Cranfield University

School of Applied Science

PhD
2007

Dirk Ansorge

Soil Reaction to Heavily Loaded Rubber Tracks and Tyres

Prof. Richard J. Godwin

Presentation 12.10.2007

This thesis is submitted in fulfillment of the requirements for the Degree of the Doctor of Philosophy.

ABSTRACT

The importance of undercarriage design with respect to its effect on soil density changes grows with the size of harvest machinery. Therefore this study elucidates the mechanics of soil displacement caused by different undercarriage systems of combine harvesters on soil.

The soil displacement caused by different undercarriage systems at maximum working weight was measured by embedding tracers into the soil in both the soil bin laboratory and the field studies. The effects of different tyres, tracks, and whole undercarriage systems on soil density increase were significant. The results from whole machine systems were validated with field experiments using fish-hooks for measuring displacement on a sandy loam and a clay soil. The draught force of a tine loosening the soil after the passage of whole machines was also investigated.

With an increase in speed, soil density increase was reduced. The implement tyre evaluation emphasized the importance of tyre width, diameter, and inflation pressure on soil density increase. The evaluation of whole machine systems showed that the influence of rear tyre size on additional soil density increase is larger for wheeled than for tracked undercarriage systems. The strong layer at the surface from a track is able to carry the rear tyre without further compaction of the soil below leading to an overall soil displacement similar to a wheeled machine of 1/3 of the weight. The evaluation of different track systems emphasized the effect of the number of rollers on soil physical parameters. Variations in a high belt tension range showed only small effects.

A novel approach was developed determining virgin compression line parameters in-situ from contact pressure, rut and working depth enabling an easy adjustment of a model to given soil conditions and a successful prediction of soil displacement for tyres. The in-situ approach can be used for tracks, but a different VCL results. The in-situ VCL was validated with small scale plate sinkage tests and compared to results from triaxial cell testing. Results from triaxial tests showed that the VCL depends on the relation of major and minor principel stresses. Ancillary experiments were carried out to shed light on longitudinal soil movement and the influence of lugs and pressure history on soil displacement. In addition a new heuristic model involving load per perimeter length was tested and the “punching failure” of soil observed justified with theories from literature.

Ancillary experiments showed that the dense layer at the surface from the tracks originates from a backward soil movement limited to the uppermost 150 mm. The lug influence of both tyres and tracks was insignificant from 200 mm depth downwards. From heuristical data analysis the load per perimeter length was identified as an important variable. Peaked pressure history caused about 1/3 more sinkage than constant contact pressures.

ACKNOWLEDGEMENTS

I want to thank Prof. Dr. Dick Godwin for suggesting this interesting topic, enabling the project and his great support during the work. Without him I would never have been able to achieve what I did in my time at Silsoe and never had learned so much.

Without the financial support from Dr. Helmut Claas and Dr. Hermann Garbers this work would not have been possible and this is very gratefully acknowledged. Jan Willem Verhorsts help in carrying out the day – by – day topics was important – thank you very much. Trevor Tyrrell and Paul Moss did me a huge favour by organizing combine harvesters for the field trials and supplying tyres as they didn't arrive in time from Germany.

For the continuous support on fighting Cranfield's "paper war" and Dick's diary I would like to thank Sandra Richardson very much indeed.

Very special thanks must go to Dr. James L. Brighton for his enormous support in the construction process and his challenging questions. Thanks must go to Dr. Ian James as head of the thesis committee meeting who always challenged my data analysis.

Without the help of the technicians in the soil bin Simon Stranks and Roy Newland the results would never have been gained. Phil Trolley was always there when I needed another hole drilled and never ever let me down. Many thanks to Bob Walker and Peter Grundon for their help during the field work.

Great thanks to Dr. Walter Zuern for his continuous support and ideas during the whole work and for proof reading. The moral support of Denise Türk during the work is highly appreciated ☺.

TABLE OF CONTENTS

List of Figures

List of Tables

A list for the figures and tables in the Appendix is given at the beginning of the Appendix.

NOMENCLATURE

Abbreviations:

CI	confidence interval
DBD	dry bulk density [g/cm^3]
LSD	least significant difference
LPPL	load per perimeter length [t/m]
VCL	virgin compression line

Symbols:

A	contact area [m^2]
B	diameter of plate [m]
c	cohesion [kN/m^2]
d	displacement [mm]
F	force [kN]
m	mass [kg]
p	probability level
P	power [W]
s	change in vector length per unit of depth [mm/mm]
S	Sinkage [mm]
t	time [s]
U	circumference [mm]
v	speed [m/s]
z	depth [mm]
Z_I	critical sinkage depth
η	draught efficiency
κ	draught to weight ratio
σ	slip
ξ	concentration factor
σ	pressure [kPa]

σ_h	horizontal pressure component [kPa]
σ_v	vertical pressue component [kPa]
σ_p	passive earth pressure [kPa]
χ	shape factor
γ_c	critical density for cone formation [Mg/m^3]
γ_i	initial density of soil [Mg/m^3]
γ_f	final density [Mg/m^3]
ϕ	angle of internal friction [degree]

Units:

h	hour
Hz	$second^{-1}$
l	liter
m	metre
m^2	square metre
N	newton
Pa	pascal
s	second
W	watt

Factors:

mega (M)	10^6
kilo (k)	10^3
centi (c)	10^{-2}
milli (m)	10^{-3}
micro (μ)	10^{-6}

1 INTRODUCTION

1.1 Background

This thesis investigates the process of soil compaction caused by combine harvesters (total weight 30 – 33 t) equipped with tyres or tracks and enlightens the discussion about the possible impact of modern harvest machinery on soil physical parameters. It follows from an earlier study conducted by Ansorge (2005, a) who investigated the effect of axle loads between 21 – 24 t carried on self propelled wheels and a track on soil density increase under controlled laboratory conditions. The study showed a clear benefit of the "Terra Trac" driving system compared to wheel type systems in uniform and stratified soil conditions. Soil displacement was reduced to 50 % for the tracks compared to the wheels at an overall load of 12 t and 10.5 t, respectively. In uniform soil conditions there was no significant increase in penetrometer resistance compared to the control below 400 mm depth. Reducing the inflation pressure for a tyre to half the recommended inflation pressure reduced soil deformation by 25 %.

Subsequently to Ansorge (2005, a) it was necessary to account for the interaction of the rear axle wheels following the front axle investigated previously to evaluate the impact of whole harvester machinery on soil physical parameters. For a tracked combine harvester it is important to quantify the possible additional soil compaction caused by the pass of the rear wheels following the front axle to investigate whether the benefit of tracks reported by Ansorge (2005, a) is maintained after a subsequent wheel pass and to compare it to wheeled combine harvesters. To support the discussion of alternative wheel configurations an evaluation of possible wheel systems was carried out with respect to their potential for reducing changes in soil physical properties compared to current wheel configurations. The influence of the time of contact on changes in soil physical properties was investigated determining the effect of speed on soil strain and relating the speed used for the experiments to real harvest speeds. This experiment allowed to quantify the additional soil density increase on headlands due to reduced speed and may help understand some of the track characteristics observed by Ansorge (2005, a). Different rubber track belt tensions and rubber track types were evaluated with respect to changes in soil physical properties enabling to possibly derive guidelines for future track design and to compare current products.

The results were verified in the field on two soil types at higher moisture content with full size tracked and wheeled combine harvesters. This supports the credibility of the results with respect to their validity in practice.

The alleviation of soil compaction is highly cost intensive. Therefore the forces on a deep tillage tine were measured after the passage of wheels and tracks in both laboratory and field soil conditions. This revealed information concerning the required energy input to loosen the soil after the passage of wheeled and tracked combine harvesters.

From the study of two models for predicting soil compaction Ansorge (2005, a) revealed that they were not appropriate for reliable predictions without modifications of the soil properties. Hence, an alternative approach to gain the soil properties for predicting soil compaction was taken and verified with data from both soil bin laboratory and field experiments.

During the study ancillary experiments and data analysis were carried out. The origin of the beneficial strong layer picked up by Ansorge (2005, a) in penetrometer resistance after the passage of tracks was investigated. The influence of lugs on vertical soil displacement has been a point of long discussions and hence was evaluated. Analysing the data scatter obvious when plotting soil density increase with respect to contact pressure lead to the parameter load per perimeter length. The influence of peaked vs. average contact pressure on sinkage was examined to evaluate and quantify possible differences. The vertical punching soil failure observed by Seig (1985), Trein (1995), Ansorge (2005, a), Antille (2006) and in this study was explained with plate sinkage and passive earth pressure theory.

During the process of writing the thesis the following three papers have been published in / submitted to / are in prepararion for submission to *Biosystems Engineering*:

- Ansorge, D. and Godwin, R.J.: The Effect of Tyres and a Rubber Track at High Axle Loads on Soil Compaction: Part 1: Single Axle Studies. Biosystems Engineering (2007), doi:10.1016/j.biosystemseng.2007.06.005

- Ansorge, D. and Godwin, R.J.: The Effect of Tyres and a Rubber Track at High Axle Loads on Soil Compaction: Part 2: Whole Machine Studies. Submitted

- Ansorge, D. and Godwin, R.J.: The Effect of Tyres and a Rubber Track at High Axle Loads on Soil Compaction: Part 3: Prediction Studies. In Preparation.

The following paper has been submitted to the *Journal of Terra Mechanics*:

- Ansorge, D. and Godwin, R.J.: An In-situ Determination of Virgin Compression Line Parameters for Predicting Soil Displacement Resulting from Agricultural Tyre Passes

A detailed literature review concerning soil compaction in general, its implications on crop growth, and alleviation is given in Ansorge (2005, a) and Ansorge and Godwin (2007). That work additionally includes a review on the controversy concerning tracked vs. wheeled machines. Consequently this section will give a summary and deal with publications which were published in the meantime. A brief summary on soil compaction models is provided, too; the detailed literature review on soil compaction models is given in Section 6.1.

A review monograph concerning soil compaction, its consequences and counter measures summarizing in detail the current state of knowledge was published by Hakansson (2005). For an introduction into the issue of soil compaction it is highly recommended. According to Van den Ploeg et al. (2006) agriculture is responsible for the increased threat of flooding due to a reduced infiltration rate caused by modern agricultural machinery. Unfortunately, this publication lacks data to back up its statements. In contrast, Godwin and Dresser (2003) and Dresser and Godwin (2004) showed that by improved soil management the infiltration rate would reduce the peak in flood hydrographs by 20 %.

Watts et al. (2005) found that maximum rut depths are caused by heavy trailers rather than tractors and moreover showed that crawler tractors created the least soil damage suggesting the use of tracked undercarriage systems. A similar benefit of tracks was found in an in-field investigation on undercarriage systems for a sugar beet harvester by Brandhuber et al. (2006). The tracked type undercarriage system caused less reduction in hydraulic conductivity than its wheeled counterpart.

The effect of wheel traffic on runoff and crop yield was investigated by Li et al. (2006), whereby they have found that controlled traffic seems to be the most beneficial solution for both high yields and reduced compaction. This agrees with results from Tullberg (2006).

Little extra has been reported since Ansorge (2005, a) with respect to tracks.

Excellent reviews of existing soil compaction models were compiled by Seig (1985) and Defossez and Richard (2002). The performance of two elastic and two elasto-plastic models was compared by Chi et al. (1993) in predicting stress and strain of a sandy loam soil and clay. Chi et al. (1993) point out that the assessment of soil parameters is mostly the largest source of error. Therefore a soil compaction model which can account for different soil conditions is of great value for machine designers and soil managers to evaluate the impact a machine pass can have under given soil conditions. Tyre and agricultural machinery manufacturers could evaluate tyre specification and axle configuration, respectively, at the design state. This thesis will describe a simple approach to obtain the slope and intercept parameters of a virgin compression line from contact pressure and soil density changes and use this with the model COMPSOIL (O'Sullivan et al., 1998) for a spectrum of soils. Following this approach, designers, advisers and farmers could assess the field impact of machines from a knowledge of the inflation pressure and the resulting rut depth. In contrast to the models SOCOMO (van den Akker, 2004) and TASC (Etiennen and Steinmann, 2002) COMPSOIL is actually able to quantify the soil density increase rather than simply stating a danger of soil compaction for given loads and inflation pressures. A detailed literature review on soil compaction models is given in Section 6.1.

Overall a significant volume of work has been conducted in the area of soil compaction and as a result the soil physical principles of soil compaction appear to be clear, but its real implications with the soil conditions are less so. The results depend on the soil conditions and the author's interpretation. With the exception of Ansorge (2005, a) laboratory studies were limited to loads smaller than 5 t and no published results have been found on the performance of tracks in laboratory conditions. This study aims to extend the laboratory investigation from Ansorge (2005, a) into the effects of whole undercarriage systems with high axle loads on both wheels and tracks. Additionally the findings in the soil bin laboratory will be compared to a field experiment.

1.2 Aim

To elucidate the mechanics of soil displacement causing compaction by combine harvester wheels/tyres and tracks at high axle loads on uniform soil conditions in controlled laboratory conditions and in field.

1.3 Objectives

Objectives:

1. To investigate the effect of:
    a. multi - wheel systems as shown in Figure 1
    b. the time of contact and the length of the contact patch
    c. the size and inflation pressure of a rear combine tyre following the passage of the front implement
    d. different track configurations on soil physical properties
    e. the load and inflation pressure of a light weight combine harvester

on soil physical properties in controlled laboratory and field conditions.

2. To evaluate and develop existing soil compaction models to predict the effects of wheels/tyres and tracks on soil physical properties.
3. To determine the relative effects of wheels/tyres and tracks on the resulting tillage forces.

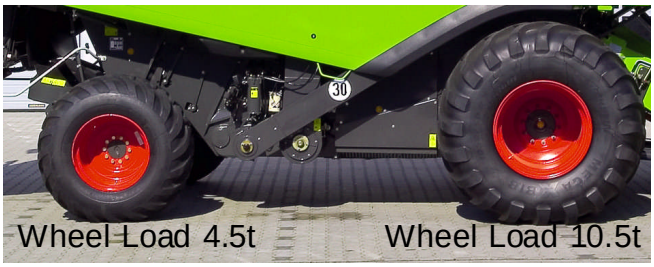

Traditional Wheel Configuration

Alternative Wheel Configuration 1 (Tandem)

Alternative Wheel Configuration 2

Alternative Wheel Configuration 3

Figure 1: Alternative multi - wheel configurations

1.4 Outline methodology

1. Review the relevant literature from the international public domain and restricted data at Cranfield University at Silsoe.
2. The tyre / track and the tillage tine force studies will be conducted using the single wheel / track tester built by Ansorge (2005, b) with a uniform soil condition in a controlled laboratory environment. The following will be investigated in detail:

a) the soil compaction of multi wheel systems compared to track data from Figure 1. Hence answering the question whether multi-wheel systems have similar soil compaction characteristics as tracks
b) the influence of time of contact on soil compaction parameters to illuminate the effect of reduced traffic speed on increased soil compaction in headlands and to simulate a long contact time as it occurs with a track
c) the additional soil compaction caused by a rear tyre after the passage of a tyre or a track
d) the soil compaction characteristic caused by tracks. In particular answer the question "what causes the dense layer close to the surface detected by Ansorge (2005, a)?"
e) the soil density increase of a wheeled combine harvester at 11 t in comparison to a modern one on tracks at 33 t
f) the draught force of a subsoiler to loosen the soil after the passage of a tracked and a wheeled machine
g) the vertical soil failure found by Ansorge (2005, a)

3. The full size combine studies will be conducted in field conditions on different soil types.
4. The effects on soil properties to be determined by changes in:
   a) Soil displacement
   b) Penetration resistance
   c) Rut characteristics
   d) Dry bulk density
   e) Pressure distribution in the soil

   Hereby each measurement is replicated three times.
5. Data analysis and explanation of results.
6. The further development of the compaction prediction models of Smith / O'Sullivan / van den Akker including triaxial cell tests and plate sinkage tests to derive virgin compression line parameters for the prediction of soil displacement.

2 EXPERIMENTAL METHODS

This chapter contains a description of the experimental environment in both the laboratory and the field (Section 2.1) followed by a detailed explanation of the measured parameters (Section 2.2) and a description of test procedures utilizing the triaxial test cell apparatus (Section 2.3).

2.1 Experimental Environment and Set Up

This section specifies the details on soil conditions, test set up, and tyres and tracks utilized in the soil bin laboratory in which the drive units of full size combine harvesters were simulated. Additionally the details of the field site experiment with full size machinery are provided; i.e. soil conditions, machine configurations and experimental set up.

2.1.1 Soil Bin Laboratory Conditions

The study was conducted in the soil bin laboratory of Cranfield University, Silsoe. The soil bin is 20 m long, 1.7 m wide, and was prepared to a depth of 750 mm with a soil processor. The soil used was a sandy loam (Cotternham series; King, 1969) with 17 % clay, 17 % silt and 66 % sand and water content was maintained at 10% dry base. A uniform soil condition was prepared to a dry bulk density of 1.4 g/cm^3 chosen to represent soil with a relatively low bearing capacity where tracks and large size tyres would have value in agricultural practice. The initial penetrometer resistance of such a soil is shown in Figure 2.

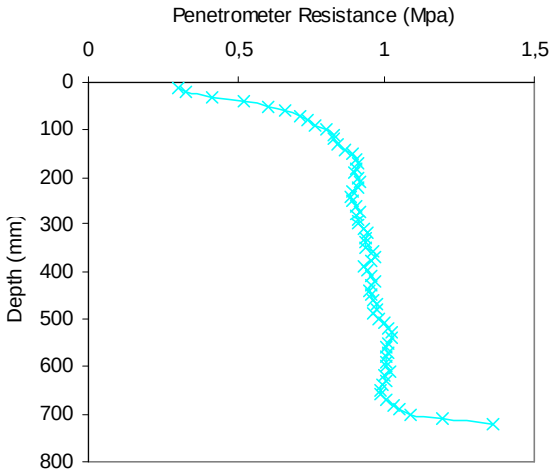

Figure 2: Initial penetrometer resistance profile from the soil bin prepared to uniform soil conditions

2.1.1.1 Test Frame

To be able to test the harvester tyres and the track on the front axle a test apparatus was designed and built in accordance with the requirements of the study and the soil bin. The apparatus, shown in Figure 3 with a track unit before (left) and a 900 mm section width tyre after a run (right), allows the application of 0 – 14 t onto a self propelled wheel or track mounted to a standard Claas Lexion axle using a hydraulic cylinder. A detailed description of the single wheel/track tester used can be found in Ansorge (2005, b).

Figure 3: Single Wheel/Track test apparatus with a track (left) and a tyre (right)

The implement tyres which are fitted to the rear axle of a combine harvester, were placed in a test rig towed by the soil processor of the soil bin whereby the tyre is mounted to a continuous axle supporting the frame which takes up the load boxes supplying the required load. In this test rig the load has to be taken off after each run.

2.1.1.2 Tyres and Tracks

The details of all tyres and tracks loaded to 1.5 – 12 t are given at the beginning of each chapter on results. The list of rear tyres loaded to 4.5 t and undercarriage configurations used to simulate machines in the range of 11 – 33 t is provided in Section 3.2. Detailed information on tracks at 12 t load is given in Sections 3.3.1 and 3.3.2 for different belt tensions and track types, respectively. The self propelled tyres run at approximately 10 % and the rubber tracks at approximately 5 % slip (Ansorge, 2005, b).

2.1.2 Field Studies

2.1.2.1 Soil Conditions and Soil Preparation

Two field sites were chosen with soil types of a sandy loam (Cotternham series (King, 1969) with a particle size distribution of 65.7 % sand, 17.2 % silt and 17.1 % clay (Ansorge, 2005, a)) and a clay (Wicken series with a particle size distribution of 12 % sand, 25 % silt and 62 % clay (Spoor and Godwin, 1979)), respectively. Using these two soil types enabled both the verification of soil bin results in the field on the same soil type and the expansion of the study onto a clay soil.

The sandy loam field site was split in two parts, see Figure 5. One was subsoiled five weeks before the investigations were carried out and the second one was shallow tilled four weeks before. Both sites had not been cropped or subject to other tillage operation for the previous 1.5 years. The clay field, shown in Figure 6, was only shallow tilled four weeks beforehand. This site was located within an oil seed rape crop, however due to pigeon damage it had a large area without crop on which the investigations were conducted. Direct drilling of the oil seed rape was the only tillage operation for 1.5 years.

The subsoiling operation was chosen to obtain a very weak soil condition, similar to the uniform soil bin conditions. A subsoiler was operated at 350 mm depth at 1 m leg spacing. The working direction was 90 degrees to the travel direction of the combine harvesters. The shallow tillage operation was chosen for the second site on the sandy loam and on the clay to level the surface and gain a uniform surface. Underlying variances could not be removed, but it provided field conditions likely to be found in a harvest with precipitation. Shallow tillage was carried out with cutting discs followed by tines running at 100 mm depth followed by D-D rings.

2.1.2.2 Machines

The study was carried out with two Lexion 580, Type 586, built in 2005, each with a 316kW engine, and shown in Figure 4. One machine was equipped with wheels and the second with the “Terra Trac” sytem on the front axle. The wheeled machine with identification No 58600515 had 800/65 R32 tyres on the front and 600/55-26.5 tyres on the rear axle. On the tracked machine with identification No 58600525 the Claas Terra Trac system

had been mounted on the front axle and 600/55-26.5 tyres on the rear axle. The front and rear tyres were inflated to 2.5 and 1.4 bar, respectively.

Figure 4: The combine harvesters taken into the field

For the field trials both machines were equipped with a 9 m header and the traveling speed of the machines was approximately 1 m/s, thus similar to soil bin speed. This slow speed (in comparison to real working conditions) was necessary to target the measurement spots. The aim was to make a relative comparison, not necessarily replicating exact harvest speeds, and hence the speed itself is not significant on the relative difference as long as both machines operate at the same speed. However, the speed in exact harvest conditions could influence the outcome eventually.

2.1.2.3 Experimental Set Up

The initially planned treatments with numbers one to five (locations shown in Figure 5 and Figure 6) were the tracked combine harvester with full (1) and empty grain tank (3), a wheeled combine harvester with full (2) and empty grain tank (4) at recommended inflation pressure for maximum machine weight and the wheeled combine harvester at +1 bar on top of the recommended inflation pressure (5). This additional inflation pressure of 1 bar was selected because of theoretical ideas leading to an infield possibility to gain the slope and intercept of the virgin compression line for the given soil type and conditions.

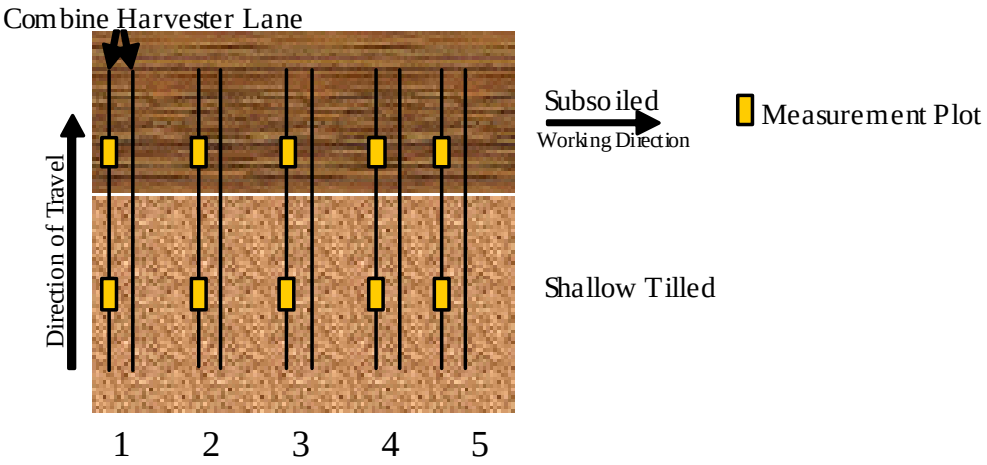

Figure 5: Sandy loam field layout, with shallow tilled and subsoiled parts

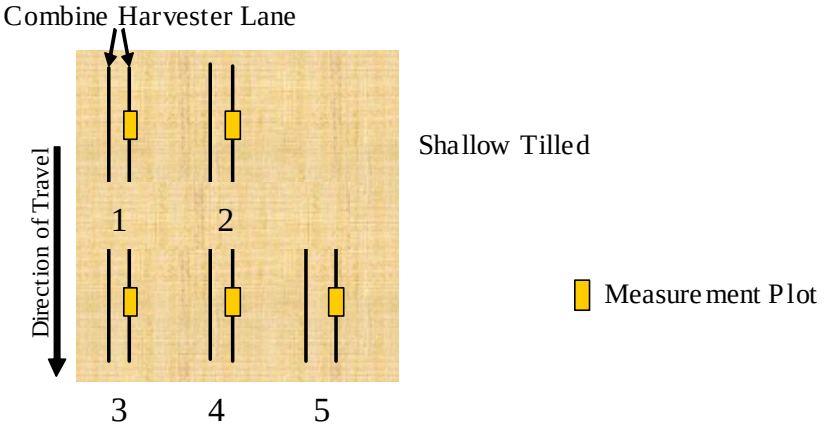

Figure 6: Clay field layout

Due to very wet weather conditions and the fact that the combine harvesters need to run with their grain tank open when harvesting or filled with grain, the variations were reduced to only those with an empty grain tank. As a consequence the plots originally created for the treatment with a full grain tank were converted to a replication of the empty grain tank in the same field. During data analysis this proved to be sensible due to the high variation of the measured parameters in the field and the increased amount of data points to strengthen the statistical analysis. A full grain tank would have added 6 – 7 t to the total weight of the machines depending on moisture content of the grain.

The left track of a machine (looking in travel direction) was always chosen for the measurement to avoid errors from load differences between the left and right of the machine

track; the load difference can amount to 200 – 400 kg depending on the equipment of the machine (Verhorst, 2006).

Measurements were replicated within a wheel rut at 2 m distance from each other as indicated by the yellow marks in Figure 5 and Figure 6. The field was assumed to be uniform, hence measurement replications were taken in a particular area to describe the behavior at a given point with high resolution. The uniformity was later confirmed by comparing the control measurements in penetrometer resistance at the different locations - no significant variations could be found. Gaining a further replication by using empty machines alone proved to be statistically sensible.

2.2 Measurements of Parameters

2.2.1 Soil Displacement

Soil displacement was measured with two different methods. In the soil bin laboratory talcum powder lines were used as in Ansorge (2005, a) and slightly improved. In the field a new method utilizing fishing hooks was introduced.

2.2.1.1 Soil Displacement Measurement in Soil Bin Laboratory

A novel “non - invasive” procedure inspired by a technique of Trein (1995) was used to determine soil displacement (strain) and effective density change. This was achieved by placing longitudinal talcum powder lines into the soil during preparation and the measuring the change in their relative position following each passage of a tyre or track. Four sets of talcum powder lines were placed along the length of the soil bin. The position of the talcum powder lines is located from the digitized output of two drawstring transducers connected to a pin drawn to each talcum line appearing in the profile as a point, when the length of each draw string is recorded. Knowing the length of each drawstring and the distance between the drawstring transducers, it is possible to calculate the vertical and horizontal coordinates of each point using triangulation formulae. As shown in Figure 7 two points on either side in the undisturbed area are taken as a control and linearly interpolated visualized with the white line to gain the initial coordinates of the central talcum powder points. Compared to the approach taken by Trein (1995) visualization has been enhanced

as the talcum powder is much easier to locate than the paint used earlier while maintaining high accuracy.

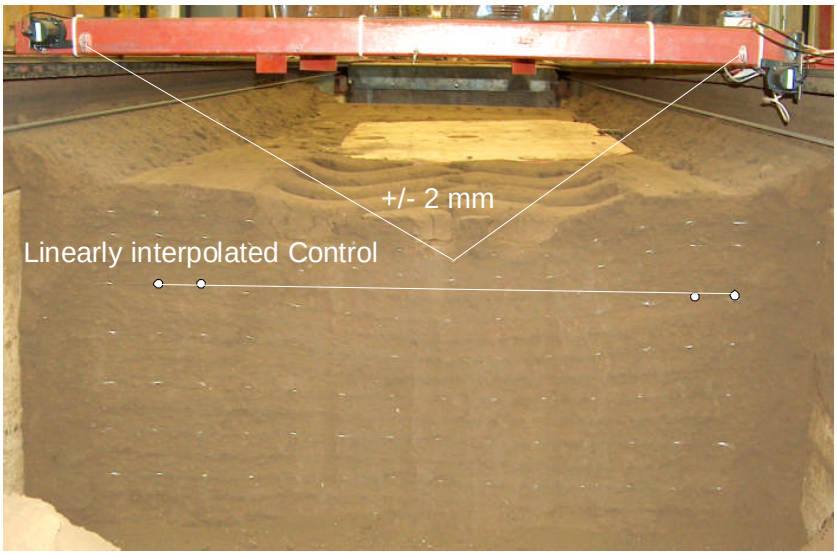

Figure 7: Vertical cut through soil with points of talcum powder and the drawstring transducers in the initial condition

The mechanical accuracy of the measurements was assessed by printing an imaginary cut through the soil bin profile with a large CAD plotter and measuring the position of the points with the drawstring transducers. Hence the true position of every single point was known and then compared to its measured position. This comparison showed that the individual position of a single point can be measured to an accuracy of +/- 2 mm, and the depth of a layer can be measured to within +/- 0.5 mm due to the repeated measurements within a layer. Having digitized the initial and the final positions of the talcum powder points, it is possible to draw a vector diagram of the soil movement from the initial coordinate to the final. Such a vector diagram is shown in Figure 8 for an 800 mm section width tyre at 10.5 t load and 2.5 bar inflation pressure (800/10.5/2.5).

The vectors in Figure 8 exhibit near vertical soil displacement with little sideways movement. This type of displacement was seen for all treatments.

To be able to compare the different treatments in one diagram the length of the central four vectors was averaged for each depth. This average vector length representing the soil displacement of the central 300 mm for the rut is plotted against depth in Figure 9 for the

800/10.5/2.5 tyre. Vectors with greater displacement, as shown by the solid line, show a greater change in soil density and a smaller displacement as shown by the broken line indicate smaller changes in soil density.

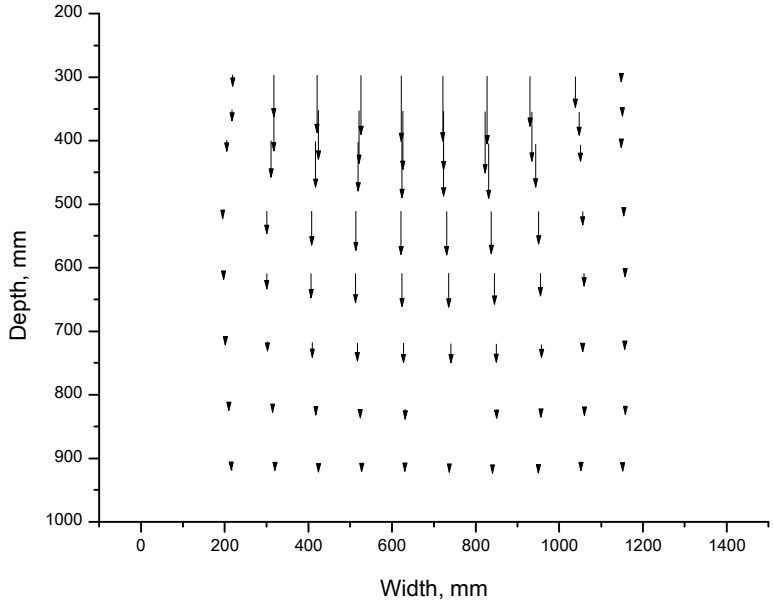

Figure 8: Vector diagram of soil movement after the pass of an 800/10.5/2.5 tyre

Figure 9 shows soil displacement as a function of depth, which can be described in the depth range from 0 – 500 mm by a linear function with the following equation which only holds true for *d(z)* being positive or zero:

$$d(z) = d_0 - s \times z$$

Eq. 1

where: d is the soil displacement in mm at a given depth z; d_0 is the displacement at the surface in mm; s is the change in vector length per unit of depth in mm/mm; and z is the depth in mm.

The slope can be taken as a direct measure for an increase in soil density because it determines the change in soil movement per unit of depth which consequently is accompanied by an increase of soil density. The following example visualizes the concept: assuming a layer has an initial thickness of 10 mm and its surface has moved 5 mm and its bottom face has moved by 4 mm, the remaining 1 mm has been taken up by the layer, i.e. its thickness has been reduced from 10 to 9 mm and which in consequence increased the soil density of the layer. Then soil movement decreases by 0.1 mm/mm and in turn soil density increases by 10%.

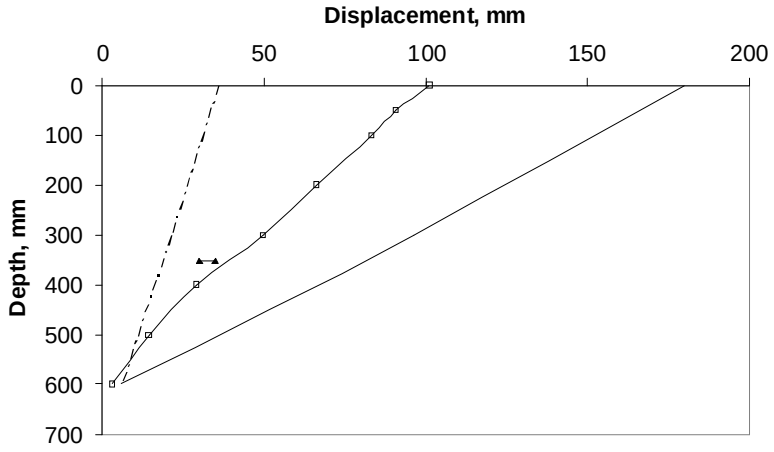

Figure 9: Soil displacement vs. depth after a pass of an 800/10.5/2.5b: □ 800/10.5/2.5; - - 5% and - 30% increase in density; and▲ LSD

When Eq. 1 is differentiated with respect to depth, the displacement change, i.e. the average increase in soil density is derived:

$$-\frac{\Delta d(z)}{\Delta z} = -d'(z) = s$$

Eq. 2

Thus $|s|$ is a direct measure of the relative increase in soil density caused by vertical soil movement and will be used to compare the treatments.

The method to determine density increase by measuring soil displacement with the drawstring transducer is much more accurate than the gravimetrical method as shown by detecting significant differences between individual treatments. The maximum error in measuring the depth of a layer is +/- 0.5 mm which would result in less than 1% error in soil density increase in the worst case; i.e. if all points over the 500 mm depth range line up in such a way that the top has a larger displacement of + 0.5 mm than in reality and the bottom has 0.5 mm less than in reality. This is unlikely due to the large amount of measurements and handling errors do not exist with the drawstring method.

The curvature of the soil displacement graph raised the question whether a linear function was appropriate. Fitting different regression functions to the soil displacement data justified the linear regression function approach described earlier for a depth range from 0 – 500 mm depth. Each full regression model function included both a non linear and a linear

term. In the majority only the linear term proved to be significant. Moreover, the influence of the non-linear term on curvature did not always lead to desired outcome. Depth functions $\sqrt{z}, \ln(z), \exp^{-z}, \frac{1}{z}, and \frac{1}{z^2}$ all created high curvature close to the surface and could not describe the curvature at depth properly. $z^2, z^3, and \exp^z$ showed the curvature at the desired depth. z^2 was able to trace the original data best. Still, 8 out of 15 analyzed data sets reduced to the linear model while for the remaining 7 both parameters were significant. If the reading at 600 mm depth is disregarded, 11 out of 15 reduce to the linear model. Therefore the general approach taken to describe the soil displacement data with a linear function is justified. Although for some experiments the relationship is too simple, this appears to be the only sensible possibility for comparisons of treatments.

2.2.1.2 Soil Displacement Measurement in Field

The high resolution of the results gained by Ansorge (2005, a) measuring soil displacement with talcum powder stripes in the soil bin created the demand for the same parameter to be measured in the field experiment. The talcum powder stripes idea could not be realized as this would destroy the initial soil structure and thus not provide real infield conditions. Alternative methods had to be found whilst maintaining soil structure yet picking up soil movement. Therefore two methods were seriously contemplated:

1.) Drilling small holes and filling them with differently colored sand to known depths. Hereby one would drill a hole to a given depth, say 400 mm. Then filling 100 mm of sand of one color into it, using a packer to make sure it is entirely filled up to the required height. This is followed by 100 mm of differently colored sand and repeating the process up to the surface. Thereby one would know at which depths the initial boundaries of the differently colored sands are situated. By digging a profile after the treatment the depth of the boundaries could be measured against a benchmark outside the rut area. This method is shown schematically in Figure 10.

2.) To use triple headed fishing hooks placed at a known depth. Basically a fishing hook, with a fishing line of known length attached to it, is pushed into the soil with a rod. Once the approximate depth for the fishing hook is reached, the rod is pulled out. Then the barbs of the treble fishing hook engage with the surrounding soil. Afterwards the fishing line is

tightened and the length sticking out of the ground is measured to a reference surface. Knowing the initial length of the fishing line and the excessive length gives the depth at which the hook was placed. After the run the fishing hook is carefully dug out following the fishing line leading to it. Once the top of the hook can be seen, however before it is taken out entirely, the fishing line is tightened and its length above the original reference surface is measured again. This is the final position of the hook and the amount of soil movement relative to the reference surface is the difference in length of the fishing line above the reference surface. This method is sketched in Figure 11.

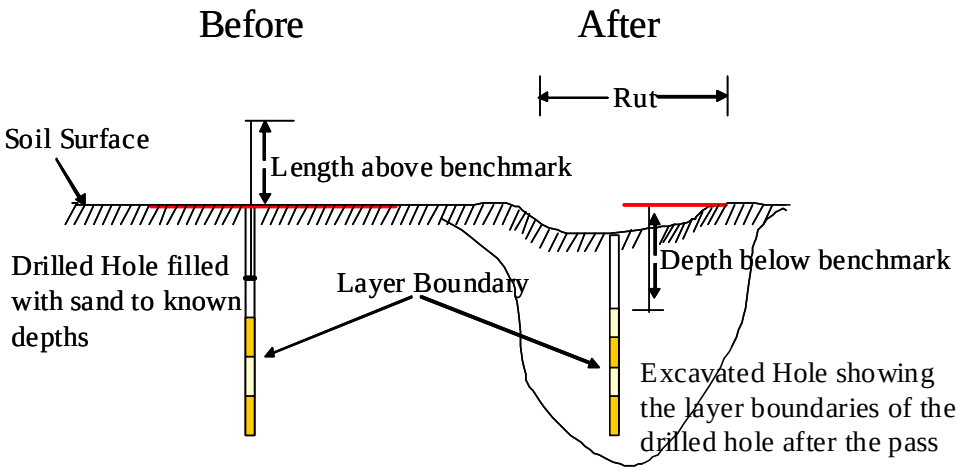

Figure 10: Differently colored sand method to determine soil displacement in the field

Both methods engage with the surrounding soil and follow the movement of the soil during the treatment. As the distance from the surface to the fishing hooks reduces, caused by the compacting soil, the hook has to be dug out to make sure the fishing line is tight and straight again. This reduction in distance from the soil surface to the hook has the advantage that one can be sure that the fishing hook is not physically restrained by the fishing line when it is pressed into the surface during the passage of the vehicle.

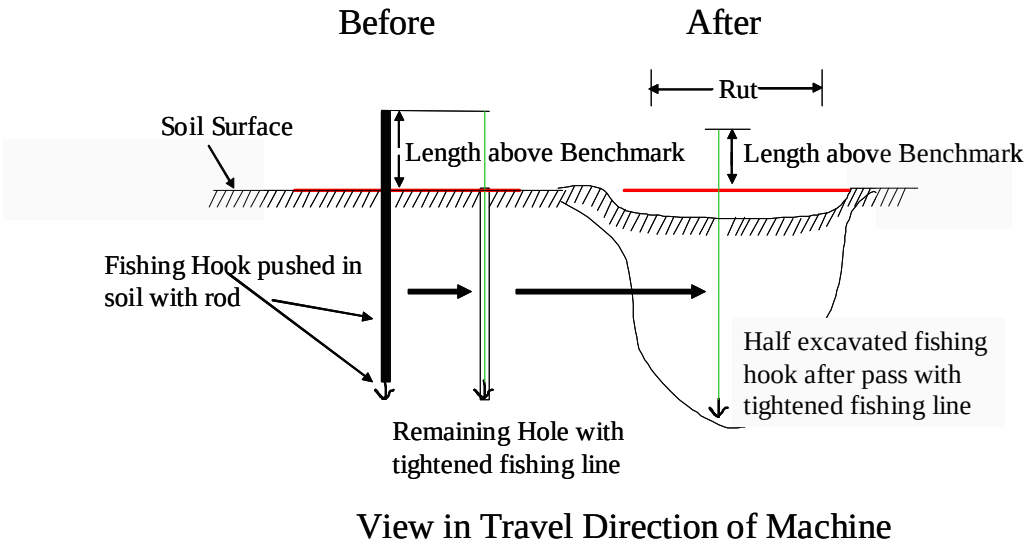

Figure 11: Fishing hook method

Finally the fishing hook method with triple headed fish hooks was selected as filling the holes with sand to a known depth seemed too challenging regarding field conditions with a hole of a diameter not bigger than 5-10 mm in order to minimize soil disturbance. Earth worm holes and other cavities of similar size to the sand hole are able to pick up sand during, but more importantly, after being filled and in the first steps of compaction, hence causing errors to the changes in the depths of the boundaries of the color layers.

The fishing hook method was verified in soil bin experiments against the talcum powder line measurements and gave good agreement as shown in Figure 12. The slope was similar and only the offset varied slightly. This is not significant as only 7 fishhooks were compared to approximately 120 talcum powder points.

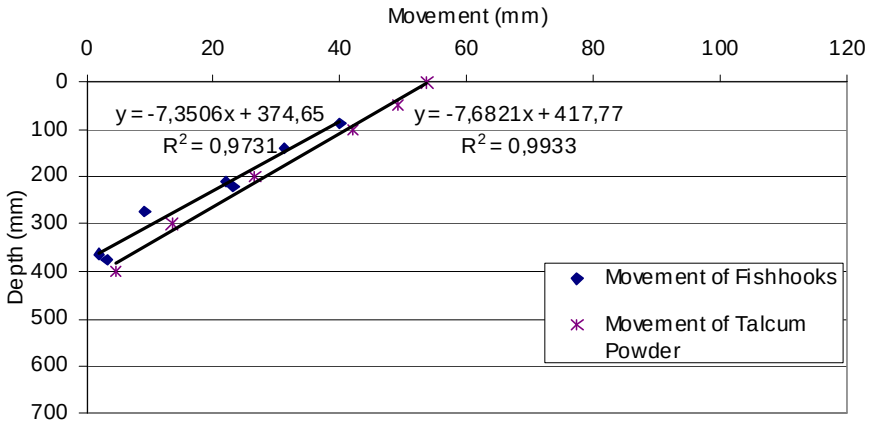

Figure 12: Movement of talcum powder and fishhooks in the soil bin under the same experiment

Depending on the expected soil displacement of a certain treatment and soil condition the number of fishing hooks was varied by varying the amount of depth locations at which hooks were placed. The distribution of the fishing hooks with depth is shown in Table 1. All depths were replicated three times. The rut depth was taken as the surface/highest reading in the following analysis enabling regression lines including the surface.

Table 1: Intended placement depths of fishing hooks for treatments

Treatment	Measured Depths (mm)	Total Hooks
Sandy Loam, Subsoiled		
Tracked Machine with full grain tank (1)	100, 200, 300, 400, 500, 600	18
Wheeled Machine with full grain tank (2)	100, 200, 300, 400, 500, 600	18
Tracked Machine with empty grain tank (3)	150, 250, 350, 450	12
Wheeled Machine with empty grain tank (4)	150, 250, 350, 450	12
Wheeled Machine with high inflation pressure (5)	150, 250, 350, 450	12
Sandy Loam, Shallow Tilled		
All treatments (1 – 5)	150, 300, 400	9*5
Clay, Shallow Tilled		
All treatments (1 – 5)	100, 200, 300, 400, 500	15*5

After placing the hooks in the soil, their uniform distribution was verified. During this process additional fishing hooks were added to the treatments at depths shown in Table 2.

Table 2: Depth and amount of additional fishing hooks for uniform distribution in sandy loam

Treatment	Depth (mm)	Amount of additional Hooks
Subsoiled 1	600	2
Subsoiled 3	450	2
Subsoiled 4	450	2
Shallow Tilled 1	400	3

The initial distribution over depth for the fishing hooks is shown in Figure 13, Figure 14, and Figure 15 for the sandy loam subsoiled, shallow tilled and for the clay, respectively. It shows that they are well distributed, and cover the required depth range.

Figure 13: Fishing hook distribution in the sandy loam subsoiled

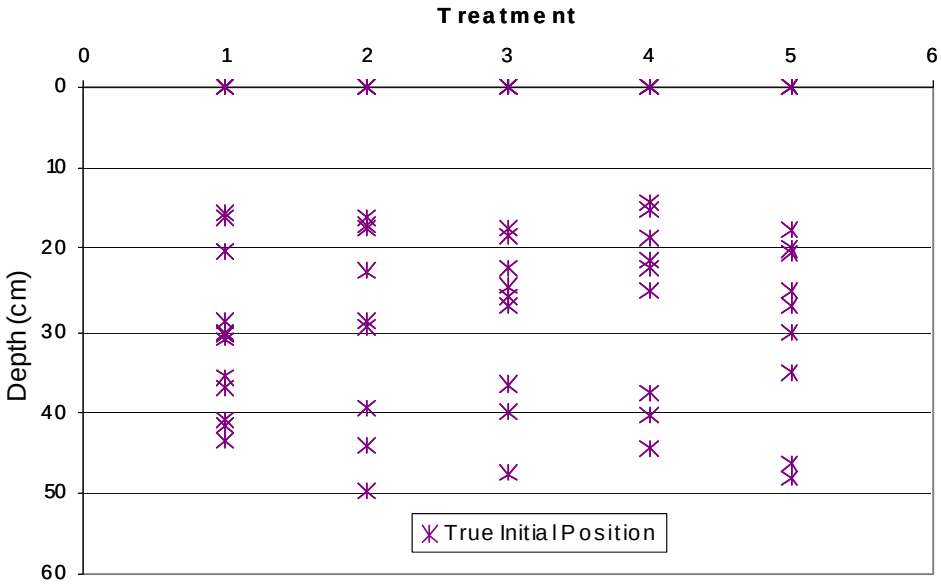

Figure 14: Fishing hook distribution in the sandy loam shallow tilled

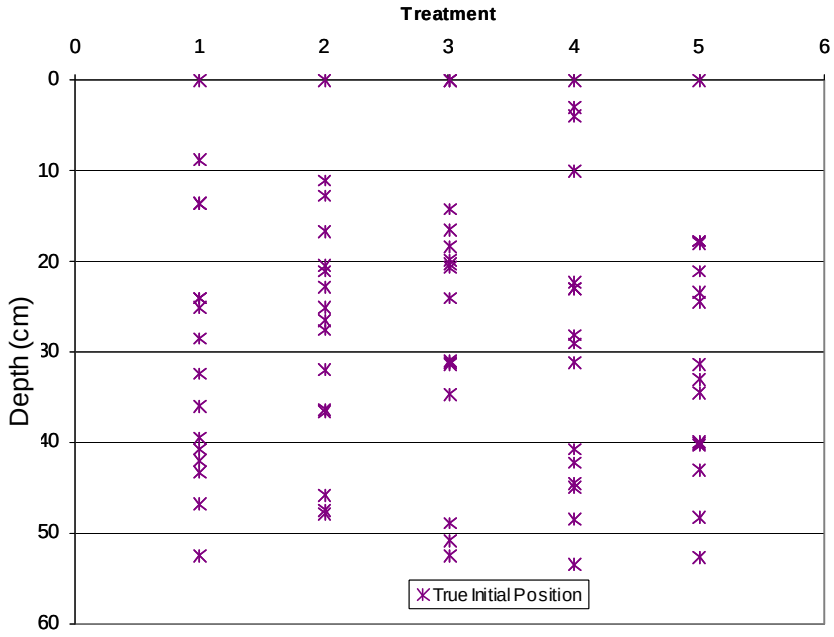

Figure 15: Fishing hook distribution in the clay

A photograph showing how the fishing hooks were dug out including the ruler laid across the hole and resting on the reference surface is shown in Figure 16. This also shows how the fishing line can be identified. The surface visible in Figure 16 was marked with yellow construction site spray to enable easy reference after the passage of the combine harvester.

Figure 16: Excavation of the fishing hooks together with the ruler for surface reference

Before the fishhooks were placed into the soil a shallow tillage operation was carried out to a depth of 100 mm to smooth the surface as detailed in Section 2.1.2.1. However, a rain period of 3 weeks delayed the actual experiment. Consequently the soil including the refer-

ence surface could settle. Following Spoor and Godwin (1984) a 15 % settlement was assumed for this soil, tillage operation, and time period between preparation and final excavation resulting in a depth offset of 15 mm. As all fishhooks were placed below the cultivation depth, all are affected by the same amount and consequently final displacement was increased by 15 mm for all fishhooks.

2.2.2 Penetrometer Resistance

Cone penetrometer resistance was determined by measuring the force necessary to push a 125 mm^2, 30^o cone into the soil. A detailed explanation of the soil mechanics influencing penetrometer resistance is given by O'Connell (1972). The data was automatically digitally recorded in 10 mm depth increments and afterwards exported to an Excel file for data analysis. The data was plotted as penetrometer resistance with respect to depth. Cone penetrometer resistance was measured across the soil bin in ten places (1- 10) at 120 mm spacing for both the initial control and the three replicated positions of the wheel/track passage. This resulted in diagrams such as Figure 17 a).

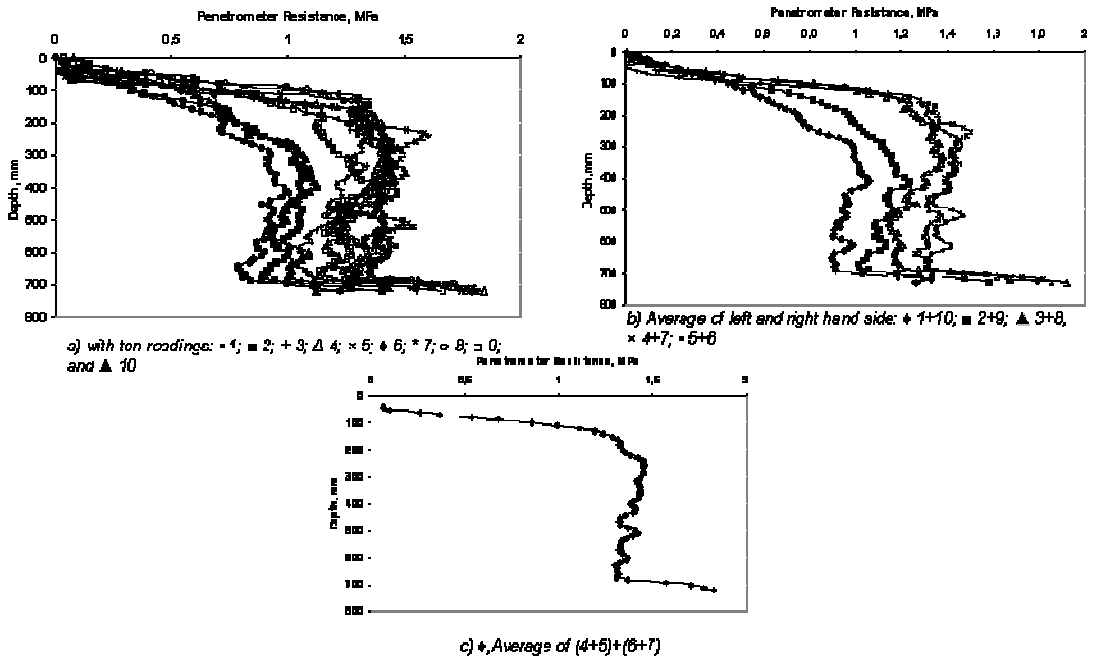

Figure 17: Penetrometer resistance across the soil bin for the 900/10.5/1.9 tyre

The increase in measured penetrometer resistance at 700 mm depth is due to the penetrometer sensing the bottom of the soil bin. Consequently, the last five readings were always disregarded for statistical analysis. As the data in Figure 17 a) shows for the 900/10.5/1.9

tyre, there is symmetry between the left (1, 2, 3) and the right (10, 9, 8) hand side of the soil bin with the highest values in the centre (five and six). Thus measurements taken at symmetrical positions relative to the centre of the rut have similar readings and consequently these readings were averaged resulting in the curves shown in Figure 17 b).

The curves 4+7 and 5+6 in Figure 17 b) coincide so giving the possibility of averaging them and thus creating one penetrometer resistance curve per treatment representing the average of the centre 4 points of measurements or the centre 360 mm of the rut. This mean curve is shown in Figure 17 c). The same procedure was applied for the initial control.

2.2.3 Dry Bulk Density

Two different methods to determine dry bulk density were used. In the soil bin only a density ring was utilized and in the field measurements both, a density ring and a gamma ray probe (Troxler) were used.

2.2.3.1 Gravimetrical Density Measurement

Dry bulk density (DBD) was measured gravimetrically at depths of 0, 250, and 500 mm, with three replications before and after each run, at the centre of the track mark in the soil bin. A cylindrical ring (60 mm diameter and 51.5 mm deep) was pushed into the soil and excavated. The surplus soil was carefully cut off and the soil sample from the cylinder weighed and dried for 48 h at 105^{o} C. The dry soil was weighed and soil water content determined from the weight difference. Dry bulk density was calculated from the given volume of the cylinder and the dry weight.

2.2.3.2 Nuclear Density Measurement Gauge

With the aim to gain a more precise resolution of the increase in soil density a nuclear density gauge, namely a Troxler 3430, was used to measure soil density. With this measurement device a gamma source is positioned at a known depth in the soil in a previously created access hole. Once the gamma source is in position and switched to transmitting mode, the detectors located within the gauge count the received radiation, which depends on the dry bulk density and the depth of location of the source within the soil. From this the ma-

chine derives the average dry bulk density which is mainly influenced by the DBD at the position where the source is located (Gameda et al., 1987). Figure 18 shows the used Troxler. As this is a radioactive measurement device the measurements were subcontracted to ACS Testing, Ltd, Dorset, BH16 6LE.

The absolute accuracy of a Troxler 3430 is not very high in determining DBD, however, the experiment is set up to determine relative differences between the single treatments and therefore the device should be suitable (ACS, 2006). Gameda et al. (1987) derived a similar conclusion when comparing a single probe (like the Troxler) to a dual probe (whereby both transmitter and recorder are located within the soil at the same depth a given distance apart from each other). Overall the dual probe showed a higher accuracy, but both methods gave consistent results. In determining absolute dry bulk density the authors suggest that each type had to be calibrated on a soil with known density before it is taken to the field to gain accurate absolute dry bulk density readings. As the aim of this field experiment is to accomplish a relative comparison of treatments by measuring dry bulk density before and afterwards it is not necessary to do a calibration. Following Gameda et al. (1987) the vital assumption of consistency of readings within one soil type is provided.

The marked ruts before the run and the places of measurements for the Troxler and the fishing hooks including the reference surface are shown in Figure 19.

Figure 18: The Troxler on a field plot

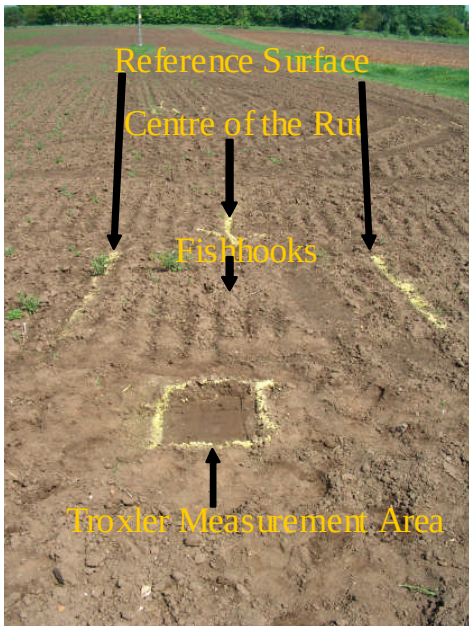

Figure 19: Placement of Troxler, fishhook and reference surface in test area

The soil dry bulk density was determined in the depths of 50, 100, 200, and 300 mm (the maximum depth possible for the system). At one location before and after the pass of the combine harvester three access holes were made and each depth was measured once within a hole. Relative densities before and after the passage of the combine harvester were recorded.

2.2.4 Rut Depth

Rut displacement and rut area were measured using a profile meter. The profile meter with its rods was placed over the rut and the rods were lowered into the rut and fixed in their position. Then the device was taken out and the shape of the rut and thereby the area of disturbance was reproduced on a sheet of paper. The area on the paper was measured using a planimeter. This method gave the total area of displacement. The width of the rut and depth were measured. All these measurement were done in three replications. For further information on rut measurements see Davies et al. (1973).

2.2.5 Pressure Measurement

Using ceramic pressure transducers embedded at the top of a 100 mm diameter aluminum tube the pressure exerted by the tracks when rolling over the soil was measured at 250 mm

depth. The data was recorded at 50 Hz sampling rate onto a laptop computer using Daisy Lab 7 software and a Doc Book for digital data processing. Detailed explanations and methodology can be found in Dresser et al. (2006).

2.2.6 Draught Force Measurement for Subsoiler Tine

On uniform soil conditions after the passage of a tracked and a wheeled undercarriage system a subsoiler tine was pulled through the soil at 350 mm depth. The draught force was measured using an octagonal draught force transducer (Godwin, 1975). Afterwards the loosened area was measured by excavating all the loose soil and measuring the area with a profilemeter. This area includes the initial rut area which therefore was subtracted of the entire loosened area. From the area and force specific draught force can be calculated.

2.3 Triaxial Cell Test Apparatus

The triaxial cell test apparatus was used both to determine virgin compression lines (VCLs) in order to conduct a comparison to the in-situ VCL created from tyre passes and to conduct small scale plate sinkage tests for a further justification of the in-situ VCL approach and some of the ancillary experiments in Chapter 7.

2.3.1 Determination of Virgin Compression Lines (VCL)

A VCL for the sandy loam soil of the soil bin was gained using the triaxial testing apparatus GDS LAB DYNTTS 2 Hz which can apply axial loads in any wave form up to 2 Hz and an axial load of 10 kN with a cell pressure of 3 MPa. The apparatus is shown in Figure 20.

To prepare a sample the soil bin soil was wetted to about 8 – 10 % moisture content and afterwards 825 g of soil filled in three layers into a 70 mm diameter and 140 mm high cylinder where each layer was precompacted to 1.4 g/cm^3 representing the density of the soil in the soil bin. A rubber sleeve was put into an 80 mm diameter tube and the rubber was folded over at one end to put this rubber membrane over the sample later, thereby protecting it from the water in the cell. Then a small amount of talcum powder was sprinkled in the rubber sleeve which allowed the soil sample to slide into it frictionless. Now the sam-

ple was taken out of the preparation pipe and slid into the rubber. A Perspex plate was put on top and bottom of the sample into the rubber sleeve. The overlong rubber was located on the top Perspex with two O – rings. Then the sample was carefully put onto the plunger in the triaxial cell and the rubber membrane at the bottom slid over the plunger and was located with o-rings on the plunger. Then the cell itself was placed over the sample and bolted onto the base while ensuring that the sealing was in place to keep the water inside when pressurizing the cell. The air outlet on top of the cell is opened and water is let into the cell while the air comes out at the top outlet. Before the cell is totally filled with water, the water level in the cell volume controller is checked and if necessary refilled by letting it suck water out of the cell. In this process the outlet valve needs to be open to allow air replacing the water which was sucked out.

Figure 20: Complete triaxial cell apparatus (top left), the cell itself (top right), and the load cell on the perspex on the sample (bottom)

The remaining air is let out of the cell and then the sample is docked to the force transducer on top by moving the plunger up electronically and screwing the force transducer down onto the top Perspex by hand for the last 10 – 20 mm to control that the force transducer just touches the Perspex not applying any load. Once the sample is docked, the cell filled

with water and the air outlet is closed again, the test procedure was carried out with a PC controlling the triaxial test apparatus. For this investigation axial load, axial displacement, cell volume and radial pressure were needed to be measured. These are automatically measured by the software during testing. As the samples are not saturated the compressibility of air was ignored because in comparison to soil it is very large. For the entire investigation changes in matrix suction were not accounted for, because when a machine traffics the field or the soil in the soil bin is compacted the same change in matrix suction will take place at the given moisture content.

2.3.2 Plate Sinkage Procedure

The plate sinkage tests were undertaken in the triaxial cell test apparatus with a 140 mm diameter cooking pot filled with soil which had taken the handle off and thus fitted into the 160 mm diameter cell of the triaxial apparatus. A 72 mm diameter and 5 mm deep metal ring was glued to the bottom of the pot locating it centrally on the plunger of the triaxial cell.

Rectangular contact patches simulating the tested tyres and the Claas Terra Trac were cut out of wood simulating the width and length of the contact area on a scale of 1:20 which resulted in a contact area and force scale of 1:400. This small scaling might not reproduce the same sinkages, but the major aim was to investigate them relative to each other.

In order to be able to place the wooden plates in the centre of the pot filled with soil, 2 diagonal lines were constructed intersecting exactly in the center of the pot. Where these two lines were resting on the wall of the pot four little slots were sawed into the wall giving the location for the strings in subsequent preparations. The strings had weights on either side to pull them tight when locating the wooden plate below. As these two strings crossed each other exactly in the centre of the pot the wooden plate with lines connecting diagonally opposite corners and crossing each other in the centre of the plate was put below the strings and the two crosses lined up directly below each other making sure that the plate is placed in the centre of the cooking pot which is necessary to apply the load centrally onto the plate in the triaxial cell.

The cooking pot was filled with soil in the following manner:
2320 g of soil with 9 % moisture content were uniformly crumbled with no soil aggregates of more than 5 mm diameter remaining. Then 1160 g were weighed into the cooking pot and afterwards compressed by 15 mm with a 120 mm diameter plate. Afterwards the remaining 1160 g of soil were weighed into the pot and the sample was compacted by 15 mm again which left the 120 mm high pot filled to 100 mm. With a volume of 1.615 l (140 mm diameter filled to 105 mm height) and a dry weight of the soil of 2119 g the resulting DBD was 1.312 g/cm^3.

Then the plate was placed in the centre of the pot as previously described and the pot was put into the triaxial cell. The sample was docked and the chosen load application carried out. Force, time and sinkage measurements were automatically taken by the triaxial apparatus. The force was usually applied to replicate a pressure measurement of the soil bin from Ansorge (2005, b) as shown in Figure 21 (right) and only for the comparison study of average to peak pressure (7.4) applied as shown in Figure 21 (left). The average pressure was the same for both curves. The scales are relative. The Y-axis symbolizes the proportion of the total load applied at any given time within the cycle whereby the relative time scale is represented by the X-axis. For 0.5 Hz the cycle time is 2 s, thus 1000 corresponds to 2 s. After the experiment the pot was taken out and the soil removed, crumbled and the entire procedure repeated again.

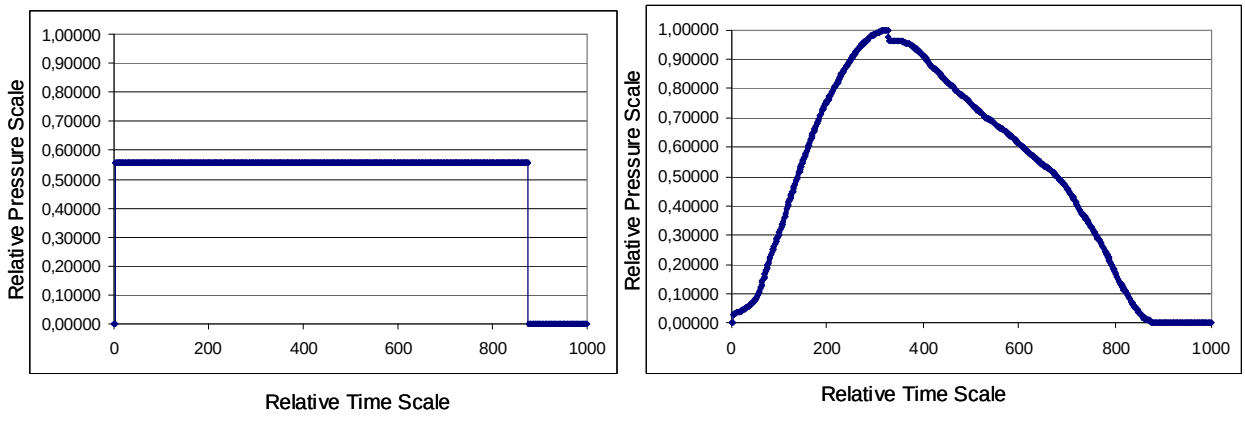

Figure 21: Left hand side: average pressure; right hand side: peak pressure replicating true tyre pass data from the soil bin. Both curves are on relative scales

2.4 Statistical Analysis

For the statistical analysis a statistical analysis software was used (SAS, 2003) assuming a probability level of 0.05. This means that the probability for obtaining the tested result from a random population was less than 5%. Normal distribution of the data was verified before the statistical analysis was conducted. All parameters were analyzed using generalized linear models to determine whether there were significant differences between control and run, between single tyres and tracks, and interaction over depth where parameters had been taken. To account for variances within the process of taking measurements covariance parameters were identified where appropriate on level of measurements and their replications. As measurements were taken in the same soil bin several times per run statistically they have to be treated as repeated unpaired measurements (Piepho et al., 2004). Normal probabilities were used for multiple comparisons as well because the standard errors of the different treatments were close together and differences are implicated by analyzing the data. This method is suggested by Nelder (1985).

3 LABORATORY STUDIES INTO UNDERCARRIAGE SYSTEMS

This chapter containing the results of the laboratory study begins with the introductory experiments concerning repeatability and traveling speed followed by the evaluation of the effects of implement tyres and whole combine harvester undercarriage systems on soil physical parameters. Finally track parameters are more deeply investigated in terms of the influence of belt tension from a friction driven track systems and different rubber track systems on soil physical parameters. Details on the laboratory set up are given in Section 2.1.1. A description of the methods can be found in Section 2.2.1.1 for soil displacement, in Section 2.2.2 for penetrometer resistance, in Section 2.2.4 for rut parameters and in Section 2.2.5 for pressure profiles which were only measured in the track studies.

3.1 Introductory Study into Soil Laboratory Settings

The repeatability of results was confirmed and the influence of speed was evaluated ensuring the appropriateness of the laboratory settings.

3.1.1 Repeatability of Results

Due to the time consuming preparation and data collection procedure, each treatment was usually only carried out once and repeated measurements taken which was taken into account in the statistical analysis. To ensure repeatability of the results in the soil bin, one treatment was carried out twice. As Figure 22 shows, results were repeatable if the soil bin was prepared to the same initial conditions and the same treatment was applied for a 600 mm section width tyre laden to 10.5 t and inflated to 2.2 bar (680/10.5/2.2).

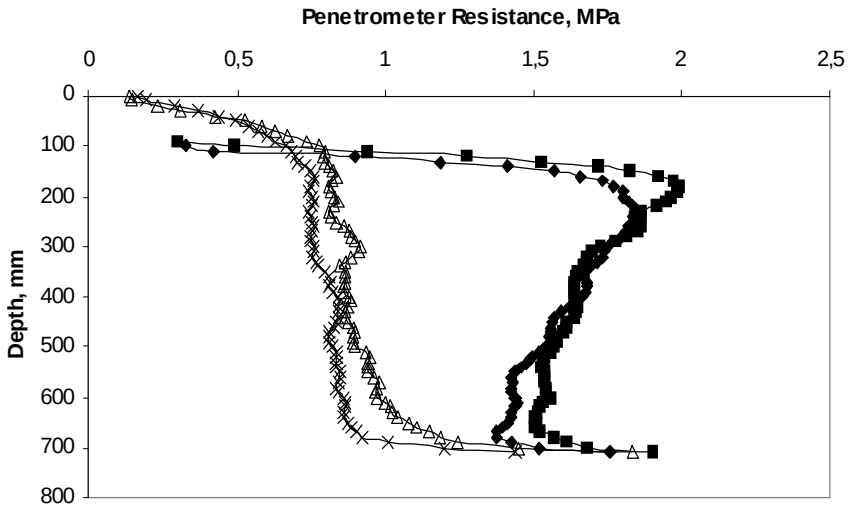

Figure 22: Repeated treatments with near identical initials and results: ♦ 680/10.5/2.2 Test 1; ■ 680/10.5/2.2 Test 1; Δ Initial Test 1; and × Initial Test 2

3.1.2 Evaluation of Travel Speed

Aboaba (1969) pointed out the influence of speed of travel in relation to the sinkage of a roller pulled over a loose soil surface. From this work arose the question as to whether the speed of 0.85 m/s used for the investigations by Ansorge (2005, a) causes a much higher soil compaction than field work carried out at 1.5 - 2 m/s. For this investigation three speeds were chosen, 0.28 m/s as the slow variant, 0.85 m/s as normal speed, and 1.52 m/s as high speed. The tyre used was a 900/65 R32 Continental laden to 5 t and inflated to 0.5 bar.

3.1.2.1 Penetrometer Resistance

The penetrometer resistances for the three speeds for the 900/5/0.5 tyre are shown in Figure 23. An increase in speed decreased penetrometer resistance. Statistically significantly different were only the run at 0.28 m/s compared to the one at 0.85 m/s. The deepest reading of the run at 1.52 m/s was an outlier caused by the penetrometer hitting the concrete floor of the soil bin. There was no statistically significant difference in penetrometer resistance between the runs at 0.85 m/s and the one at 1.52 m/s.

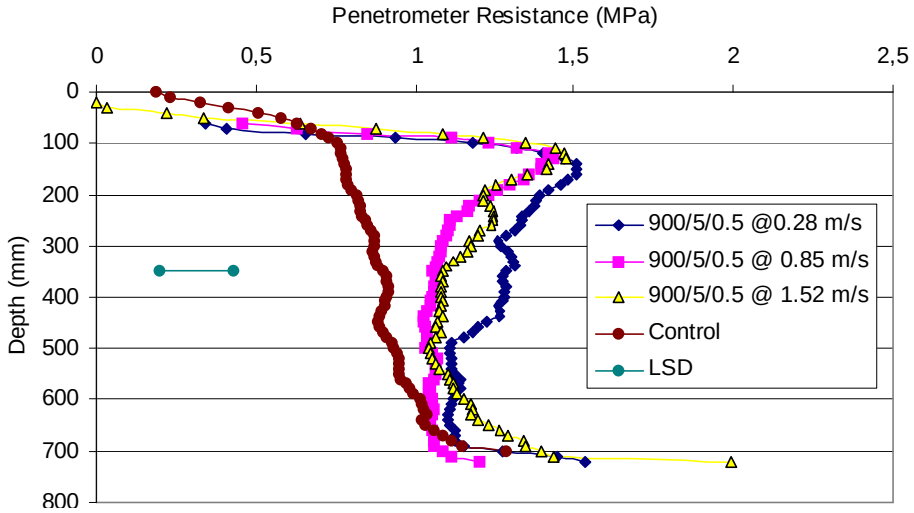

Figure 23: Penetrometer resistance at three speeds and a multi pass of the 900/5/0.5

3.1.2.2 Soil Displacement

Soil displacement caused by the three different speeds is shown in Figure 24 without the surface value and the last value at 600 mm depth to remove the systematic outliers originating from the lugs at the surface and the bottom of the bin. With increasing speed soil displacement decreased. Statistically all combinations were significantly different from each other with p-values between 0.014 and < 0.0001 whereby the LSD is 3.6 mm. In the speed range from 0.29 m/s up to 0.85 m/s the soil seemed more prone to changing its behavior than at speeds higher than 0.85 m/s. In Figure 25 the influence of speed on the average increases in DBD is evaluated; the average increase in DBD is gained as described in 2.2.1.1 utilizing the slope of the soil displacement graphs of Figure 24.

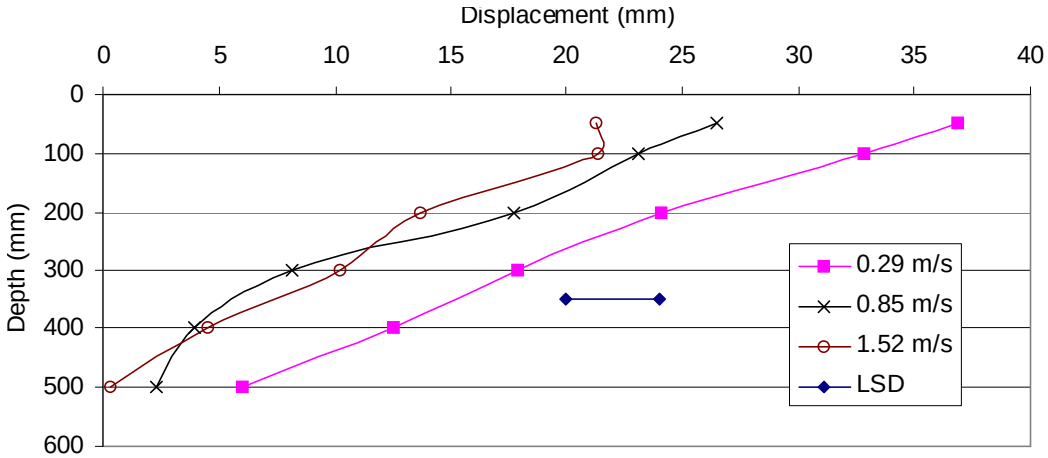

Figure 24: Soil displacement vs. depth for different speeds for the 900/5/0.5

Figure 25 shows a linear decrease in DBD increase with increasing speed. The general offset in displacement over the entire depth visible in Figure 24 was not represented adequately with the slope for the run at 0.29 m/s. Hence the increase in DBD seemed to decrease linearly and not curvilinear with speed as the overall shape of the curve from Aboaba (1969) implied. The increase in DBD at 0.85 m/s was approximately 20 % greater than at 1.52 m/s. However, this difference is not accompanied by an offset as for 0.29 m/s. Therefore the speed of 0.85 m/s used by Ansorge (2005, a) seems suitable as compromise between real field travel speeds and operational safety.

The greater increase in density originating from the experiment at 0.29 m/s emphasizes the possible damage caused to headlands due to slower machine speeds when turning.

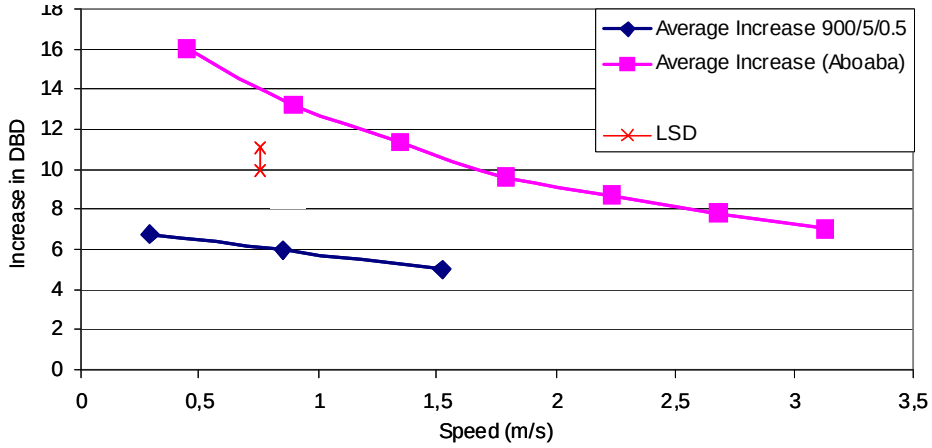

Figure 25: Average increase in DBD vs. speed for measured data and multi pass experiment and literature

3.1.2.3 Rut Parameters

Rut parameters shown in Table 3 support the findings in soil displacement (Section 3.1.2.2). Cross sectional area, rut width, and maximum rut depth all decreased with increasing speed.

Table 3: Rut parameters for different forward speeds, statistically identical values are followed by the same letter (a, b or c)

Treatment	Area (m^2)	Width (m)	Max. Depth (m)
900/5/0.5 at 0.28 m/s	0.0276 a	0.81 a	0.07 a
900/5/0.5 at 0.85 m/s	0.0179 b	0.68 b	0.055 b
900/5/0.5 at 1.52 m/s	0.0168 b	0.69 b	0.053 b
LSD	0.0037	0.037	0.007

3.1.2.4 Discussion and Conclusion

The data showed the significant influence of speed on soil displacement. Aboaba (1969) did not give an explanation why this was the case. Assuming soil could physically be described as a damper-spring system, this behavior would be due to the time depending elongation of the damper. The longer a force is applied, the more the damper contracts, i.e. soil compacts. The speed of 0.85 m/s used in the soil bin created marginally more soil displacement than common harvest speed at about 1.5 m/s. If the speed was significantly reduced to 0.29 m/s, the impact would be bigger. Thus 0.85 m/s was considered a reasonable compromise between operational safety and the replication of real speeds. The result of a speed at 0.29 m/s compared to the other two visualizes the possible damage occuring in headlands originating from slower speed.

3.1.3 Gravimetrically Measured Dry Bulk Density

Dry bulk density was measured for all experiments gravimetrically as described in Section 2.2.3.1. However, due to the large variations reported by Ansorge and Godwin (2007) details on gravimetrically measured dry bulk density are only given in the Appendix 2. The sensitivity of the soil displacement measurement was significantly greater and therefore the focus will be on that measure.

3.2 Evaluation of Implement Tyres and Whole Combine Harvesters

Following Ansorge (2005, a) it was important to investigate the effect of the additional passage of the rear tyre on the soil when considering whole machines. Particularly interesting was the question whether the advantage gained by using tracks at a total load of 12 t in comparison to tyres at a total load of 10.5 t (the smaller load accounts for the lighter undercarriage system) could be maintained after the passage of a rear tyre at a load of 4.5 t. To conduct this study first rear tyres are evaluated on their own. Details of the rear tyre specifications including the load of 4.5 t and the corresponding inflation pressure are shown in Table 4. The abbreviation used for the single rear tyres is listed, too.

Table 4: Rear tyre specifications

Tyre	Load (t)	Inflation Pressure (bar)	Abbreviation
500/70 R24	4.5	2.3	500-70/4.5/2.3
500/85 R24	4.5	1.4	500-85/4.5/1.4
600/55 – 26.5	4.5	1.4	600/4.5/1.4
710/45 – 26.5	4.5	1.0	700/4.5/1.0

Afterwards whole common combine harvester undercarriage system comparisons will be conducted. Additional machine configurations will be investigated as detailed in Figure 1. Table 5 gives a listing of all the simulated machine configurations with tyre, track, load, and inflation pressure combinations and assigns an abbreviation to each.

The 680-700 was assumed to act as a dual tyre configuration on the front axle. Due to the width restriction of the soil bin, no true dual configuration with two 680 tyres side by side could be realized. Hence, the load was halved for one tyre and for simplicity no interaction between the two tyres was assumed. This assumption is justified due to the punching type of soil failure already observed by Ansorge (2005, a) and explained in Section 7.5.

Table 5: Whole machine configurations used and abbreviation (Red = Modern Harvester with total load of 30 t and wide front tyre; Green = Modern Harvester with total load of 33 t and Terra Trac on front axle; Blue = Modern Harvester with total load of 30 t and narrow tyre option; Brown = Alternative Wheel Configurations with 30 t total machine load; Grey = Older Machine with 11 t on medium tyre size)

Front Axle			Rear Axle			
Tyre	Load (t)	Inflation Pressure (bar)	Tyre	Load (t)	Inflation Pressure (bar)	Abbreviation
900/60 R32	**10.5**	**1.9**	**710/45-26.5**	**4.5**	**1.0**	**900-700**
900/60 R32	**10.5**	**1.9**	**500/70R24**	**4.5**	**2.3**	**900-500/70**
Three Idler Track	**12**	**-**	**710/45-26.5**	**4.5**	**1.0**	**Track-700**
Three Idler Track	**12**	**-**	**500/70R24**	**4.5**	**2.3**	**Track-500/70**
680/85 R32	**10.5**	**2.2**	**500/85R24**	**4.5**	**1.4**	**680-500/85**
680/85 R32	**7.5**	**1.5**	**680/85R32**	**7.5**	**1.5**	**680-680**
680/85 R32	**5.5**	**0.9**	**710/45-26.5**	**4.5**	**1.0**	**680-700**
900/60 R32	**5**	**0.5**	**3 Passes Same Tyre**			**900X3**
23.1-26	**4**	**1.2**	**11.5/80-15.3**	**1.5**	**2**	**23-11**
680/85 R32	**7**	**1.6**	**(2) 500/70R24 (3) 500/85R24**	**3.5 3.75**	**1.3 1.1**	**680Alt**

3.2.1 Penetrometer Resistance

Penetrometer resistance for the rear tyres is shown in Figure 26 and was close for all rear tyres with no statistically significant differences. The higher readings at the greatest depths were due to the concrete floor of the bin.

The increase in penetrometer resistance caused by additional pass with the rear tyre can be seen in Figure 27 for the track at 12 t and the 900/10.5/1.9. For both the additional pass caused a significant increase in penetrometer resistance, uniformly for the track and with a large increase in the top 400 mm only for the 900 mm section width tyre.

Penetrometer resistance for the different undercarriage systems is shown in Figure 28 and differentiates into two distinct groups. Figure 29 contains the group with a high penetrometer resistance at the surface and a decrease with depth. This penetrometer resistance resembles the track like behavior and consequently Figure 29 contains the track-type undercarriage systems (23-11, the 680-700) including multiple passes (900X3 and 680 Alt) as their

penetrometer resistance has a similar characteristic as the tracks. When taking the 680-700 into consideration, the additional pass of the 680 on the outer side creating a wider rut must be kept in mind as this machine was run on 680 dual tyres on the front axle.

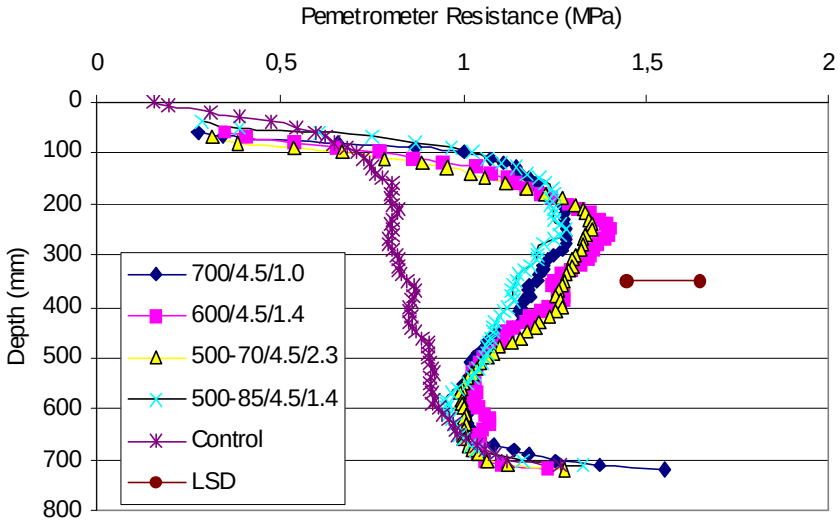

Figure 26: Penetrometer resistance for the rear tyres

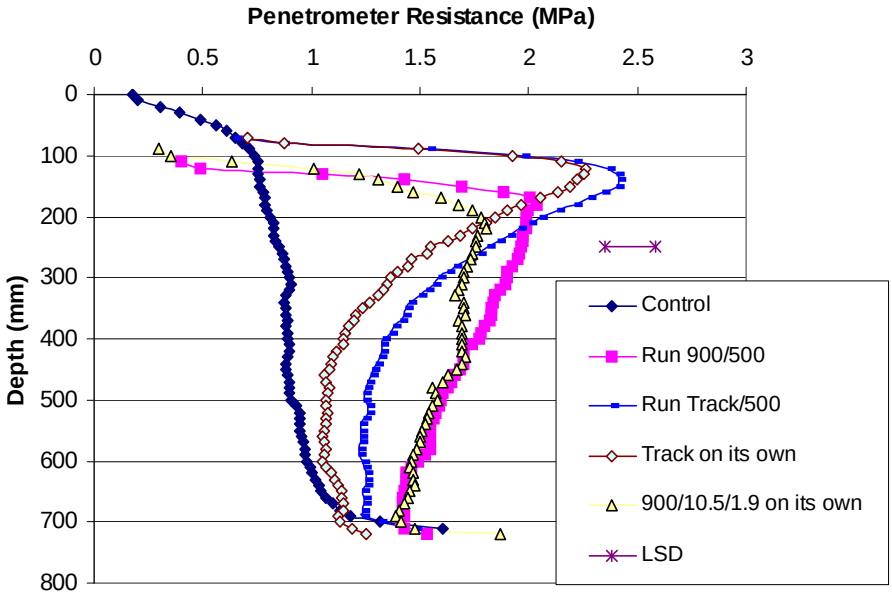

Figure 27: Penetrometer resistance with and without influence of rear tyre

The second group had a more constant decrease rate with depth in penetrometer resistance and is shown in Figure 30 and resembles the typical penetrometer resistance caused by tyre-type undercarriage systems. Hereby the values were lower at the surface compared to the group with the peak at or close to the surface, yet higher below 250 – 300 mm depth.

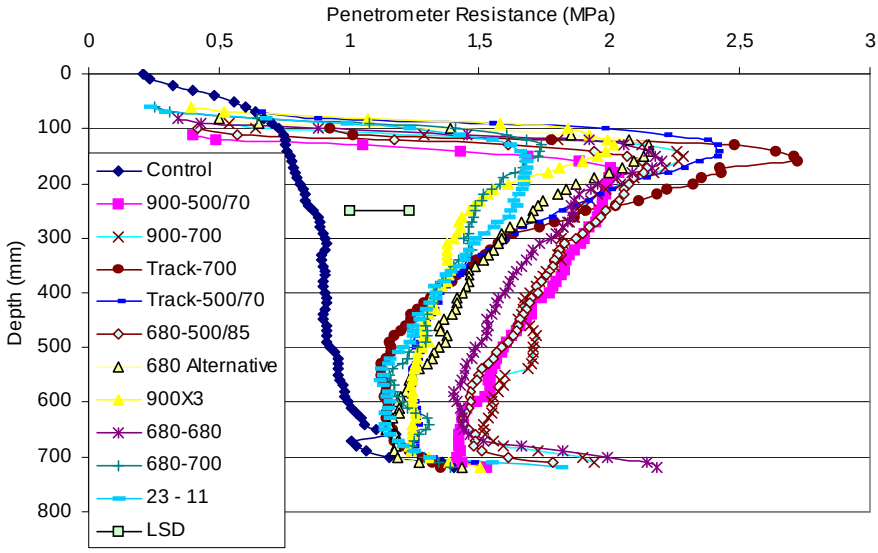

Figure 28: Penetrometer resistance for different undercarriage systems

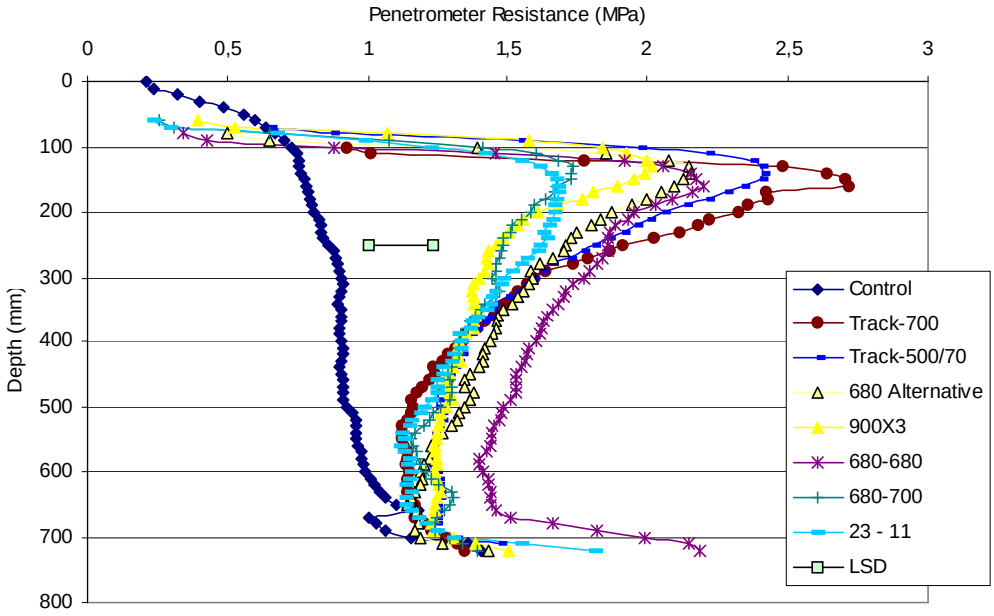

Figure 29: Group of track type penetrometer resistance including 680-680

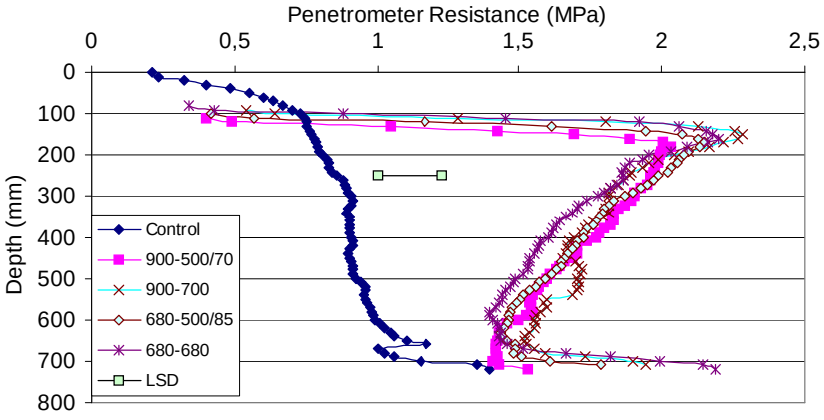

Figure 30: Group of wheel type penetrometer resistance

The 680-680 was in the range of wheeled machines and is included in both diagrams as for the tracked types with the peak at the surface it creates the highest penetrometer resistance below 300 mm and for the wheeled type the least.

Statistically these two groups could be partially defined whereby the 680-680 was not significantly different from either. Full statistical details are given in Table 6 whereby the average penetrometer resistance is given for each treatment. The statistical analysis considered the penetrometer resistance with depth profile, too, such that this average comparison takes account of the individual change in penetrometer resistance with depth.

Table 6: Average penetrometer resistance for whole machine treatments

(similar penetrometer resistance followed by the same letter)

Treatment	Penetrometer Resistance (MPa)	Group
Control	0.87	
23-11	1.329	A
680-700	1.349	A
900X3	1.352	A
Track-700	1.386	AB
Track-500/70	1.437	AC
680Alt	1.510	AD
680-680	1.612	DCB
900-500/70	1.631	DC
680-500/85	1.676	D
900-700	1.698	D
LSD	0.23	

3.2.2 Soil Displacement

As there was no difference among the penetrometer resistances for the different implement tyres the evaluation of soil displacement after the pass of the rear tyres was particularly interesting. Figure 31 shows the soil displacement depending on inflation pressure and size of the contact area. Larger contact areas and lower inflation pressure, respectively, reduced soil displacement. The 500-70/4.5/2.3 caused most soil displacement due to its high inflation pressure and small contact patch compared to all other rear tyres (p-values ranging from <0.0001 to 0.032). Statistically all other combinations were similar. The similarity of the 500-85/4.5/1.4 and 600/4.5/1.4, with contact areas of 0.41 and 0.39 m^2, respectively,

compares to the case of the 680/10.5/2.2 and the 800/10.5/2.5 from Ansorge (2005, a). Again, the higher section width tyre with similar inflation pressure as the wider tyre created similar soil displacement. Therefore the larger section height accounts for the smaller section width. The potential difference in carcass stiffness of cross ply (600/4.5/1.4) vs. radial (500-85/4.5/1.4) tyre did not have an influence. The 700/4.5/1.0 tyre was not able to utilize its large section width and low inflation pressure to create a significantly smaller soil displacement although having the largest contact area of 0.47 m^2.

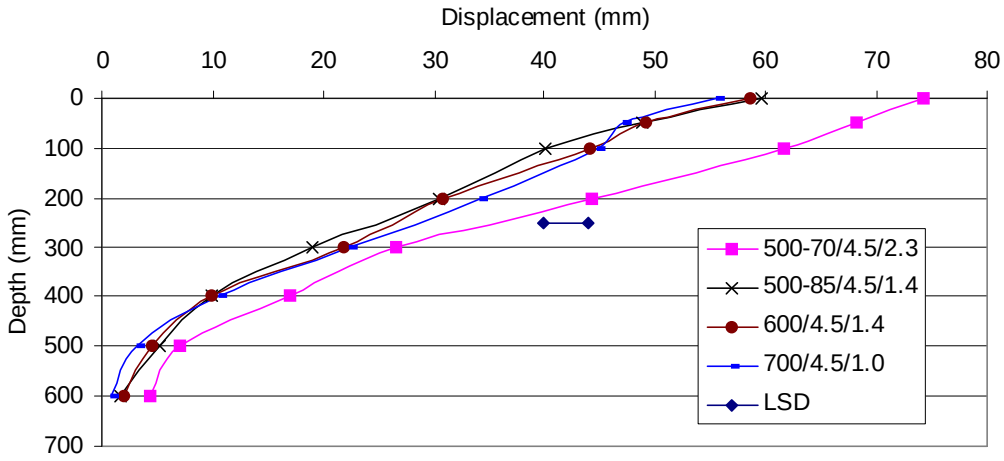

Figure 31: Soil displacement vs. depth for the rear tyres

The average increase in soil density caused by the implement tyres was similar to the 800/10.5/1.25 tyre, both increasing soil density by 12%; half the load on a smaller tyre increased density by a similar amount to the total load at half the recommended inflation pressure.

In order to investigate the additional soil displacement caused by the rear tyres, Figure 32 contains the soil displacement caused by the front axle on its own and after the additional pass of the rear tyre. After the pass of a track, the extra soil displacement from the rear tyre can be neglected. The same held true for the 900/10.5/1.9 followed by the 700/4.5/1.0. However, if the 900/10.5/1.9 was followed by the 500-70/4.5/2.3 soil displacement increased considerably. Thus, the rear tyre size was crucial in relation to soil displacement after the pass of a soil protecting tyre, yet it was not crucial after the pass of a track as long as the load could be carried and distributed by the strong layer at the surface created by the track. The strong layer phenomenon originating from the track will be discussed in 7.1.

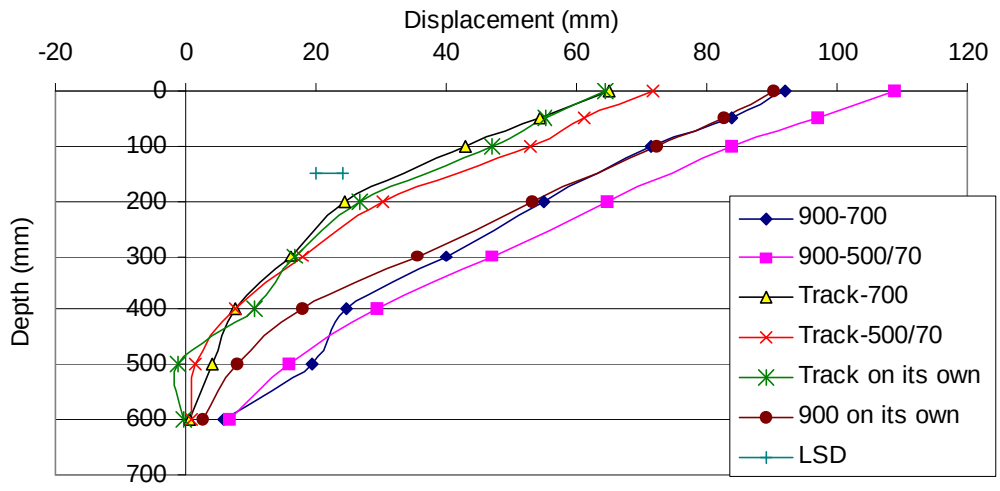

Figure 32: Soil displacement caused by the front implement and total soil displacement caused by the rear implement

For entire undercarriage systems the two distinct groups obvious in penetrometer resistance were obvious in the soil displacement data in Figure 33, too. Here the wheel type undercarriage systems showed a significantly larger soil displacement i.e. increase in soil density than the track type undercarriage systems. Statistically there could be more differences proven. The two tracks were statistically the same and so is the 680-680 to the 900-700. The 23-11 is equal to the 680-700. All other combinations are significantly different from each other.

The two groups are split up in Figure 34 for the wheel type soil displacement and in Figure 35 for the track type soil displacement.

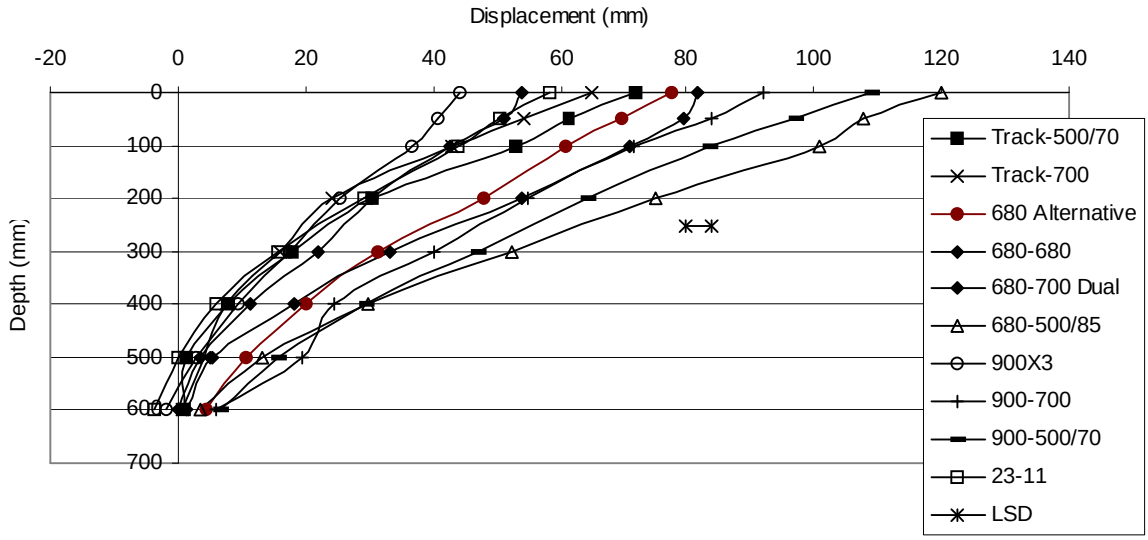

Figure 33: Soil displacement for different undercarriage systems

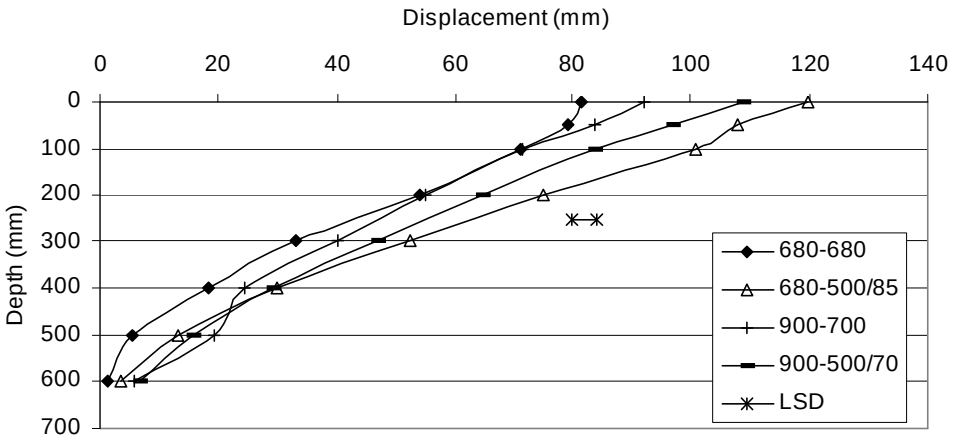

Figure 34: Group of wheel type soil displacement

The similarity of the 680-680 to the 900-700 in Figure 34 was surprising as this tyre carried less load and operated at a lower inflation pressure than the 900-700. However, the result was caused by the fact that the 680-680 combination passes the soil twice; particularly with the same load in the 2nd pass as in the 1st pass and thereby further compacting the soil. In comparison the subsequent pass of the 700 in the 900-700 combination caused only mariginally more soil displacement as shown in Figure 32.

Most of the track type soil displacement graphs were close together. Only the 680Alt showed a larger offset from the entire group of soil displacement graphs in Figure 35.

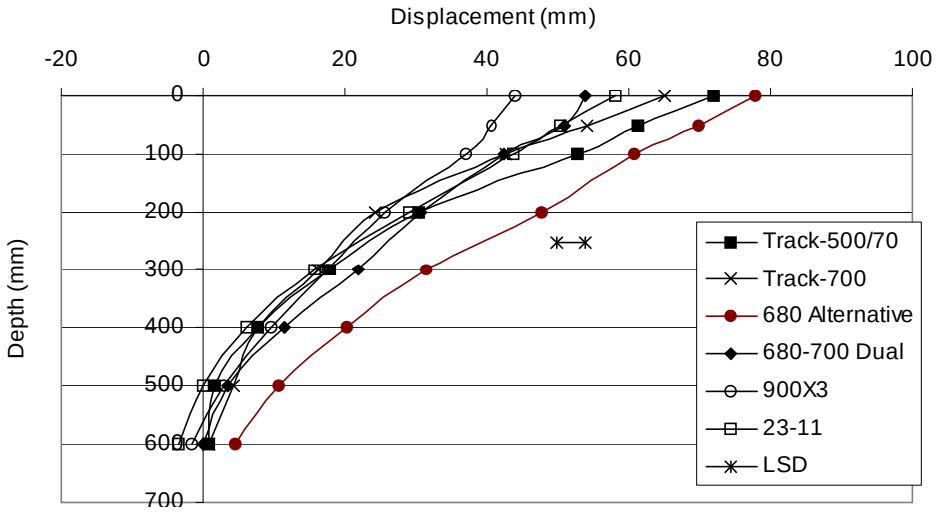

Figure 35: Group of track type soil displacement

Particularly interesting was that all of the graphs approach zero soil displacement from a depth of 500 mm downwards. Only the 680Alt maintained a residual soil displacement alike wheel type undercarriage systems in Figure 34. Hence, all other track type undercar-

riage configurations were able to keep the soil displacement in a range where it could be alleviated. In most field situations no soil displacement at this depth would be expected due to the stronger subsoil. All the above is summarized in Table 7.

Table 7: Soil displacement in soil bin laboratory caused by individual machine configurations

Treatment	Average Position	Statistical Grouping
23-11	598.86	A
Track– 500/70	617.01	B
Track-700	613.97	B
680–500/85	649.95	
680–Alt	626.70	
900X3	608.57	
900 – 500-70	643.05	
900 – 700	636.70	C
680 – 680 (four equal size tyres)	634.76	C
680 – 700 (duals on front axle)	599.62	A
LSD	4.0	

The fact that the 23-11 representing a load total machine weight of 11 t caused similar soil displacement as the entire range of other machine configurations carrying loads between 30 – 33 t emphasized the possibilities of good undercarriage design to maintain soil displacement at a level similar to lighter machines which have been used in agriculture for the last 30 years. This allows the assumption that no further damage would be expected if soil displacement was maintained within that range. Hereby, the smaller area traveled due to increased working width is not taken into consideration. From the result of the 900X3, 23-11, and 680-700 compared to the 680-680 and 680Alt it seems beneficial if wheel loads can be maintained at approximately 5 t. If this is achieved, soil displacement is similar to that of the tracked undercarriage systems.

3.2.3 Rut Parameters

Rut parameters shown in Table 8 correspond reasonably well with the results from Section 3.2.2. An increasing tyre width caused an increased rut width. The depths of the rut mirror the results shown in Figure 31. The rut area was the product of rut width and rut depth; therefore the 500-85/4.5/1.4 caused the smallest rut area although it did not cause the least

soil displacement. Yet its relatively narrow width and shallow rut depth resulted in the smallest rut area. Hence, rut depth corresponds more closely with soil compaction.

Table 8: Rut parameters for different rear tyres. Treatments followed by different letters are statistically significantly different

Treatment	Area (m^2)	Width (m)	Depth (m)
500-70/4.5/2.3	0.0333 a	0.56 a	0.093 a
500-85/4.5/1.4	0.0234 b	0.52 b	0.075 b
600/4.5/1.4	0.0298 a	0.61 c	0.077 b
700/4.5/1.0	0.0296 a	0.68 d	0.072 b
LSD	0.0037	0.037	0.007

The rut parameters for whole undercarriage systems in Table 9 showed similar characteristic as the soil displacement measurement (Section 3.2.2). The cross sectional area split up into two groups and so did the maximum rut depth, too. The width was determined from the initial width of the implement.

Table 9: Rut parameters for different undercarriage systems. Treatments followed by different letters are statistically significantly different

Treatment	Area (m^2)	Width (m)	Max Depth (m)
900/10.5/1.9 followed by 500-70/4.5/2.3	0.0668 a	0.89 a	0.112 a
900/10.5/1.9 followed by 700/4.5/1.0	0.0627 b	0.9 a	0.1 b
T3 followed by 500-70/4.5/2.3	0.0401 c	0.67 b	0.09 c
T3 followed by 700/4.5/1.0	0.0362 d	0.71 c	0.075 d
680/10.5/2.2 followed by 500-85/4.5/1.4	0.0691 a	0.77 d	0.13 e
680/7/1.6 followed by 500-70/3.5/1.3 followed by 500-85/3.75/1.1	0.0386 c , d	0.65 b	0.08 d
680/7.5/1.5 followed by 680/7.5/1.5	0.0552 e	0.72 c	0.099 b
680/7.5/1.5 followed by 700/4.5/1.0	0.0312 f	0.68 b c	0.065 f
23-11	0.0321 f	0.55 e	0.073 d
LSD	0.0037	0.037	0.007

3.2.4 Discussion and Conclusions

In general the width and inflation pressure of the tyre determined the amount of soil displacement and thereby soil compaction caused by a tyre. This confirmed the results of An-

sorge (2005, a), Antille (2006), and Stranks (2006). Interesting to note was the fact that three of the four tested implement tyres achieved similar results although differing in section width and inflation pressure. An increased section height was able to account for a reduced section width.

For whole undercarriage systems the benefit of the tracks shown by Ansorge (2005, a) was maintained after the additional passage of the rear axle tyre. A typical wheeled combine increased the soil density by 19 % compared to a tracked machine with an increase of 14 %. Thereby the effect of the rear axle tyre size had a less effect on soil conditions following a front axle track unit than a tyre. Soil displacement increased by 6 mm compared to 12 mm for the tyre over the same depth range and extended to a shallower depth (300 mm) after the track. This was due to the bearing capacity of the stronger layer in the top 150 mm observed from the penetrometer studies.

A hypothetical three axle tyre configuration with 5 t load per tyre caused similar vertical soil displacement compared to a track followed by a rear tyre and to a dual configuration on the front axle. An undercarriage unit with a track unit on the front axle and a gross weight of 33 t resulted in a similar vertical soil displacement to that of an 11 t combine harvester on commercially fitted normal front and rear tyre sizes. A hypothetical 3 axle machine with unequal tyre sizes and load caused intermediate soil compaction compared to that of a tracked and a wheeled machine. An equal weight distribution on two 680-tyres caused nearly as much soil compaction as a traditional wheeled combine configuration on 900 – 700. From this the conclusion can be drawn that a maximum wheel load of 5 t on appropriately inflated tyres has the same impact on soil density changes as the rubber track. Therefore fitting a track on a combine has a similar impact as reducing axle loads to 10 t while using large section width/height tyres and maintaining whole machine weight. Important to note is the residual soil displacement between 500 – 600 mm depth for wheel type undercarriage systems. Soil displacement for track type undercarriage systems has decreased to zero at about 500 – 600 mm depth, but the 680Alt, 680-680, and all common combine harvester tyre combinations maintain a residual soil displacement highlightening their possible impact on the subsoil.

The overall configuration of the undercarriage system of the combine harvester was more important than individual weight on a single axle.

3.3 Track Studies

The benefits found for TerraTracs by Ansorge (2005, a) raised the question how different belt tensions influence soil physical properties, i.e. what benefit could be gained from higher tension and what damage might be caused by less tension. Additionally of interest became how different track types compare to the TerraTrac. Thus, in a first instance the rubber belt tension was evaluated and in the second part, different track type units were evaluated. Additionally to penetrometer resistance, soil displacement, and rut characteristics, longitudinal pressure profiles described in Section 2.2.5 were measured for these treatments.

3.3.1 Evaluation of the Effect of Rubber Belt Tension

This section aims at evaluating the influence of belt tension in the Claas TerraTrac system on soil physical properties. Therefore the three idler Claas Terra Trac unit was run at a higher belt tension of 200 bar (20 t belt tension) and at a lower belt tension of 50 bar (5 t belt tension) whereby results were compared to the data gained at the common pressure of 160 bar (16 t belt tension) from Ansorge (2005, a). A belt pressure of 160 bar is necessary for the TerraTrac as it is friction driven and hence relies on belt tension to develop draught.

3.3.1.1 Penetrometer Resistance

Penetrometer resistance for the TerraTrac at the three belt pressures is shown in Figure 36. There is a trend that shows that the peak penetrometer resistance reduces with increasing tension. In tendency the unit at 50 bar created the highest peak in penetrometer resistance close to the surface and its decrease in penetrometer resistance with depth was smaller than for higher pressures. At 200 bar the peak at the surface was smallest and therefore the penetrometer resistance at depth marginally smaller. However, taking the entire curves into consideration, no significant differences were found.

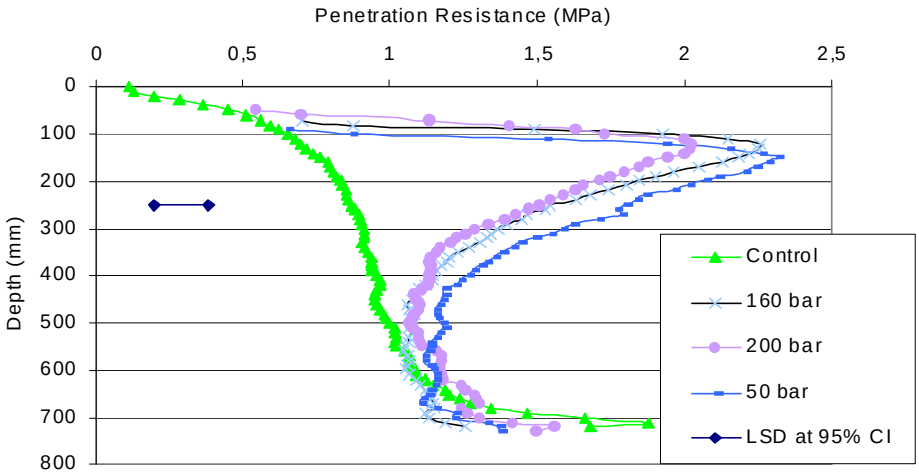

Figure 36: Penetrometer resistance vs. depth for the Claas unit at three belt pressures

3.3.1.2 Soil Displacement

Soil displacement for the normal belt tension at 160 bar in Figure 37 showed a larger soil displacement than both the 50 and 200 bar experiment and was statistically significantly different from the unit at 200 bar (p=0.0059). The soil displacement data for the belt tension at 160 bar originates from Ansorge (2005, a). Hence, the difference in soil displacement is most likely due to both the variation in soil bin preparation due to possible changes on the soil processor and this particular run of the track at 12 t from Ansorge (2005, a) being an outlier showing more soil displacement, too. The penetrometer resistance given earlier in Section 3.3.1.1 for the experiment at 160 bar originates from this study and consequently was in line. The talcum powder lines for this particular experiment were used alternatively to evaluate the influence of lugs on vertical soil displacement as detailed in Section 7.2. When the unit was operated at 200 bar, it caused the least soil displacement. At 50 bar, rut depth and soil displacement were larger, but no statistical difference could be detected. Over the entire depth soil displacement for the unit at 50 bar varied slightly, however, was always bigger than the soil displacement at 200 bar.

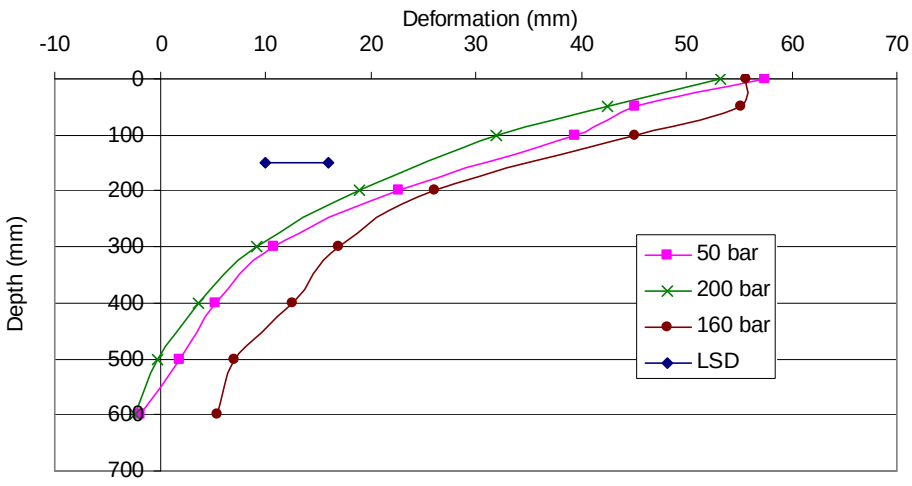

Figure 37: Soil displacement vs. depth for the Claas unit at three belt pressures

3.3.1.3 Pressure Profiles

The pressure profiles for the three belt pressures are shown in Figure 38. The pressure profiles did not vary significantly due to the different belt tensions.

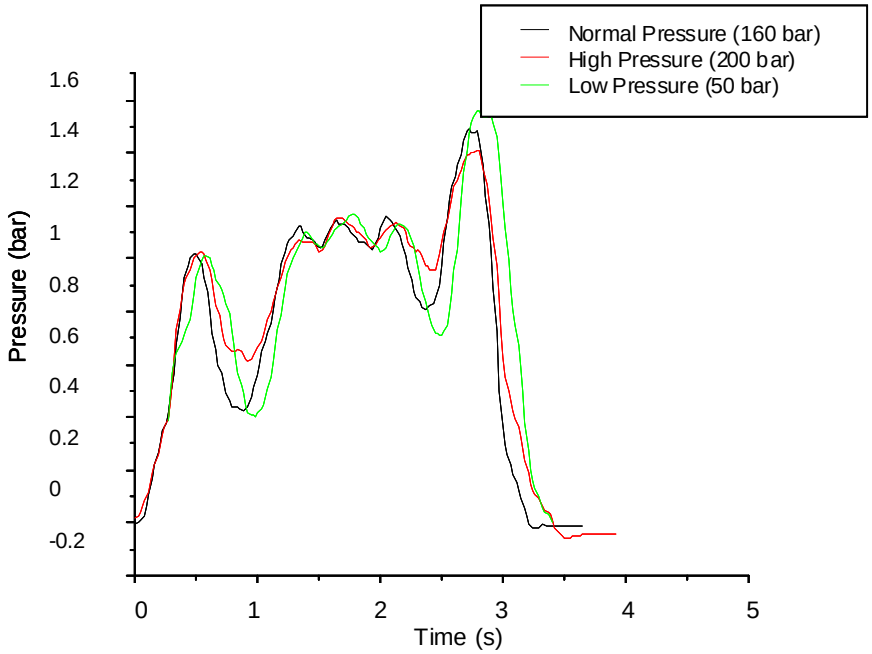

Figure 38: Pressure trace in soil below different belt pressures of Claas unit

The peak pressures below the front and the central rollers were the same, however, the pressure peak below the rear roller decreased slightly with an increase in belt tension. The minimum between both the front and the mid-rollers and the rear roller increased with an

increase in belt tension resulting in an overall smoother pressure profile. However, as Figure 39 indicates, there is no statistically significant difference between the different pressure profiles. The large minimum pressure in relation to the contact pressure is due to the two central minima having an overall relatively high pressure.

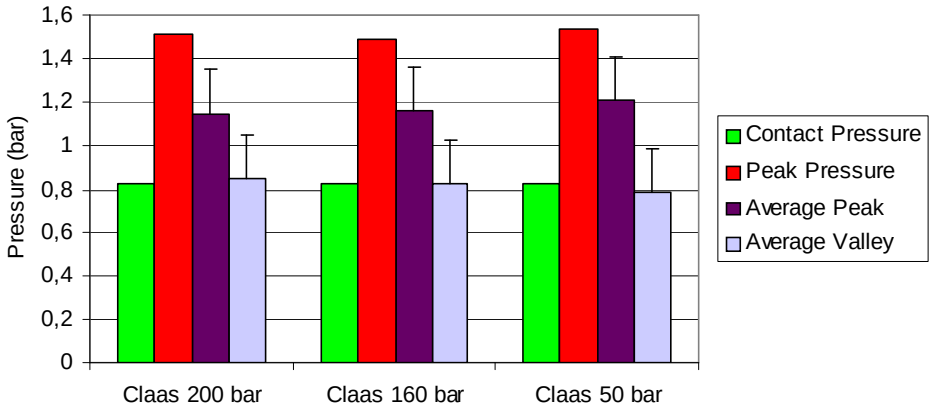

Figure 39: Pressure summary for different belt tensions

3.3.1.4 Discussion and Conclusions

The effect of belt tension on soil physical properties is limited in the range of belt tensions tested for this friction driven rubber track unit. The small effect on soil physical properties is in accordance to the similar pressure profiles measured in the soil. The small effect of belt tension on pressure profiles is due to the fact that the tension coefficient of the track (belt tension in relation to weight carried on both tracks) is 21 % at a belt pressure of 50 bar as tension is 5 t and the load is 24 t. Wong (2007) has shown that depending on roller configuration only small effects of belt tension could be identified, especially when the tension coefficients were larger than 20 %. The overlying soil above the pressure cell situated at 250 mm may smooth some of the differences possibly seen closer to the surface already, too (Berli et al. 2006).

Therefore it can be concluded that varying the belt tension of a friction driven track unit has only limited effect on soil physical properties due to the residual belt tension necessary to provide the friction for propelling. However, the tendency is that higher tensions produce less compaction.

3.3.2 Evaluation of Different Types of Rubber Tracks

The performance of the TerraTrac in comparison with tyres measured by Ansorge (2005, a) raised the question how alternative sprocket driven track units compare with respect to their influence on soil physical properties. Therefore 3 alternative track units were compared to the TerraTrac; all run at a load of 12 t. The alternative units were namely a Westtrack, a Stocks, and a prototype called SPT. The characteristics of the units are detailed in Table 10 and a photograph of each is given in Figure 40. All units had the same belt width of 750 mm except the TerraTrac with a width of 635 mm.

Table 10: Characteristics of rubber track units

Track Unit	Belt width (mm)	Centre front-rear roller length (mm)	Contact length (mm)	Number of rollers	Contact Pressure (bar)
TerraTrac	635	1825	2300	5	0,83
Westtrack	750	1600	1850	5	0,86
Stocks	750	1460	1750	4	0,92
SPT	750	1400	1750	3	0,92

Figure 40: Track units; TerraTrac, Westtrack, SPT, and Stocks (clockwise from top left)

3.3.2.1 Penetrometer Resistance

The penetrometer resistance for all track units and the control is shown in Figure 41. All units created pronounced peaks at the surface as previously found by Ansorge (2005, a) whereby the SPT unit exhibited the least decrease in penetrometer resistance with depth. Both, the Westtrack and Stocks unit were statistically significantly different from the SPT unit with p-values of 0.0136 and 0.0475, respectively. Other combinations were not significantly different.

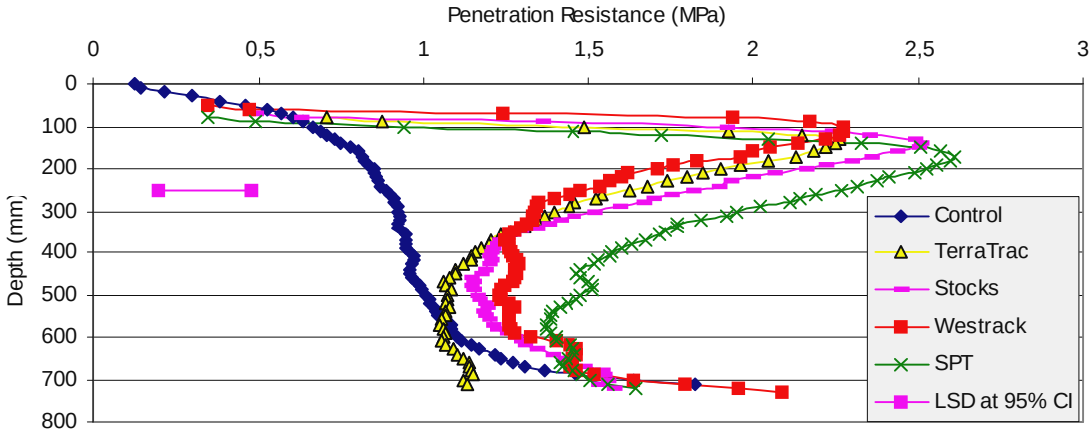

Figure 41: Penetrometer resistance vs. depth for different track units

3.3.2.2 Soil Displacement

The soil displacement diagram for the different track units is shown in Figure 42. Westtrack and Stocks created the least soil displacement followed by the TerraTrac unit at 50 bar belt pressure (the TerraTrac at normal belt pressure was excluded due to the reasons detailed in Section 3.3.1.2). SPT caused the most soil displacement. Statistically only the SPT unit was significantly different from all other units with a p-value ranging from <0.0001 to 0.0034. Reasons for the differences will be explored in section 3.3.2.5.

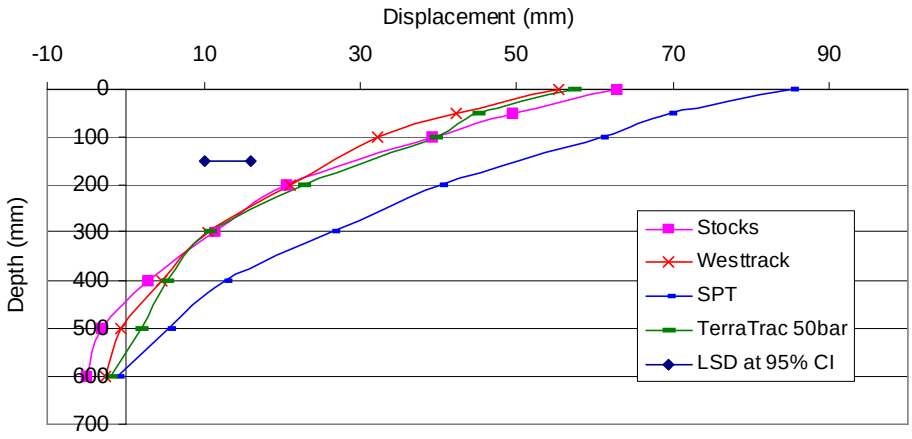

Figure 42: Soil displacement vs. depth for different track units

3.3.2.3 Longitudinal Pressure Profiles

The pressure profiles for all treatments are shown in Figure 43. Absolute pressure varied from a minimum of 0.4 bar from one unit to a maximum of 1.8 bar of an other unit. Mainly the curves were distributed at 1.2 – 1.4 bar. The difference in time of pressure application was due to the individual length of each track unit. The Stocks unit showed the most uniform pressure application. The peak in the centre of the profile of the Westtrack unit indicated that its 3 mid-rollers were sitting lower than the front and the rear roller as the pressure was decreasing below the front and the rear roller compared to the centre. The TerraTrac unit showed the typical Claas pressure profile with increasing pressure peaks from the front to the rear. On the contrary, the SPT unit had the highest peak below the centre of the unit and a strong decline in pressure to the rear roller. This was due to the load being applied off-centre towards the front of the unit aiming for an equal pressure distribution under drawbar pull. Pressure data from an 800/10.5/2.5 run was included for reference showing the highest peak, but contact time was half of that of the track units.

To statistically analyze the pressure-time histories the rectangularity was estimated. To do this each curve was divided by its maximum value resulting in a relative pressure ranging from 0 – 1. This data was averaged and the closer the average was to 1, the more rectangular, and consequently uniform, the pressure profile was. Typical values were approximately 0.55. This is shown in Figure 44 whereby the 95% - CI bars are included.

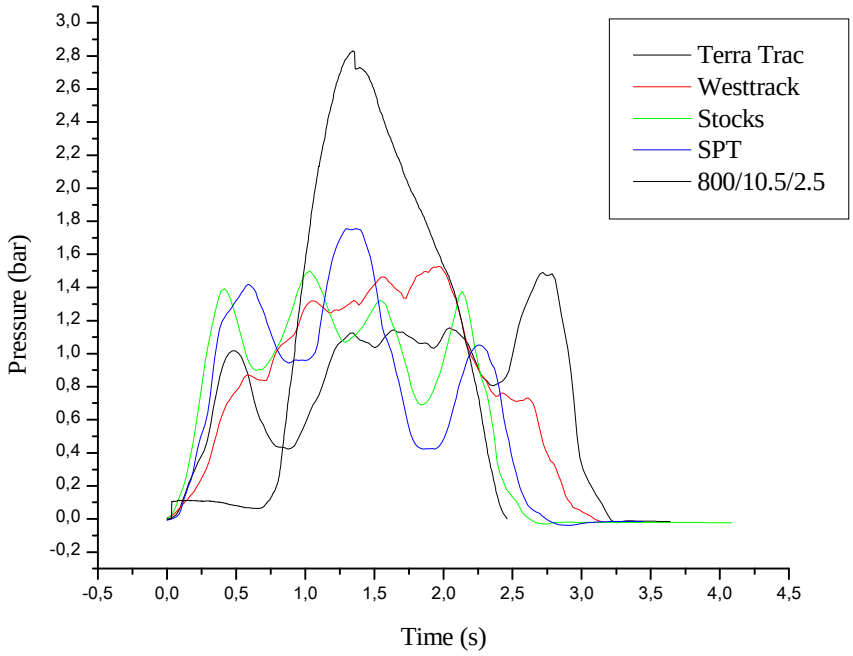

Figure 43: Pressure profiles for track units including a 800/10.5/2.5 for reference

The statistical analysis showed that the pressure application was only significantly different for the SPT unit with a rectangularity measure of 0.51 from the Stocks unit with a rectangularity measure of 0.61 (p-value 0.0067). The two remaining track units and the tyre show similar values of approximately 0.55. As the rectangularity of a tyre was within the range of tracks, it could not be used as a distinguishing characteristic. In Section 7.4 the significance of peak vs. average pressure in sinkage will be demonstrated and thus shows the importance of high rectangularity.

Figure 45 shows the average contact pressure, maximum peak pressure and the average maxima and minima for the different units. The minima are always significantly smaller than the maxima except for the Westtrack which due to the triangular pressure profile has a more uniform pressure profile. Minima of all other units are similar, too. The average minima can be bigger than the average contact pressure as this calculation does not account for time. The peak pressures are always significantly higher than the average maxima except for the Stocks supporting a uniform pressure distribution seen already.

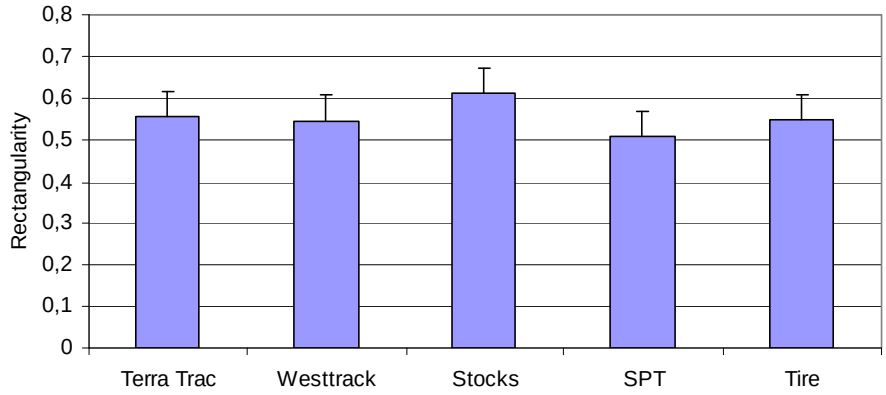

Figure 44: Rectangularity for different track units

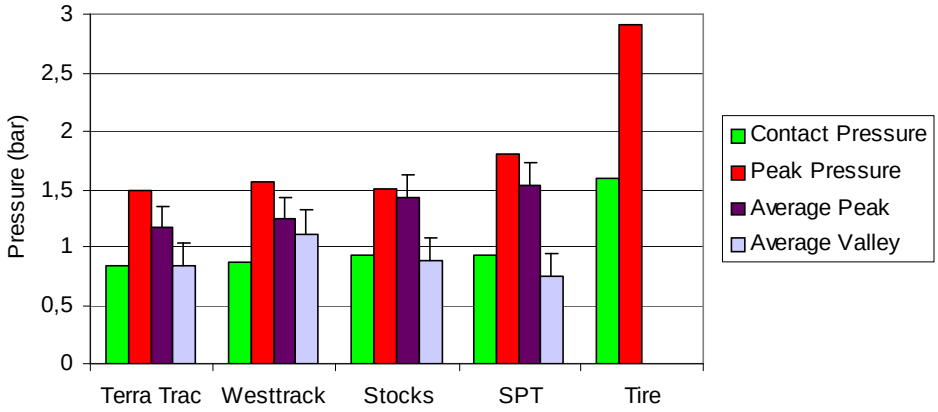

Figure 45: Pressure summary for different track units

3.3.2.4 Rut Parameters for Belt Tension and Track Evaluation

The rut parameters for both the influence of belt tension and the comparison of tracks are given in Table 11.

Table 11: Rut parameters for track evaluation

Treatment	Area (m^2)	Max. Rut Width (m)	Max. Rut Depth (m)
Stocks	0.052 a	0.85 a	0.094 a
SPT	0.062 b	0.87 b	0.127 b
Westtrack	0.049 a	0.82 c	0.090 a
TerraTrac 50 bar	0.039 c	0.68 d	0.090 a
TerraTrac 160 bar	0.033 d	0.68 d	0.075 c
TerraTrac 200 bar	0.031 d	0.69 d	0.078 c
LSD	0.0041	0.018	0.006

The width of the different units depended on the belt width. The TerraTrac had a belt width of 635 mm whereas all other units ran with 750 mm wide belts. This had the consequence that the rut area for these treatments was bigger. The rut depth corresponded to some extent to the results of the soil displacement measurements. For the TerraTrac unit max rut depth and rut area were smallest compared to Stocks, SPT, and Westtrack although no difference was apparent from soil displacement measurement. The TerraTrac at 50 bar belt tension created as well a significantly deeper maximum rut depth and larger rut area than at 160 and 200 bar.

3.3.2.5 Discussion and Conclusions

The performance of the Stocks and Westtrack units compared to the TerraTrac unit could be attributed to the wider belt. The wider belt enabled them to reduce contact time while maintaining similar contact pressures. Yet, contact time could not be the mere reason as both, the Stocks and SPT unit, had 0.68 s less contact time than the TerraTrac unit, however, the soil displacement below the SPT unit was highest. A smooth pressure distribution is essential. The more rollers there were in a track unit and the closer together these rollers were, the more uniform became the pressure application as demonstrated by the Stocks unit. If the TerraTrac unit was equipped with the wider belt of the other units, it would most likely outperform them.

Although the previous section could not show a large effect of belt tension on soil physical parameters for a friction driven rubber track system, the low belt pressure of the SPT is an additional reason for its larger impact on soil physical properties. This is in accordance with Wong's (2007) requirement for high belt tension and reasonable roller distribution. The Appendix contains a brief theoretical background of sinkage caused by tracks applying Bekker (1960).

For track development it can be concluded that there is an optimum amount of rollers. Too few rollers are disadvantageous as the Stocks unit outperforms SPT. But above a treshhold value, the benefit from additional rollers becomes marginal (comparison of Stocks to the Westtrack unit) which agrees with Wong (2001) and Bekker (1960).

3.4 Interactions of Carriage System, Load, and Speed on Soil Displacement

This Section contains interesting cross references between unlinked data originating from the evaluation of the influence of speed and the evaluation of the rear tyres on soil displacement.

Figure 46 shows that a track at 12 t causes similar soil displacement as an implement tyre carrying about 1/3 of the load. Moreover, the soil displacement is reduced to zero at 500 mm depth for the track. This pronounces the overall ability of the TerraTrac to spread high payloads uniformly while causing a minimum amount of compaction. The TerraTrac carries 2.67 times the load of the implement tyres and causes the same soil displacement. This is very similar with the comparison the the T12-700 and 23-11 in Section 3.2.2 whereby the tracked undercarriage system carrying 33 t causes similar soil displacement as an 11 t wheeled combination.

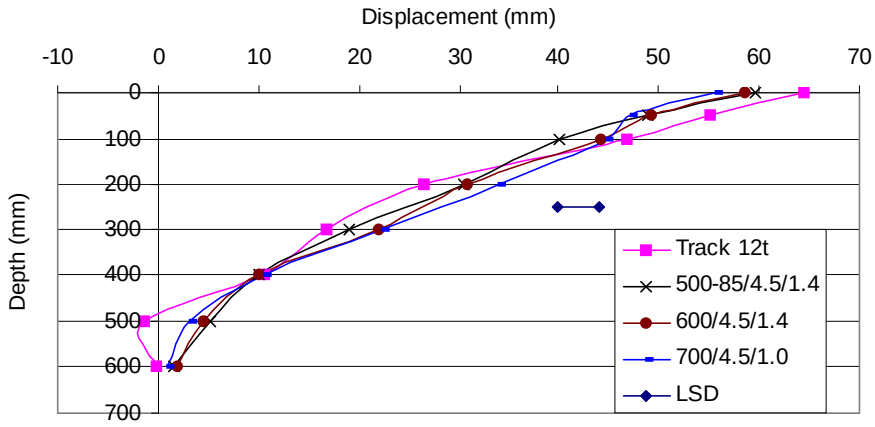

Figure 46: Soil displacement vs. depth for implement tyres and the track at 12 t

Figure 47 shows that three passes of a 900/5/0.5 tyre have the same impact on soil displacement as one pass at a much slower speed emphasizing the effect of speed on soil displacement. This again pronounces the potential damage to headlands where slow speeds are common. In this critical range from 0.29 m/s to 0.85 m/s a decrease of speed to approximately 1/3 increases soil displacement; consequently the increase in soil density results in the same amount as three passes of the same tyre at the higher speed. Fortunately for most of the field, speeds do not become as small. As Section 3.1.2 showed, for higher speeds the accompanying decrease is not as pronounced anymore.

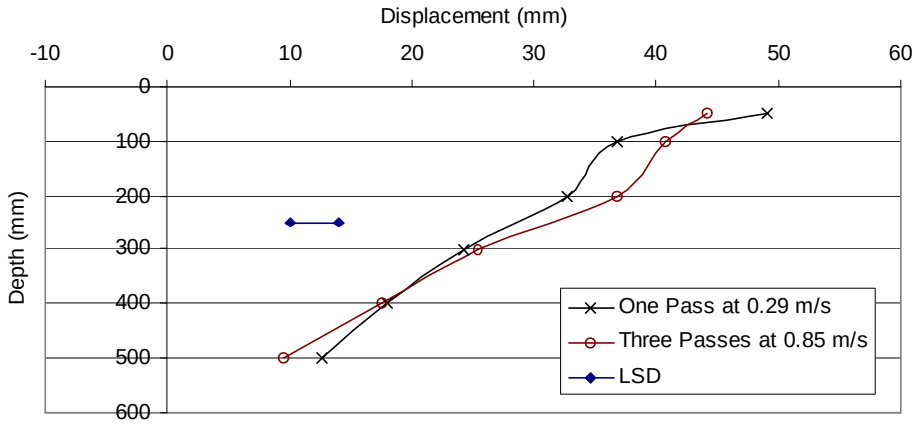

Figure 47: Soil displacement vs. depth for 900/5/0.5 at 0.29 m/s and after three passes at 0.85 m/s.

3.5 Conclusions on Soil Bin Laboratory Study

- Experiments in the soil bin laboratory can be replicated when the same soil conditions and experimental setup is used.
- The influence of speed on soil displacement could clearly be shown whereby the speed studied (0.85 m/s) resulted in a soil displacement approximately 20 % greater than typical harvest speeds (1.52 m/s). However, as this was the same for all such treatments it did not influence the conclusions drawn.
- The benefit of tracks with respect to soil displacement, penetrometer resistance, and rut depth from Ansorge (2005, a) is maintained after the additional passage of the rear axle.
- Tracked machinery caused significantly less soil displacement, rut depth and a strong decline in penetrometer resistance with depth compared to wheeled machines.
- The size of the rear tyre was more crucial after a passage of a wheel on the front axle than after the passage of a track.
- A tyre combination representing a combine harvester at 11 t on medium tyre size caused similar soil displacement compared to a tracked machine at 33 t. A dual and a hypothetical three axle machine caused similar soil displacement compared to a tracked machine. A tandem front axle machine causes intermediate soil displacement between tracked and wheeled machines. A machine on 4 equal sized tyres

caused similar soil displacement as a traditionally wheeled machine, but with a smaller soil displacement at depth.

- Only if wheel load was maintained below 5 t for large section width / diameter tyres, no residual soil displacement between 500 – 600 mm depth was apparent as it was for track type units.
- The possible variation in belt tension of a friction driven track unit (TerraTrac) between 50 and 200 bar affects the resulting soil displacement and pressure distribution below the track insignificantly.
- An evaluation of different track types resulted in the fact that there is an optimum amount of rollers. Additional rollers have only a slight impact, but less rollers can increase soil displacement significantly. Belt tension for sprocket driven track units should be kept in mind as too low a pressure can increase soil displacement, too. All standard track units achieved similar results, a prototype unit created significantly more soil displacement due to the reduced number of rollers.
- The soil displacement caused by implement tyres (4.5 t) usually fitted to the rear axle of a combine was within the range of a rubber track at 12 t.
- A larger section height can compensate for a smaller section width as shown by Ansorge (2005, a), too.
- Passes at low speed on the headlands can cause the same soil displacement as three passes of the same tyre at operation speeds.

4 FIELD STUDY WITH FULL SIZE COMBINE HARVESTERS

In spring 2006 a field study was conducted aiming to verify soil bin results on a sandy loam and clay soils with full size combine harvesters. For the detailed field set up, refer to Section 2.1.2. A description of parameter measurement can be found in Section 2.2 for penetrometer resistance, rut depth and DBD which were measured similar to the soil bin. Soil displacement was measured using fishing hooks and a gamma ray probe was used as well to measure DBD as detailed in Sections 2.2.1.2 and 2.2.3.2, respectively.

The scatter of the measurements in the field results is much larger than in the soil bin laboratory, with high probability due to the inhomogeneities, e.g. variations in water content, soil texture and structure, etc. in the field soil.

4.1 Results of the field experiment

4.1.1 Soil Displacement

Due to the pattern of the observed soil displacement data from the fishhook experiments shown exemplarily for the clay soil in Figure 48, different regression functions were evaluated, quadratic, 1/x, logarithmic, and root functions, respectively, all including a linear term. Attempting to describe the data of all three soils with quadratic and 1/x functions including a linear term reduced mainly to linear functions. Fitting logarithmic and root functions, the linear terms disappeared in the majority of cases, but the differences of the R^2 for the linear, the logarithmic, and the square root functions are marginal with less than 2 % for the clay and the subsoiled sandy loam. The R^2 is greater than 0.7 for the wheeled configurations and exceeds 0.45 for the tracked treatments. As Figure 48 shows the linear term is appropriate because it has zero displacement at a depth where the majority of data from this depth and below is zero. This confirms the findings discussed in 2.2.1.1 assuming to approximate soil displacement by a linear function.

On the shallow tilled sandy loam plot, no coherent picture was gained. For the track data all models reduced to a linear regression function with R^2 greater than 0.7. But for the wheeled treatments, the full model (linear plus quadratic) fitted best with R^2 greater than 0.75. However, as full models had never been chosen before, and the particular data distri-

bution was strongly influenced by the missing measurements in the surface 150 mm, no consequences will be drawn for the overall analysis.

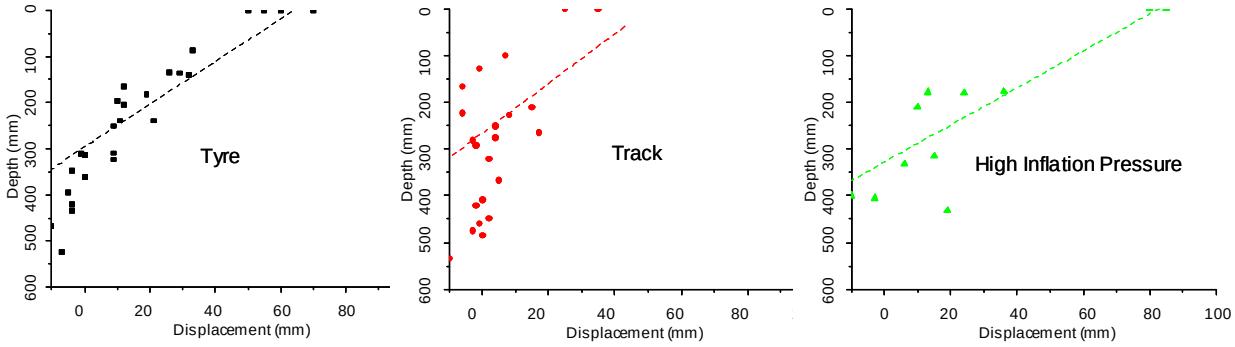

Figure 48: Soil displacement vs. depth on clay soil for individual treatments fitted with linear regressions

Therefore linear regression functions were chosen to evaluate the single treatments on the different soils as overall they showed the same R^2 than more complicated functions and allowed simple comparisons.

4.1.1.1 Clay Soil

Figure 49 shows the movement of the fishing hooks vs. depth. From this graph it would be difficult to detect differences between single treatments. Therefore a statistical regression analysis for the movement of the fishhooks was carried out and revealed significant differences in the slope and intercept of the regression lines for the clay.

The parameters of a statistical regression analysis are shown in Table 12. Take note that in the diagrams the depth is used as the dependent variable, yet the statistical analysis was carried out with the soil displacement depending on depth (Eq. 1) whereby the slope s of the line represents the density increase of the soil.

Table 12 clearly shows that all slopes were negative and all intercepts were positive indicating soil displacement below every single treatment. This was confirmed as for all CI the lower and upper boundary had the same algebraic sign. The slope and intercept were similar for the two tracks, as were the two normal tyre treatments. The replications of the track and the tyre overlap with their confidence intervals but none of the means was included in the CI of the other treatment and hence they could be regarded as statistically significantly

different. Due to the similar relationships and in order to reduce the variation to obtain the effect of track vs. tyres, the data of each were pooled together. This pooled data is shown in Figure 50 and the statistical parameters are listed in Table 12. Grouping the data together produces a more coherent picture, because the number of data points per group increased. The data points and the corresponding regression lines are shown in Figure 50. The slope of the regression line for the track was significantly different from the one for the tyres. There was as well significant difference between the results of the tyre and the tyre at high inflation pressure. Moreover the slope was larger indicating more soil compaction than for a tyre at normal inflation pressure which was accompanied by a larger intercept on the X-Axis; thus creating overall a larger soil displacement and hence soil compaction.

From the slope it could be concluded that on average the tracked machine increased soil density by approximately 9 %, the wheeled machine by 16 %, and at high inflation pressure by about 20 %. These values had the same magnitude compared to the results from the sandy loam soil in the laboratory study (13 % and 18 % for tracked and wheeled machines, respectively).

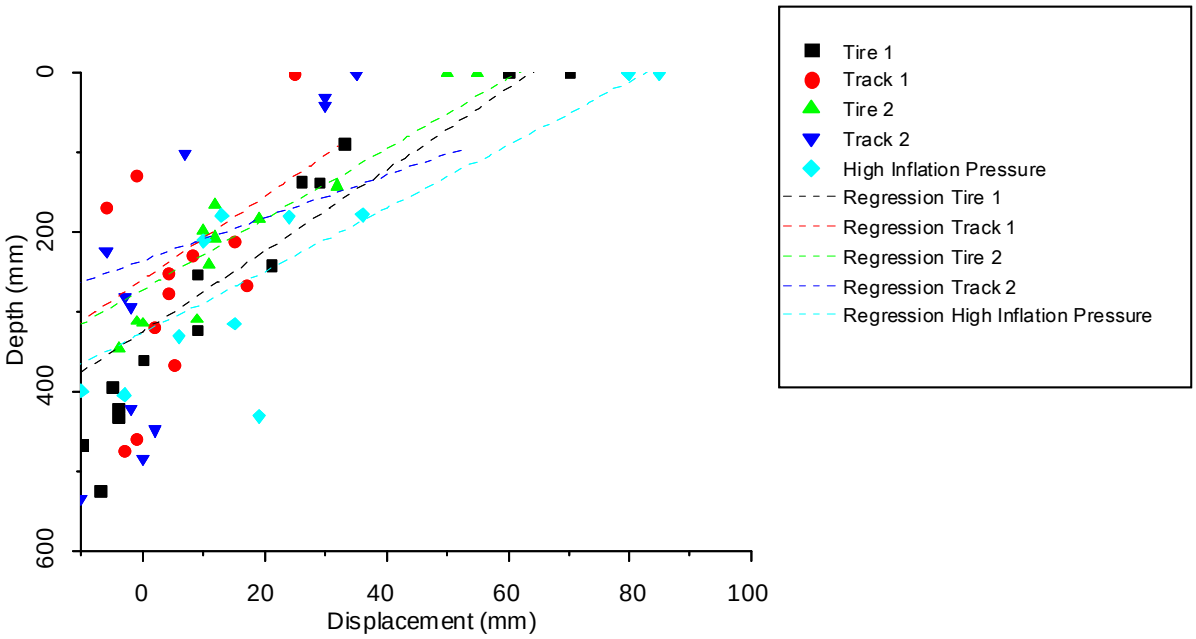

Figure 49: Soil displacement and regression lines for clay with individual groups

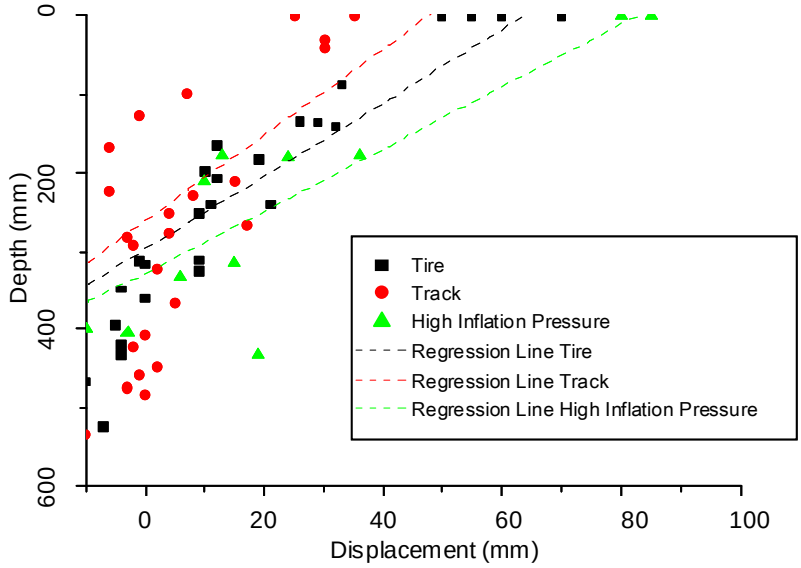

Figure 50: Soil displacement and regression lines for clay with pooled groups

Table 12: Regression line parameters for displacement on clay soil

Treatment	Intercept d_0 (mm)	95% - CI Int.	Slope s	95%-CI Slope	R^2
Individual Groups					
Tyre 1	51.1	37.3 – 64.9	-0.148	-0.193 - -0.103	0.756
Tyre 2	47.4	31.5 – 63.3	-0.169	-0.224 - -0.115	0.746
Track 1	23.6	7.5 – 39.7	-0.087	-0.142 - -0.032	0.455
Track 2	21.7	3.5 – 40.0	-0.086	-0.144 - -0.029	0.450
High	70.0	51.8 – 88.2	-0.203	-0.260 - -0.140	0.802
Combined Groups					
Tyre	49.0	38.7 – 59.2	-0.157	-0.191- -0.123	0.727
Track	22.7	11.6 – 33.9	-0.087	-0.123 - -0.051	0.454
High	70.0	51.8 – 88.2	-0.203	-0.260 – -0.140	0.787

4.1.1.2 Sandy Loam Subsoiled

In this section only the diagrams with the pooled data will be shown and discussed because of the experience gained in the analysis in the previous section. For completeness data for both the pooled and the individual groups was included in Table 13. As can be seen graphically from Figure 51 and numerically from Table 13, the track and the tyre were statistically significantly different. The track created the smallest soil displacement. This was in agreement with Ansorge (2005, a), Section 3.2 and with the results found on clay.

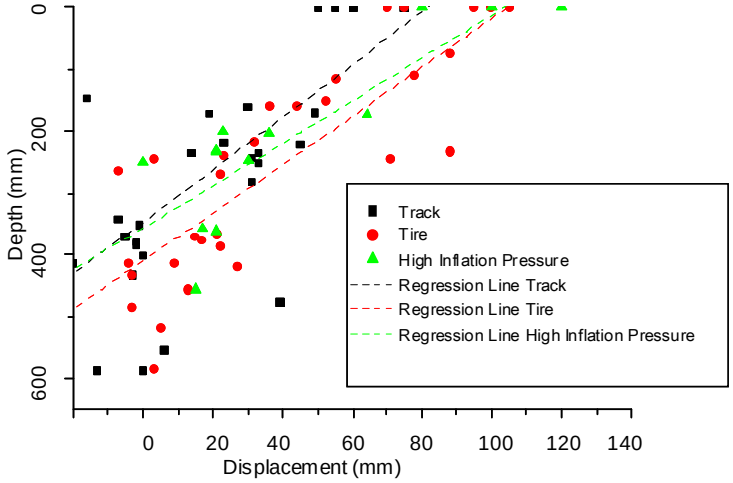

Figure 51: Soil displacement and regression lines for sandy loam subsoiled with pooled groups

Table 13: Regression line parameters for displacement on sandy loam subsoiled soil

Treatment	Intercept d_0 (mm)	95% - CI Int.	Slope s	95%-CI Slope	R^2
Individual Groups					
Tyre 1	78.9	57.7 – 100.1	-0.163	-0.235 – -0.091	0.629
Tyre 2	94.9	77.8 – 112.2	-0.206	-0.259 - -0.152	0.804
Track 1	66.6	56.0 – 77.3	-0.179	-0.216 - -0.142	0.886
Track 2	39.3	13.5 – 65.1	-0.078	-0.154 - -0.004	0.285
High	89.0	68.3 – 109.7	-0.226	-0.303 - -0.150	0.777
Combined Groups					
Tyre	86.0	73.0 – 99.0	-0.182	-0.225 - -0.141	0.715
Track	49.5	35.3 – 63.7	-0.113	-0.158 - -0.068	0.462
High	89.0	68.3 – 109.7	-0.226	-0.303 – -0.150	0.777

The high inflation pressure tyre resulted in a larger slope and hence caused larger soil displacement than the tyre with normal inflation pressure. Yet this difference was not statistically significant due to smaller number of replications. This emphasised the benefit of more data points for field experiments. With natural variance, it was not possible to statistically confirm results with less than 20 fish hook measurements. Overall the tracked combine harvester on the subsoiled sandy loam soil increased soil density by approximately 11 %, the wheeled combine harvester by approximately 18 % and at higher inflation pressure by 23 %. These numbers were higher than the results from the soil bin laboratory as expected due to weaker soil condition.

4.1.1.3 Sandy Loam Soil Shallow Tilled

The soil displacement for the shallow tilled soil pooled together is shown in Figure 52. From the curves in the graph it was difficult to argue whether differences between treatments were significant or not. Overall displacement is small due to the high soil strength.

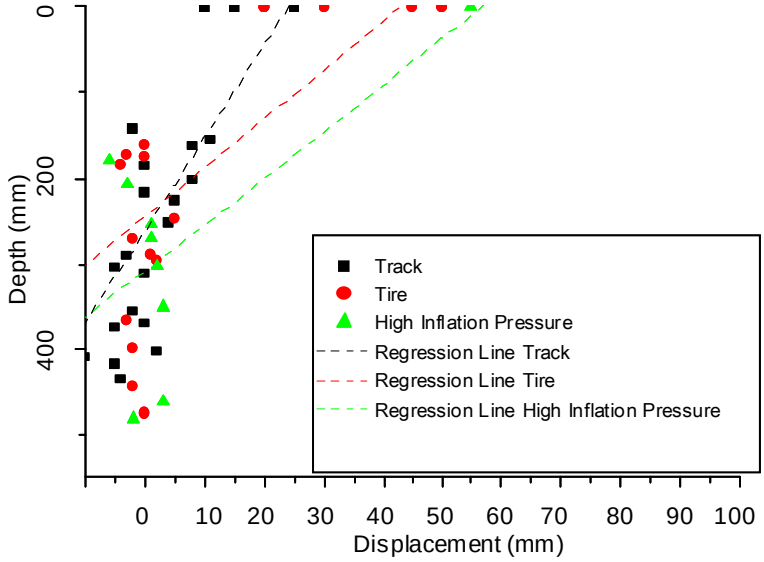

Figure 52: Soil displacement and regression lines for sandy loam shallow tilled with pooled groups

Table 15 illustrates that the regression lines for all treatments were significantly different from zero, indicating that consequently soil displacement occurred. From the overlapping CI it could be seen that the data from the track experiment had a significantly smaller intercept than the data from the tyre, but the slope and hence the density increase was not significantly different. Both intercept and slope of the regression line from the track experiment were statistically different from the tyre at high inflation pressure. But the data from the tyre at high inflation pressure was not significantly different from the one at recommended inflation pressure. The tracked combine harvester increased soil density by approximately 7 %, the wheeled machine by approximately 9 % and at high inflation pressure by about 12 %.

Before the statistical analysis was conducted the uniform distribution of the data was generally confirmed. In this particular case the data was skewed to the right due to the surface readings suggesting a LN-transformation of the data. Yet as it can be seen from Table 15

this transformation did not make a difference to the results, only the R^2 and the differences decreased. Due to the smaller R^2, the transformation was rejected.

Table 14: Regression line parameters for displacement on sandy loam shall. tilled soil

Treatment	Intercept d_0 (mm)	95% - CI Int.	Slope s	95%-CI Slope	R^2
Individual Groups					
Tyre 1	17.5	5.9 – 29.0	-0.069	-0.069 – -0.116	0.594
Tyre 2	34.2	14.7 – 53.7	-0.114	-0.187 - -0.039	0.574
Track 1	19.1	13.2 – 25.0	-0.085	-0.085 - -0.044	0.781
Track 2	17.0	7.8 – 26.2	-0.069	-0.106 - -0.034	0.679
High	42.4	23.9 – 61.0	-0.121	-0.187 – -0.055	0.656
Combined Groups					
Tyre	25.8	14.9 – 36.6	-0.091	-0.134 - -0.049	0.519
Track	17.9	13.1 – 22.8	-0.065	-0.083 - -0.065	0.711
High	42.4	23.9 – 61.0	-0.121	-0.187 – -0.055	0.656

Table 15: Regression line parameters for displacement with LN transformed data on sandy loam shallow tilled soil

Treatment	Intercept d_0 (mm)	95% - CI Int.	Slope s	95%-CI Slope	R^2
Individual Groups					
Tyre 1	15.2	11.5 – 18.9	-0.019	-0.035 – -0.004	0.525
Tyre 2	16.9	9.6 – 24.3	-0.024	-0.052 - -0.004	0.291
Track 1	15.9	14.0 – 17.9	-0.018	-0.025 - -0.012	0.729
Track 2	17.4	9.3 – 25.4	-0.037	-0.068 - -0.005	0.436
High	18.9	15.0 – 22.7	-0.022	-0.036 - -0.009	0.604
Combined Groups					
Tyre	16.1	12.4 – 19.7	-0.022	-0.036 - -0.007	0.342
Track	16.5	12.9 – 20.2	-0.025	-0.038 - -0.004	0.393
High	18.9	15.0 – 22.7	-0.022	-0.036 - -0.009	0.604

4.1.2 Penetrometer Resistance Results

20 penetrometer resistance readings were taken in the center line of the wheel rut before and after each treatment. Due to stones, mouse holes and other physical soil disturbances 10 penetrometer readings of each experiment were dismissed in subsequent data analysis. The average remaining readings are shown in the following graphs. Similar to the soil displacement data of the track and the tyre the two replications were averaged. Ansorge

(2005, a) discussed the importance of taking control and final readings of penetrometer resistance from the same spot due to soil differences, but this did not apply on these field sites as it could be shown that the controls for different treatments were identical.

In general penetrometer resistance readings were not very sensitive in picking up differences between the treatments due to the high moisture content of 21 % for the sandy loam field and 36 % of the clay field.

4.1.2.1 Penetrometer Resistance on Clay

On the clay site there were no differences between the treatments and even not between the treatments and the control.

The controls for all treatments are shown in Figure 53 and do not exhibit any difference. The average of all controls vs. the average of each treatment is shown in Figure 54. From the LSD plotted it could be seen that there were no statistically significant differences, although a denser soil was indicated as far as 200 - 300 mm depth for the control vs. treatment groups as both the track and the tyre were consistently higher than the control. The treatment with the high inflation pressure always interfered with the control line. This could be due to both less replications taken for the high inflation pressure treatment and the high initial variation within the data expressed in the large LSD.

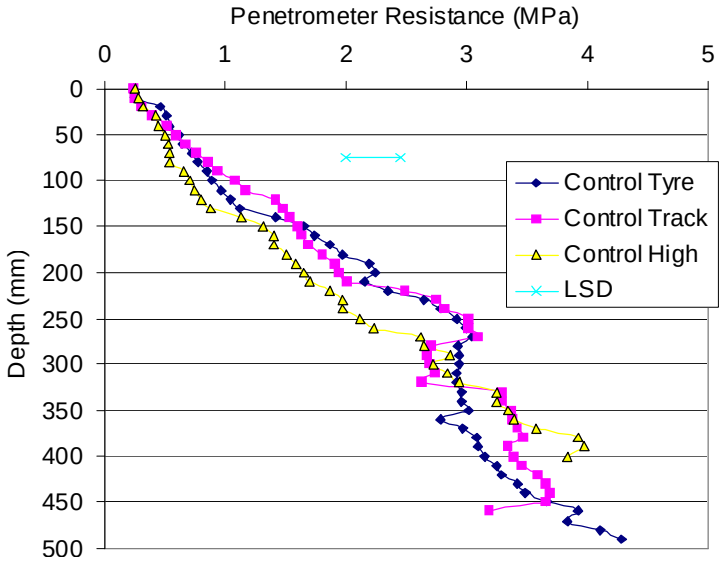

Figure 53: Penetrometer resistance for the controls on the clay side

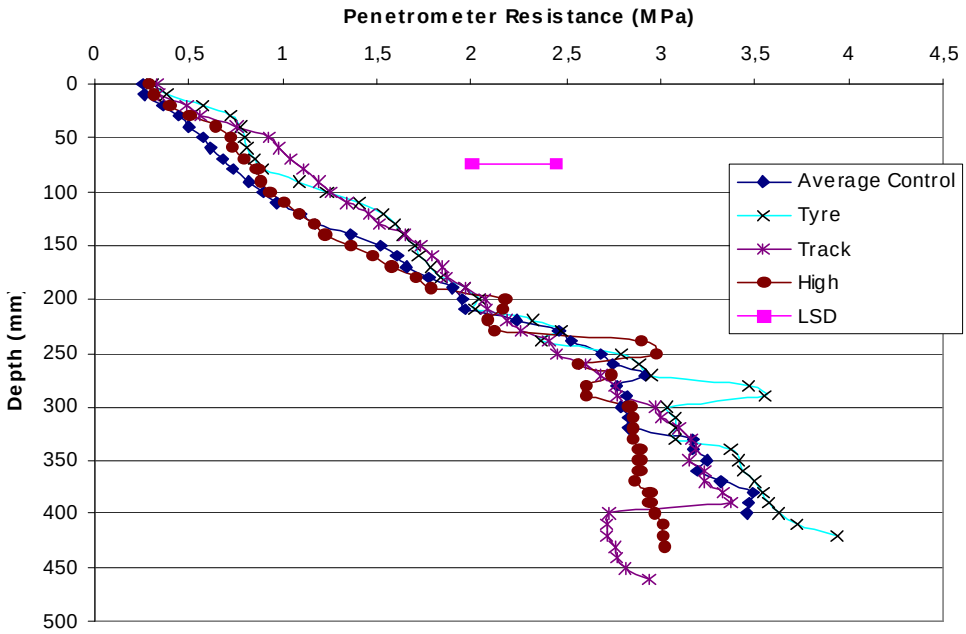

Figure 54: Penetrometer resistance for clay control and the pass of a wheeled, tracked and a wheeled machine with high inflation pressure

Clay penetrometer resistance was influenced by the clay sticking to the cone and shaft due to the high moisture content. It was not significantly affected by the single treatment. Interesting to note was the increased variation below 250 to 300 mm depth. During the excavation of the fishing hooks the reason became clear. It was the maximum working depth ranging to about 250 mm depth on this field. Below 250 mm the AP horizon changed to a B/C horizon of virgin clay mixed with stones.

4.1.2.2 Penetrometer Resistance on Shallow Tilled Sandy Loam

Controls for different treatments in the shallow tilled sandy loam soil are shown in Figure 55. There were no significant differences so one control was used.

Similar to the clay data, there were no significant differences between either the runs themselves or even the control and the run as obvious from Figure 56. Because of the amount of interference amongst the different treatments close to the surface it did not allow any conclusion. Maximum working depth on the clay was found to be between 250 – 300 mm; in the shallow tilled sandy loam it seemed to be at about 300 mm depth from the graph. This was confirmed when excavating the fishing hooks.

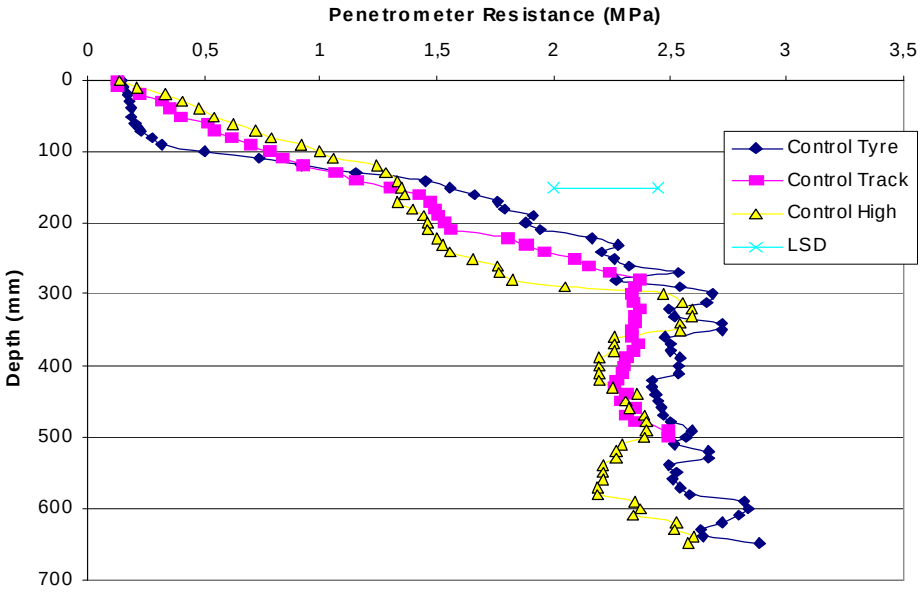

Figure 55: Penetrometer resistance for the controls on the sandy loam shallow tilled side

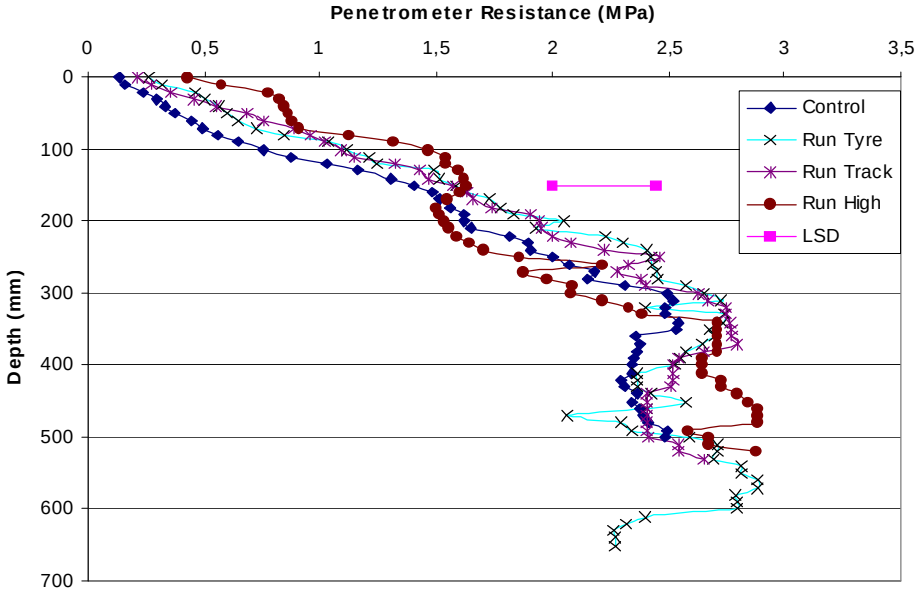

Figure 56: Penetrometer resistance for sandy loam shallow tilled control and the pass of a wheeled, tracked and a wheeled machine with high inflation pressure

4.1.2.3 Penetrometer Resistance on Subsoiled Sandy Loam

Similar to the controls of the penetrometer resistance for the sandy loam shallow tilled and the clay soil, the controls for the subsoiled treatment shown in Figure 57 did not display significant differences. In this diagram the working depth of the subsoiler preparing the

soil for the investigation can be seen between 300 – 350 mm, the bottom of a tine tip and the unloosened "heap" in between, respectively.

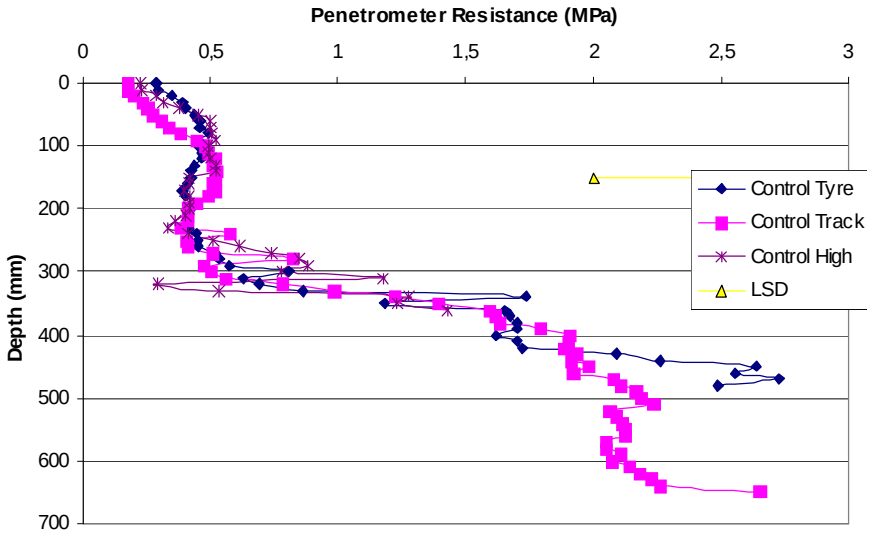

Figure 57: Penetrometer resistance for the controls on the sandy loam side which has been subsoiled

Due to the very loose surface the only significant differences in penetrometer resistance among any treatments could be detected when looking at Figure 58. All treatments were significantly different from the control. The track treatment was significantly different from the tyre treatment between 100 – 300 mm depth. Due to fewer replications in the high inflation pressure treatment, this curve showed a lot of variation.

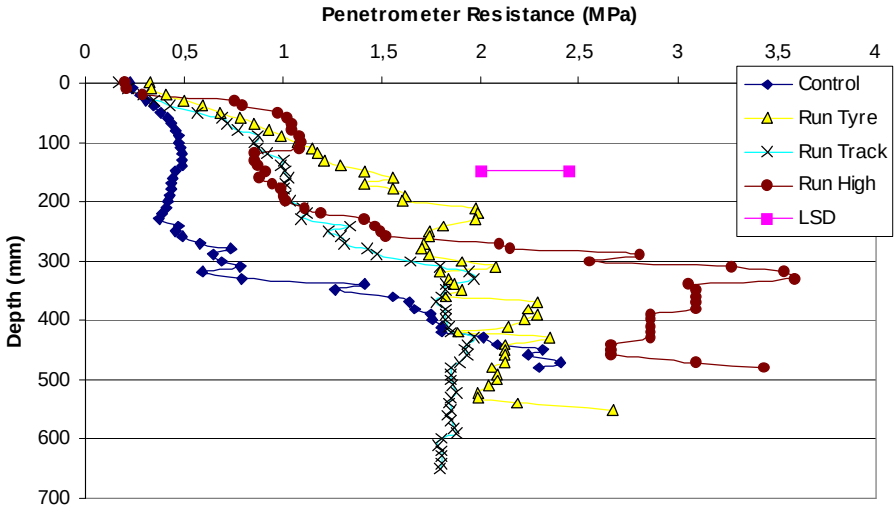

Figure 58: Penetrometer resistance for sandy loam subsoiled control and the pass of a wheeled, tracked and a wheeled machine with high inflation pressure

In summary the tyre treatment caused tendency to significantly higher penetrometer resistance than the track. Due to fewer replications for the tyre at high inflation pressure the results of this had higher variation masking its stronger influence on the soil.

4.1.2.4 Summary of Penetrometer Resistance on Sandy Loam

When plotting the penetrometer resistance curves for both final sandy loam curves into one diagram, shown in Figure 59, the wheeled machine created similar penetrometer resistance for the subsoiled site as for the shallow tilled sandy loam site to a depth of 200 mm. This emphasized the benefit of the track on a very weak soil. Below 250 mm depth the variance of the controls for both sites affected the final result. The penetrometer resistance for the shallow tilled site was slightly less than 2.5 MPa whereas for the subsoiled site it was less than 2.0 MPa below 300 mm depth.

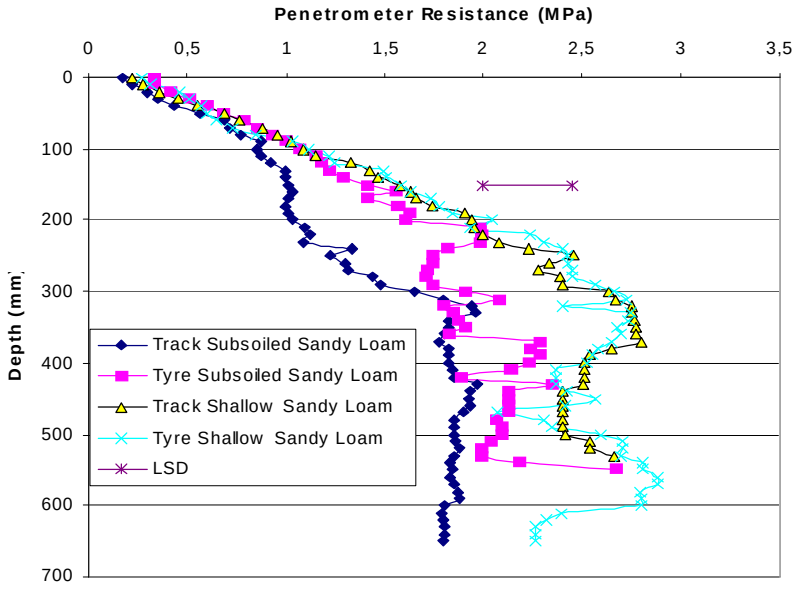

Figure 59: Penetrometer resistance diagram after the pass of a tracked and a wheeled machine on both sandy loam soil conditions

4.1.3 Analysis of Rut Depth

Looking at Figure 60 the differences between the single treatments could be shown visually. The wheeled machine with high inflation pressure on the left hand side caused the largest rut depth followed by the wheeled machine at normal inflation pressure in the centre. The tracked machine on the far right hand side caused the least rut as expected from measurement of all soil physical parameters.

High Inflation Normal Inflation Tracked Machine

Figure 60: Rut depths on sandy loam soil

The differences became more obvious when looking at the ruts in sandy loam field shown in Figure 61. This picture looked into the subsoiled part which was followed by the shallow tilled part in the back.

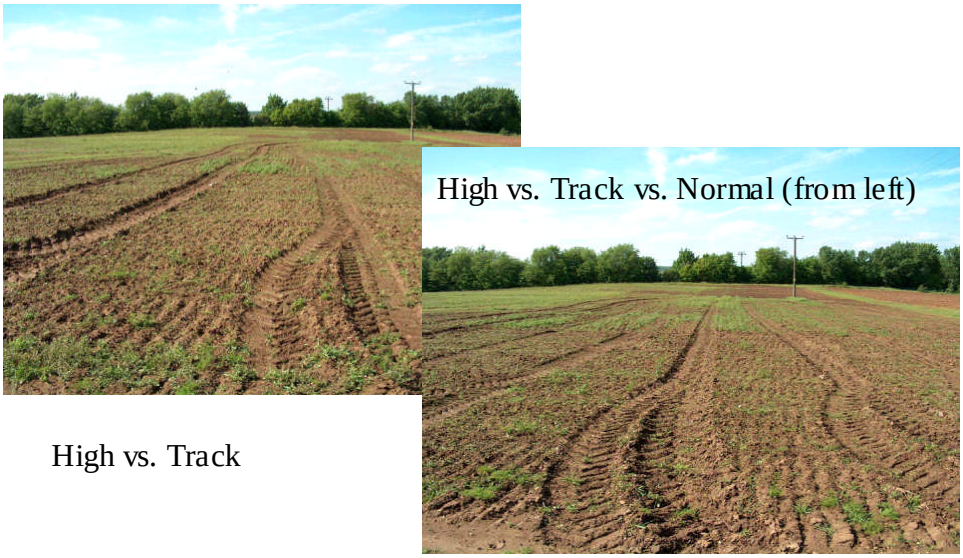

High vs. Track

Figure 61: Ruts depths on sandy loam soil from further above

The measured rut parameters for the field trials are summarized in Table 16 and Table 17. Table 16 shows the average values for every single treatment, Table 17 shows the single track and tyre treatments pooled together.

Looking at the statistical differences in Table 17 does not result in a coherent picture for all treatments. Treatments were sometimes similar to different treatments on the same soil

type, e.g. on the subsoiled plot the tyre and the tyre at high inflation pressure were statistically the same concerning the average rut depth. Hence, an analysis of variance was carried out with the parameters tyre, soil and tyre soil interaction to ease the comparison of different treatments when looking at Table 17. All three parameters were significant and the results in relation to the measured parameters and statistical differences amongst treatments and amongst soil types are shown in Table 18 and Table 19, respectively.

Table 16: Rut parameter field trials including all treatments

Treatment	Aver. Max Depth (mm)	Aver. Aver. Depth (mm)	Aver. Width (mm)
Subsoiled Track 1	90	55	920
Subsoiled Track 2	102	70	903
Subsoiled Tyre 1	112	80	873
Subsoiled Tyre 2	120	103	907
Subsoiled High	152	100	953
Shallow Track 1	48	20	670
Shallow Track 2	50	18	790
Shallow Tyre 1	43	23	873
Shallow Tyre 2	63	47	810
Shallow High	73	55	830
Clay Track 1	55	25	857
Clay Track 2	60	35	860
Clay Tyre 1	82	63	850
Clay Tyre 2	88	52	830
Clay High	105	82	830

All treatments are significantly different with regard to their maximum rut depth and average rut depth, however, average rut width was the same for all treatments. The significant difference in maximum rut depth and average rut depth in the field experiments confirmed the results from the soil bin.

As soil displacement, soil density and penetrometer resistance were mainly influenced by rut depth, this clear result put emphasis on the differences seen in penetrometer resistance and soil displacement.

Table 17: Rut parameters, same treatments averaged together, statistically same values are followed by the same letter

Subsoiled	Aver. Max Depth (mm)	Aver. Aver. Depth (mm)	Aver. Width
Average Tyre	116 a	92 a	890 a
Average Track	96 b	63 b	912 a
Average High Pressure	152 c	100 a	953 b
Shallow Tilled			
Average Tyre	53 d	35 c	842 c
Average Track	49 d	19 d	730 d
Average High Pressure	73 e	55 e	830 c
Clay			
Average Tyre	85 f	58 e	840 c
Average Track	58 d	30 c	858 c
Average High Pressure	105 b	82 f	830 c
LSD	9	9	39

Table 18: General statistical analysis of rut parameters in relation to treatment (statistically different treatments are followed by different letters)

Treatment	Aver. Max. Depth (mm)	Aver. Aver. Depth (mm)	Average Rut Width (mm)
Tyre	85a	61a	857a
Track	68b	37b	835a
High Inflation	110c	79c	871a
LSD	9	9	39

The statistically identical rut width for all treatments was due to the fact that the rear tyre of a tracked combine harvester did not run in line with the track, but approximately 15 cm offset resulting in the same rut width as a wheeled combine harvester with front tyres wider than the belt of the track, but the rear tyres running in line. To reduce the trafficked area of the field it was strongly recommended to let the tyres run in line with the front axle.

Following the differences seen between the treatments, the question arose whether these were individually influenced by the soil type, too. From Table 19 it was obvious that all measured parameters were significantly influenced by the soil type.

Table 19: General statistical analysis of rut parameters in relation to soil type (statistically different treatments are followed by the same letter)

Soil Type	Aver. Max. Depth (mm)	Aver. Aver. Depth (mm)	Average Rut Width (mm)
Subsoiled	121a	86a	920a
Shallow Tilled	59b	37b	800b
Clay	83c	55c	840c
LSD	9	8	36

Significant differences between the plot which received a subsoil treatment and the shallow plots were expected as initial soil density and therefore soil strength for the subsoiled plot was much lower. The significant differences between the shallowly tilled clay and sandy loam confirmed the theoretically expected difference due to soil strength.

Comparing the results of the high inflated tyre vs. the tracked machine on the left hand side of Figure 61 showed the significant differences seen in rut depth visually in a the sandy loam subsoiled plot. On the right hand side the ruts caused by the normal inflated tyre can be seen, too, followed by the tracked machine on the left and in the far left the pronounced ruts are caused by the high inflation pressure tyres.

Consequently in first instance an analysis of soil compaction caused by drive systems can be performed visually. However, as Ansorge and Godwin (2007a) showed on a stratified soil condition in the lab, the rut depths might be identical but the soil displacement might not. Therefore if differences are obvious, then these are there. However, if no differences are seen there can still be differences in the underlying soil.

4.1.4 Gravimetrical Dry Bulk Density

In each treatment DBD was determined gravimetrically at two depths (150 and 300 mm) with three replications. Three control measurements were randomly taken on each field site before the experiment was conducted.

An analysis of variance was carried out for all the DBD data and showed that there were significant fixed effects from the treatment itself, the soil type, the depth at which the probe was taken and a significant interaction between the treatment and the soil type.

Analyzing the data with respect to the overall effect of the treatment across all soil types showed that all treatments were significantly different from the control, yet there are no significant differences between the treatments. The estimated densities for the treatments were in corresponding order as the soil bin results and the results previously discussed. Table 20 shows the summary of this data.

Table 20: DBD for field treatments, statistically identical DBD followed by the same letter

Treatment	Estimated DBD (g/cc)	SE	DF
Control	1.352 a	0.0198	29
High Inflation Pressure	1.518 b	0.0214	29
Normal Inflation Pressure	1.517 b	0.0171	29
Tracked Machine	1.499 b	0.0171	29

The fixed effect of the soil type over all treatments showed a significant difference for both sandy loam soils from the clay treatment. The results from subsoiled and shallow tilled sandy loam were statistically identical which lead to the conclusion that the sandy loam soil had been compacted to a similar final state, indifferent from their initial density (data shown in Table 21). This was confirmed when looking at the penetrometer resistance in Figure 59 whereby the final penetrometer resistance was identical for the wheeled machine on both the shallow tilled and the subsoiled part of the sandy loam, but the track could maintain the subsoiled sandy loam at a lower final penetrometer resistance.

Table 21: DBD for soil types and, statistically identical DBD followed by the same letter

Soil Type	Estimated DBD	SE	DF
Clay Shallow Tilled	1.318 a	0.017	29
Sandy Loam Subsoiled	1.551 b	0.016	29
Sandy Loam Shallow Tilled	1.546 b	0.016	29

Analyzing the interaction of treatment and group is shown in Table 22. Due to the large variances the amount of significant differences was small, but the trends agreed with previous data in this chapter, the thesis and in Ansorge (2005, a).

Table 22: Estimated DBD for treatments and controls, statistically identical DBD followed by the same letter

Effect	Estimated DBD (g/cc)	SE	DF
Control Clay	1.271 a	0.034	29
Control Sandy Loam Shallow Tilled (SLT)	1.463 b	0.034	29
Control Sandy Loam Subsoiled (SLS)	1.323 a	0.034	29
High Inflation Pressure on Clay	1.318 a	0.042	29
High Inflation Pressure on SLT	1.563 c	0.034	29
High Inflation Pressure on SLS	1.672 d	0.034	29
Normal Inflation Pressure on Clay	1.349 a	0.030	29
Normal Inflation Pressure on SLT	1.597 c e	0.030	29
Normal Inflation Pressure on SLS	1.605 d e	0.030	29
Tracked Machine on Clay	1.333 a	0.030	29
Tracked Machine on SLT	1.581 c e	0.030	29
Tracked Machine on SLS	1.582 d e	0.030	29

The moisture content on the clay site was 36 % and on the sandy loam subsoiled part 20.5 % and the shallow tilled part 21.5 %.

4.1.5 Density Measurements with Nuclear Density Gauge

Figure 62 shows the DBD before and after the passage of tracked, wheeled and high inflated wheeled combine harvesters in the field on the different field sites. Statistically accounting for treatment and depth was significant in explaining the variation. There was no interaction between depth and treatment, showing for all treatments a similar behavior with depth. Figure 62 a) shows the results for the clay soil where the DBD for the control was in tendency higher than after the passage of the machines. Apart from the machine at high inflation pressure the control and the passage were not significantly different from each other however, the experiment has a smaller value than the control. This was interesting as it would mean that driving over the soil with a combine harvester would in fact loosen the soil. As this was not possible, it could only be due to the swelling of the clay caused by

precipitation in-between taking control measurements and taking measurements after the experiment. This was indicated by the soil moisture content, too, which was lower when the control measurement was taken. Due to the questionable results on the clay soil no further discussion will be made. It showed the accuracy or better inaccuracy of the transmitting radiation method in determining DBD.

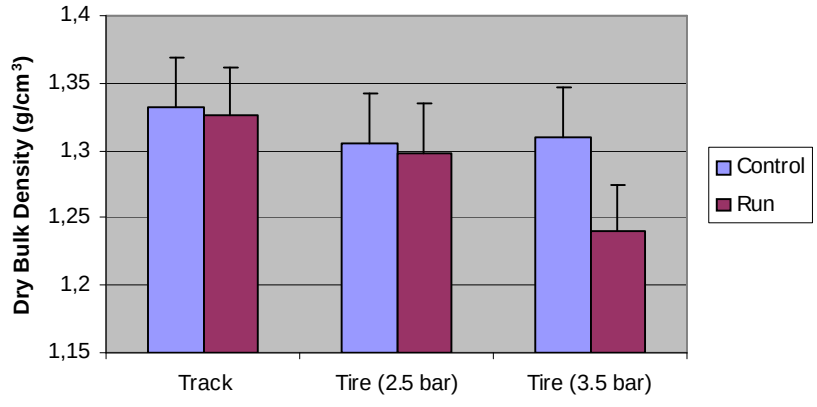

a)

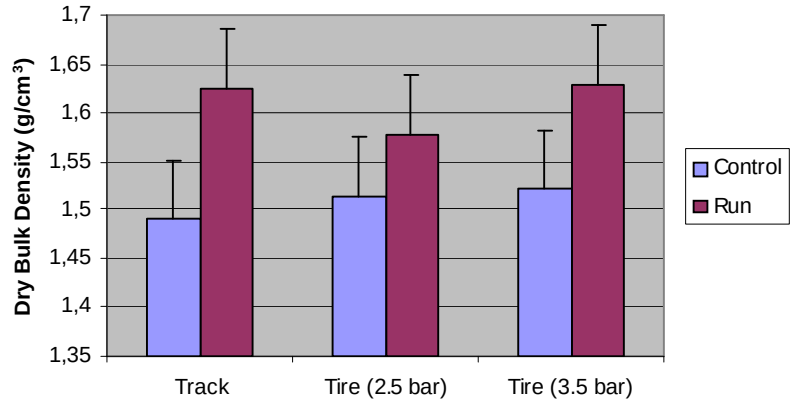

b)

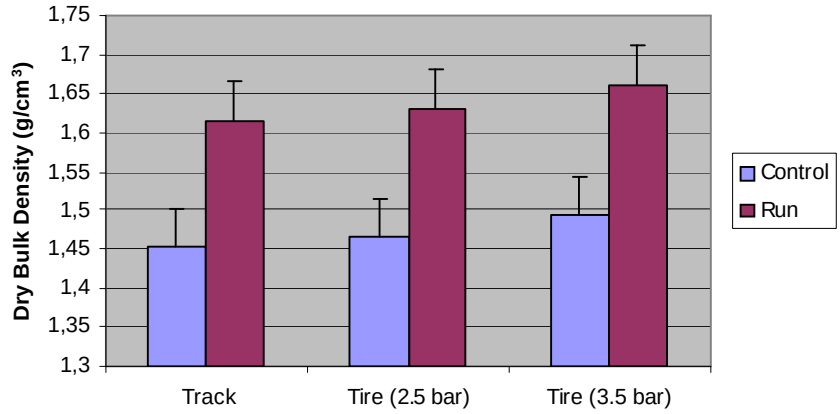

c)

Figure 62: Gamma ray dry bulk density measured for clay (a); sandy loam shallow tilled (b); sandy loam subsoiled (c).

Figure 62 b) shows the DBD for the experiment on the shallow tilled sandy loam measured with the Troxler. All runs were significantly higher than the control and there were again neither significant differences amongst the controls, nor the runs themselves. In absolute numbers the high inflation pressure tyre experiment caused a 0.004 g/cm^3 higher DBD than the track experiment. This marginal difference was surprising and as the results of the Troxler on clay compared to all the previous parameters showed must be caused by the insensitivity of the method.

The tyre at normal inflation pressure had the smallest DBD after the run. Appart from the clay data shown in the previous paragraph this was the only time ever, that a tracked machine caused in tendency more soil compaction than a wheeled machine at normal inflation pressure. This does not agree with all other measured soil physical parameters.

The measurements taken in the subsoiled sandy loam showed a significant increase from the control to the measurement taken after the pass of the machinery. There was no significant difference between the controls as can be seen in Figure 62 c). It includes the 95 % CI for the control and the run measurements. The absolute values for the run measurements showed the same tendency as the fishhook method with the lowest density for the track experiment followed by the tyre at normal inflation pressure followed by the high inflation pressure tyre. However, none of these differences were significant.

4.2 Discussion and Conclusion on Field Study

The benefit of the rubber tracked machine in comparison to the wheeled machine was shown in field on sandy loam and clay soils with respect to reduced rut depth, soil displacement, and penetrometer resistance. This confirmed the findings from the soil bin laboratory and field study from Ansorge (2005, a) and Chapter 3. The average increase in soil density in the field on both soil types was similar to the one found in the soil bin laboratory study, but reaching only to a more shallow depth.

The penetrometer resistances did only show differences on the most pronounced case, the subsoiled sandy loam. On all other occasions the soil was too wet. Interestingly the penetrometer resistance on the sandy loam exhibited a similar pattern after the pass of a wheeled machine on both subsoiled and shallow tilled sandy loam. The tracked machine

was able to maintain penetrometer resistance at a smaller level on the subsoiled part pronouncing the ability of the track to maintain loose soil states.

The rut parameters showed the clearest picture of all measured parameters. A visual assessment of the ruts led to the same conclusion as drawn from rut depth and soil displacement measurement by means of fish hooks. Measuring soil displacement by means of placing fishing hooks into the soil provided a sensible way of measuring soil movement in the field while minimizing initial soil disturbance.

Due to the large inherent variation of the data gained with the nuclear density gauge this device proved not to be useful even for assessing relative changes in soil dry bulk density. Therefore the use of this measurement is not recommended.

5 ALLEVIATION OF SOIL COMPACTION

After harvest machinery has passed over the soil, it might be appropriate, possibly necessary, to alleviate the compaction caused. The question is how a wheeled undercarriage system compares to a tracked undercarriage system in this respect and whether the differences seen in soil physical properties are transmitted to the draught force of a tine. Therefore this chapter investigates the required draught force of a subsoiler to loosen the soil after the passage of both a wheeled and a tracked undercarriage system in controlled laboratory conditions and in the field. The method for this chapter can be found in Section 2.2.6.

5.1 Literature Review

For loosening soil an implement has to be driven or pulled through it inducing soil failure; most times the implements are pulled. Usually a tine or tine – similar – implement is utilized for this purpose. Tines cause a crescent failure of the soil whereby soil shears at an angle of 45 degree down to the critical working depth which depends on tine geometry and can either be estimated (6 times the width of the tine in depth) or calculated according to Eq. 20 with the extensions of Eq. 21 to Eq. 23 in Godwin and Spoor (1977). Below this depth lateral failure occurs whereby the soil in front of the tine is only pushed sideways. Crescent failure causes a much higher working and draught efficiency than lateral failure and is consequently beneficial. The effects of soil conditions and tines geometry for the optimum soil loosening are discussed in detail by Spoor and Godwin (1978). Prediction models summarized and further developed by Godwin and O'Dogherty (2003) can be used to calculate both the vertical and draught force necessary for pulling a tillage implement.

When loosening a deeply compacted soil care has to be taken not to cause severe re-compaction when traveling the soil subsequently as the loosened subsoil is very sensitive to re-compaction. This re-compaction can merely be evaded utilizing very light machinery, controlled traffic or by a combined operation of deep loosening and surface cultivation with drilling. Mouldboard ploughing following deep loosening can induce significant re-compaction independent of the tractor wheels operating in the furrow or on the surface (Soane et al., 1986). Practical suggestions are given by Spoor and Godwin (1981) for loosening soil compaction.

However, according to Arvidsson and Hakansson (1996) not all consequences of soil compaction in the topsoil can be alleviated by tillages. The authors reported an effect of topsoil compaction on yield up to 5 years after the whole field was trafficked, although annual ploughing was performed.

5.2 Draught Force for Subsoiler in Laboratory Study

On uniform soil conditions after the pass of the track at 12 t followed by the 500-70/4.5/2.3 rear tyre, and after the 680/10.5/2.2 followed by the 500 – 85/4.5/1.4 a winged subsoiler tine was operated at 350 mm depth measured from the virgin surface and draught force recorded using an octagonal ring transducer. Afterwards the loosened area was measured using a profilemeter. The actual area in which the tine operated ("tine area") was calculated by subtracting the measured rut area from the loosened area. All numbers are given in Table 23. Due to the large rut area, the draught force was smallest for the wheeled combination and highest for the track. To correct for the rut area, specific draught force was calculated using the tine area. Draught force for the control was 40.7 kN/m^2, after the track including a rear tyre it was 70.8 kN/m^2 and after the pass of the wheeled under carriage system it was 84.5 kN/m^2.

Table 23: Area and draught force of subsoiler

Implement	Loosened Area (m^2)	Rut Area(m^2)	Tine Area(m^2)	Draught Force (kN)
Control	0.1111	0	0.1111	4.5
Track	0.1108	0.0401	0.0707	5
Wheel	0.1147	0.0691	0.0456	3.86

5.2.1 Consequence of Draught Force for Subsoiler in Real Situations

For practice specific draught force does not reveal the most important information. Absolute draught force at a given depth is more crucial to find a tractor being capable of the operation. The absolute draught force for a tine obeys the following relationship:

Absolute Draught Force= Spec. Draught Force * Loosened Area

Eq. 3

Spec. Draught force and loosend area follow in general the equations:

Loosened Area = a * Working Depth ^{b}

Spec.Draught Force = c * Working Depth

Eq. 4

whereby a, b, and c are empirically determined constants; i.e. for a sandy loam soil in this condition the values are approximately 1.4, 1.15, and 0.1-0.4, respectively. The linear relationship between working depth and spec. draught force was mentioned by Spoor and Godwin (1978).Eq. 4 can be substituted in Eq. 3 to express absolute draught force depending on working depth.

From the profiles gained in the experiment the loosened area was estimated if the subsoiler tine ran 100 mm deeper. This gave three data points for each the track and the tyre enabeling the fit of a regression curve to determine the relationship of depth to loosened area. Knowing from Spoor and Godwin (1978) that specific draught force increases linearly with depth, the single draught force measurement for each treatment in section 5.2 was sufficient to derive a regression line.

It was possible to determine the following graph showing absolute draught force depending on working depth by substituting these empirically gained equations into Eq. 3:

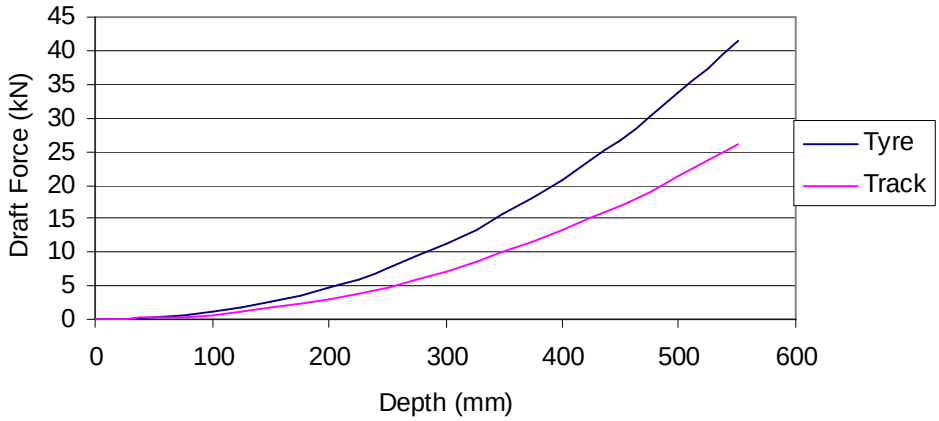

Figure 63: Draught force vs. depth for a subsoiler tine after the pass of a tracked and a wheeled combine harvester

From the penetrometer resistance for different undercarriage systems in Figure 28 the appropriate working depth on such a loose soil to alleviate the compaction caused by the pass of a combine harvester was set to 350 mm for the track as here the shape of the curve did

not change quickly anymore. For the tyre it was set to 450 mm as this is the maximum working depth commonly used and it is difficult to find equipment to work at greater depths. Going back into Figure 63 the chosen working depth of 350 mm for a track and 450 for a tyre resulted in 10 kN and 27 kN draught force, respectively.

For practical calculations the following assumptions were made:

- Loosening both wheel/track marks in one go => doubling the above draught force
- Approximately 1600 m track length per ha assuming a cutterbar width of 7.5 m and field efficiency of 0.83
- Working speed for subsoiling 2 m/s or 7.2 km/h

Knowing the required draught force the appropriate tractor weight can be calculated. For sustained working a slip σ of 13 % should not be exceeded resulting in a draught to weight ratio κ of 0.35 for a dry stubble field (Kutzbach, 2003). Therefore the weight of the machine has to be 1/0.35 times the required draught force. With the required draught force of 2*10 kN and 2*27kN, respectively, the tractor pulling the subsoiler after the tracked combine harvester has to weigh 57 kN and after the wheeled combine 154 kN.

The efficiency of the whole tractor is the product of the efficiency of the transmission and the draught efficiency η. With the given slip σ and draught to weight ratio κ η results from:

$$\eta = \frac{\kappa}{\kappa + \sigma} * (1 - \sigma)$$

Eq. 5

With the numbers from above η becomes 0.72. Gear box efficiency can be assumed to be about 0.85 (Kutzbach, 2003). Hence total efficiency results in 0.612. Running at 2 m/s, a tractor efficiency of 0.612 and a draught force requirement of 2*10 kN for the tracked and 2*27 kN for the wheeled machine results in power requirements of 65.4 kW and 176.5 kW, respectively. In Table 24 the tractor requirements are summarized.

Table 24: Power and weight requirement for tractors pulling a subsoiler

Treatment	Power Requirement (kW)	Weight Requirement (kN)
Loosening after Track	65	57
Loosening after Wheel	177	154

These requirements result in the tractor sizes shown in Table 24 necessary to conduct the operation (only examples, not necessarily all available and possible tractors included). Occasionally one example is put in not fitting the requirement.

Table 25: Required tractor specification to pull the subsoiler
(Specifications as in May 2006)

Brand	Required after Track	Required after Wheel
Claas	Ares 557 (75 kW, 48.2 kN plus additional weight of 10 kN)	Atles 936 (184 kW, 9.026 plus possible additional weight of 15kN) *Not heavy enough for requirement from* Table 24*!*
		Xerion (224 kW, 130 kN plus additional weight of 25 kN)
Fendt	Farmer Vario 409 (70 kW, 50 kN plus additional weight of 7 kN)	Vario 924 (186 kW, 88 kN plus additional weight of 32 kN) *Not heavy enough for requirement from* Table 24*!*
		Vario 930 (228 kW, 89,5 kN plus additional weight of 50 kN) *At the limit for requirement from* Table 24
John Deere	6220 (70 kW, weight not specified, yet should be sufficient with some additional)	8520 (217 kW, 140 kN max weight) *At the limit for requirement from* Table 24
		8230 (177 kW, 140 kN max weight, can be increased to 180 kN if demanded by customer)

According to Nix (2001) the category of tractors necessary after the tracked machine can be operated at 7.95 £/ha, the tractors necessary after the wheeled machine can be operated at 24.71 £/ha. These costs include all costs except the operator. The difference of nearly 17 £/ha would pay for the operation of two additional small tractors.

A different but simple approach just looks at the additional fuel consumption. The draught force difference between the track and the tyre was 17 kN. Taking the efficiencies from above into consideration, this resulted in 55.5 kW power per traffic lane. When assuming an engine efficiency of 45 % (Kutzbach, 2003) this meant 123.5 kW burning diesel which

in an hour accumulates to 123.5kWh. One liter diesel contains 9.8 kWh, resulting in 12.6 l /h more fuel. Relating this to fuel per ha, it was 6.3 l/ha. With the increasing fuel prices, just the difference in fuel cost could make a tracked combine harvester more efficient than a wheeled machine and justify the additional cost of 1£/acres (Tyrrell, 2005).

5.3 Draught Forces of Subsoiler in Field Situation

The same winged subsoiler utilizing the same method as in the soil bin was mounted to the back of a MB Trac 1300 and the draught forces at different depths in the ruts of the combine harvester treatments measured in the field. The data in Figure 64 and Figure 65 generally looks different than expected from normal draught force vs. depth curves as for example stated in Godwin and O'Dogherty (2003) whereby draught force increases exponentially with working depth. In these field experiments draught force did not increase strongly with depth between 200 – 350 mm depth for the clay and 150 – 250 mm for the sandy loam which is due to the lateral soil failure caused by the high moisture content of the soil of approximately 20 - 25 % for the sandy loam and about 35 % for the clay.

The draught force is plotted against depth for the clay soil in Figure 64. As mentioned before, draught force did not change between 200 – 350 mm and thus no regression functions were fitted to the data. Due to the small length of wheel ruts from the combine harvester at high inflation pressure the corresponding draught force data was not included in Figure 64. When loosening the soil in the rut after the pass of a wheeled combine harvester at normal inflation pressure a higher draught force was measured than for the rut created by the tracked machine, 25 kN per leg compared to 22 kN per leg, respectively. Correspondingly draught force for the control in the clay was smallest with 18 kN per leg.

Comparing the clay field to the sandy loam field overall, absolute draught forces decreased by approximately 33 % when looking at Figure 65 and comparing it to Figure 64. Due to the field set up and the necessity to gain constant working speed before taking measurements, draught force was only measured in the subsoiled plot on the sandy loam soil. The final working depth is slightly shallower on the sandy loam soil as the rut depths are deeper for the subsoiled part where the measurements were taken. Similar to the clay soil the draught force did not change significantly with depth.

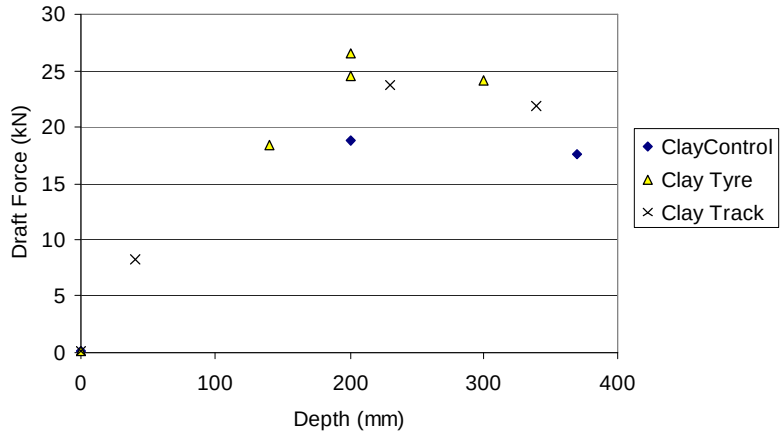

Figure 64: Draught force for subsoiling on the clay soil after the pass of combine harvesters

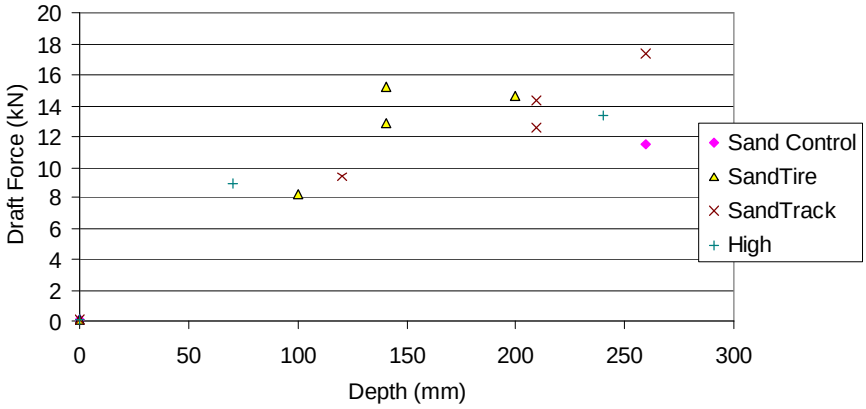

Figure 65: Draught force for subsoiling on the sandy soil after the pass of combine harvesters

On the sandy loam soil, pulling the subsoiler leg after the wheeled machine at normal inflation pressure required approximately 15 kN draught force per leg compared to about 13 kN for the tracked machine and 11 kN for the untrafficed soil (control). After the wheeled machine at high inflation pressure about 13 kN are necessary, too, however, only one data point was available for this treatment due to the short length of travel of the machine at high inflation pressure in the field. Consequently this configuration will not be discussed further.

The increase in draught force for the track was 18 % on the sandy loam and 22 % on the clay compared to the control. The increase of the wheeled machine was 36 % on the sandy loam and 39 % on the clay compared to the control. These similar increases indicated that the total effect of the machines onto the soil was similar, as on both soil types the relative

differences were similar. On either soil the pass of the tracked machine increases the required draught force by approximately 20 % compared to the control and the pass of the wheeled machine increased the required draught force by approximately 40 %. Thus the pass of the wheeled machine increased draught force by double the amount than the tracked machine.

5.4 Discussion and Conclusions on Draught Force

Draught force necessary to loosen soil after the passage of a wheeled machine is significantly higher than after a tracked machine on sandy loam in both the soil bin laboratory and the field. On the sandy loam soil in the laboratory and in the field experiment measured draught force was about 50 % greater for the wheeled machine than for the tracked machine. On the clay soil in the field, draught force was as well significantly higher for a wheeled machine compared to a tracked machine with a difference of 30 %. The increase in draught force is in accordance with the greater soil density caused by a wheeled compared to a tracked undercarriage system.

The increases mentioned above do not take into account that subsoiling after the pass of a wheeled machine should be carried out at a greater depth than after a tracked machine. Using laboratory results, a subsoiler run at 350 mm after a tracked machine and at 450 mm after a wheeled machine results in an additional 6.3 l/ha between the treatments from the laboratory data. Under these circumstances, power and weight requirements tripled from loosening a track rut to loosening a wheel rut.

Field results were harmed by the high soil moisture content. It did not create the soil failure necessary for loosening the soil above the tine, instead plastic failure was observed.

6 SOIL COMPACTION MODELS

The availability of a reliable and user friendly soil compaction model would enable researchers, machinery designers, manufacturers, farm advisers and farmers to evaluate the impact of machinery on soil density at the respective design selection and use stages. An important requirement is the option to quickly assess soil parameters, ideally in the field, to account for different soil conditions and enable accurate predictions for different soil conditions. With such a tool it would be possible to determine the impact of vehicles on the increase in soil density ahead of the treatment. The chosen approach to assess soil parameters will be compared to traditional methods and verified in field.

This chapter contains a literature review (Section 6.1), followed by a comparison of the pressure prediction of different soil compaction models and a sensitivity analysis (Section 6.2). After this a novel “in-situ” method to derive VCL parameters will be introduced and validated both in the soil bin and in the field (Section 6.3). In the following Section 6.4 the approach to derive VCL parameters in-situ is validated for tracks. Then, the method developed in the soil bin laboratory with tyres and track is utilized by small scale plate sinkage tests (Section 6.5), further validating the entire approach. In the following Section 6.6 the VCL parameters gained in the soil bin are compared to parameters determined using the classical triaxial cell test apparatus. In a subsequent step (Section 6.7) traditional plate sinkage predictions using the Bekker approach are compared to the measured rut depths. A mathematically drawn similarity found in literature between triaxial and plate sinkage tests will be subsequently discussed (Section 6.8). Finally (Section 6.9) the possible influence of peak vs. average contact pressures on the developed methodology will be considered and the chapter closes with an overall discussion and conclusion (Section 6.10).

Appendix 1 contains additional detailed information concerning Sections 6.2 throughout to 6.8. Consequently, some of the figures given in the thesis sections will be repeated in the Appendix allowing the reader to easily follow the argumentation.

6.1 Literature Review

The material in the literature review was selected to provide 1) an overview of model types, 2) an update on published material since the more recent reviews, 3) review the pos-

sibilities to obtain the mechanical parameters of the soil, and 4) derive a conclusion from literature.

6.1.1 Theoretical Background of Soil Compaction Models

Preliminary soil compaction models can be divided into empirical models and soil mechanics models. The available soil mechanics models describe qualitatively the true impact of different treatments on soil compaction. However, quantitatively they fit best the data they were originally generated for. Reasons for this are the influence of organic matter, soil moisture content, soil type, and physical soil structure on both pressure transmission within the soil and on soil compactability.

At a first glance these facts increase the attractiveness of empirical models. However, to generate an empirical model one has to use large amounts of input data in order to make it reliable and applicable in a range of situations. The second drawback is the fact that it contributes little to the fundamental understanding of soil physical behavior and soil physical laws.

Soil mechanics models are usually a combination of soil mechanical principles and numerical techniques. Most models use either a finite element analysis or some approach which can be categorized into elastic theory and minor extensions of it. The advantage of taking the elastic theory approach is that it is a simple route for improvement and cannot only predict stress, but predict both stress and strain using Young's Modulus and Poisson's Ratio. A slightly different approach based on the elastic theory is the critical state soil mechanics which aims on describing volumetric soil response in regard to soil hydrostatic and shear stress. This was implemented by both Schofield and Wroth (1968) and Kurtay and Reece (1970). A detailed description of elastic soil modeling is given by Wulfsohn and Adams (2002). The authors describe the basics beginning with a purely elastic behavior following Hooke's law (which was utilized by Soehne, 1953 and all approaches based on his work) and finishing with a detailed explanation of Critical State Soil Mechanics. On the contrary FEA models are difficult because they require many empirically determined input parameters. Critical state soil mechanics theory was initially developed for saturated clay soils, and later used to explain behavior of agricultural soils for example by Spoor and Godwin (1979). Towner (1983) describes the stress state in partially saturated soils with

respect to critical state soil mechanics, whereby he states that the theory of critical state soil mechanics is valid for partially saturated soils, however, it should be kept simple as the total stress states have not been proven yet, but can well be used as a working hypothesis. The study by Adams and Wulfsohn (1998) showed that the critical state soil mechanics can explain agricultural soil behavior and that it is possible to identify critical state soil mechanics parameters for unsaturated soils. The critical state concept is applicable to unsaturated soils both quantitatively and qualitatively except that the critical state parameters depend on the soil moisture content according to Hettiaratchi and O'Callaghan (1980), Hettiaratchi (1987), and Kirby (1989). Additionally they found that it is reasonable to use total stress and consequently ignore soil moisture tension. Following these authors it is possible to utilize the complex critical state soil mechanics framework to describe soil compaction.

An example of an empirical soil compaction model is the one developed by Adam and Erbach (1995) who empirically measure soil compaction by determining the depth to which DBD changes less than 5%. They could fit one exponential equation to the data similar to Bekker (1960) as the depth of soil compaction was not significantly affected by the water content on the silty clay loam used for their investigation.

Excellent reviews of soil compaction models were done by Seig (1985) and afterwards by Defossez and Richard (2002). Both summarized and grouped the different approaches to predict soil compaction at their times.

6.1.2 Latest Soil Compaction Models

Since the last reviews on soil compaction modeling by Seig (1985), Defossez and Richard (2002) and Ansorge (2005, a), Keller et al. (2007) have created a model called SOIL FLEX. It includes the soil displacement approaches of O'Sullivan et al. (1998), Bailey and Johnson (1989), and Gupta and Larsson (1982). In all the models used soil strength increases with strain, i.e. strain hardening applies. Gupta and Larson (1982) describe volume change with a relationship between bulk density and the logarithm of the major principal stress. Bailey and Johnson (1989) describe the natural volumetric strain in dependence of octahedral normal stress and octahedral shear stress. O'Sullivan et al. (1998) (COMPSOIL) use a critical state soil mechanics approach whereby the specific volume

depends on the natural logarithm of the mean normal stress. This approach is described in detail by Ansorge (2005, a). Thus in SOIL FLEX the user can choose the theoretical background he wants to utilize. Stress distribution is based on Söhne (1953) with an added shear component. For stress distribution in the contact area a variety of approaches can be selected. In section 6.2 two of these predictions will be compared to results of both Ansorge (2005, a) and this study.

Within SOIL FLEX this work will only consider the model COMPSOIL as this requires the least amount of parameters to be estimated while maintaining all output parameters. COMPSOIL only needs an estimation of the slope and intercept of a virgin compression line. For subsequent passes the slope of the recompression line has to be calculated. Thus overall only three parameters are needed. Gupta and Larson (1982) need similar parameters, a reference bulk density and a reference stress state on the VCL, i.e. an intercept of the VCL; and the slope of the VCL. Additionally the model of Gupta and Larson (1982) requires the slope of the bulk density vs. degree of water saturation curve and the desired degree of saturation minus the actual saturation at a reference bulk density. Thus this model requires an additional three parameters and moreover, the recompression index is equal to zero, assuming no elastic rebound, which can lead into difficulties predicting subsequent passes. The model of Bailey and Johnson (1989) requires four compactability coefficients of which two are dimensionless and two have dimensions of [kPa^{-1}]. The empirical determination of this number of coefficients requires a large data set to adapt the model to a certain soil condition. Keller et al. (2007) give for each of the three models pedo-transfer functions from literature to be able to adapt each individual model to given soil conditions. However, determination of variables from pedo-transfer functions is time consuming as it involves extended laboratory testing.

Another approach concerning soil compaction models and the prediction of soil compaction was developed by Diserens and Spiess (2004) (TASC for “Tyre/Tracks and Soil Compaction”) and is based on the principles of Etienne and Steinmann (2002) who developed a stress distribution model utilizing the approach of Newmark (1940) for stress propagation in the soil. This model is in theory and approach similar to the model from van den Akker (2004) (SOCOMO; described in detail by Ansorge 2005, a), yet it takes a different approach in both calculated pressure distribution and the occurrence of soil compaction. It merely looks at the soil pressure rather than a combined failure criteria as in SOCOMO.

The approach of Etienne and Steinmann (2002) was empirically developed using Bolling pressure probes. Soil stresses were measured at three depths and compared to the predicted results from 5 different approaches; three types of Söhne (1953) each with a different concentration factor, a combined Boussinesq and Froehlich approach, and the Newmark (1940) model. The approach by Newmark (1940) only differs by the concentration factor from Söhne (1953) as Newmark (1940) always assumes a concentration factor of 2. Stress propagation in the soil is determined using the Newmark (1940) approach as it showed the closest agreement between measured and predicted values. However, the stress decrease at the surface was larger than predicted; therefore a variable in addition to soil type and working depth was introduced determining stress decrease in the topsoil. This variable depends on the surface soil strength because stress decrease is smaller with depth for a stronger soil. This is the only input variable concerning soil conditions and is determined with a screw driver. Depending on the force necessary to push the screw driver into the soil, the soil can be qualified in soft, medium, and hard. This basic principle was extended into a model by Dieserens and Spiess (2004). It contains nearly all common agricultural and forestry tyres and tracks as input options whereby contact pressure data is stored within the model. Once the tyre or track option is selected, only load, inflation pressure, working depth, and the strength of the topsoil determined with the screwdriver test have to be entered. The model then determines the pressure distribution in the soil and states if there is a danger of subsoil compaction or not. If the pressure decreases to less than 1 MPa within the working depth, the model implies no danger of subsoil compaction, but if the pressure is higher than 1 MPa below the working depth, it assumes subsoil compaction. Additionally pressure bulbs and maximum pressure over depth curves are given. The model can compare up to four different tyre or track systems in one analysis.

A great advantage of TASC is its user friendliness when compared to SOCOMO which gives similar outputs. In contrast to the models SOCOMO and TASC, COMPSOIL is able to quantify the soil density increase rather than simply stating a danger of soil compaction for given loads and inflation pressures.

6.1.3 Approaches to derive Critical State Parameters and the Influence of Water

For the critical state soil mechanics model e.g. for COMPSOIL the slope and intercept of the VCL have to be determined. Following the traditional approach from Schofield and

Wroth (1968) critical state parameters are usually obtained from triaxial cell tests. A description of the procedure can be found by Leeson and Campbell (1983). However, multiple tests are necessary which are rather time consuming. Improving this Kirby et al. (1998) derive all critical state soil mechanics parameters from one constant cell volume triaxial test. Kirby (1998) developed a further method to estimate all critical state soil mechanics parameters from shear box tests. This, however, requires multiple testing, but is less time consuming than conducting triaxial tests.

Gregory et al. (2006) calculated the slope of the virgin compression line and the precompression stress from compression test data and show that the accuracy of the prediction of the parameters increases when the clay content increases.

A totally different approach is taken by Gurtug and Sridgaran (2002), who, "*out of coincidence*" obtained compaction characteristics of soils from plastic limit tests for fine grained soils. The plastic limit test can even be reproduced if the procedure is carefully followed.

However, as the following authors stated, there are differences between triaxial measurements and field conditions. Jakobsen and Dexter (1989) point out that due to the shorter loading time soil is not completely compacted in the field and consequently, the field parameters can not be readily derived from measurements in the laboratory from samples of small size. Roscoe (1970) comes to the same conclusion that the laboratory measurements do not represent real field conditions. Hence deriving a methodology to gain them from tyre passes and quantifying the difference to triaxially gained parameters is even more important. Chi et al. (1993) analyse the prediction behaviour of elasto plastic models and critical state soil mechanics models and derive the conclusion that the main source of error in prediction is the variability of soil physical properties among samples. This emphasizes the advantage of an infield determination of necessary variables as sample size increases tremendously when taking the ruts of machines in consideration compared to small samples fitting into triaxial cells which can differ from each other and no true replication of field conditions is possible as stated by Roscoe (1970) and Jakobsen and Dexter (1989).

The moisture content influences both, stress concept and critical state parameters. The work by Jennings and Burland (1962) indicates that it is not the total effective stress which controls the behaviour of partially saturated soils, it is rather the sum of the stress and wa-

ter/air potential individually. There is some evidence that this appears to apply for both sand and clay soils. This conclusion can be drawn as Jennings and Burland (1962) experienced changes in soil behaviour which are not accounted for by the effective stress principle. However, as it is possible to draw the influence of water content on soil physical properties rather than on stress, effective stresses can be used again as pointed out in section 6.1.1. Therefore it is necessary to be able to adapt critical state soil mechanics parameters to the given moisture content. This requires the effective moisture content to stay constant during compaction which can be assumed for short term loadings such as from tyre passes in the field.

Wheeler and Sivakumar (1995) showed that the intercept of VCL increases with an increase in suction, whereby the slope showed little variance with suction in the range of 100-300 kPa. But the slope falls significantly if the suction is reduced to zero. Toll and Ong (2003) developed a function which relates critical state soil mechanics parameters to the degree of saturation in a normalized form by referencing them to the saturated state. It can be a good way of adding the influence of water content on soil compaction and critical state soil mechanics parameters. A typical critical state soil mechanics modelling approach was undertaken by Blatz and Graham (2003), but the authors added the influence of soil moisture tension to the stress strain relationship and its recovery from swelling. A review of recent models which account for and do not account for the influence of soil water content is included in the paper by Gallipoli et al. (2003). Following the review the authors create a yield surface to incorporate changes in void ratio from drying and use it to account for different soil moisture contents. However, this approach is also based on triaxial tests.

Ghezzehei and Or (2001) showed that wet soils have viscoplastic behaviour with a well defined yield stress and nearly constant plastic viscosity. However, rapid transient loading is often too short for complete viscous dissipation of the applied stress which results in an elastic component (viscoelastic behaviour) whereby low water contents and fast loadings increase the elastic component of displacement. In general high water contents decrease viscosity and shear modulus.

The depth to which an increase in soil density is measurable is not influenced by the water content (Adam and Erbach, 1995) and thus the influence of the water content may be ignored to some extent, as under wet conditions the soil is compacted to the same depth,

however, the overlying layers can be compacted significantly more. The general influence of water content on predicted soil displacement was shown by Defossez et al. (2003) who further improved SOCOMO with respect to water content. Still with adjusted parameters, the deviation between measured and predicted values was larger than the 95%- CI.

From all the studies into soil mechanical parameters, it can be concluded that an in-situ approach to determine VCL parameters from tyre passes would be beneficial.

6.1.4 Basic Considerations on the Modeling of Soil Compaction

The fact that plenty of work was conducted concerning the prediction of soil compaction while at the same time no model is able to suit different conditions entirely rose the question why this is the case. Basically soil can be regarded as a granular media and it should obey the physical laws of granular media. Therefore the author did an extended literature review concerning the physics of granular media. A summary of the most recent findings was edited by Hinrichsen and Wolf (2004). Most research was done concerning the flow of granular media. At the peak of the review the author read an article by Haff (1997) concerning the difficulties in predicting the behavior of geological granular systems. Haff (1997) points out the fact that the prediction is difficult “not because of the lack of knowledge in physics of geologists, rather because of a complex behavior of environmental material (sand, soil, galaxies etc.)”. If a granular medium consists of a well grained and evenly shaped powder, physical laws can be developed and the material obeys these laws. However, as soon as either the powder is not well grained and/or not evenly shaped these physical laws cannot be transferred one to one onto a different powder as the variables triggering this behavior cannot be either specified accurately or even specified. The following example points out this behavior excellently. In pure water one molecule is identical with another. Each has the same shape, size and weight. However, already sand, which in soil scientist circles is regarded as uniform and “easy” to predict, differs from one grain to another in mass, size, shape, and friction. Thus all these values have to be averaged and a particular investigation in a controlled laboratory environment can be repeated as long as it is possible to keep the average values sufficiently close. The behavior of the naturally best sorted and particularly well grained sand dunes is difficult to predict even after in depth investigations. Thus, moving from sand to soil adds the difficulty of non identical grains as size distribution varies a lot and does not merely contain sand. Thus the shape of the parti-

cles varies even more. The organic matter content of real field soil adds to the difficulty of the system as it changes across a field. Not to mention the implication of water content on the behavior of soil, particularly cohesion and friction (Spoor and Godwin, 1979).

In the following examples are chosen to show the effect of certain parameters on grain behavior and the complexity of the physics involved.

Delie and Bouvard (1997) show that spherical inclusions are easier to compact than angular inclusions. The effect of particle size and bond strength on the breakage of lactose agglomerates was shown by Ning et al. (1997). The effect of humidity in monodisperse glass beads on quasi - static behavior of granular media was shown by Fraysse (1997). Even the rotation of particles changes mechanical behavior of granular media, i.e. the failure and dilatancy of the media (Oda et al., (1997)).

The characteristics of force distributions in granular media is shown by Radjai et al. (1997). The authors show that the contact network consists of two complementary sub-networks. Firstly a strong sub-network ranging through the whole media and carrying a force larger than the average force. Secondly, the weak sub-network carrying less than the average pressure. The weak sub-network is responsible for the dissipation of the stress whereby the forces decay in a power law function. In the strong sub-network forces have a decreasing exponential distribution. As the contacts in the strong sub-network are non-sliding contacts, these contacts carry the whole deviatoric stress. These results are based on a numerical simulation of a few thousands of particles in two dimensions and are expected to theoretically agree with the real soil conditions.

6.1.5 Discussion and Conclusions on Literature

All the results from above show the important decision every scientist has to make when trying to model the behavior of granular material. It is a decision between the trial to come to a mere physical approach including all variations and differences between different media in one equation or a more general approach just accounting for the behavior of the material observed while being robust against inherent variations at the grain level. The approach taken by Etienne and Steinmann (2002) with their screwdriver test is a good example of a general approach accounting for large variations and being robust on the grain

level. Critical state soil analysis might be an appropriate way if it was possible to define critical state soil parameters either directly or at least indirectly with a test as easy as for example the screwdriver test. The advantage of the critical state soil analysis is the possibility to predict real changes in soil density, rather than "just" defining a threshold value above which soil compaction is expected to happen.

6.2 Comparison of Soil Compaction Models

The variety of approaches used to model and estimate soil compaction rose the question how their performances compare and whether it is possible to tune variables such that the predictions agree with the measured data. This is only a digest of the entire comparison. The detailed version can be found in the Appendix 11.1.1. Most soil compaction models give different final outputs ranging from final DBD (O'Sullivan et al., 1998/COMPSOIL) through the prediction of an area of excess of soil stability (van den Akker, 2004/SOCOMO) to just a danger of soil compaction (Etienne and Steinmann, 2002/TASC). Their common basis is the calculated stress propagation in the soil leading to the final prediction of soil compaction. Thus comparing their performance in stress prediction to measured stresses in the soil bin can determine the accuracy of these models. Therefore this section contains a comparison of soil compaction models with respect to pressure prediction followed by a sensitivity analysis of COMPSOIL and SOCOMO.

6.2.1 Comparison of Pressure Prediction

The vertical stress propagation predicted by SOCOMO, COMPSOIL, and TASC was compared to measured stresses from the soil bin during the project conducted by Ansorge (2005, a).

COMPSOIL overpredicted the stresses compared to the measured stresses in all cases considered; hence showed poor agreement between measured and predicted values. SOCOMO showed the closest prediction to the measured parameters at the soil surface, although the predicted soil stresses were too high except for one data point. At depth the TASC model gave good estimations and predicted soil pressures closer to the measured ones than SOCOMO. It is not clear why or how, yet interestingly stress decrease with depth seems too small for SOCOMO compared to reality.

There was close agreement between the predicted and the measured soil pressures despite the detailed differences stated above. Hence, the pressure prediction cannot explain the large differences between measured and predicted soil displacement found by Ansorge (2005, a). Therefore parameters translating the pressure distribution into soil behavior have to be responsible for the disagreement.

The benefical effect of the simple surface screw driver test included in TASC to account for soil variability, raises hopes for a possibile improvement of predicting soil behavior utilizing an easily obtained parameter describing soil physical behavior and improving prediction accuracy. TASC is the only model with such a feature. All other models involve laboratory testing or at least laboratory test equipment to assess soil strength.

Estimation of Contact Pressure

The semi-empirically estimated contact pressure from O'Sullivan et al. (1998), which is equal to σ_1 in their model, is in good agreement with the contact pressure determined from measured contact area and tyre load from Ansorge (2005, a) and this study as shown in Figure 66. The slope of the regression line is close (-2.5%) to 1 and the coefficient of determination (R^2) is high. In comparison to this the contact pressure estimation utilizing the super ellipse of Keller (2005) shown in Figure 67 has a smaller R^2, the slope deviates more from 1 and in addition the intercept is also larger.

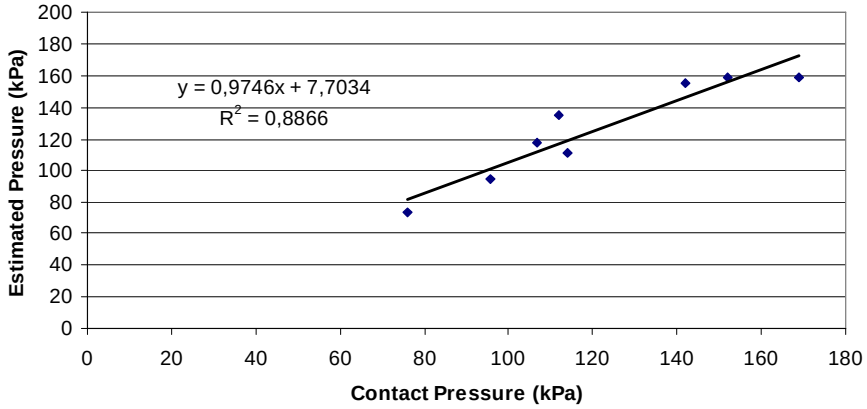

Figure 66: Estimated pressure from O'Sullivan et al. (1998) vs. contact pressure for tyre loads

Utilizing Keller's (2005) super ellipse as input contact stress in SOILFLEX did not result in an improvement of stress predictions within the soil.

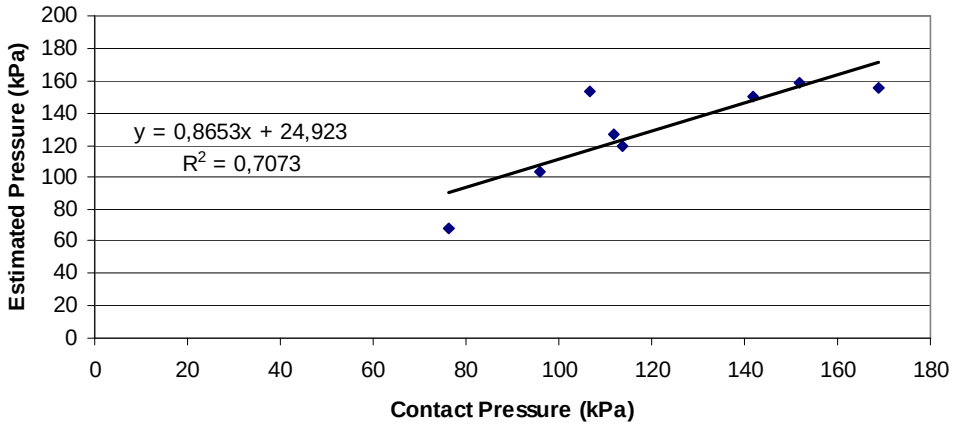

Figure 67: Estimated pressure from Keller (2005) vs. contact pressure for tyre loads

6.2.2 Sensitivity Analysis of Soil Compaction Models

The small differences in stress propagation predicted by the models (Section 6.2.1) cannot be the reason for the significant differences between predicted and measured soil deformation found by Ansorge (2005, a). This raises the question as to whether the default initial soil parameters used by the models are appropriate for the given soil type and conditions. Consequently a sensitivity analysis of SOCOMO and COMPSOIL was conducted (TASC only computes stresses).

SOCOMO

One of the most important parameters determining soil compaction is the value of preconsolidation stress in the soil for the SOCOMO model (van den Akker, 2004). Preconsolidation stress shows to which mechanical and hydraulic stresses the soil has been laden to in its history. Thereby indicating to which amount of stress the soil can be laden without further unrecoverable volume change (Baumgartl and Koeck, 2004); a detailed explanation is given by Ansorge (2005, a) or Gregory et al. (2006).

The prediction by the model only agrees to a certain extend with the experiments. Changes of preconsolidation stress produced variations in soil failure only up to a certain threshold

value. A further increase in preconsolidation stress did not produce a consecutive decrease in soil failure as expected. Full details can be found in Appendix 1/1.1.2.1.

COMPSOIL

The model SOILFLEX (Keller et al., 2006) provides the possibility to change critical soil mechanics parameters embedded in COMPSOIL directly while keeping both initial DBD and soil moisture content as given in the experiment. From theory an increasing magnitude of the slope of the virgin compression line means that increases in DBD result from smaller pressure changes. A decreased intercept means less pressure for the same DBD.

With a reduction in the intercept soil compaction increased significantly. With a slope of ~ 0.15 the results came into the range measured in the soil bin by Ansorge (2005, a). The recompression lines were not changed because their influence can be ignored for single passes. Changing VCL parameters it was possible to improve predictions significantly.

6.2.3 Discussion and Conclusions on Comparison of Soil Compaction Models

The comparison of measured and calculated pressure showed some deviation, yet the magnitude is too small to explain the differences in soil compaction seen especially with COMPSOIL. Changing critical state soil parameters to fit the data seems a promising way to adapt a soil mechanics models for a particular soil. Following the proposal for an in-situ access to VCL parameters in Section 6.1.5, this will be the aim of the following Section.

6.3 Derivation of VCL Parameters from Soil Bin and Validation/Evaluation

The compression behaviour of soil is shown in Figure 68 as a function of soil volume depending on the exerted pressure. The soil indicates a semi-logarithmic relationship of volume with pressure. If the pressure is plotted on logarithmic scale and the volume is replaced by the relative density of the soil, the virgin compression line (VCL) is derived. The VCL as defined by Schofield and Wroth (1968) is a unique function relating the relative density of a soil at a given moisture content to the natural logarithm of the spherical pressure it is subjected to. According to their definition spherical pressure is the arithmetical

average of major, intermediate, and minor principal stresses: σ_1, σ_2, and σ_3, respectively. As mathematically this is also the definition of the mean normal pressure p, this thesis will use the term mean normal pressure after O'Sullivan et al. (1998). Therefore the virgin compression line basically describes soil density in dependence of exerted stress.

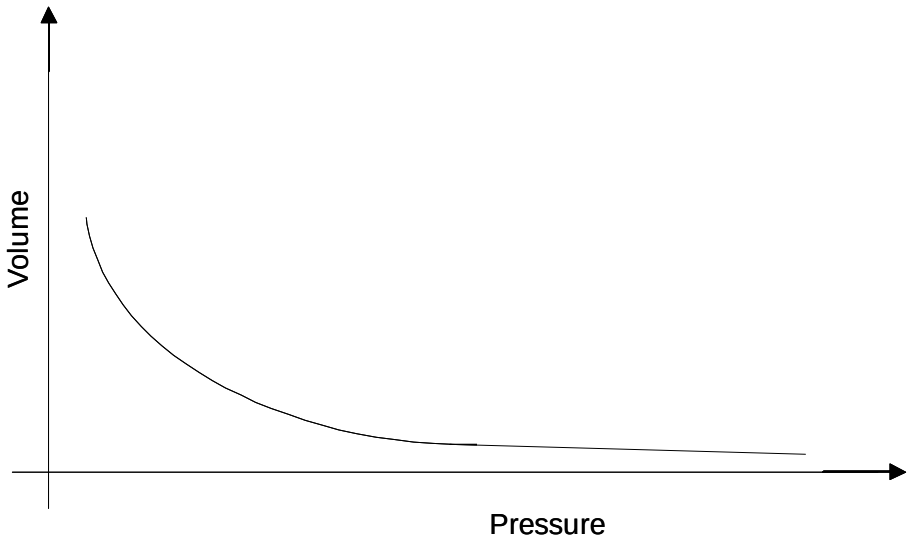

Figure 68: Compression behaviour of soil

An approach to gain information about the VCL is to investigate the slope of the soil displacement curves from this work and the work by Ansorge (2005, a) in the soil bin laboratory. Soil density can be gained from initial density and the slope of the soil displacement curves which were assumed to be linear over the upper 0.5 m for each treatment as first assumed by Ansorge (2005, a) and in detailed reconsidered in Section 2.2.1.1. The contact pressure can be calculated below a tyre from the known area and known load, assuming uniform stress distribution over the contact area. The exerted stress for the VCL model is in some relation to this contact pressure. Knowing the initial soil stress exerted by the roller during soil bin preparation and knowing the resulting initial soil density gives the first point on the virgin compression line. Knowing the increase in density for different contact pressures the virgin compression line can be created and the recompression line could be gained from multi passes. If in a future step it was further possible to determine the virgin compression line just from tyre sinkage at two different inflation pressures, a very important characteristic of soil compaction could easily be determined in the field.

In a first step (Section 6.3.1) this "in-situ virgin compression line (in-situ VCL)" will be derived from theoretical considerations. Afterwards (Section 6.3.2) the in-situ VCL is created utilizing treatments from the soil bin. The in-situ VCL will be validated with independent soil bin laboratory data (Section 6.3.3) and the entire concept validated in field conditions (Section 6.3.4). In the subsequent section (Section 6.4) the in-situ approach will be applied to tracks. Then the in-situ VCL approach is repeated with small scale plate sinkage experiments (Section 6.5). After gaining the slope and intercept of the in-situ VCL, these parameters will be verified in a triaxial cell test apparatus (Section 6.6).

6.3.1 Theoretical Considerations

The Cam-Clay model COMPSOIL (O'Sullivan et al., 1998) provides an estimation of soil displacement for a sandy loam soil from tyre data and DBD whereby COMPSOIL calculates VCL parameters depending on moisture content.

An initial comparison of soil displacement measured by Ansorge (2005, a) for a sandy loam to the data predicted by COMPSOIL using the VCL parameters suggested by O'Sullivan et al. (1998) is given in Figure 69 originating from Ansorge (2005, a). This shows very large deviations for both uniform and stratified soils, which in turn suggests that either the soil specific parameters used to describe the sandy loam soil of the model are not adequate to describe the sandy loam soil used in the soil bin or there are substantial errors in the model. The latter is unlikely as O'Sullivan et al. (1998) demonstrated close agreement. Consequently the VCL parameters for the sandy loam of the Cotternham Series (which was used by Ansorge (2005, a) and this study) have to be different from the sandy loam soil described by O'Sullivan et al. (1998) and used by the original COMPSOIL model and hence need to be determined.

A VCL is usually obtained from plotting the relative density (ratio of the maximum soil density (2.66 g/cm^3) to the resulting dry bulk density) against mean normal pressure measured with triaxial cell tests. For the assessment of the in-situ VCL in the soil bin the relative density is obtained by adding the average density increase measured by Ansorge (2005, a) and this study to the initial soil density. Mean normal pressure is obtained from the contact pressure following a transformation after O'Sullivan et al. (1998).

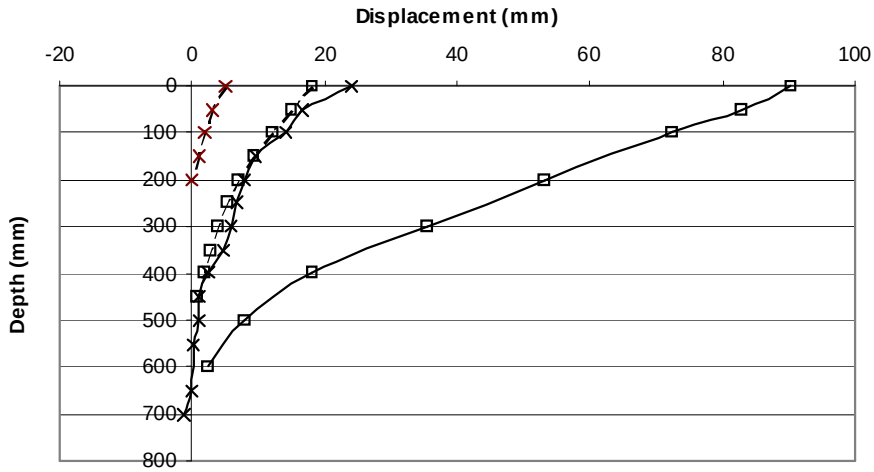

Figure 69: Measured (solid line) and predicted (broken line) soil displacement for 900mm section width tyre at 10.5t load and 1.9bar inflation pressure on uniform (□) and stratified (×) soil conditions (measured data from Ansorge, 2005, a)

This approach does not take into account the elastic recovery of the soil, and consequently will potentially yield a VCL indicating the soil to be slightly too strong.

A calculation, detailed in Appendix 11.1.2.1, yields a 0.87 % error from neglecting elastic recovery for the relative density measurement indicating a marginally stronger soil. This small error is accepted as it will affect all treatments similarly.

6.3.2 Practical Derivation of VCL Parameters

As shown in 6.2.1 the semi-empirically estimated contact pressure from O'Sullivan et al. (1998), is in good agreement with the contact pressure determined by Ansorge (2005, a) and this study. The confining pressures σ_2 and σ_3 can be derived from the following equation gained by O'Sullivan et al. (1998) from empirical regression lines:

$$\ln\frac{\sigma_1}{\sigma_n} = c_1 * z - c_2 * A + c_3 * \xi$$

Eq. 6

where z is the depth (m), A is the contact area (m^2) and ξ is the concentration factor. c_1, c_2, and c_3 are constants whose values are given in the Appendix and depend on the calculated stress ratio.

To calculate σ_2 and σ_3 Eq. 6 would have to be solved for all tyres at each depth within the soil. To simplify the approach a depth z of 0.4 m representing the average depth in the soil profile and a contact area A of 0.8 m^2 were assumed and ξ was varied from three to five representing possible soil conditions (dense to soft) as proposed by Fröhlich (1934). The resulting dependencies of σ_2 and σ_3 on σ_1 are given in Appendix 11.1.2.2.

In a first approximation $\xi = 5$ was chosen to calculate p from the contact pressures given in Table 26 of the treatments by Ansorge (2005, a) and this study. Knowing the initial density of 1.38 g/cm^3 and the average increase, final density can be calculated. Relative density (RD) is gained by dividing final dry bulk density (Final DBD) into 2.66 g/cm^3. The average increase (AvI), the final DBD and RD are also given in Table 26.

Table 26: Treatments and corresponding increase in DBD, final DBD, relative DBD and σ_2 and σ_3, contact pressure and mean normal pressure for $\xi = 5$

Treatment (Section width[mm]/Load [t]/Inflation Pressure [bar])	AvI (%)	Final DBD (g/cm^3)	RD	$\sigma_2 + \sigma_3$ (kPa)	Contact Pressure (σ_1) (kPa)	P (kPa)
900/5/0.5	5.66	1.458	1.817	29	76	35
500-70/4.5/2.3	14.27	1.577	1.681	54	142	65
500-85/4.5/1.4	11.06	1.533	1.729	42	110	51
600/4.5/1.4	11.00	1.532	1.730	43	114	52
700/4.5/1.0	10.59	1.526	1.736	36	96	44
900/10.5/1.9	17.30	1.619	1.637	43	112	52
800/10.5/2.5	17.36	1.620	1.636	64	169	78
800/10.5/1.25	11.59	1.540	1.721	41	107	49
680/10.5/2.2	17.73	1.625	1.631	58	152	70
Roller		1.380	1.928	22	58	26

Figure 70 shows relative density vs. mean normal pressure. A logarithmic regression line was fitted to the data points representing the in-situ VCL for the sandy loam soil at a mois-

ture content of approximately 9 % at which the experiments were conducted. The VCL for the sandy loam soil given by O'Sullivan et al. (1998) is also included for reference.

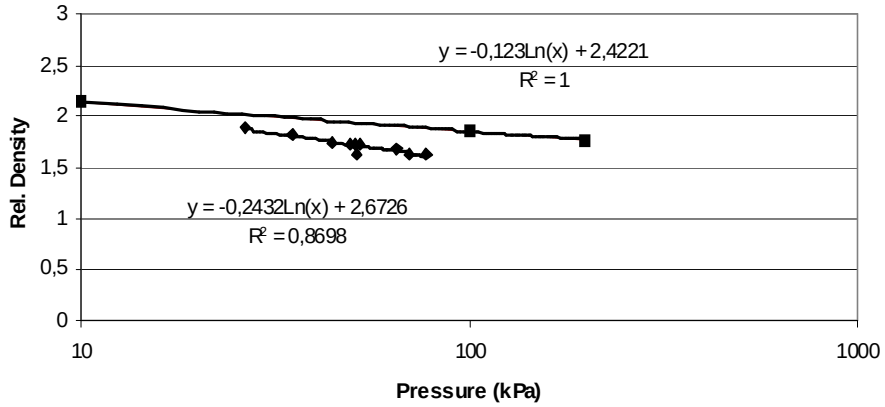

Figure 70: Virgin compression line for sandy loam soils ■ from O'Sullivan et al. (1998) and ♦ from the soil bin studies based on the average density increases from Ansorge and Godwin (2007a)

The intercept and slope of the in-situ VCL were used in COMPSOIL. The prediction performed with these modified parameters is compared to the measured data in Figure 71 for six individual tyres and close general agreement was achieved. Soil displacement is successfully predicted using COMPSOIL and the parameters of the in-situ VCL obtained from the soil bin experiments with a heuristically chosen concentration factor of ξ=5 suits best. The effect of other ξ is evaluated in Appendix 11.1.2.2.

Fitting linear regression functions through the top 500 mm of the measured and predicted data of Figure 71 estimating the average increase in soil density as described by Ansorge and Godwin (2007a) and plotting the measured against predicted average density increase results in close agreement as shown in Figure 72 to within +/- 2 % errors. The data is spread randomly around the line of slope 1 and does not exhibit a general offset confirming the choice of ξ = 5. Fitting a linear regression line shows a marginal overprediction of 0.8% and the R^2 = 0.85 confirms the overall effectiveness of the technique.

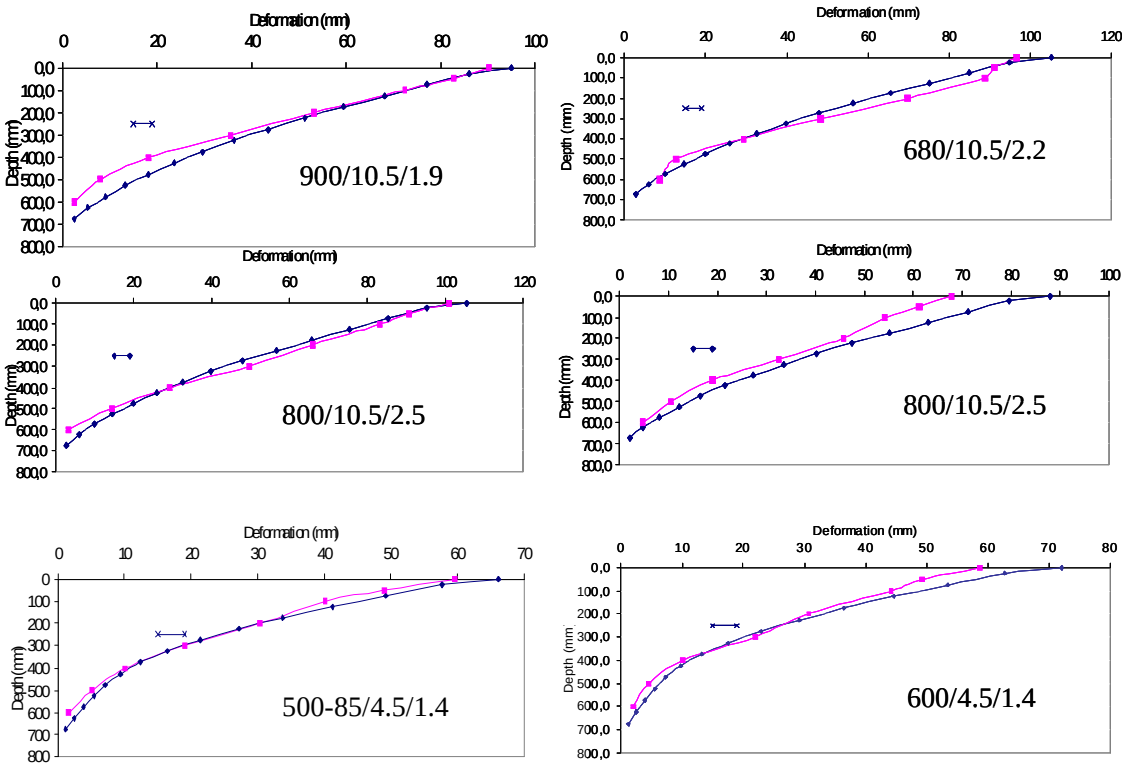

Figure 71: Measured (■) and predicted (♦) soil displacement for tyres with a concentration factor of 5. Least significant difference (LSD) at 95 % is also shown

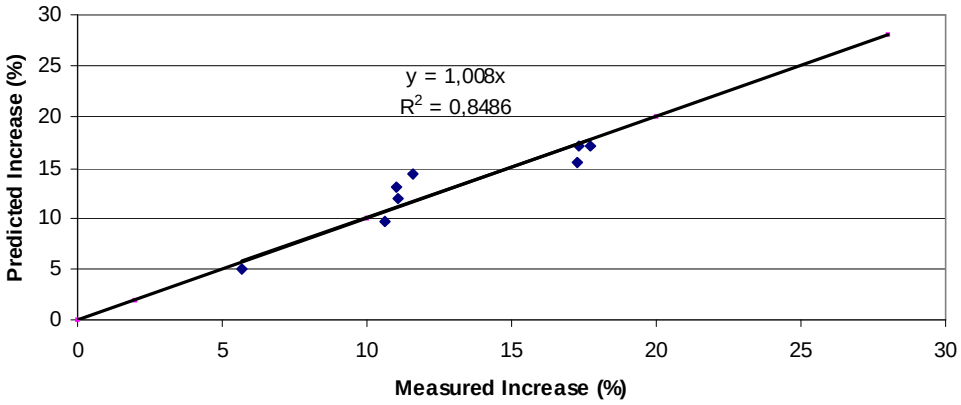

Figure 72: Measured vs. predicted average percentage increase in soil density

6.3.3 Prediction of Independent Data

It was an important step to be able to show that COMPSOIL is self consistent with a soil specific VCL which is able to reproduce the input data used to derive the specific VCL. However, for complete justification of the approach the modified model will be compared

with four other data sets from the same soil but not utilized for the development of the in-situ model. To do this:

1. Data generated by Antille (2006) using the single wheel tester designed by Ansorge (2005, a) with the same tyres at identical loads and inflation pressures with more dense (1.6 g/cm^3) and less dense (1.2 g/cm^3) soil conditions. This aimed at justifying the appropriateness of this VCL more generally for different initial dry bulk densities.
2. Data generated by a pass of the 900/10.5/1.9 tyre on stratified soil conditions simulating field conditions and investigating the ability of the model to deal with different soil densities within the same profile. This data originated from work of this thesis and Ansorge (2005, a).
3. Data generated by two sets of multiple (3) passes on the uniform medium soil condition. The tyre used was the 900 mm section width tyre, having the 900/10.5/1.9 and 900/5/0.5 configuration, respectively. This was targeting the performance of the model with respect to loading-unloading cycles and included the opportunity to adjust the recompression and reloading parameters. The data originated from Ansorge (2005, a).
4. Data from this thesis which was generated by the passage of whole combine harvesters and used to explore the possibility to predict the soil displacement after a pass of whole combine harvesters over medium soil conditions.

6.3.3.1 Dense and Loose Soil

Following the ability to reproduce the input results as shown above, the prediction is extended onto different densities of the same soil type. Therefore the results from Antille (2006) were compared to the theoretical predictions. Antille (2006) used the same high axle load tyre configurations as Ansorge (2005, a) with the same soil type and water content, only at a looser DBD of 1.2 g/cm^3 and at a denser DBD of 1.6 g/cm^3. The accuracy was evaluated from the calculated average density changes for the predicted and the measured soil displacement shown in Figure 73 and plotted against each other in Figure 74.

From Figure 74 a close agreement can be seen between the measured and the predicted increase in soil density for the data from Antille (2006). The accuracy is within an absolute error of +/- 3 %. The linear regression line shows that the increase is underpredicted by 1.5% compared to the 1:1 line, however, linearity of the data is confirmed with an R^2 of 0.95.

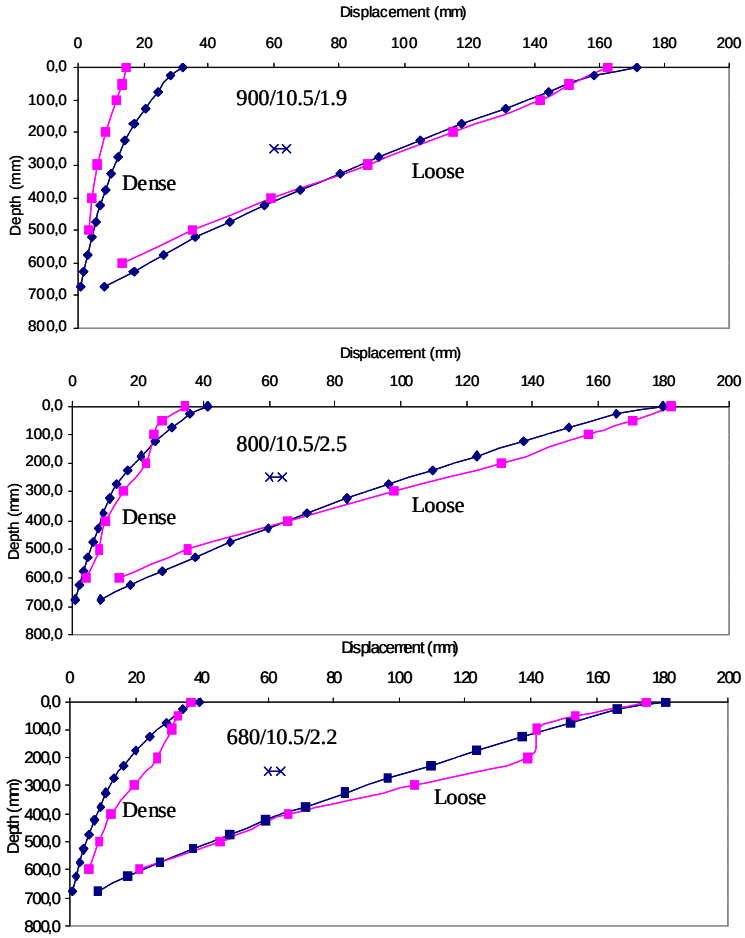

Figure 73: Measured (■) and predicted (♦) soil displacement for tyres on loose (1.2 g/cm^3) and dense (1.6 g/cm^3) soil conditions. The least significant difference (LSD) at 95 % is also shown

Data from the medium density was used to derive the VCL parameters and it is capable of predicting soil density increase for different initial DBD's. Thus this justifies the concept of a VCL for a soil at given moisture content in general and in particular for this soil type.

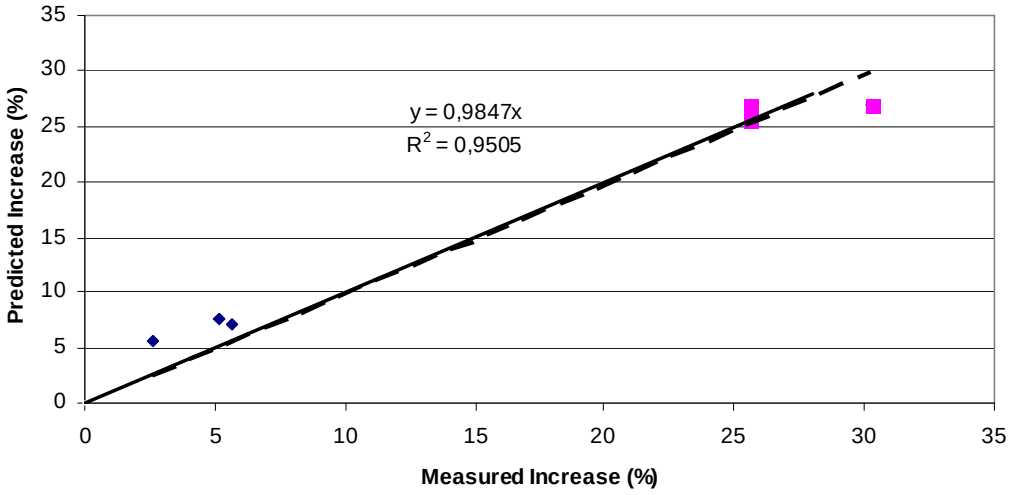

Figure 74: Predicted vs. measured increase in soil displacement for the data from Antille (2006) on dense (1.6 g/cm^3) (♦) and loose (1.2 g/cm^3) (■) soil. Regression line is dashed and 1:1 relationship solid

Moreover the initial DBD from which the in-situ VCL parameters are derived allows a prediction of soil density increase in denser and in looser soil conditions. Thus the in-situ VCL is independent of the initial density it was created for as assumed for general VCLs in theory. The close agreement was achieved with a ξ of 5 and shows the robustness of the approach against this parameter which technically influences pressure distribution within the soil and is depending on the initial density.

The close agreement on higher and lower bearing capacities justifies an extension of the investigation of the capability of the model to predict soil compaction in the more complex cases given below.

6.3.3.2 Stratified Soil Conditions

The next step was to compare the performance of the in-situ model for different soil densities within one soil profile. Hence, the stratified soil conditions used by Ansorge (2005, a) were simulated with the in-situ model using densities of 1.45, 1.62, and 1.55 g/cc for the zones: above 200 mm, between 200-325 mm and 325-750 mm, respectively. As can be seen from Figure 75 the predicted and measured soil displacement agree well in shape indicating that the compaction behavior of the soil is correctly predicted. However, a general over prediction is visible over the whole depth starting with 14 mm at the surface and de-

creasing to 2 mm at depth. The large difference at the surface can be attributed to the sampling error caused by the lugs. Overall the deviation is mostly enclosed by the LSD showing close agreement.

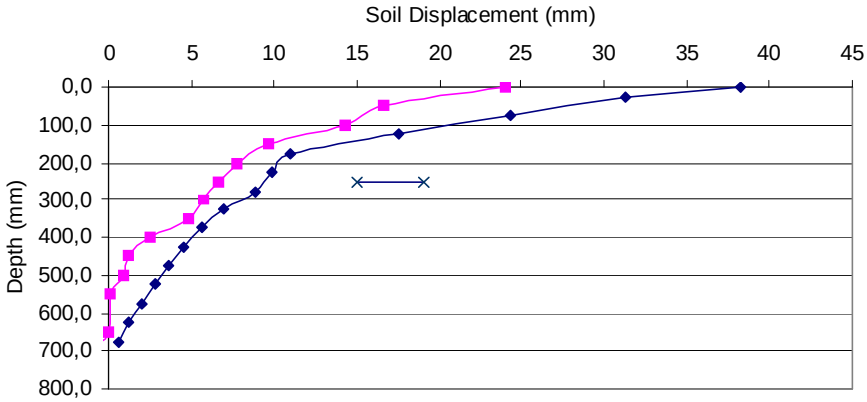

Figure 75: Predicted (♦) and measured (■) soil displacement on stratified soil conditions after the pass of a 900/10.5/1.9. The least significant difference (LSD) at 95 % is also shown

6.3.3.3 Multi-Pass Experiment

Figure 76 shows the results of predicting soil displacement after 3 passes of 900/10.5/1.9 and 900/5/0.5 tyres over a uniform medium dense soil with an initial DBD of 1.38 g/cm^3. These were compared to the measured values from Ansorge (2005, a). This comparison aims particularly at the evaluation of the behavior of the model with respect to the slope of the recompression line (RCL) which determines soil behavior at the beginning of reloading (the second cycle in a loading-unloading sequence). The smaller the slope of the RCL the more soil compacts in the consecutive loading cycles and has undergone less strengthening than one with a larger RCL slope.

As the close agreement between measured and predicted data shows, the model predicts the soil behavior correctly for subsequent passes without the necessity to adjust the RCL. The slope of the RCL = 0.0327 as defined by O'Sullivan (1998) can be maintained for this sandy loam. In general a close agreement at the surface is achieved and only displacement behavior at depth differs slightly when the displacement approaches zero anyway whereby the deviation is still within the error of measurement.

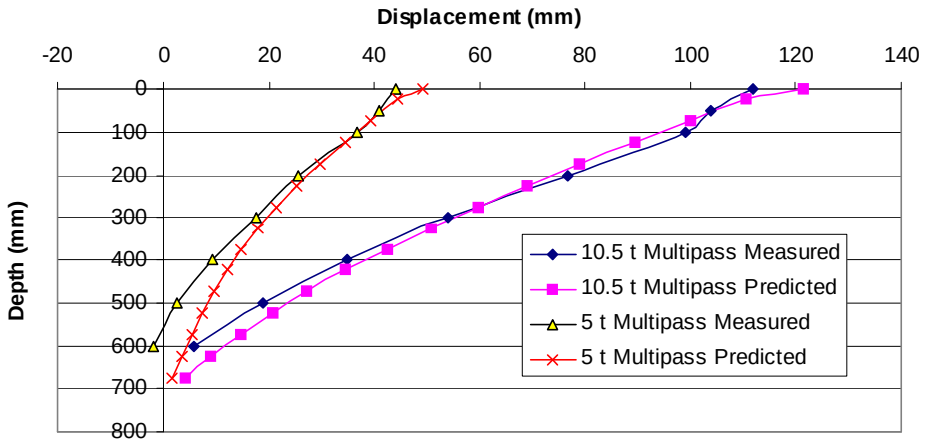

Figure 76: Predicted and measured soil displacement after 3 passes of a 900 mm tyre at 10.5t and 5t loads at 1.9 and 0.5 bar inflation pressure, respectively

6.3.3.4 Passes with complete vehicles

Figure 77 shows the predicted soil displacement below vehicles after the pass of the front and the rear axle. In general a close agreement was obtained between the measured and predicted soil displacement.

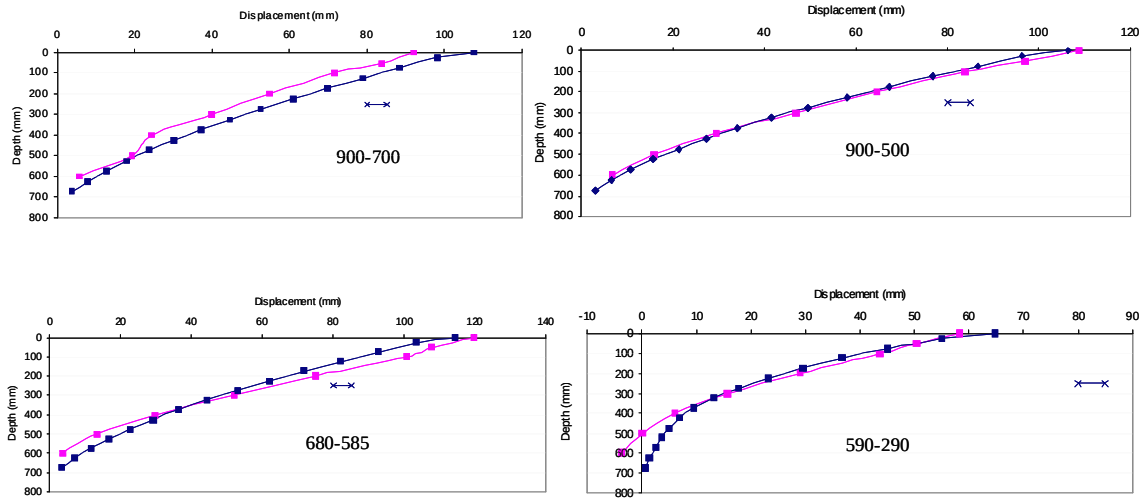

Figure 77: Predicted (♦) and measured (■) soil displacement on uniform soil conditions after the pass of a combine harvester with different tyre and load combinations. The least significant difference (LSD) at 95 % is also shown

To summarize the ability to predict soil displacement after multiple passes from either a three front axle pass or whole machines the slope of the measured and predicted soil displacement lines were calculated and plotted against each other in Figure 78. The agreement between measured and predicted soil displacement is high. The average increase in DBD was predicted to within +/- 1.5 % for all treatments except the 680-585 with +3%. The slope shows that the overall increase in density is underpredicted by 5 % compared to the 1:1 line with an R^2 of 0.85.

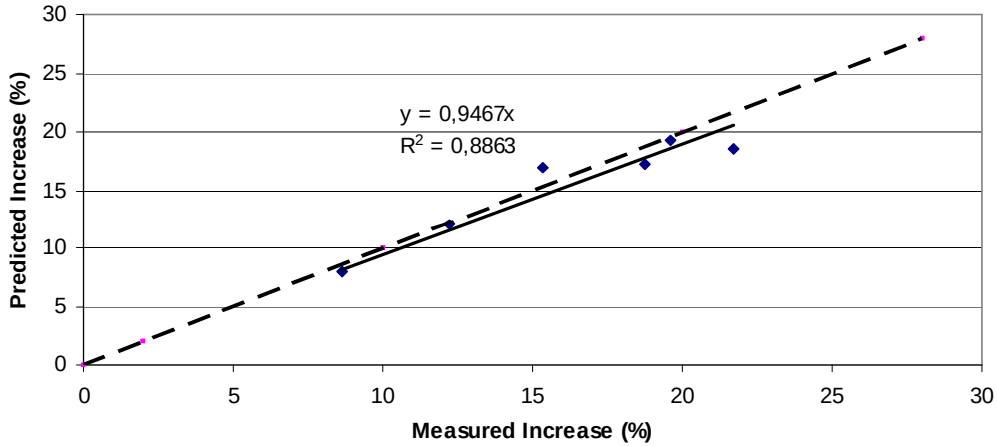

Figure 78: Predicted vs. measured increase in soil displacement for multi passes from whole machines or front axles. Also shown is the 1:1 relationship (broken line)

6.3.4 In-field determination of VCL

This section contains the soil displacement data from field experiments whereby the approach to gain the slope and intercept from tyre passes as explained in 6.3.1 will be validated on both a clay soil and a sandy loam soil. On both soils ξ of 4 and 5 will be evaluated. It is shown that the rut depth is sufficient to estimate the increase in DBD due to the uniform density increase over a known depth (either working depth or soil type depended on DBD profile in field).

6.3.4.1 Clay Soil

The combine formed rut depths of 57.5 mm and 82 mm on the clay loam field soil for low and high inflation pressure, respectively, resulting in an average increase in DBD of 9.6

and 13.7 % by assuming that the top 600 mm of soil uniformly increased in DBD. Initial DBD was 1.27 g/cm^3 and resulted in relative densities of 1.911 and 1.843 when adding the increase in DBD for the low and high inflation pressure, respectively. Contact pressure was estimated according to O'Sullivan et al. (1998), and resulted in a mean normal pressure of 52.9 kPa and 55.9 kPa for the low and high inflation pressure, respectively at ξ of 5 following the calculations given in detail in Section 6.3.2. At ξ of 4 the corresponding pressures were 57.5 kPa and 60.8 kPa. In Figure 79 the relative density is plotted vs. mean normal pressure for both concentration factors and a logarithmic regression line is fitted to each set of data resulting in the corresponding in-situ VCLs for the clay soil.

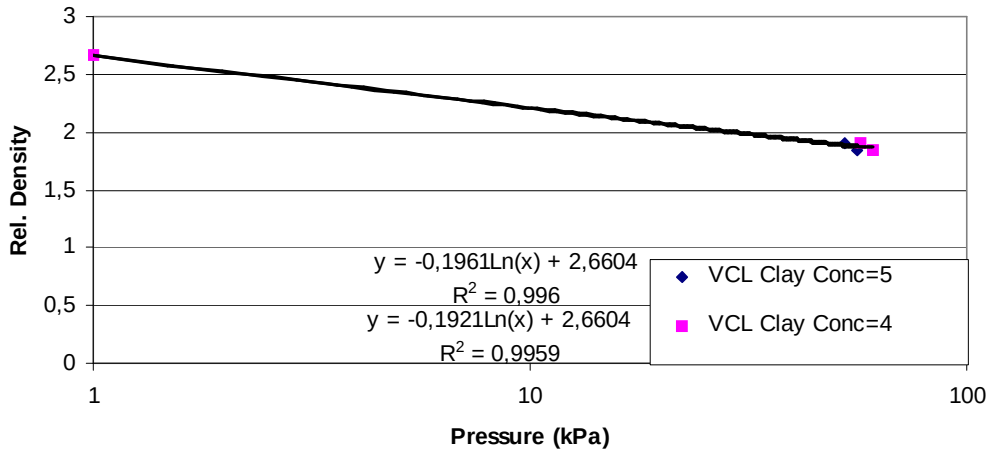

Figure 79: VCL for cay soil gained in field experiment

If the slope of -0.1961 and the intercept of 2.6604 corresponding to a ξ of 5 are fed into COMPSOIL, soil displacement for these field conditions is predicted for the high and normal inflation pressure machine configuration and compares to the measured data as shown in Figure 80 by the dash-point-dash line. Doing the same with slope and intercept gained from ξ of 4, the prediction compares to the measured data as shown by the dashed lines in Figure 80. When comparing the effect of ξ to the predictions for both inflation pressures, ξ of 4 is closer to the measured data and therefore on the clay soil this appears more appropriate. Predictions of contact pressure from COMPSOIL are probably better close to the recommended inflation pressure explaining the closer fit to the data of the appropriately inflated tyre.

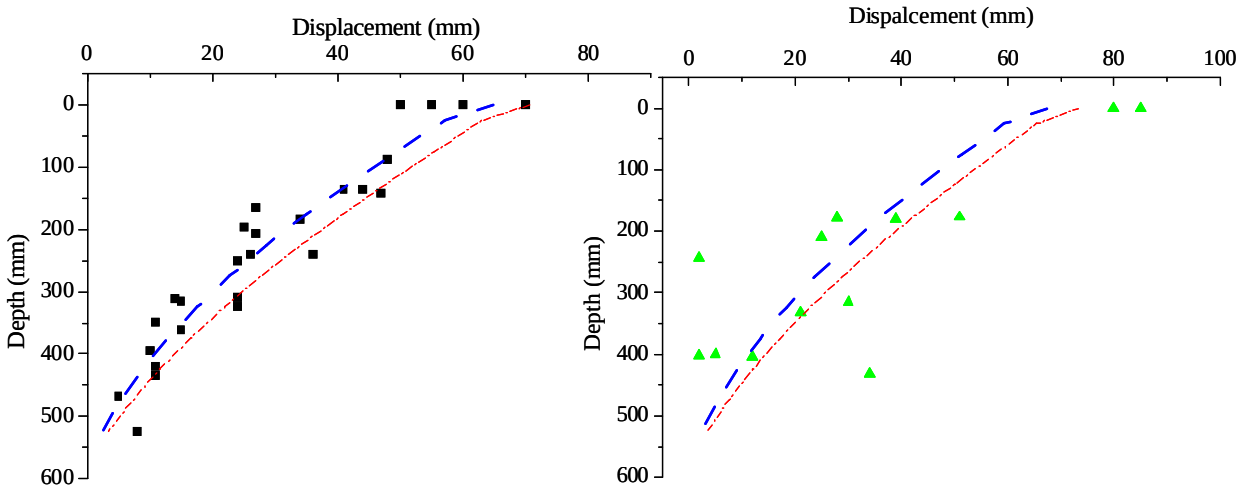

Figure 80: Predicted vs. measured soil displacement on clay soil in field for ξ of 4 (- - -) and 5 (-·-) at normal (2.5 bar) [squares] and high inflation pressure (3.5 bar) [triangles]

6.3.4.2 Sandy Loam Soil

In this section the data from both the sandy loam shallow tilled and subsoiled experiments will be pooled to gain the slope and intercept of a VCL. The identical procedure as described in the previous section was used to gain the slope and intercept of the VCL. In Appendix 1/1.4.2 a split of the VCL according to the different tillage treatments is provided showing marginal differences and the DBD profile is given, too.

The resulting VCLs for a ξ of 4 and 5 are shown in Figure 81. The predicted soil displacement for the VCLs is shown in Figure 82 for the shallow tilled soil. Soil displacement is larger for a ξ of 5 compared to a ξ of 4. Overall a ξ of 4 fits better in the field, however, using the VCL created in the soil bin on the same soil type with a ξ of 5 was found to fit best. This is due to the fact that the VCL from the soil bin contains more and better defined data points. The field experiment was conducted at a moisture content of approximately 20 % while the soil bin experiment was conducted at about 9 %. The good agreement in predicted soil displacement using the soil bin VCL is due to a similar distance from optimum moisture content for compaction which is at about 15 % moisture content for a sandy loam soil.

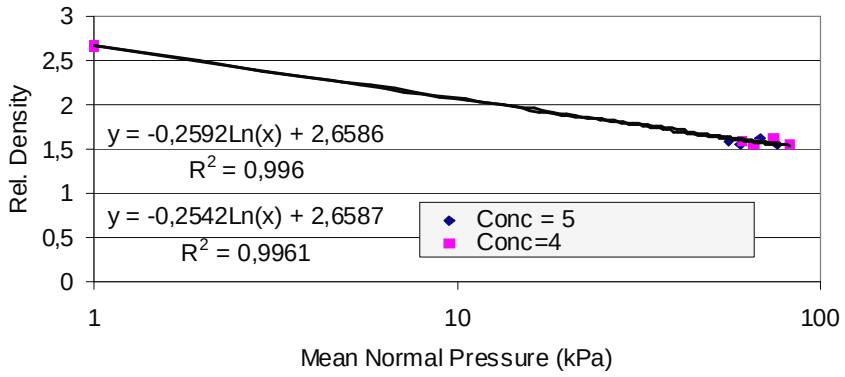

Figure 81: Virgin compression lines from two concentration factors of field experiments on sandy loam soil

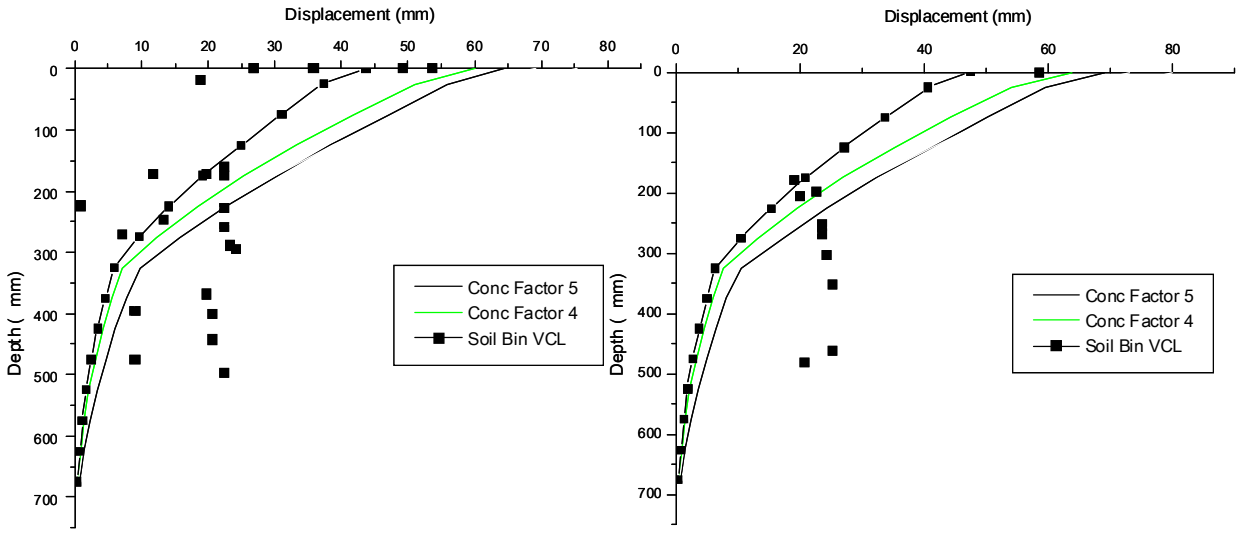

Figure 82: Measured (points) and predicted (lines) soil displacement for the normal (2.5 bar) (left hand side) and high inflation pressure (3.5 bar) (right hand side) treatment on shallow tilled sandy loam soil

Predicted vs. measured data for the sandy loam soil subsoiled is shown in Figure 83. ξ of 4 fits the data for the normal inflation pressure better than ξ of 5. However, at high inflation pressure a ξ of 5 seems more appropriate because it overcomes the under estimated soil displacement for this passage. Thus on this soil condition no clear recommendation can be given concerning ξ.

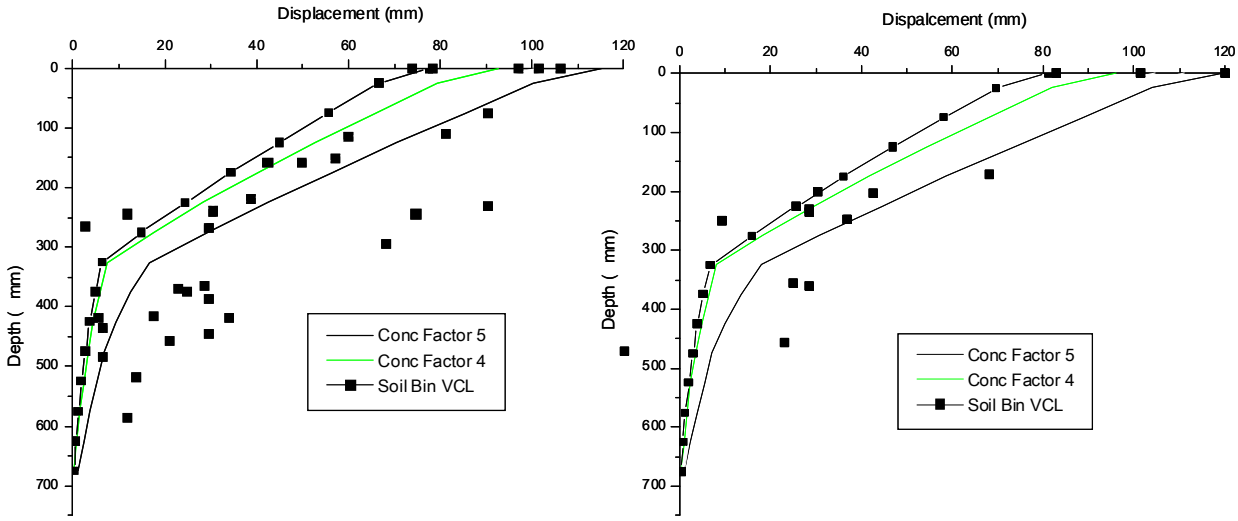

Figure 83: Measured (points) and predicted (lines) soil displacement for the normal (2.5 bar) (left hand side) and high inflation pressure (3.5 bar) (right hand side) treatment on subsoiled sandy loam

Overall it seems as if a ξ of 5 is appropriate to describe the pressure propagation for a sandy loam soil and a ξ of 4 to describe a clay soil. This can be explained by their different particle size distribution which overall gives the sandy loam a coarser network compared to the clay.

6.3.5 Discussion and Conclusions on in-situ VCL

The approach from Etienne and Steinemann (2002) utilizing a screw driver test to describe soil strength at the surface triggered the idea of developing an easy accessible way to measure soil specific parameters. With the in-situ VCL approach presented here, such a possibility has been found. A new approach to gain the slope and intercept of a soil and water content specific in-situ VCL was derived from easily accessible tyre and soil data. The approach was successfully validated both in the soil bin laboratory and in the field. Necessary parameters are tyre load, inflation pressure, tyre width and diameter, rut depth, uniform soil density depth or working depth, and density of this soil.

From this, it was possible to provide a relatively simple critical state soil mechanics soil compaction prediction model (COMPSOIL; O'Sullivan et al., 1998) with soil specific

VCL parameters. The predicted soil displacement was highly accurate. The models of Gupta and Larson (1982) and Bailey and Johnson (1989) which require more input parameters can hardly be more accurate, however, the larger amount of input parameters these need make them unsuitable for such an in-situ approach. Chi et al. (1993) point out that the derivation of critical state soil mechanics parameters is the largest source of error when comparing soil compaction model predictions to real data. This source was reduced here due to the small number of necessary parameters and the large sample size.

It was possible to use a soil mechanics model based on critical state soil mechanics theory (Schofield and Wroth, 1968) and gain its soil specific soil physical parameters from simple empirical measurements. This allowed qualitative but more importantly quantitative correct predictions.

The output from COMPSOIL is more distinct than for models such as TASC (Diserens and Spiess, 2004) or SOCOMO (van den Akker, 2004) which only predict soil stresses. Although the screw driver test for TASC is easier to perform than gaining an in-situ VCL, the additional information gained from COMPSOIL due to the accurate soil displacement and soil density increase prediction with depth make the additional effort worthwhile. Thus the in-situ VCL approach improves considerably the user-friendliness of COMPSOIL due to the ability to adapt easily to different soil types.

Considering the different approaches taken to derive VCL parameters, the approach described here to gain an in-situ VCL has the advantage of easily accessible information and very large sample size compared to any laboratory based approach. The large sample size and in-field test avoids the major issue of variations with small sample testing for critical state soil mechanics models as pointed out by Chi et al. (1993) when investigating the accuracy of soil compaction models. The sample size is of concern for the approach taken by Gurtug and Sridgaran (2002) who obtained compaction characteristics from plastic limit tests for fine grained soils as these are usually carried out with only a few grams of soil. Compared to the improvement of Kirby et al. (1998) who derive all critical state soil mechanics parameters from one constant cell volume triaxial cell test, the field test only provides the information for soil compaction, but without any laboratory equipement. No pedo - transfer functions as for example included by Keller et al. (2007) in SOILFLEX are necessary as the approach can be repeated on any soil type and the resulting in-situ VCL will

be specific to that particular soil type. The same holds true for water content as the method simply can be repeated at any given moisture content and a water content specific in-situ VCL will be derived. This is a great simplification taking the work of Wheeler and Sivakumar (1995), Toll and Ong (2003), Blatz and Graham (2003) and many others into account trying to link critical state soil mechanics parameters to soil moisture content. It was possible to account for water content not with soil stresses but as an influence on critical state soil mechanics i.e. soil physical parameters as found by Hettiarachi and O'Callaghan (1980), Hettiarachi (1987) and Kirby (1989).

The robustness of the entire approach against the concentration factor introduced by Fröhlich (1934) was surprising, but agrees with the findings of Etienne and Steinmann (2002) who are able to predict soil stresses independent of soil type with one concentration factor. Interestingly their concentration factor is 2 and the one most commonly used in this study is 5. However, for the work here, 5 is most appropriate.

With respect to the physics of granular media, the framework of critical state soil mechanics theory embedded in COMPSOIL is regarded as an approach which is sensitive enough to describe soil density changes accurately by means of a physical concept (critical state soil mechanics theory, Schofield and Wroth, 1960), while at the same time it is stable against variations at the grain level. Much work has been conducted to describe factors influencing the physics of granular media at the grain level, yet it is virtually impossible to account for all of them in one model. The orientation of particles changes mechanical behavior according to Oda et al. (1997), particle size determines the strength of particle according to Ning et al. (1997), Delie and Bouvard (1997) found that spherical inclusions are easier to compact than angular inclusions. All these effects are averaged and thus do not affect the predicted soil displacement utilizing the in-situ VCL.

At the onset of the in-situ approach it was mentioned that the error originating from disregarding the elastic recovery of the soil when deteriming the in-situ VCLs would be ignored as the error is small. The entire section proved this assumption to be correct due to its high accuracy. The validation in the field even confirmed the validity of the whole approach on a different soil type. Now there is a method available which has been validated on the two of the most opposing soil types found in arable agriculture – a sandy loam and a clay soil.

The approach satisfies the requirements in the introduction of the Chapter. COMPSOIL embedded in SOILFLEX using the in-situ VCL approach enables researchers, machine designers, manufacturers, farm advisers, and farmers to evaluate the impact of their machinery on soil density at the respective design selection and use stages.

In future work consideration should be given to the behavior of tyre contact patches at different inflation pressures. When they deviate from the recommended inflation pressure either way, contact pressure predictions may be improved leading to a closer agreement of soil displacement prediction to measured data.

The next section carries the in-situ VCL approach to tracks. Afterwards the whole in-situ VCL is repeated on a small scale plate sinkage experiment and finally compared to triaxially derived VCLs.

6.4 Compaction Prediction using in-situ VCL for Rubber Tracks

Figure 84 shows the VCLs for only tyres, only tracks, and including both. The resulting R^2 decreases from 0.87 to 0.63 if tracks are added to tyres. A VCL only including the tracks and the roller shows a greater R^2 of 0.82. The slope and intercept of the VCLs indicate that the tracks show a different soil compaction behavior compared to tyres. The contact pressure of tracks results in a smaller relative density than for the corresponding tyres.

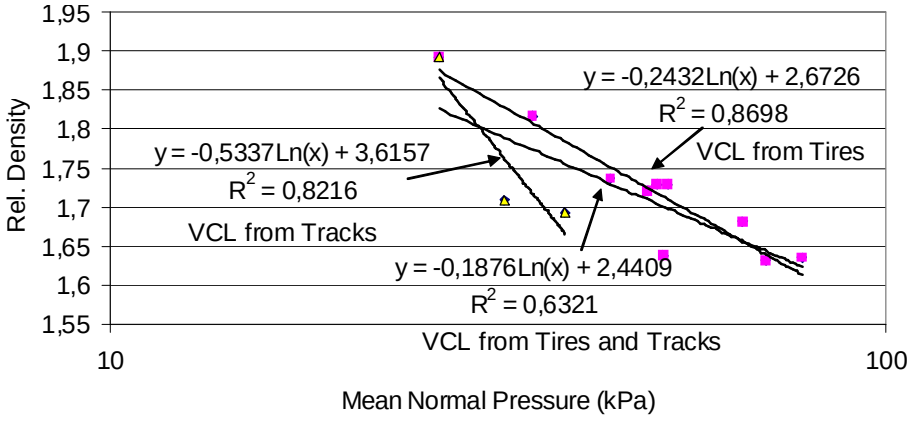

Figure 84: VCL gained from contact pressure and density increase measured from soil displacement including tracks

The slope for the VCL without the tracks is steeper compared to the one including both tyres and tracks characterising the relative density change less prone to changes in mean

normal pressure if tracks are added. However, the intercept decreases when tracks are included, leading to a weaker soil characteristic. The mere track VCL has the greatest slope and hence is most prone to changes in mean normal pressure.

The prediction of an in-situ VCL gained including the track data is compared to the measured increase in DBD in Figure 85 and shows a high correlation coefficient and only a slight underprediction of the regression line indicating predicted increase in DBD to be 10% too small. However, compared to Figure 72 which shows the prediction without the track data the correlation coefficient is smaller and the slope of the regression line differs by 9 % rather than 1%. Therefore, not selecting the tracks to create the in-situ VCL is justified for tyres due to the different compaction characteristic of tracks. To predict tracks most accurately it is recommended to use merely tracks.

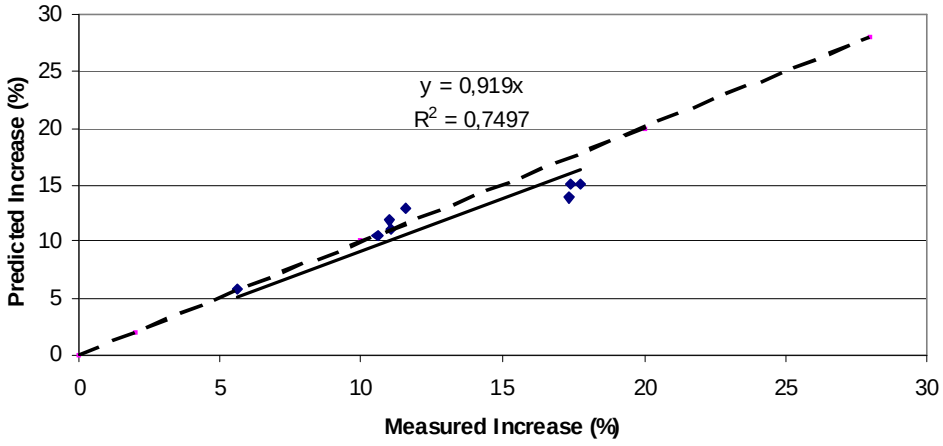

Figure 85: Predicted vs. measured increase in DBD for the VCL created including track data. Also shown is the 1:1 relationship (broken line)

Figure 86 compares the prediction of rubber tracks using the in-situ VCL for both tyres and tracks and tracks on their own to the measured data of the TerraTrac at 12 t with common and 50 bar belt tension. The unequal weight distribution of the track was partially replicated with an uneven load distribution on the different tyres simulating 4 rollers of the track; 2 t on the first roll at 60 kPa followed by twice 3 t at 80 kPa and finally 4 t at 100 kPa on the last roller on the 680 mm section width tyre. If the roller preparing the initial soil condition is not included into the VCL (regression line not shown), soil displacement is largely overestimated as obvious from Figure 86. Including the roller, the rut depth at the

surface stayed similar, but the characteristic with depth changed exhibiting a larger change at the surface than at depth (below 400 mm) as expected.

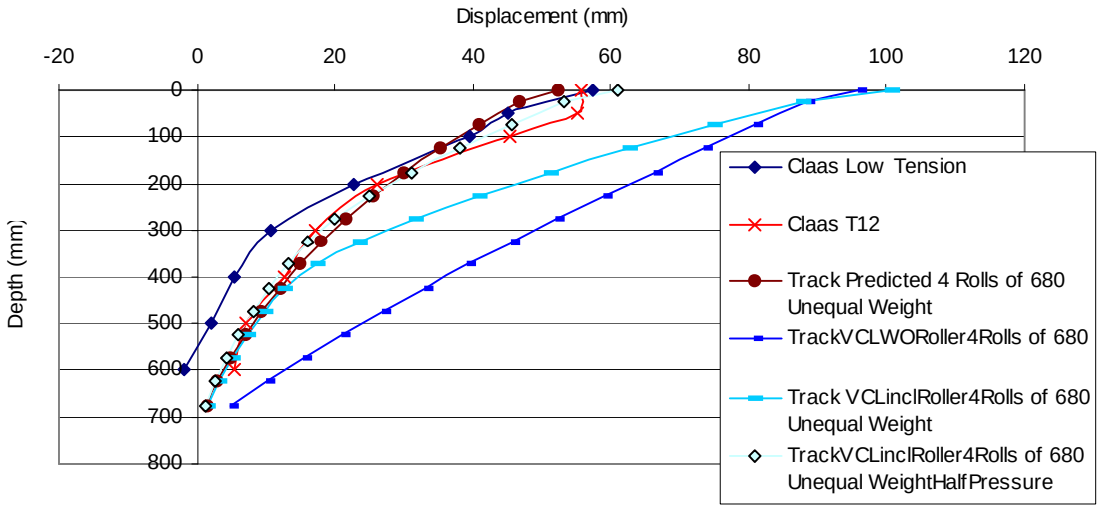

Figure 86: Predicted sinkage for tracks using individual VCL

Subsequently halfing all inflation pressures put the line closer to the measured data. Using the in-situ VCL of tyres and tracks made soil displacement with depth more linear which it in reality is not. Thus the track specific VCL predicted the track at normal belt tension most closely, although this is regarded as an outlier. It was not possible to predict the shape of the soil displacement and particularly no residual soil displacement from the TerraTrac measured at 50 bar belt tension, although rut depths agreed well.

Hence, to model tracks accurately the same methodology as previously developed for tyres seems promising. However, to be able to evaluate different track types, “something else” or some other methodology would have to be developed.

6.5 VCL from Plate Sinkage Data from Triaxial Cell

The section utilizes small scale plate sinkage experiments to gain an in-situ VCL with the same methodology. This will further validate the in-situ approach as it is on a totally different scale, but using the same procedure. The plate sinkage method is explained in section 2.3.2 and the contact patches which are used have also been used for the work described later in Section 7.3. Similar to the soil bin a uniform soil density increase over the

entire depth was assumed as no sideways movement of the soil could be detected. The resulting in-situ VCLs are shown in Figure 87.

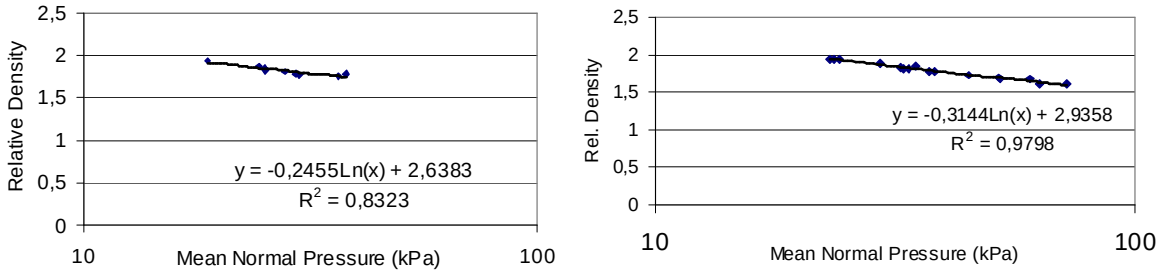

Figure 87: Virgin compression line for plate sinkage tests with different plate sizes (left) and different pressures on same plate (right)

The function for the different plates (left hand side of Figure 87) indicates a slightly weaker soil as the one for the same plate with different loads on the right hand side. Feeding the slope and the intercept of these VCLs into COMPSOIL gave a close agreement to the measured data as shown in Figure 88.

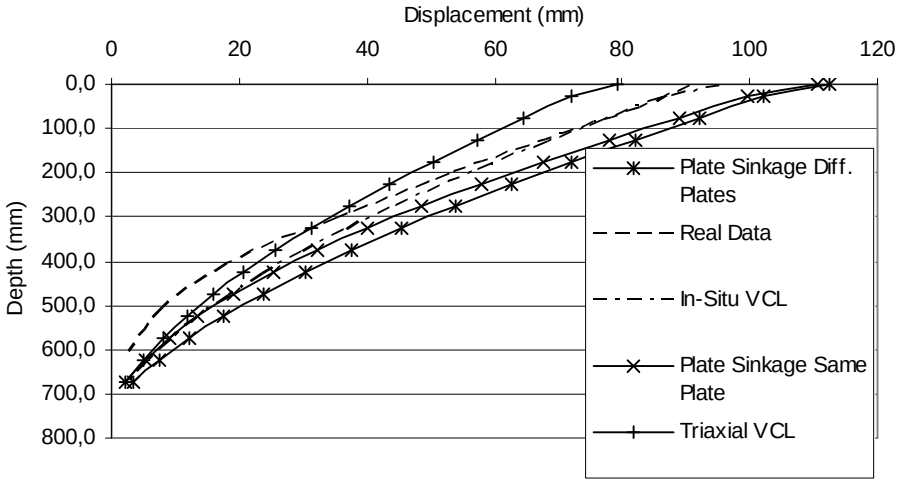

Figure 88: Measured and differently predicted soil displacement for the 900/10.5/1.9 on uniform soil conditions

The VCL parameters created with the plate sinkage tests predict the 900/10.5/1.9 tyre closer to its real data than the appropriate parameters from triaxial cell test data; whereby axial and radial load is applied at the same time as described later in Section 6.6.2. Still, the best estimation is gained with the in-situ method using tyres.

This result justifies the approach taken with the estimation of the VCL parameters only from contact pressure and rut depth when knowing the DBD profile with depth of the soil. It furthermore describes an alternative approach on a smaller scale to derive VCL parameters with the same procedure in-situ. This may have the advantage that field conditions can be assessed empirically before machines are used. However, for most farmers it is easier to take machines into the field and measure the rut depths than to conduct these sinkage tests. If in future work it was possible to link these small scale plate sinkage experiments to drop cone results (Godwin et al., 1991) a neat approach for a farmer friendly method not using whole machines might be created.

6.6 Triaxial Cell Test Apparatus VCL Compared to in-situ VCL

In this section the in-situ VCL will be compared to a VCL gained with triaxial test equipment. The entire methodology for the triaxial cell test apparatus can be found in Section 2.3.1. Initially confining pressure will be applied followed by an investigation of the system and water compressibility. Subsequently axial and radial pressure will be applied trying to mimic real soil loading conditions occurring during the passage of a wheel. At the end all the different prediction results of the varying VCLs will be compared. The full details of the entire section are given in Appendix 11.1.5.

6.6.1 Confining Pressure Applied

In the first sequence only confining pressure was applied as this is the commonly referred way in literature to obtain a VCL according to Leeson and Campbell (1983). In the second sequence an axial stress higher than confining pressure was applied.

6.6.1.1 Influence of Time of Loading

Samples at one density and one moisture content (10%) were loaded to 100 kPa, unloaded and then reloaded up to 250 kPa. Loading times ranged from 30 – 360 min because the short loading time from the soil bin experiment could not be repeated due to the impossibility to change cell pressure instantaneously. The different loading times did not influence the VCLs significantly and agreed well with a VCL gained from the tyre passes in the soil bin if the mean normal pressure was set equal to σ_1; (“Full Pressure” in Figure 89). This

"Full Pressure" approach is practically not sound as it sets intermediate and minor principal stresses equal to the major principal stress. As a result a soil is predicted too strong when its parameters are used as input variables in COMPSOIL.

6.6.1.2 Influence of Moisture and Initial Soil Density

The influence of moisture content and initial soil density was investigated in fast loading tests. In the range of 8.2 – 12.5 % moisture content the samples appear independent of moisture content as they merge between 100 – 200 kPa depending on their initial densities ranging from 1.31 g/cm^3 to 1.54 g/cm^3. No influence of initial density is expected, however, the independency of moisture content in this range was not expected. Probably the range of only 4 % was too small. Again, these curves are close to "Full Pressure" from the soil bin experiment as shown in Figure 89. Overall the repeatability of results was within +/- 15 % when applying confining pressure.

The necessity to actually adjust a VCL for different sandy loam soils can be seen when comparing the VCLs of different authors in Figure 89. The VCL obtained from this experiment and which represents a typical VCL result applying confining pressure is intermediate between those from O'Sullivan et al. (1998) and Leeson and Campbell (1983).

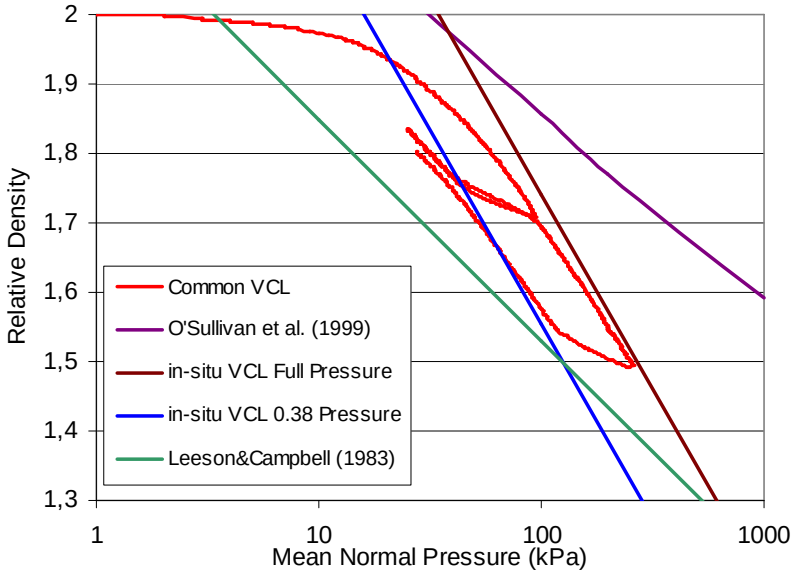

Figure 89: VCLs from O'Sullivan (1998), Leeson and Campbell (1983), and the one gained by confining pressure.

6.6.1.3 Water and System Compressibility

The previous relationships do not take the water compressibility and the elasticity of the triaxial system into account. Therefore the elastic response of the system including the water was evaluated by pressurizing the cell without a sample three times up to 350 kPa and relieving the pressure again to determine the effect on the apparent volume change which in turn would influence the relative density. Considering the compressibility of the system, which has been disregarded in the previous figures, shifts the VCL further away from the origin on the horizontal axis making the soil to appear stronger as shown in Figure 90.

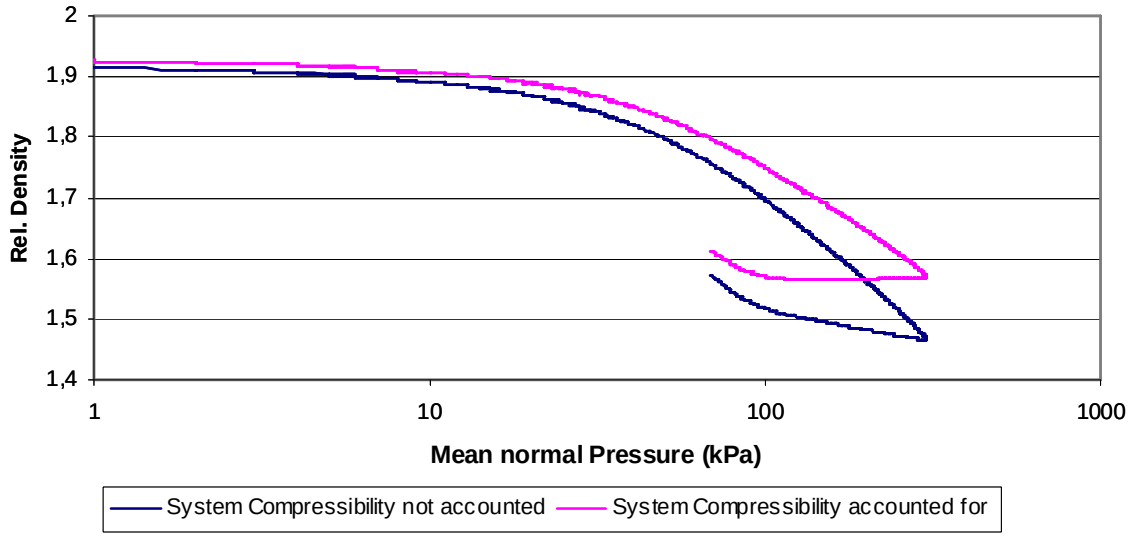

Figure 90: VCL with and without compensation for water compressibility

Water compressibility was not taken into account in the previous discussion as it is identical for all curves and would only shift them in total and not have an influence on their relations amongst each other.

6.6.2 Axial and Radial Pressure

As there was poor agreement for the VCL from the soil bin gained by the tyre passes and the VCLs created with radial pressure in the triaxial test apparatus the idea arose to apply radial and axial pressure simultaneously replicating stress conditions during a tyre pass as implied by Eq. 6 in Section 6.3.2. Radial pressure was set to 25 kPa and axial load was applied replicating the instant loading time and magnitude of a tyre pass in the soil bin.

According to Eq. 6 the resulting σ_1 should be approximately 130 kPa because of the relation of σ_1 to the sum of σ_2 and σ_3 being 0.38 as shown in Appendix 11.1.2.2.

These experiments resulted in a VCL less strong (details given in Appendix11.1.5.2) compared to soil bin VCL. Therefore the idea followed to apply axial load by moving the piston a known distance in a given amount of time while recording the resulting axial force. As now the axial load is applied slowly, radial pressure can be well maintained and the cell volume change is equal to the compacted soil volume.

Using the parameters of the VCL created only from cell volume change resulted in a closer agreement between the predicted and measured soil displacement using COMPSOIL. However, as shown with the loading cycle in Figure 91 the relation of σ_1 to σ_2 and σ_3 was never larger than three which means that the stress state expected from Eq. 6 in the soil bin was not reached in the triaxial cell. At first a confining pressure of 25 kPa was applied to the sample. When axial load was applied the cell pressure dropped due to the contracting sample and became stable at about 19 kPa when the compaction of the sample was in equilibrium with the rate of water being pumped into the cell. Axial load increased up to a threshold value of 68 kPa and then slowly decreased whereby the stress difference between major and minor principal stress cannot become larger because the sample started to fail in shear.

The influence of differences in σ_1 to σ_2 and σ_3 can be seen in Figure 92 where the VCLs differ significantly if σ_1 is bigger than σ_2 and σ_3. The VCLs with different confining pressure than axial load are much closer to the in-situ VCL than if only radial pressure is taken into account. The axial-radial loaded VCL was repeated five times and corrected vor water compressibility and is shown in Figure 92. The standard deviation was 6kPa for the pressure and 0.03 for the rel. density.

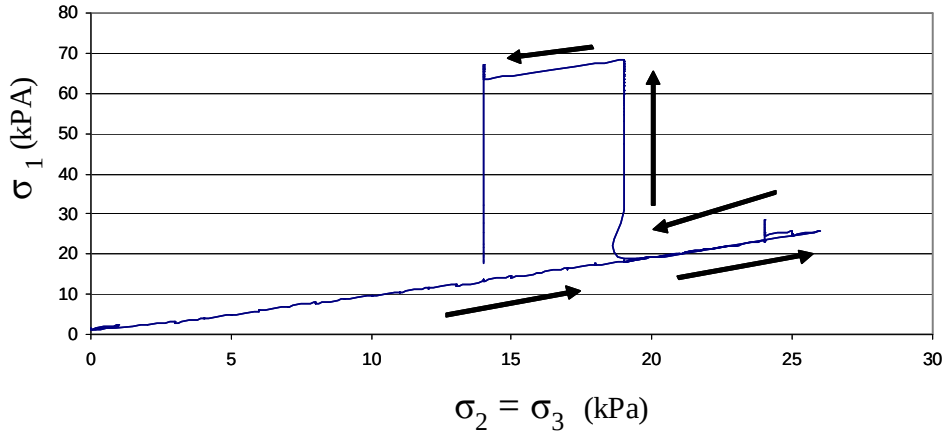

Figure 91: σ_1 in relation to σ_2 and σ_3 during the virgin compression test loading

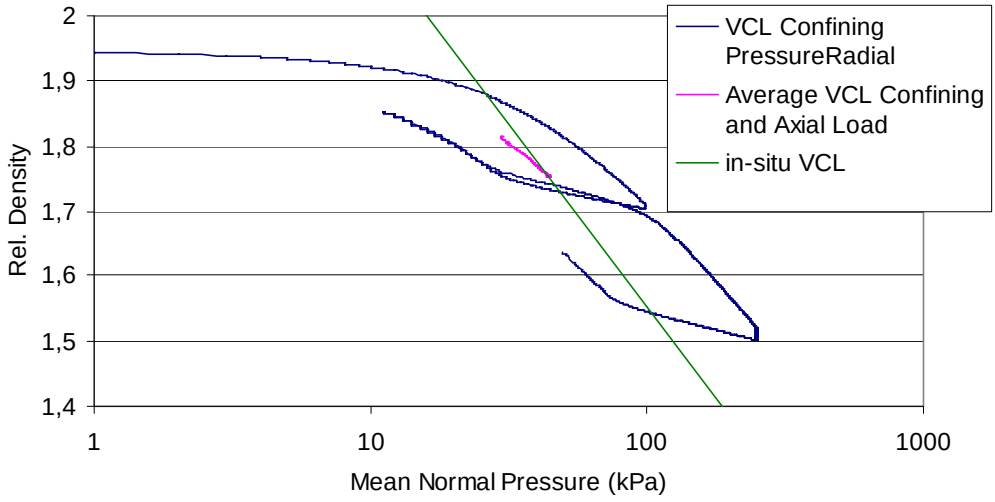

Figure 92: Virgin compression lines for radial and averaged radial-axial loading with sandy loam soil at 9 % moisture content; water compressibility taken into consideration

6.6.3 Implications of Triaxial VCLs on predicted Soil Displacement

After Section 6.3 derived and validated an in-situ VCL for predicting soil displacement with COMPSOIL, Section 6.5 validated the in-situ VCL approach with small scale plate sinkage tests, now this Section investigates the ability to predict soil displacement caused by the 900/10.5/1.9 tyre from triaxally gained VCL parameters. The slope and intercept of the triaxially gained VCLs in Sections 6.6.1 and 6.6.2 is used with COMPSOIL and the results are compared in Figure 93 to the real data for the different approaches.

The “in-situ VCL full pressure” gained by assuming contact pressure being equal to mean normal stress agrees well with a typical VCL from the triaxial tests whereby only confining pressure has been applied (“VCL Spherical Pressure”). However, this underestimates soil displacement by a factor of 2.

If constant confining stress is applied and an axial load impact similar to that in the soil bin is applied, and if the height change is additionally to the cell volume change taken into account (“VCL A+R Height / Quick”) soil displacement is largely overestimated. With only cell volume change (“VCL A+R Quick”) the approach is closer to the prediction with the tyres, however, slightly underestimates the resulting sinkage.

If the axial load is applied slowly by a constant strain rate and only cell volume change is taken into consideration (“VCL A+R Slow”) the correct shape is obtained and it underestimates total displacement less than “VCL A+R Quick”. If in the slow case height change is taken into consideration, too, “VCL A+R Height / Slow” shows a closer agreement at the surface, but the entire shape of the curve changed making it less appropriate. Thus the VCL which shows the closest agreement to the in-situ VCL in the previous Section provides the parameters for the closest prediction.

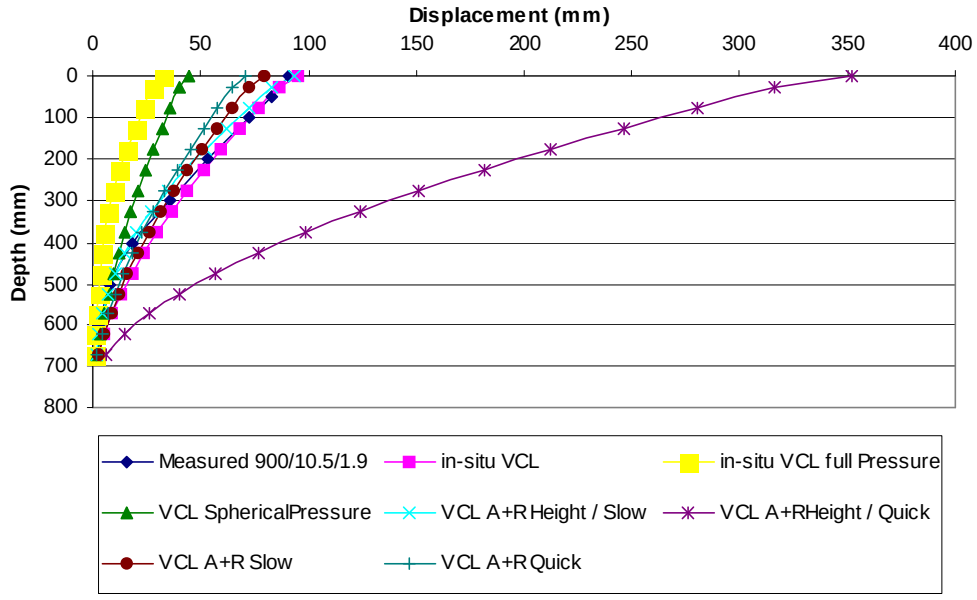

Figure 93: Comparison of prediction of 900/10.5/1.9 tyre with different triaxially gained VCLs to describe

The following Figure 94 compares in detail the average VCL gained from axial and radial loading but only considering cell volume change and the VCL gained from mere confining

pressure to the initial soil data and in-situ prediction. Soil displacement for the two triaxially gained VCL predictions is overestimated at depth and underestimated at the surface. Rut depth and shape of the soil displacement curve was predicted closest utilizing the in-situ VCL which again pronounces the quality and success of this method. It appears that the triaxially gained VCLs describe the soil displacement behavior more linearly than it actually is and than it is predicted with the in-situ VCL.

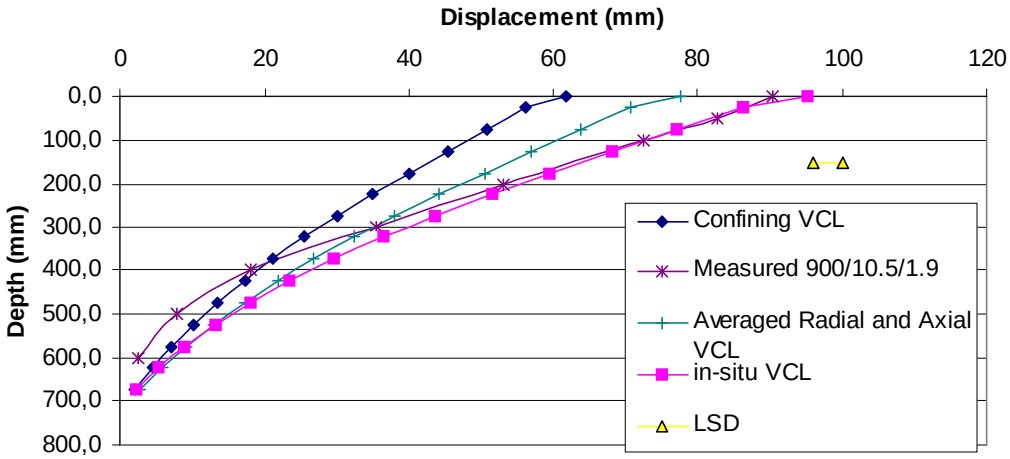

Figure 94: Predicted soil displacement using averaged VCLs at 1.4 g/cm^3

Very interesting is that VCLs which should uniquely describe soil density change with pressure depending on mean normal pressure differ significantly if σ_1 is larger than σ_2 and σ_3, i.e. if additional axial load is applied. The VCL depends on the stress state of σ_1, σ_2, and σ_3 and only if these represent real field conditions the VCL does correspond with the VCL gained from the passage of the tyres.

6.6.4 Discussion and Conclusions on triaxially gained VCLs

It was possible to determine a VCL which is similar to the one gained from the in-situ approach. However, the approximate relationships of σ_1, σ_2, and σ_3 as occurring from a tyre pass have to be maintained, because it was shown, that the slope and intercept of the VCL depends on that relationship. In general, a VCL is not unique to a given soil with given moisture content; it depends on the relationship of minor and major principal stresses.

Overall comparing the success in predicting soil displacement from tyre passes the in-situ VCL achieved a higher accuracy than any triaxially gained VCL. For a rough estimation

the triaxially gained VCL can give a sufficiently good estimate and show the relationships amongst individual treatments. However, to predict real sinkages occurring in the field, which might be necessary when looking at the severity of compaction on a particular site with particular machinery or trying to judge whether it is possible to cross a field with a certain equipement or not, the triaxially gained VCL may underestimate total sinkage. With the in-situ approach it would be possible, however, to derive a much more accurate prediction. If for example the question is how much damage or sinkage, depending on the point of interest, large machinery may cause, then taking smaller machines with smaller tyres and loads to the place of interest, measuring the occurring sinkage and utilizing this for the prediction of the bigger machine should give satisfying results.

Moreover, this triaxial cell test investigation proves the point of Roscoe (1970) and Jakobsen and Dexter (1989) who mention that field parameters can not be readily derived from laboratory measurements. The discrepancy can be reduced if the stress state was made more similar in the triaxial cell compared to the field, yet a slight discrepancy is maintained. It might be possible to improve this by using more dense samples, such that the relationship of minor and major principal stresses would even be closer to the ones implied by the empirical equation given by O'Sullivan et al. (1998).

The following section will report on a mathematical link between plate sinkage experiments and triaxial test data found in literature. This work has just proven that it is possible to gain in-situ VCLs with plate sinkage data, too (6.5).

6.7 Theoretical Link between Plate Sinkage and Critical State Soil Mechanics Parameters from Literature

Sime and Upadhyaya (2004) experimentally verify an inverse solution technique based on Rubinstein et al. (1994) to determine soil physical properties from a plate sinkage test which otherwise have only been gained by triaxial tests. Sime and Upadhyaya (2004) defined response surfaces for plate sinkage tests from a modified critical state soil constitutive relationship for each of the following elastic parameters: the bulk modulus and Poisson's ratio and the following plastic parameters: slope of the critical state line, slope of the virgin compression line, the initial void ratio and the intercept of the virgin compression line. To solve the entire procedure at least 16 data points are required, preferably more.

The response surface on its own is created by minimizing the sums of square errors of comparing the prediction of the parameters mentioned above to the theoretical consideration of a critical state CAM-Clay model approach. In the end the estimated/predicted parameters are compared to triaxially measured parameters. This comparison showed a "*reasonably well*" agreement for the plastic parameters, but the response surfaces for the elastic parameters were "*relatively insensitive*".

Hence, it was possible for Sime and Upadhyaya (2004) to show a link between plate sinkage and triaxial test results. However, the entire procedure is complicated and requires a large amount of data. Therefore the approach taken in this work to gain VCL parameters from tyre pass data seems much simpler. It did not yield any information concerning the slope of the critical state line or Poisson ratio or bulk modulus. However, using multi passes the slope of the recompression line can easily be evaluated providing the necessary information to adapt COMPSOIL for the elastic behavior of a soil.

The critical state concept is applicable to unsaturated soils both quantitatively and qualitatively except that the critical state parameters depend on the soil moisture content according to Hettiaratchi and O'Callaghan (1980), Hettiaratchi (1987), and Kirby (1989). Additionally these authors found that it is reasonable to use total stress and consequently ignore soil moisture tension.

6.8 Sinkage Prediction from Real and Small Scale Plate Sinkage Data

The underlying theory of Bekker (1960) to both tyre and track sinkage can be found in Appendix 11.1.7.1 and 11.1.7.2, repectively including the derivation of Bekker-specific parameters n and k in Appendix 11.1.7.3.

6.8.1 Sinkage of Tyres according to Bekker

The actual sinkage data of tyres for the soft and dense soil condition from Antille (2006) and the medium condition from Ansorge (2005, a) and this study was compared to the predicted depth from Bekker (1960). For the breadth usually the width of the tyre is used; however following a suggestion by Bekker (1960) half the length of the foot print can also be used if this is shorter than the width of the tyre. The estimated rut depth utilizing both

the width of the tyre and half the contact length is plotted against measured rut depth in Figure 95. For reference plate sinkage parameters gained from the small scale experiment in the triaxial cell are included. Figure 96 contains the large plate sinkage predictions and compares it to the predicted rut depth using COMPSOIL.

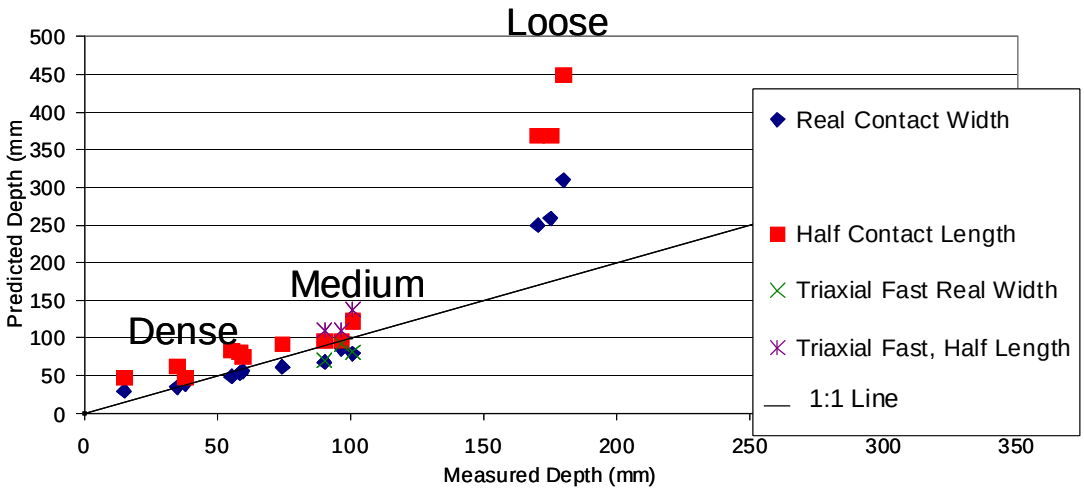

Figure 95: Predicted vs. measured depth of the tyres from plate sinkage data

The predicted and measured rut depths for the dense and medium soil condition show tolerable deviation in Figure 95, whereby using the tyre width for the shortest contact length results in a slightly underpredicted sinkage compared to using half the contact length which results in a slightly overpredicted rut depth. However, on soft soil conditions, the deviation is about 100 %. This might be due to the fact that the Bekker model assumes an infinite soil depth below, whereas in the soil bin, the maximum depth is 750 mm.

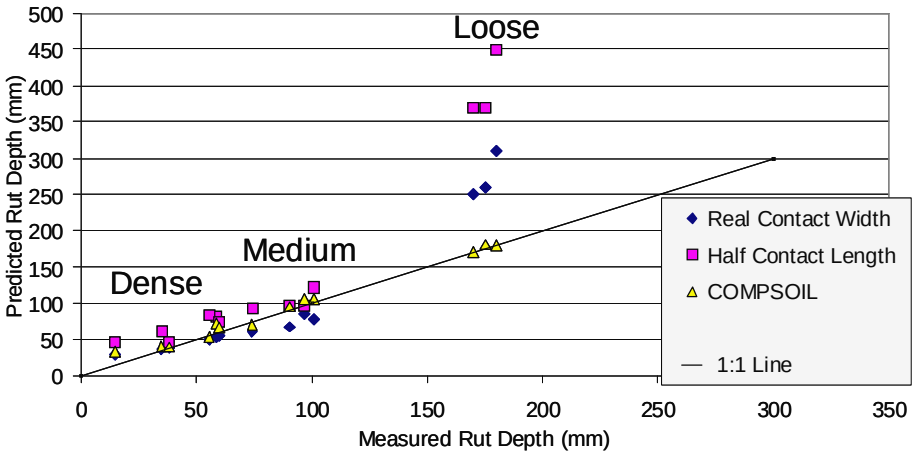

Figure 96: Predicted vs. measured depth of the tyres from plate sinkage data and from COMPSOIL

On medium soil conditions, the results could be replicated using the plate sinkage data gained from small scale contact patches in the triaxial test apparatus as described in 2.3.2. This shows that plate sinkage tests can be used for both the estimation of in-situ VCL parameters and Bekker-parameters. A mathematical justification of this was given by Sime and Upadhyaya (2004) and is explained in Section 6.7.

The advantage of the Bekker approach is, that its parameters can be measured much easier than critical state soil mechanics or VCL parameters, however, the technique still requires plate sinkage tests performed to gain the parameters. Therefore the assessment is not as straight forward as the one proposed in Section 6.3.1 with the in-situ VCL whereby the measurements can be taken from rut depths created by tyres.

Figure 96 shows that the predicted rut depths from COMPSOIL are intermediate between the Bekker approach utilizing the contact width and the one using half the contact length. From this it can be concluded that overall COMPSOIL predicts rut depths closer to the measured data, particularly on the soft soil.

6.8.2 Sinkage of Tracks

The track sinkage equation of Bekker (1960) “Track” could possibly be utilized to explain the different behavior of different tracks. However, as it assumes n to be equal to 1 which is only the case on very soft soils the predicted sinkage in Table 27 needs to be considered with care. The elastic elongation of the track (Slag) is taken into account with the “Track” equation. Besides the “Track” Table 27 includes the predictions of track sinkage gained directly from the plate sinkage approach “Plate”. Additionally the Bernstein equation (Bernstein, 1913) is included:

$$z = \frac{6 * W}{5 * r * b * k * \sqrt{D}}$$

Eq. 7

whereby r is the number of rollers in the track unit and D is equal to the diameter of the largest roller of the track unit.

According to Table 27 the general plate sinkage equation would predict sinkages too small. With “Track” assuming a slag of 0.02 sinkage is estimated too high in a range of 2 – 9 mm

depending on the unit except for PTS where sinkage would be underestimated. This is sensible as it is the unit with the least belt tension. Consequently a track slag of 0.05 results in a sinkage prediction even larger and less appropriate except possibly for the PTS. The Bernstein equation significantly underestimates sinkage except for the Stocks. Thus in general the track equation predicts sinkage most accurately. Unfortunately true track slag has not been measured during the experiments and therefore no further calibration/adjustment can be made. Overall the prediction using Bekker (1960)s equation for the sinkage of tracks probably may predict tracks most accurately if true slag data was available. Both Bekker (1960) and Bernstein lack a sensible adjustement for sinkage prediction on different soil conditions as both only consider k, but not n.

Table 27: Measured and predicted track sinkages using different approaches;
the slag i.e. elastic elongation of the track, is accounted for by the Track equation

Unit / Belt Slag	Plate (mm)	Track (mm)	Bernstein (Eq. 7) (mm)	Meas. Sinkage (mm)
Stocks/0.05	0.2	80	51	55
Stocks/0.02		64		
PTS/0.05	0.2	102	58	85
PTS/0.02		79		
Westtrack/0.05	0.1	70	36	55
Westtrack/0.02	No Slag	57	No Slag	
TerraTrac/0.05	0.15	77	29	55
TerraTrac/0.02	No Slag	62	No Slag	

6.9 The Implication of Peak vs. Average Contact Pressure on in-situ VCL

The in-situ VCL gained in 6.3 only takes average contact pressure into consideration. It does not take peak pressures underneath the tyre into consideration. If the peak pressure is taken into consideration for the in-situ VCL, rather than the average contact pressure, this would mean that the soil was stronger as it would require higher pressure to achieve the same density. However, as the triaxial cell test apparatus results in 6.6.3 indicate, if the VCL was gained by only confining pressure, the pressure should be smaller to achieve the same density, not bigger. Consequently taking the peak into consideration would not reduce the difference.

SOILFLEX takes pressure deviations into consideration. It first calculates average contact pressure according to COMPSOIL and in a subsequent routine average pressure is converted into a realistic pressure picture below the tyre whereby the peak pressure is 1.48 times higher than the average. This is slightly more uniform than the ratio of 1.77 for peak vs. average pressure which was measured and used for the calculations in Section 7.4.

Hence, the underlying model of the chosen approach takes non-uniform pressure distribution in the contact area into consideration according to the current state of knowledge. The general approach will still be valid, if in future more information is available on how the contact pressure is influenced by inflation pressure and carcass stiffness. However, this would require a re-adjustment of the VCL pressure calculations and pressure transmissions within the soil.

Work currently conducted by Miscewicz and Dain-Owens at Cranfield University at Silsoe considers some of these effects and might in future be able to give more detailed information on peak vs. average pressures.

6.10 Conclusions on Prediction Chapter

- An in-situ method was developed to gain the slope and intercept of a virgin compression line from at least two different tyre passes in the field from known weight, inflation pressure, and rut depth.
- Using COMPSOIL these parameters accurately predicted measured soil displacement caused by the unit.
- It was possible to verify the gained parameters on independently measured data on a much denser and a much weaker soil at the same moisture content and of the same soil type.
- It is possible to accurately predict whole machine configurations.
- The entire methodology was verified with infield measurements.
- Track units can be predicted with the same approach as tyres, they just need to be treated independently due to their different compaction characteristic.
- Other models within Keller et al. (2007) require more parameters to be estimated and were consequently expelled.

- With this methodology it is possible not only to state a danger of soil compaction as for example possible with TASC or SOCOMO. It is possible to gain realistic soil displacement pictures and correctly evaluate the influence of drive systems / under-carriage systems.
- Confining pressure loading times ranging from 30 – 360 min and varying moisture content between 8 – 12 % did not significantly affect the resulting VCLs.
- The VCL depends on the relations of major and minor principal stresses for mean normal stress.
- The in-situ parameters could be gained trixially if similar major and minor principal stresses were applied as occurring underneath a tyre.
- The in-situ VCL approach could be replicated with small scale plate sinkage experiments; however best prediction of soil displacement was achieved with full scale in-situ approach.
- Plate sinkage predictions worked on dense and medium soil conditions reasonably well, however, significantly overestimated rut depth on soft soil conditions.

7 ANCILLARY EXPERIMENTS AND ANALYSES

This Chapter contains ancillary experiments conducted to explain a particular behavior observed as for the strong surface layer (Section 7.1) and for the influence of lugs on vertical soil displacement (Section 7.2). Further analysis of soil density and contact pressure data lead heuristically to a new parameter load per perimeter length (Section 7.3). Particularly of interest became a comparison of sinkage caused by peak vs. average pressures from discussions with soil scientists and a lack of data in literature (Section 7.4). Finally the vertical soil failure observed in this study and others will be compared to theoretical considerations (Section 7.5).

7.1 Investigation into Track Behavior causing Strong Surface Layer

7.1.1 Theoretical explanation

The explanation for the high surface penetration resistance caused by the tracks close to the surface shown in Section 3.2 and by Ansorge (2005, a) will be considered in this section. Whilst initially of some concern, it is much more easily removed than the deeper compaction caused by the tyres (Ansorge and Godwin, 2007). This layer is also of value by reducing the subsequent amount of soil displacement caused by the rear tyres, compared to that following a wheel as shown in Figure 32.

The high penetrometer resistance was thought to originate from either vertical soil compaction close to the surface or the application of shear forces during the passage of the track.

If the high penetrometer resistance was caused by vertical soil compaction this would be visible from a change in the slope of the soil displacement curves near the soil surface. Hence, the average slope of the soil displacement lines should indicate a larger increase in soil density for the tracks than for tyres in the top 300 mm. Figure 97 shows the relevant data from Ansorge (2005, a) including the best fit linear regression lines. However, independent of the depths considered, the average slope for the tracks was always larger than the slope for the tyres with the exception of the 800/10.5/1.25, indicating less vertical soil displacement and compaction for the tracks at the surface. Hence, the peak was more likely to be caused by the shear forces applied for an extended time period by the track.

An argument supporting the hypothesis of a shear force effect was the similar vertical soil displacement caused by the rear/implement tyres to that of the rubber track (Ansorge and Godwin, 2007). However, the penetrometer resistance results for the smaller implement tyres did not show a peak close to the surface and as shown in Figure 98, merging of the data for the track and rear tyres occurred at a depth of less than 300 mm.

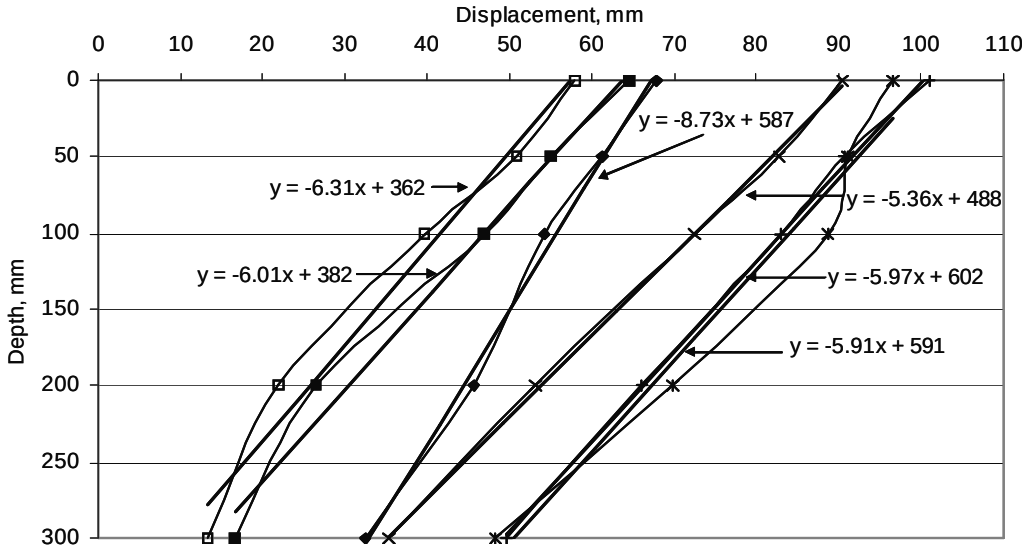

Figure 97: Displacement vs. Depth, top 300 mm with regression lines. □ track 10.5t; ■ track 12t; ∗ 680/10.5/2.2; × 900/10.5/1.9; + 800/10.5/2.5; ♦ 800/10.5/1.25

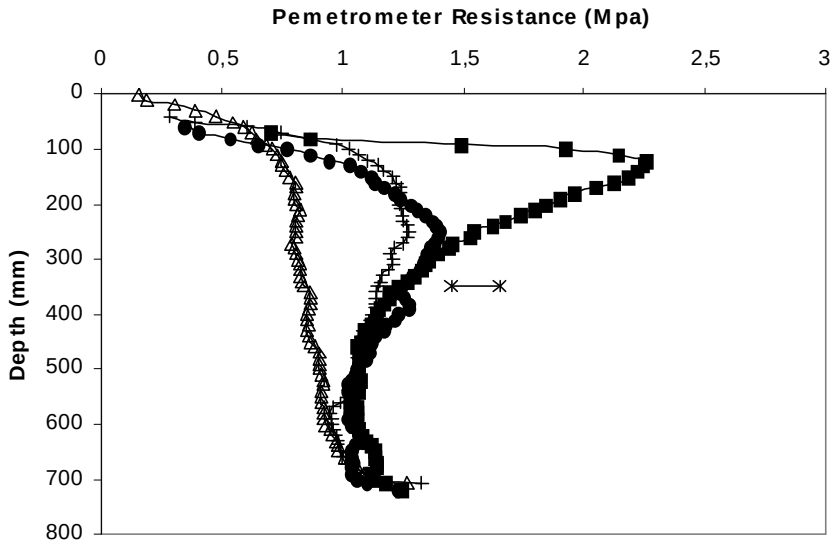

Figure 98: Penetrometer resistances for rear tyres and track at 12 t. Δ control; • 600/4.5/1.4; + 500/85/4.5/1.4b; ■ track12t ; ∗ LSD at 95% confidence level

Average contact pressure for the track was virtually identical to that of the 500-85/4.5/1.4 tyre at 83 kPa and 85 kPa, respectively (Ansorge and Godwin, 2007). For the 600/4.5/1.4 tyre a larger contact pressure of 110 kPa was measured. Nevertheless all three treatments caused similar soil displacement. Thus their increases in soil density agree well with their average contact pressures. As the true pressure distribution underneath a track was not uniform, one could argue that the dense layer was caused by the pressure peaks underneath the track; this was not visible from the study of the vertical soil displacement. Hence, neither both the absolute contact pressure or its distribution could be the cause of the higher penetrometer resistance.

The different slip behaviour of a tyre and a track could be responsible for this increase in soil strength indicated by the peak in penetrometer resistance. Calculating shear displacement resulted in twice the displacement underneath a track compared to that for a tyre according to Wong (2001). This seems rather strange as the track operated generally at a lower slip (5 %) compared to tyres (10 %) in this investigation (Ansorge, 2005, b). The shear displacement, however, is gained by the integration of slip velocity underneath the implement over the distance traveled. Hence the long contact area of the track (2.4 m) coupled with constant slip velocity led to a greater total shear displacement. The resulting constant shear strain application over the entire contact length additionally increased plastic shear displacement. Total length of the contact area for the tyre was about half (1.2 m) of that of the track, whereby the slip velocity depended on the position of the soil with respect to the tyre. The highest slip velocity occurs at the beginning of the contact patch when the tyre surface velocity is greater than that of the deformed section of the tyre under its centre line due to differences between the actual and the rolling radius (Wong, 2001). Thus shear strain decreases from the soil surface to the centre line.

The longer the soil was subjected to a force, the larger became the plastic deformation due to the spring-damper behavior of the soil during compaction as shown by Aboaba (1969) who changed the contact time of a roller by altering forward velocities. The varying slip velocity of a tyre and consequently longitudinal force cause more of an impact loading which may recover elastically.

The longitudinal soil displacement by a track and a tyre resulting from the different contact times under these given conditions will be discussed in the next Section.

7.1.2 Longitudinal soil displacement

The plastic longitudinal soil movement was measured by placing a series of 5 mm diameter vertical columns of sand into the soil at a spacing of 50 mm to a depth of 250 mm in the centreline of the path of the tyre or track. After the passage of the tyre/track these were carefully excavated along the centre line. The position of each sand column was digitized using the same methodology as for the talcum powder lines. Figure 99 shows a uniform forward soil movement after the passage of the 900/10.5/1.9. To aid the interpretation of soil movement within the column, Figure 99 includes vertical lines representing the average longitudinal position of the lower 100 mm for each sand column. The forward movement varied depending on the position relative to the lug. The columns on the back of a lug exhibited only a forward movement close to the surface, but not at depth (Column 1, 6, and 10 from left); all other columns tilted forward. The soil movement caused by a rubber track at 12 t is shown in Figure 100; these show an alternating backward and forward soil movement, whereby the backward movement was more pronounced than the forward movement. The front face of a lug appears to push the soil slightly forwards (Columns 2, 5, and 8 from left), but the remaining section of the lug and the rear area push the soil backwards. The lug-void ratios in these particular cross sections were 0.43 for the track and 1 for the tyre, representing a larger proportion of lugs for the tyre within the contact area.

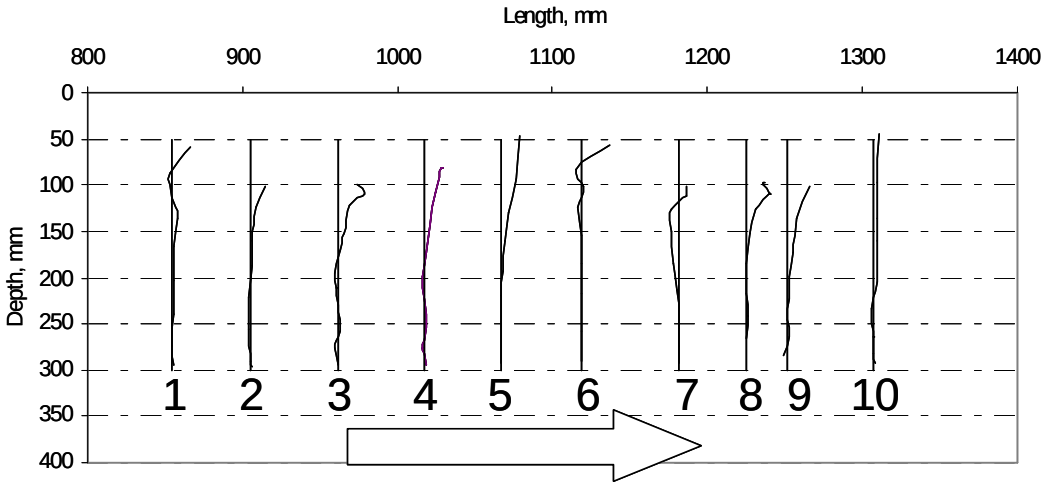

Figure 99: A digital image of the longitudinal position of the sand columns after the passage of a 900/10.5/1.9 tyre

In order to conduct a statistical analysis of the longitudinal soil movement below the tyre each column within Figure 99 was assigned either B or F to account for the tilt direction of the soil within the top 150 mm; B - indifferently to backward; F – forward. The assigned order was from left to right: BFFFFBFFFB. Within Figure 100 the sand columns of the track treatment were assigned either B, F, or I depending on whether the column was tilted backward, forward or indifferent with a shear failure below the lug and the following order was assigned: BFIBFIBFIB. The statistical analysis conducted for the entire length of each column and accounting for the treatment (track or a tyre), for the tilt direction and allowing an interaction of tilt direction with depth, revealed all parameters to significantly describe the observed sand column movement.

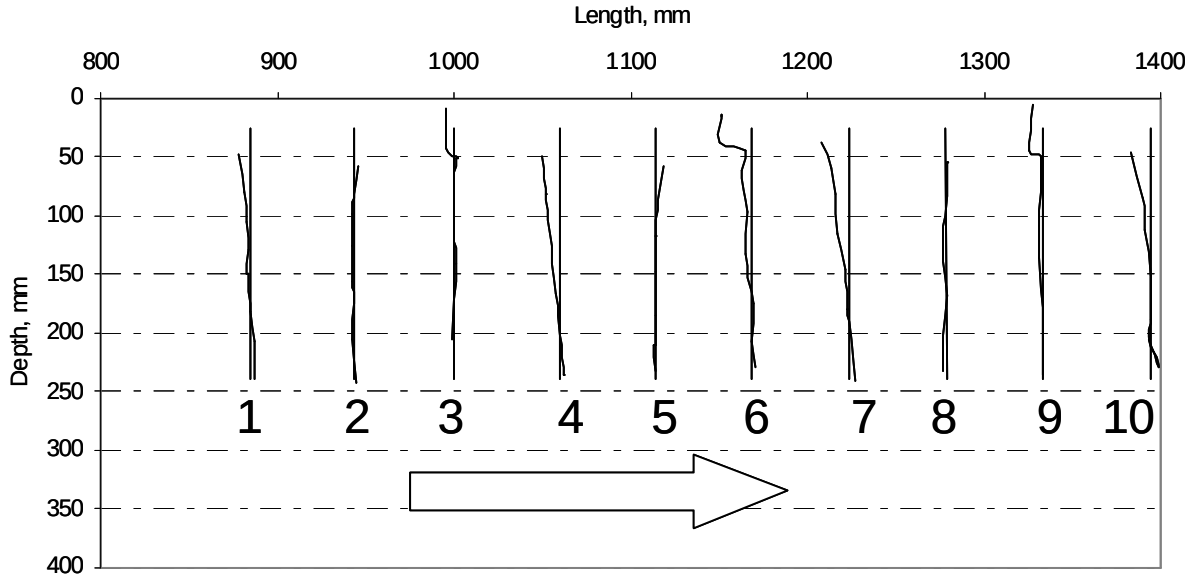

Figure 100: A digital image of the longitudinal position of the sand columns after the passage of a 12 t rubber track

To investigate the soil movement with depth the columns were divided into two parts. The lower 100 mm were taken as a reference basis and hence excluded from the comparison because of the assumption that this depth was not affected by the treatment. The assumption was confirmed by an analysis for the values from the lower 100 mm (track position -0.0008 mm, tyre position +0.0133 mm, LSD 0.51 mm). All parameters used to describe the data did not significantly influence the remaining variation and thus indicated a random distribution of the data around zero (p-values >0.9). For the upper 150 mm tilt, drive unit, and the interaction of tilt with depth were significant parameters describing the variation within the data. The mean position for the rubber track unit of the top 150 mm was -4.45

mm which was significantly different from zero. This compared to a mean position of 2.05 mm for the wheel which was not significantly different from zero with an LSD equal to 2.18 mm. Looking at the assigned tilt variables B, F, and I for both treatments, tilts B and I were negative and tilt F was significantly different from both indicating a positive, i.e. a forward soil movement.

In further support of the previous arguments it is interesting to note that the longitudinal movement which ceases at approximately 150 mm is equivalent to the point where the magnitude of penetrometer resistance drops back to that of the rear tyres (Figure 98) and even below front tyres (Figure 27).

Hence it was shown that in this very situation overall the track caused a significant backward soil movement at the surface whereas the wheel tended to cause a forward soil movement which was not significantly different from zero. As available slip data could not be accurately assigned over the distance the units travelled across the sand columns, it could be argued that the track had positive slip and the tyre negative slip thus causing these differences. However, the sand columns enclose three replications of lug-void cycles over a distance of 0.5 m and the data in Figure 99 and Figure 100 did not indicate a change in behaviour. Therefore the slip conditions could be regarded as constant with respect to longitudinal soil movement over the distance traveled and as both units are driven, it must be positive slip. Moreover penetrometer resistance randomly taken over the length of the soil bin always showed a higher surface strength for the track. These findings may change under the application of greater thrusts/slips.

According to Wong (2001) soil movement below a tyre is accompanied by a flow pattern including two opposing flow directions; except for two extreme conditions: At 100 % slip, soil will only flow backward. For a locked wheel, only a soil wedge will be formed pushing the soil forward whereby the size of the wedge depends on sinkage and the corresponding rake angle of the tyre. Any slip condition between these two extremes will include both forward and backward flow of soil. The higher the slip, the larger the backward movement will become. Following the soil trajectories given by Wong (2001) for a towed wheel, one at 37 % slip, and one at 63 % slip on a clay soil, at a slip range of about 10 – 15 % total longitudinal soil movement below a tyre could be zero due to the equilibrium of backward and forward soil flow. This was observed in this condition for the tyre. For the track on the

contrary, the bow wave and therefore forward soil movement was smaller due to the smaller rake angle and reduced sinkage. However, the backward flow pattern was more pronounced due to the constant slip conditions leading to an overall backward soil movement.

Figure 101 shows backward soil movement at the very beginning of a passage of a track/tyre and agreed with the results above. When a track started, soil was moved backwards as shown by the left hand figure which shows a clear shear failure boundary compared to the edge of the footprint from the track. In contrast, after the start of the tyre, no shear displacement could be seen, see right hand figure, although the soil lug disturbance pattern indicate high slipage at the start.

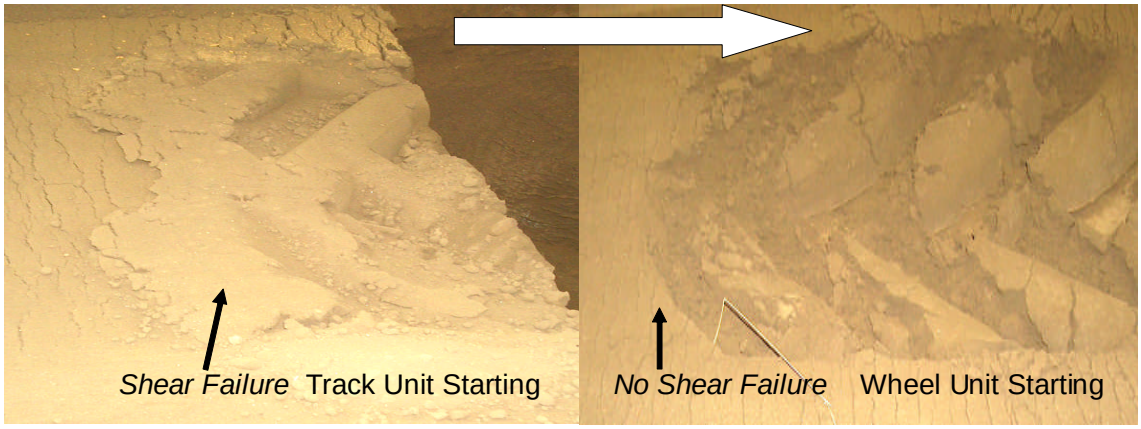

Figure 101: Soil disturbance after the track (left) and tyre (right)at the onset of movement

Therefore the following conclusions can be drawn:

- The peak in penetrometer resistance is not caused by the increased bearing capacity created by the pass of the front sprocket whereby afterwards merely the surface compacts as the load can be carried by the deeper soil because it is spread. This pronounced vertical compaction should be detectable in soil displacement curves.
- The peak in penetrometer resistance for the track is caused by the application of a constrained shear force for a long period of time (average slope in Figure 97 for tracks larger than for tyres, thus there is no additional vertical compaction close to the surface).

- A developed peak in penetrometer resistance can protect the subsoil and further compact vertically as shown with the rear tyres following a track thereby increasing its peak and possibly vertical compaction, yet the origin of an increase in peak penetrometer resistance can only be detected by looking at soil displacement and penetrometer resistance curves.

7.2 Influence of Lugs on Soil Displacement with Depth

Looking at the field surface after the passage of a tyre/track, the imprint of the lugs is very pronounced and challenges the question how deeply the lugs affect soil density increase. Information concerning the influence of lugs and inter lug area on soil compaction is limited. Whenever soil pressure was measured a difference in lugged and non lugged area could be detected (Gupta and Raper, 1994). As the authors stated the differences were not accounted for and it is difficult to account for them as their effect reduces with soil depth. Rusanov (1997) developed equations to calculate the pressure exerted by lugs on the soil at the tyre-soil interface. Way et al. (1993) found contradicting results with respect to soil density influenced by different lug heights on the same type of tyres and pressure peaks could only be found in a depth range of 160 – 280 mm (after removing outliers). The depth to which soil displacement was actually influenced by lugs had not been investigated. To shed light on this question photographs and diagrams from the talcum powder traces in the soil bin were analyzed.

When studying a soil profile after the passage of a wheel on relatively weak uniform soil condition, with an initial DBD of approximately 1.38 g/cc, lug displacement was visible to a depth of approximately 100 - 200 mm in Figure 102. This depth of lug influence was similar for all treatments.

The effect of the influence of the lugs on soil displacement is also shown in Figure 103 which represents a digital picture of the soil displacement in Figure 102. It shows the small heap on the right hand side of the centre in the third line from top, however, below this depth of 100 mm there was no further indication of lug influence.

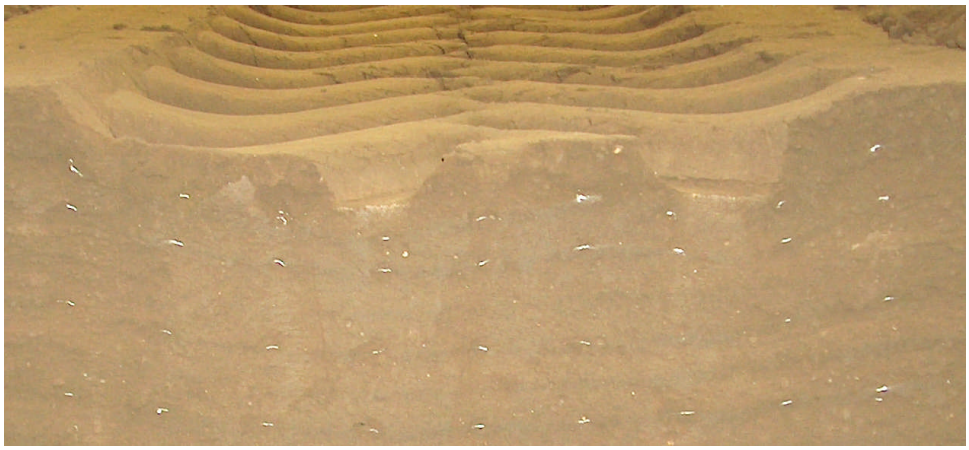

Figure 102: Soil displacement caused by lugs close to the surface after a 800/10.5/2.5; (Ansorge, 2005, a)

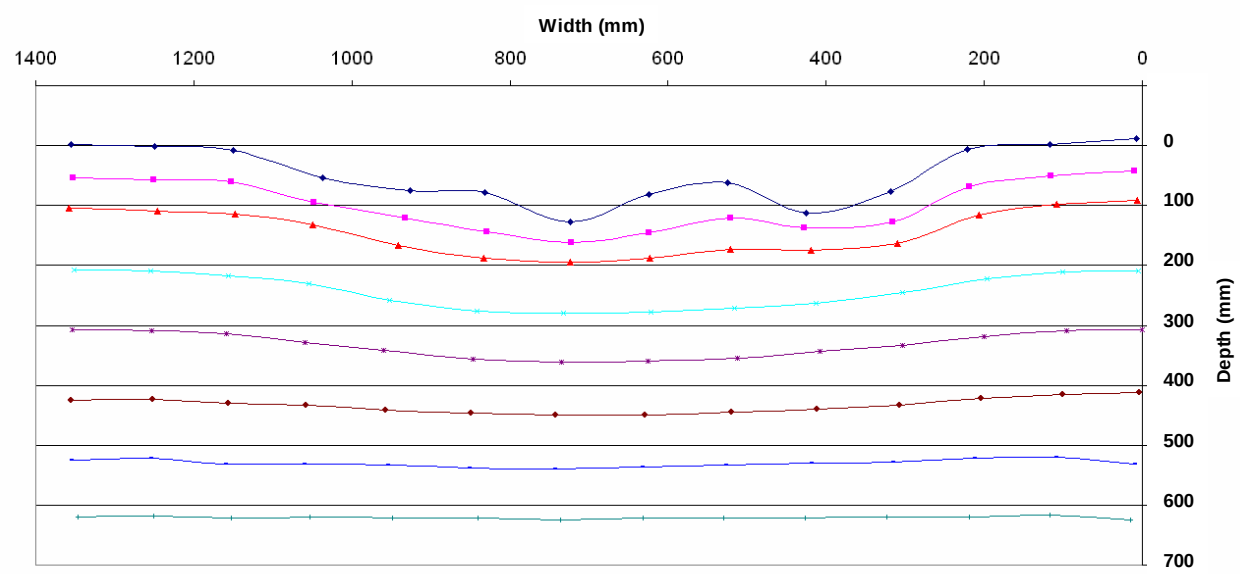

Figure 103: Soil displacement lines for 800/10.5/2.5; 2nd replication

It was difficult to analyze the data shown in Figure 103 with respect to lug influence because of the additional effect of decreasing soil displacement from the centre to the edge of the rut. To avoid this issue talcum powder lines were placed laterally along the centre line of the path of the tyre / track into the soil in order to be able to visualize the lug displacement with depth. The longitudinal cuts through the profile included the same section of the tyre/track; hence variances were only caused by the lugs. Figure 104 shows the longitudinal soil displacement lines through the profile. At the surface the regular lug pattern was obvious, however, the deeper the layer was situated the less obvious it became. Therefore a statistical analysis was carried out whereby valleys at the surface caused by lugs got as-

signed with an A while the peaks at the surface from the inter lug area got assigned a B. The explanatory power of this assignment was evaluated and as a result both, the parameter on its own and the parameter allowing for an interaction of peaks/troughs with depth were highly significant ($p<0.0001$). Normal distribution of the data was verified, too.

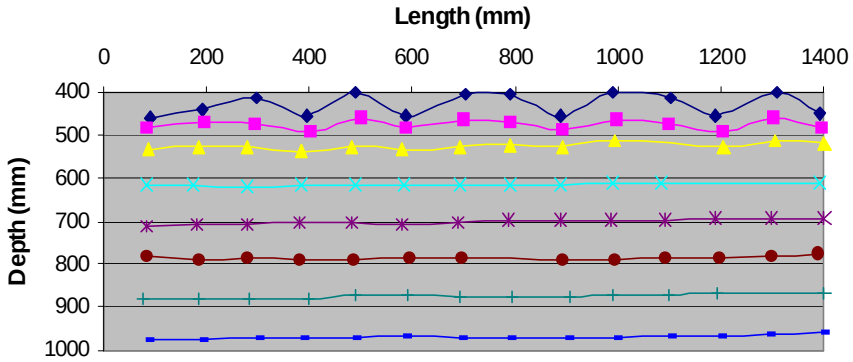

Figure 104: Soil displacement lines within a longitudinal cut for the 900/10.5/1.9

Subsequently the average peak and trough values at every depth were compared by subtracting the peak value from the trough value. The same procedure was applied for a track pass whereby peaks/troughs were assigned, too. The corresponding average numbers are shown in Figure 105 including the LSD. As obvious at the surface the difference between peak and trough was highest and decreases with depth rapidly. At 100 mm depth the difference was significant, however, from 200 mm downwards the differences were within the error probability.

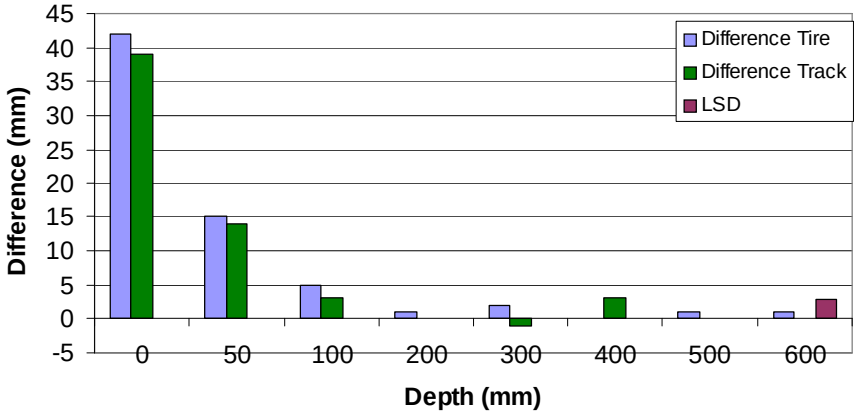

Figure 105: The average overall difference in peak and troughs values over depth. LSD at 5% error probability

Therefore it could be concluded that the influence of lugs in soil displacement measurements was limited to within the working depth. The characteristic of the lugs below the

track and the tyre was similar. The obvious differences were due to differences in the lug height and tread void ratio. The lug height for the tyre was 55 mm in the centre and 45 mm for the track. This supported the slightly larger difference for the tyre than for the track. The tread void ratio was 1 for the tyre and 0.43 for the track, i.e. the lugs cover less area under the tyre than under the track. Consequently the stress under the lugs of the tyre must be higher which further aided slightly deeper marks and leaving differences visible to a greater depth.

These results on very weak soil conditions led to the question of lug influence of lugs at the surface under a field condition. Therefore a sand layer was placed at a depth of 50 mm below the surface in a stratified soil described by Ansorge (2005, a) simulating real field conditions.

Figure 106 shows a cut lengthwise through the rut after the pass of a 900/10.5/1.9 on stratified soil conditions with the sand layer visible at a depth of 50 mm. The lugs cause a pronounced wave form in the layer of sand at this depth and situated close to the edge of the rut. Figure 107 is the same rut as the previous picture, but closer to the centre of the rut. Now the lugs were less pronounced than on the outside cut creating a wave with smaller amplitude. It can be concluded that due to the round shape of the tyre surface, leading to higher lugs on the outside, lug influence was less pronounced in the centre than on the outside. Looking at these profiles from the front, lug influence is not visible from the talcum powder lines deeper than 100 mm.

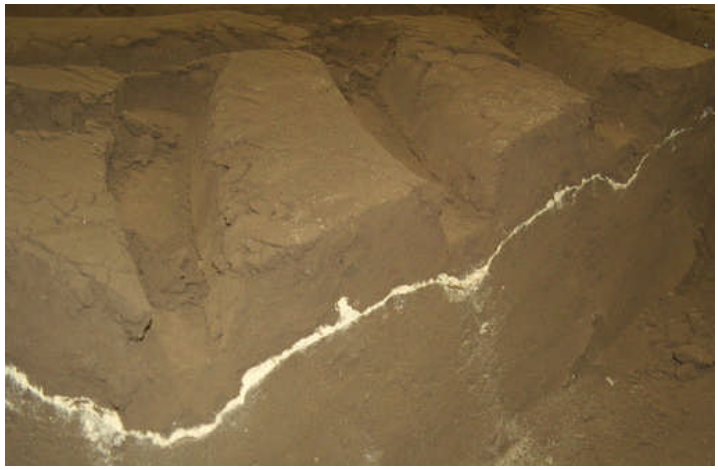

Figure 106: Lug influence close to the outside of a rut on stratified soil conditions after the pass of a 900/10.5/1.9

Figure 107: Lug influence close to the centre of a rut on stratified soil conditions after the pass of a 900/10.5/1.9

The conclusion can be drawn that soil displacement caused by lugs did not exceed the working depth of a weak uniform soil condition, i.e. it does not affect soil displacement significantly to a depth where it could not be alleviated with common tillage operations. Soil pressure measurements might indicate higher pressures due to the higher pressure caused by the lug on the soil (Gupta and Raper, 1994 and Way et al., 1993), but this pressure peak did not cause the soil to additionally deform to a critical depth. At the surface lug influence decreases when the distance to the centre of the rut decreases where the actual soil displacement is highest.

7.3 Introduction of a new Variable - Load per Perimeter Length

The following Section evolved empirically from a study relating soil density increase to contact pressure and aiming to account for the obvious variations as best as possible.

7.3.1 General Problems with Contact Pressure and First Considerations

When considering soil density increase depending on contact pressure some variation is obvious as visible in Figure 108 whereby plotting the average soil deformation caused by a single tyre or track treatment against its mathematical average contact pressure does not result in a smooth relationship. Taking the axle load into account shows that the higher axle load (quadrats) is always higher in soil deformation than the lower axle load (circles),

even when having a similar contact pressure. This supports the results from Lamande et al. (2006) based on the original theory from Söhne (1954) stating that the higher the load the more stress and consequently soil deformation is caused over the entire soil profile even if the contact pressure is the same.

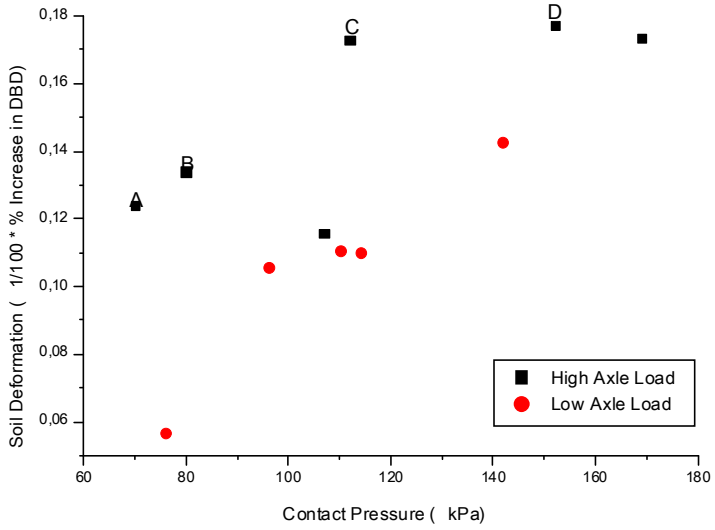

Figure 108: Soil deformation vs. contact pressure for tyre and track treatments

However, the theory from Söhne does not provide an explanation for the large deviations within a group of axle loading. Going from point A in Figure 108 to point B contact pressure increases from 70 kPa to 80 kPa, respectively 14.2 %. The corresponding soil deformation increases from 0.124 to 0.134, 8 % respectively. When looking at point C and D, contact pressure increases from 112 kPa to 152 kPa, 35.7%. Taking the previous comparison into account soil deformation should increase by approximately half, which is 15 - 20 %. Interestingly soil deformation only increases by 2.3 % from 17.3 to 17.7 %.

There is no obvious explanation for the deviation of soil deformation with an increased contact pressure. It might possibly be a diminishing rate of increase; however, considering the contact pressures of the low axle loads, no such diminishing rate is visible although reach into the same contact pressure range. To investigate the cause of the large scatter of data points, load was plotted against soil deformation. As can be seen from Figure 109 low axle loads can cause similar soil deformation as high axle loads. Per se there is no difference in soil deformation at different axle loads.

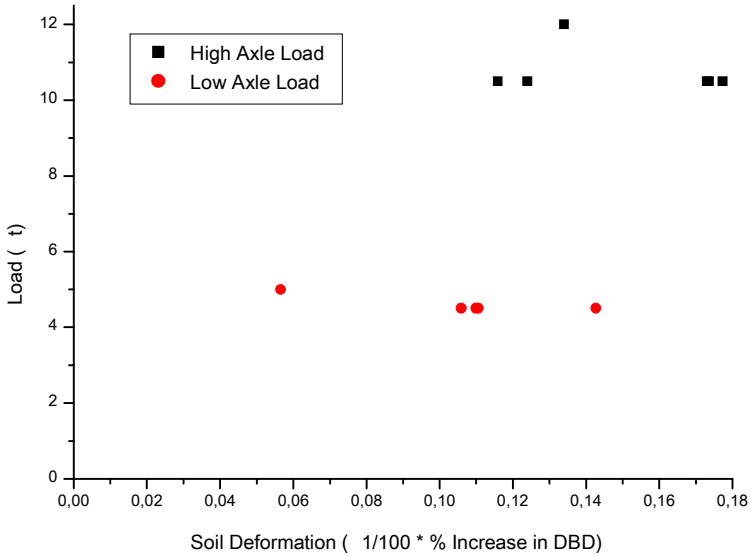

Figure 109: Load vs. soil deformation for tyre and track treatments

In a next step, load was plotted against contact pressure which is shown in Figure 110. Interesting to note is that the range of contact pressures for the two different load groups overlaps completely and not only partially as in Figure 109. In Figure 110 there is no indication that contact pressure is influenced by axle load, it merely spreads less at low axle load.

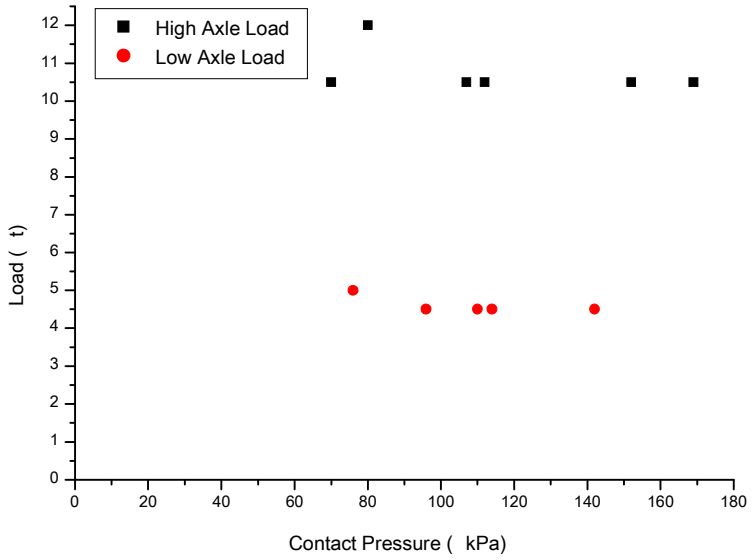

Figure 110: Load vs. contact pressure for tyre and track treatments

7.3.2 Influence of Contact Shape in Small Scale Experiment

The spread of data shown in Figure 108 with density increase plotted vs. contact pressure lead to the idea that contact geometry could have an influence. Hence, the aim was to investigate the soil behavior with different small scale plate shapes and loads simulating soil bin conditions and investigating the influence of plate geometry on sinkage.

With the plate sinkage procedure as described in 2.3.2 three plates of identical surface area (and hence contact pressure at identical loads) but different geometry were tested, a circular, a square (representing a possible tyre contact area), and a rectangular plate (exaggerating the length to width ratio of a track by 9 %), respectively. The area of each plate is 2800 mm^2 and the plates are shown in Figure 111. Each plate was tested three times at temporally average loads of 0.236 kN corresponding to 84 kPa and 0.374 kN corresponding to 132 kPa for 1.8 s whereby the load application simulated that of a tyre pass as shown on the left hand side in Figure 21.

The resulting sinkage for the three replications and treatments with an average load of 0.236 kN is plotted in Figure 112. The track shaped plate caused the least sinkage and the square plate was identical to the circular plate except for the 2nd replication. Thus a difference between the rectangular shaped plate compared to the circular and square plate can be shown. However, no clear benefit of a square to a circular plate could be shown. The corresponding force history is shown Figure 113. As visible from Figure 113 the load application was well repeated as all curves overlap. The unsteadiness of the force during the process of taking off load is due to the slow response of the force controller in comparison to the relaxation characteristic of the soil.

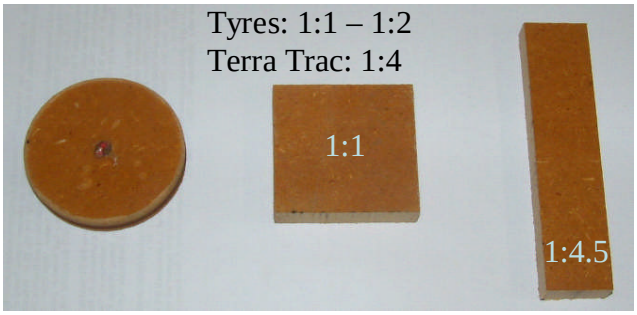

Figure 111: Plate geometry with equal area and varying perimeter length

In consequence the maximum sinkage in Figure 112 shows a small amount of noise. However, in comparison to the elastic recovery of the soil, noise is small (elastic recovery 0.8 mm and noise is 0.1 mm), and does not influence the shape of the curves, peak and relaxation sinkage measurably. Therefore no further attention will be paid to the noise.

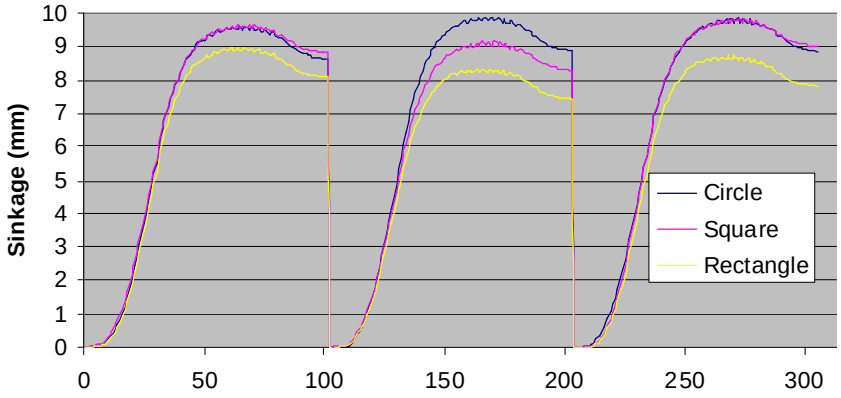

Figure 112: Sinkage at an average load of 0.236 kN for the three treatments

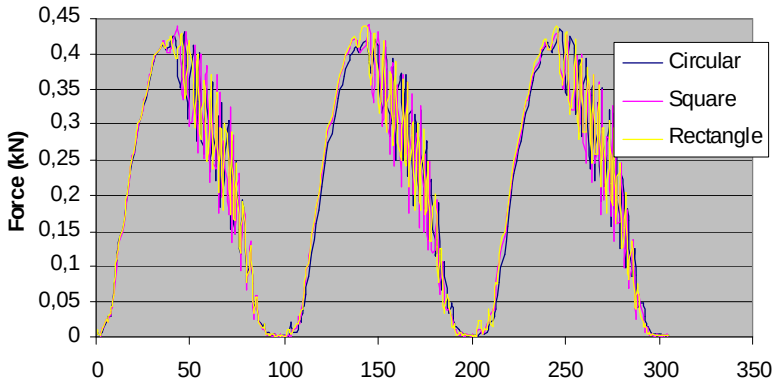

Figure 113: Force application for an average load of 0.236 kN for the three treatments

In a second phase the tests were repeated with an average load increased to 0.374 kN. The sinkage for the three treatments and three replications at higher load is plotted in Figure 114. Again the track shaped plate caused the least sinkage followed by the square plate and circular plate. Due to the higher load application the difference between the track and the circular plate increased from approximately 1 mm in Figure 112 to 2.5 mm. The force application over time is shown in Figure 115 and exhibits the same characteristics as discussed for Figure 113.

The results for both loads are summarized in Figure 116. The sinkages are the sinkages after relaxation of the soil has taken place. At 0.236 kN the rectangular plate causes a rut of approximately 7.9 mm, and the circular and square plate cause 10 % more sinkage than the track shaped plate, 8.8 and 8.7 mm, respectively. For 0.374 kN the circular plate has the largest sinkage of 18.7 mm followed by the square plate with a sinkage of 17.7 mm. The smallest sinkage is caused again by the track with 16.2 mm.

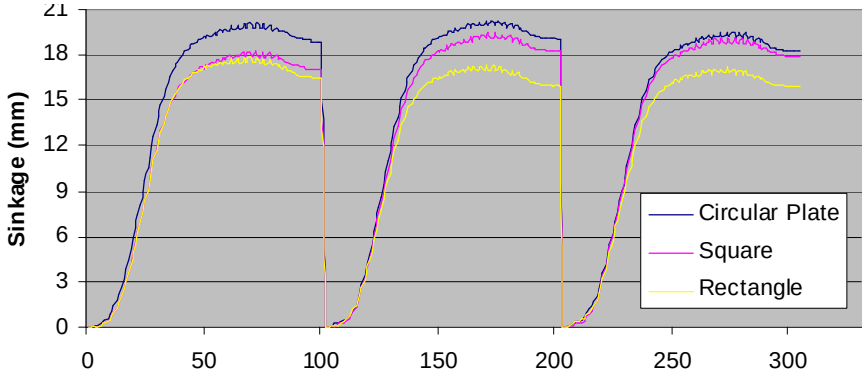

Figure 114: Sinkage at an average load of 0.374 kN for the three treatments

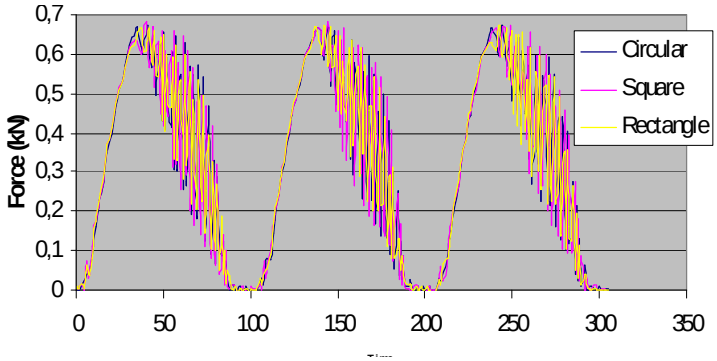

Figure 115: Force application for an average load of 0.374 kN for the three treatments

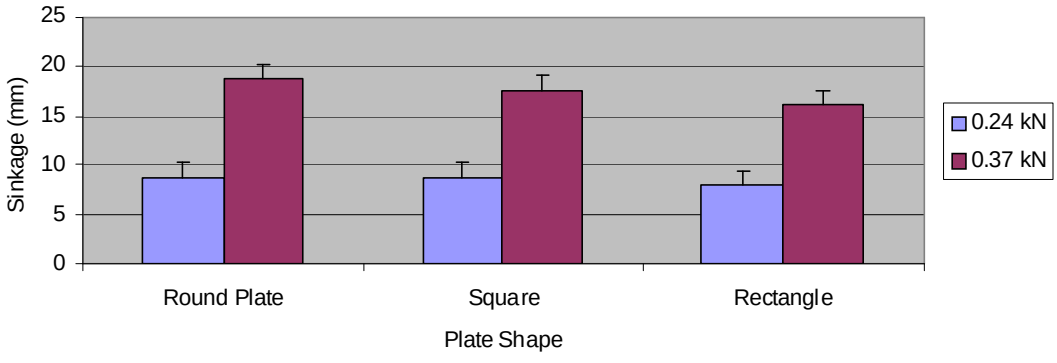

Figure 116: Summarized average sinkage for different plates at two loads including LSD

Compared to the track the square plate causes 10 % more sinkage, similar to the smaller load, and the circular plate causes 16 % more sinkage. Therefore these experiments have

shown that a long narrow contact patch can reduce sinkage compared to circular and square contact patch geometry.

The differences in sinkage behavior of the different plates observed can be evaluated depending on their shape and perimeter for this given soil condition. Therefore sinkage *S* can generally be described as:

$$S = \chi * \sigma + S_0$$

Eq. 8

whereby σ is the contact pressure and χ a shape factor determining the behavior of the plates depending on their contact area and perimeter. S_0 is a constant which should ideally be zero as at zero pressure no sinkage occurs.

The factor χ describes the individual sinkage behaviour of each plate depending on the contact pressure (if more pressures are used, plot sinkage against pressure and put linear regression function through it and use the slope of this line) is defined as:

$$\chi = \frac{S_2 - S_1}{\sigma_2 - \sigma_1}$$

Eq. 9

In the following it is attempted heuristically to understand the influence of contact area shape on soil deformation. In a first attempt χ is plotted against a form factor describing the circumference of the plates in relation to the circumference of the circle ($\frac{U}{U_{Circle}}$). Keep in mind the contact area for all plates is identical. If a straight line could be fitted through the data, it would show a linear dependency of χ on the perimeter length and hence a dependency of the sinkage on the perimeter length. As shown in Figure 117 a straight line could not easily be fitted as the square plate lies below the line.

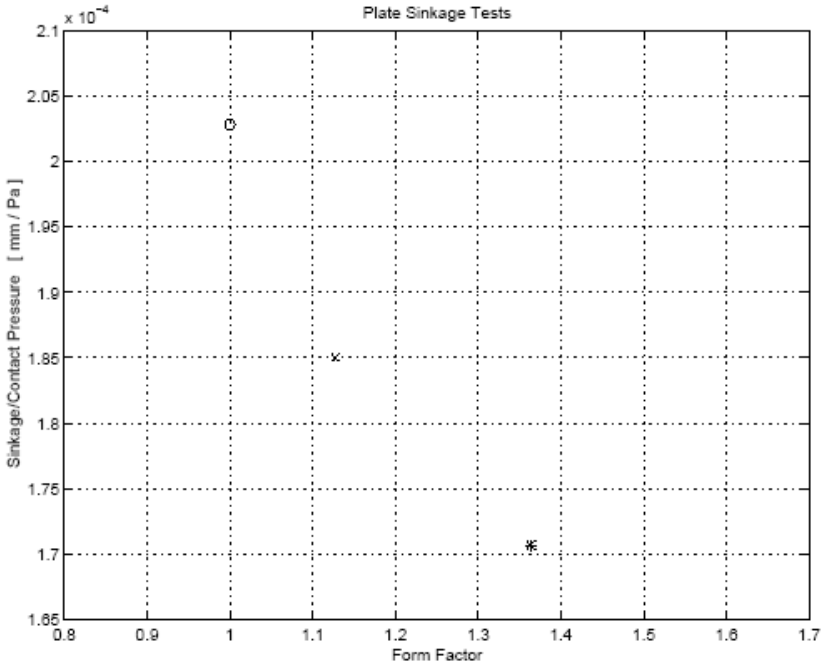

Figure 117: Sinkage/contact pressure (χ) vs. form factor

In a second attempt χ is plotted against the length of the diagonal *d* in Figure 118. In this case the square plate lies above the line connecting the outer points.

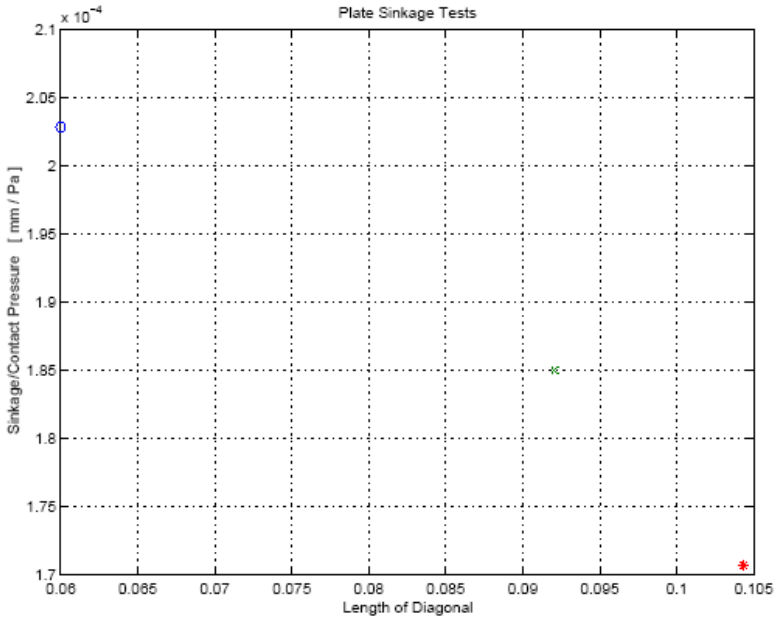

Figure 118: Sinkage/contact pressure χ vs. length of diagonal

The combination of the square plate being too high and too small resulted in the idea to plot the product of *d* and $\frac{U}{U_{Circle}}$ which resulted in the closest agreement to a straight line as displayed in Figure 119. Hence, χ can be described as:

$$\chi = c_2 * \frac{U_i}{U_{Circle}} * l_{Dia} + c_1$$

Eq. 2

whereby c_1 and c_2 are soil specific constants empirically determined. In the following Section this approach is transferred onto the experimental soil bin data from tyre and track passes.

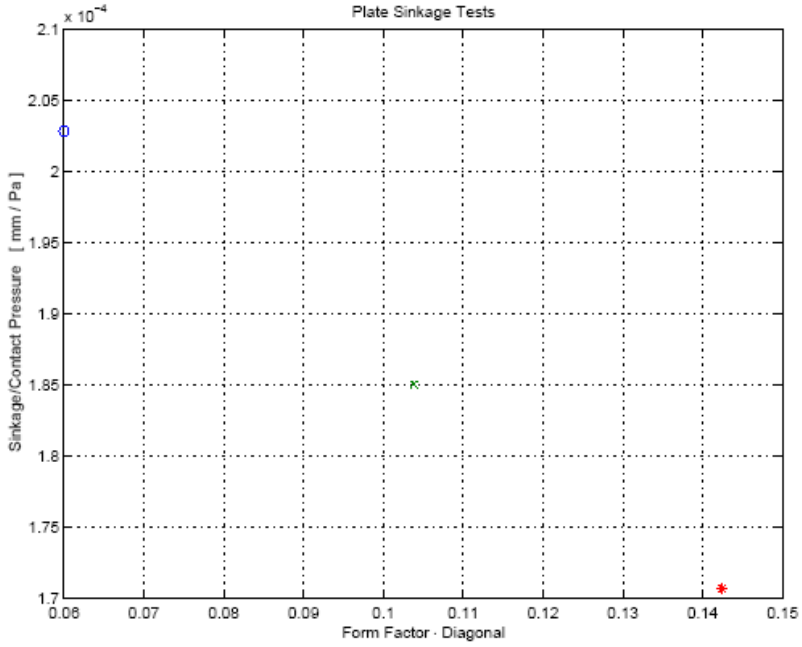

Figure 119: Sinkage/ contact pressure χ vs. form factor * diagonal

7.3.3 Application of heuristic approach to soil bin data

Figure 120 shows that if normalized sinkage is plotted against form factor for tyre/track data, the data shows a lot of variation and a linear regression line is not significant with an R^2 of 0.445 and a p-value of 0.17.

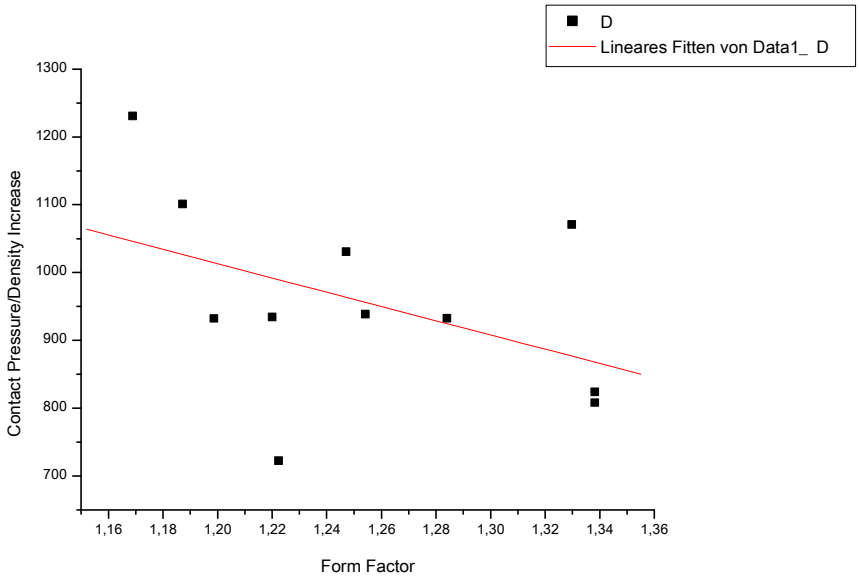

Figure 120: Contact pressure/rel. density increase vs. form factor

If in a further step normalized sinkage is plotted against the diagonal for the tyre/track data, the correlation becomes better and the linear regression function is significant with an R^2 of 0.639 and a p-value of 0.034 as shown in Figure 121.

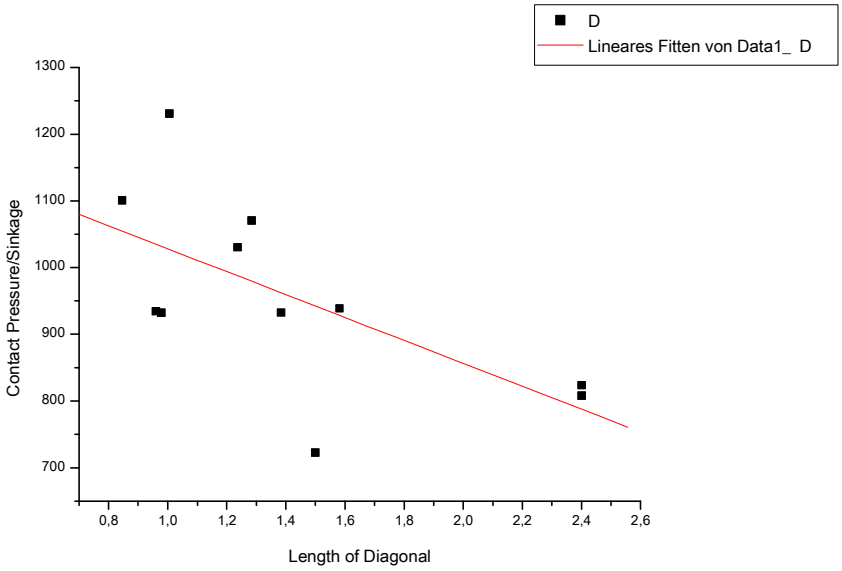

Figure 121: Contact pressure/rel. density increase vs. length of diagonal

With the unsatisfactory previous results, the last step of the theoretical approach described before is taken and normalized sinkage is plotted against the Form Factor * Length of Diagonal for the tyre/track data in Figure 122. The spread of data is similar to the previous one and so is the R^2 of 0.631 and the p-value of 0.037.

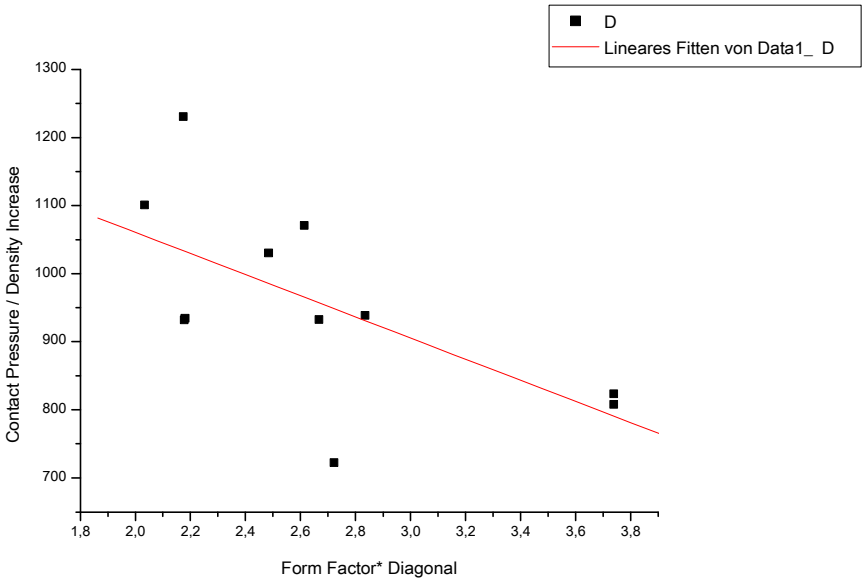

Figure 122: Contact pressure / density increase vs. form factor * diagonal

Hence, this approach is not able to reduce or better explain the observed sinkage behavior satisfactorily.

7.3.4 Derivation of Load per perimeter length (LPPL)

As the best method for describing plate sinkage in dependence of plate shape did not lead to satisfying results for the full size tyre/track data, the idea emerged that the circumference of the contact area might play an important role because of the punching failure of the soil caused by the tyres and tracks; the concept of load per perimeter length was created (LPPL). As visualized in Figure 123, the concept of the LPPL is a shear zone of limited thickness at the perimeter supporting the enclosed soil when load is applied. The effect is proportional to the perimeter length.

The data of the LPPL is plotted against measured increase in soil density Figure 124. In general soil density increase increases with an increase in LPPL, similar to the contact pressure in Figure 108, however, the spread of the data is much less with a R^2 0.858 of and a p-value of 0.0007. The fact that the LPPL is smaller for the smaller loads leads to a closer relationship between the high and the low axle load groups. Interesting to note is that all the data shows marginal noise if the 800/10.5/1.25 (the square at approximately 2.4 t/m, 0.115) is disregarded causing a much smaller increase in soil density increase than expected due to its LPPL.

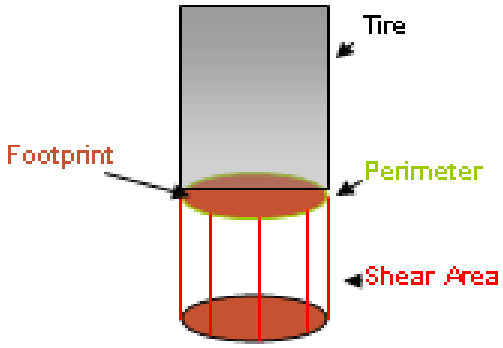

Figure 123: Footprint of a tyre with corresponding perimeter and shear area

The theory of Söhne (1954) can thus be confirmed by taking the influence of load on stress into account. If the soil has to carry a weight, which exceeds its own bearing capacity, the enclosed soil will support itself on the surrounding soil due to cohesion. The smaller the contact area, the larger in relation is this shear area and consequently the bigger is the effect of the LPPL. For a circular plate the circumference in proportion to the area enclosed decreases most efficiently with an increasing area. This is due to the fact that a circle surrounds the biggest area with the smallest circumference possible. The LPPL accounts for this and is highest for a circular plate. Consequently a long rectangular footprint maximizees the outside area load. This agrees with the benefit of the tracks as they cause the same soil displacement as the rear tyres because they have similar contact pressures and a similar LPPL.

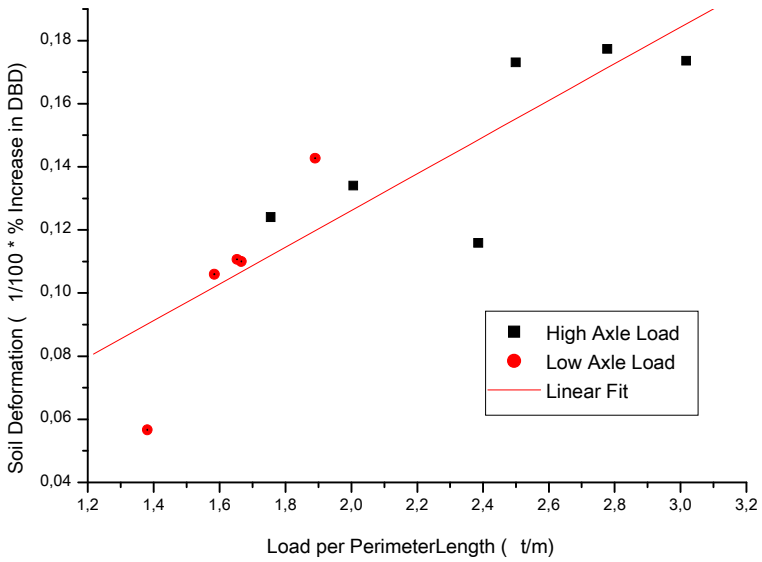

Figure 124: Soil deformation vs. LPPL for tyre and track treatments

The study from Lamande et al. (2006) confirming the theory of Söhne (1954) used identical contact pressures on different plate sizes. Thus the soil was subjected to the same pressure with each plate but with larger plates the total load increased. This resulted in twice the LPPL for the larger plate compared to the smaller one at the same contact pressure. Considering the concept of the LPPL, this might explain the larger impact of greater loads Lamande et al. (2006) observed in the subsoil and actually show that it is neither the contact pressure nor the load determining alone soil deformation and pressure distribution in the soil. It is a combination of the LPPL and the contact pressure.

The ability to describe the sinkage behavior from the soil bin experiments with the parameter LPPL reasonably well lead to a subsequent step: an investigation of the pattern of data points from small scale sinkage experiments replicating full size contact patches and plotting sinkage vs. LPPL compared to contact pressure for them. In a first instance this was investigated by using one plate and varying the applied pressure and measuring its sinkage and subsequently using different plate shapes scaled from real contact geometry.

7.3.4.1 Variation of plate sinkage with applied load/contact pressure

The response of small scale plates to applied pressure was investigated. A rectangular plate was laden to different contact pressures and the sinkage recorded. Afterwards the sinkage was plotted against contact pressure which is shown in Figure 125. A straight line fits the data exceptionally well and the intercept states that up to a pressure of 31 kPa no sinkage will take place as the soil is strong enough to carry this load without deformation.

Plotting the data against LPPL (Figure 125, left) does not reveal a different pattern. Consequently in this condition with one plate size it could not be decided which of the two parameters is able to describe the data more precisely. Due to the fact that the plate shape is the same, this is expected as with varying load contact pressure and LPPL change proportional to each other.

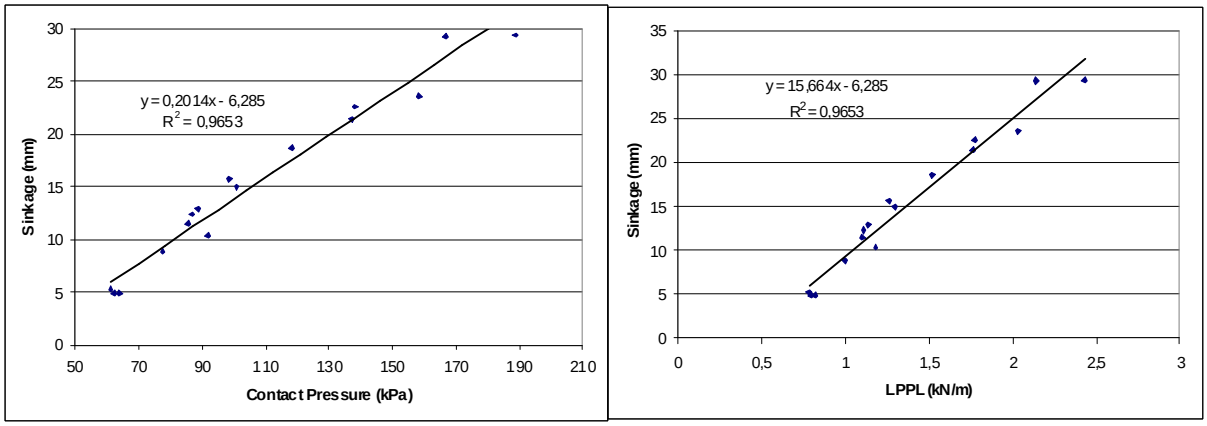

Figure 125: Sinkage of plate against contact pressure (left hand side) and against LPPL (left hand side) for plate No 1

7.3.4.2 The influence of the LPPL for different contact sizes

When introducing the parameter LPPL and plotting soil density increase against LPPL for soil bin data as shown in Figure 124 there was a clear relationship and higher correlation than with contact pressure. With scaled contact patches the question was if a similar pattern could be found. As shown in Figure 126 (left) when plotting sinkage vs. pressure a linear relationship could fit the data reasonably well. When plotting sinkage against LPPL the noise increases which is opposite to the findings in the lab.

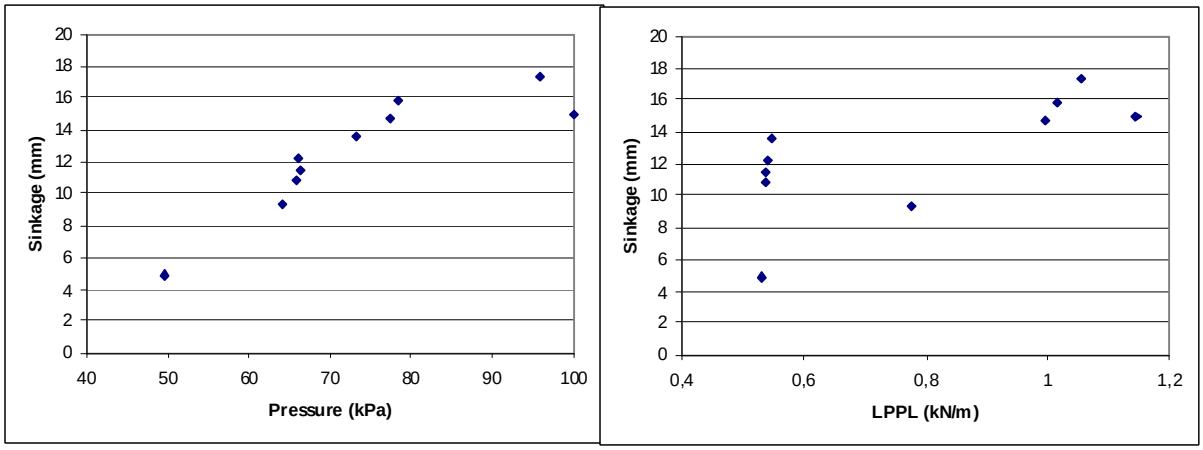

Figure 126: Sinkage vs. pressure (left) and vs. LPPL for different plate shapes replicating tyre contact patches from this study and Ansorge (2005, a)

7.3.4.3 Contact Area vs. Perimeter

These results show no coherent picture for the small scale plates between contact pressure, LPPL, and soil density increase. Therefore in Figure 127 LPPL is plotted against contact pressure for the soil bin experiment and shows two near linear relationships depending on axle load. If both, the contact pressure and LPPL data are divided by the corresponding load resulting in perimeter length and contact area which is plotted on the right hand side of Figure 127, their relationship appears to be linear. To ease further comparison, soil density increase will now be corrected for its influence of load, too.

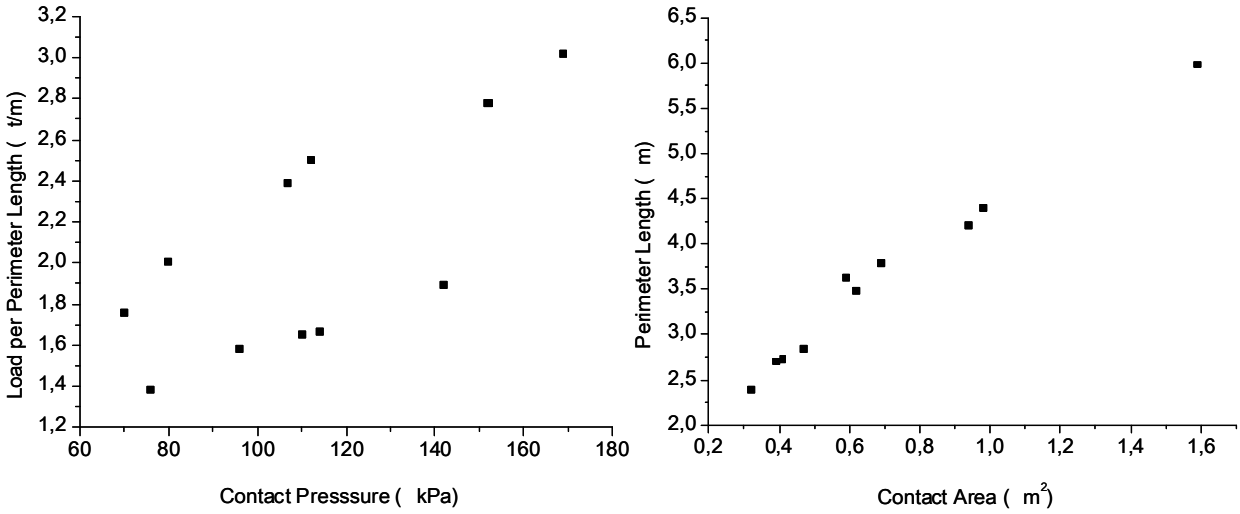

Figure 127: LPPL vs. contact pressure (left) and perimeter length vs. contact area (right)

7.3.4.4 Interaction of Contact Area and Perimeter

Since the previous Sections implied that both contact pressure and LPPL appear to have an influence on soil density increase, the following model was tested next on the soil bin experiment:

$$\mathrm{Re}l.DensityIncrease = ContactArea + PerimeterLength + ContactArea * PerimeterLength \qquad \text{Eq. 10}$$

The resulting prediction of the soil density increase is shown on the left of Figure 128 whereby a high correlation coefficient was achieved and the slope was equal to one. However, following the statistical analysis, the parameter “contact area” dropped out of this full

model which only marginally decreased the correlation coefficient as can be seen from the right hand side in Figure 128. The slight disadvantage of the prediction model was that both times the intercept was statistically significant, which ideally should be zero as at a measured density increase of zero the predicted one should be zero, too.

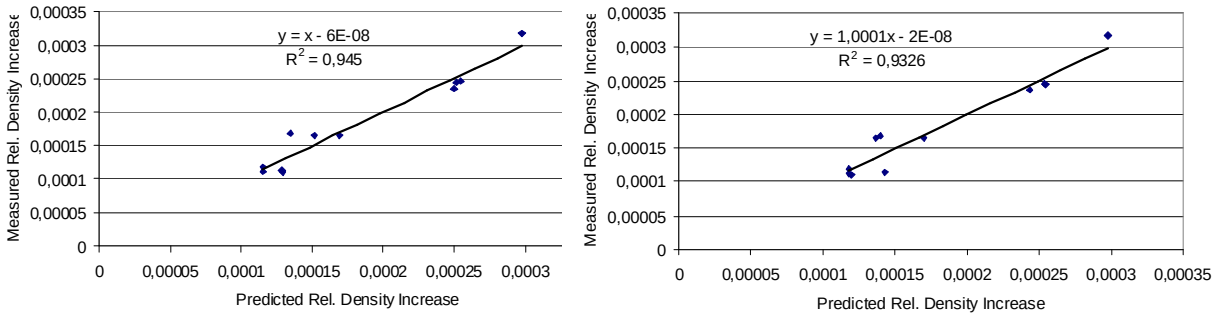

Figure 128: Measured vs. predicted relative density increase; full (left) and reduced model (right)

Therefore a further approach was heuristically taken whereby the relative density increase was described with the reciprocal of both contact area and perimeter length. Additionally the reciprocal of the interaction term again allowed an interaction between both. The result of the regression line is shown in Figure 129 on the left hand side. The correlation coefficient is highest and the slope virtually equal to one. All three parameters significantly describe the behavior and more importantly compared to the previous approach, the intercept is the only parameter not having a significant influence in explaining the data.

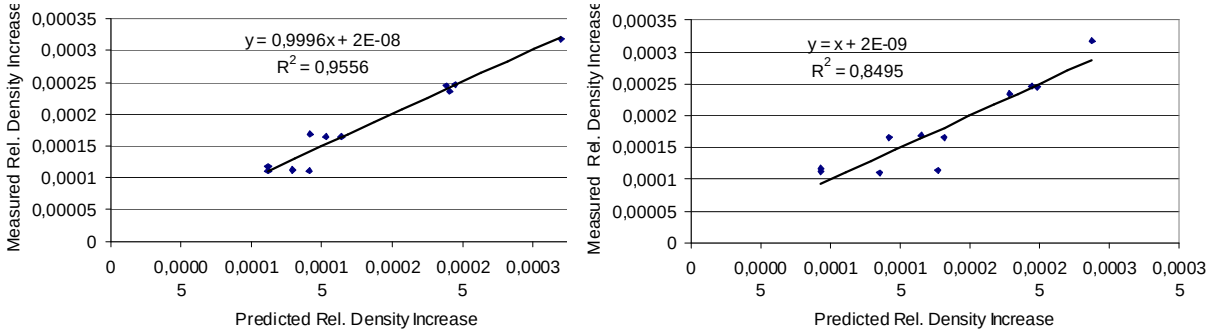

Figure 129: Measured vs. predicted relative density increase using reciprocals of Eq. 10; full (left) and empirically reduced (right) model

If the interaction term is not taken into consideration (right hand side of Figure 129) the correlation coefficient drops significantly and moreover the two remaining parameters are not significant anymore in describing the variation of the data.

Hence, a full model with reciprocal parameters explained the variation in the data best. To confirm this, the approach was utilized for the plate sinkage data from the triaxial test cell, too. Hereby the perimeter parameter drops out first, followed by the area. In the end the model remains with the interaction term being the only parameter significantly describing the variation in the data. Again, the intercept is insignificant except for the model with the interaction term only. This small scale data follows the same pattern which could be adopted for the soil bin data, too. If the parameter having the least influence would need to drop out independent of its significance, it was the perimeter. In the following reduced model, the area would drop out and as with the small scale data the interaction term remained. Hence, the same behavior pattern could be shown for both the soil bin and the triaxial data. This supports the significance of the interaction term and perimeter length in addition to contact area.

Looking at the individual terms shows an agreement in absolute values between the regression lines for the full size and scaled experiments.The general equation describing soil density increase is as follows:

$$\mathrm{Re}\,l.densityIncrease = \frac{a}{Perimeter} - \frac{b}{Area} + \frac{c}{Perimeter * Area}$$

Eq. 11

As the intercept for both full size and scaled models was not significant it was not added to the equation. The reciprocal of the area is the only negative term in the equation. This shows the contribution of the area to a reduction of the density increase is greatest for small size plates. The contribution of the perimeter to an increase in density decreases with increasing perimeter. The reciprocal of the interaction term adds to the density increase, too, in a decreasing manner as contact size and perimeter length increase. For the particular data a = 0.0013, b = 0.0003, and c = 0.0005.

It was a success to be able to describe the behavior of small scale plates with the same method as tyres although the plates only apply static pressure and do not simulate the kneading of a tyre. It can be concluded that the same link is connecting small scale plate sinkage experiments to real tyre pass data as for the in-situ VCL dapproach.

7.3.5 The Influence of Contact Time

Due to the different lengths of the plates, contact time varies when assuming the same vehicle speed for traveling. All the scaled plate sinkage experiments before do not take different contact times of the implements into consideration. Therefore a further experiment was conducted using the square plate, an intermediate rectangular plate (which had not been used before) and the long rectangular plate representing a "track". All plates had the same area and the same average load (0.236 kN) was applied. The contact time for the square plate was maintained, the contact time for the intermediate and track shape plate were adapted representing their increased contact length and assuming constant speed in a hypothetical pass. Therefore contact time for the track was 3.6 s and for the intermediate plate 2.4 s compared to 1.8 s which was previously used and is now only used for the square plate having the shortest length. The circular plate was not considered as its diameter is similar to the length of the square.

As the following diagram shows, the track creates the most sinkage due to its prolonged contact time. There is no difference between the intermediate and the square plate.

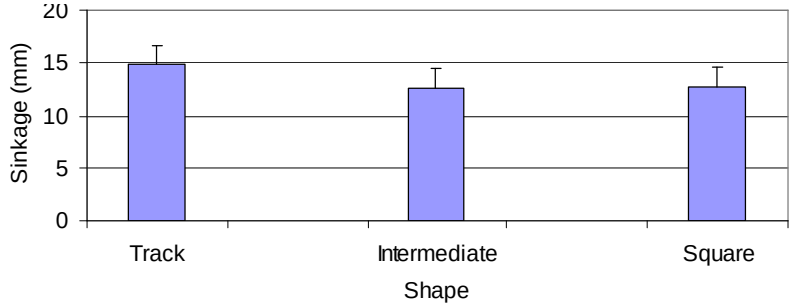

Figure 130: Sinkage for different plate shapes accounting for different contact times including 95% - CI

These results show the complexity in designing undercarriage systems. All results have to be taken into consideration simultaneously, because if only contact shape is taken into consideration one conclusion might be drawn, however, when taking contact time into account, the result might be different. These results contradict the real results from the soil bin whereby tracks caused a smaller sinkage than tyres although having a longer contact time. However, the overall reduced contact pressure is not taken into consideration in this study. Moreover, the track specific soil density increase is described in Section 6.4 for the track specific in-situ VCL and in Section 7.1 the longitudinal soil movement is investi-

gated. If it was possible to obtain vertical soil displacement data while implements were passing, probably more could be explained.

Thus in a future study it is recommended to measure the pressure and actual displacement below a track simultaneously to trace vertical displacement at varying depths while a track passes. This would enable to investigate the effect of plate geometry in more detail as it was possible to replicate the true pressure distribution below the track, too.

7.3.6 Influence of LPPL on Predicted and Measured Increase in DBD

The influence of LPPL on measured soil displacement was intensively shown. The remaining question is to which extend this was taken into consideration with existing soil compaction models. Therefore soil density increase predicted with COMPSOIL using the in-situ VCL developed in Section 6.3 was used to predict increase in DBD. The result was plotted against the corresponding LPPL in Figure 131. As it can be seen from the measured data on the left hand side compared to the predicted data on the right hand side, the overall tendency is very similar and both curves show similar curvature, too. The “outlier” in the measured term is obviously not represented in the predicted term. However, for the predicted diagram there is a similar increase in density increase for the low axle load as it was measured. The high axle load flattens, too.

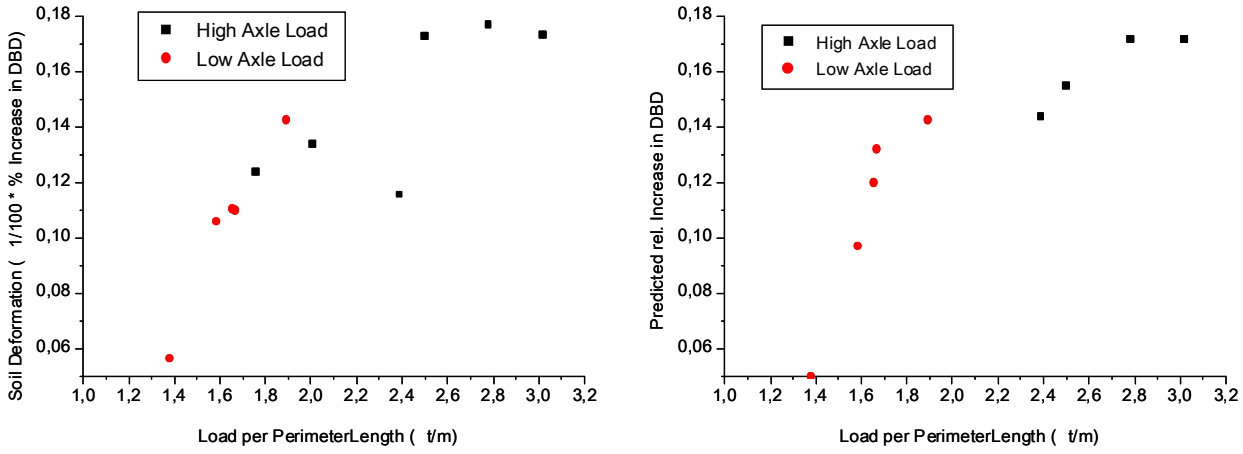

Figure 131: Measured (left) vs. predicted (right) increase in DBD against LPPL

7.3.7 Discussion, Conclusions, and further recommendations from LPPL

It was shown that both contact area and load per perimeter length describe soil displacement. The importance of the LPPL having a significant influence can further be stressed by the mere vertical soil failure which will in detail be discussed in Section 7.5.

Being able to describe the relative density increase in dependence of the reciprocal of the contact area, reciprocal of the perimeter, and the reciprocal of an interaction term between the two emphasized the overall validity of the concept as it was possible to predict the relative density increase for both full size and small scale experiments highly accurately.

The benefit of a long narrow contact patch was shown by Seig (1985) and others. With this study it was possible to actually link a parameter to the plate shape. However, for actual tyre and track design the contact time has to be taken into consideration, too. The implications of contact time on the geometry of the implement have yet to be investigated and it is recommended to measure the pressure and actual displacement below a track simultaneously to trace vertical displacement at varying depths while a track passes in a future study. This would answer the question to which extend it was sensible to take the effect of plate geometry into consideration with such experiments and whether it is necessary to replicate the true pressure distribution below the track, too, when considering contact time.

For a future total evaluation and continuation of the work the availability of TexScan can contribute to the verification of the influence above as contact areas can be determined much more accurately and so can the perimeter length.

7.4 Influence of Pressure History on Sinkage

There has been a long controversy between soil scientists and agricultural engineers about the influence of a peaked vs. a constant pressure history and their implication on resulting sinkage. In literature no information can be found concerning their effect. Thus it is not clear whether and if so to what extent sinkage is affected by the loading pattern.

The availability of a triaxial test apparatus which allows the application of axial load pattern up to 1 Hz enabled this experiment on the influence of constant vs. peak pressure. The

axial load was applied as shown in Figure 21 to two plate sizes. Each plate was randomly laden to either constant or peaked pressure, which resembled the loading cycle as if the tyre passes the soil, three times. The time integral of pressure was kept identical for both plates and histories. Thus any difference could only be caused by the difference in pressure application. The resulting sinkage is shown in Figure 132.

Plate 1 represents a large harvester tyre and Plate 2 represents the contact area of a track. In both cases the peak pressure causes significantly more sinkage than the average pressure. This result emphasizes the importance of the peaked pressures. If the pressure history could be made uniform, the soil displacement could be further reduced. The reduction in this case would have been approximately 1/3. Therefore it can be concluded that it is beneficial to minimize pressure peaks from undercarriage systems in order to reduce the impact of traffic on soil.

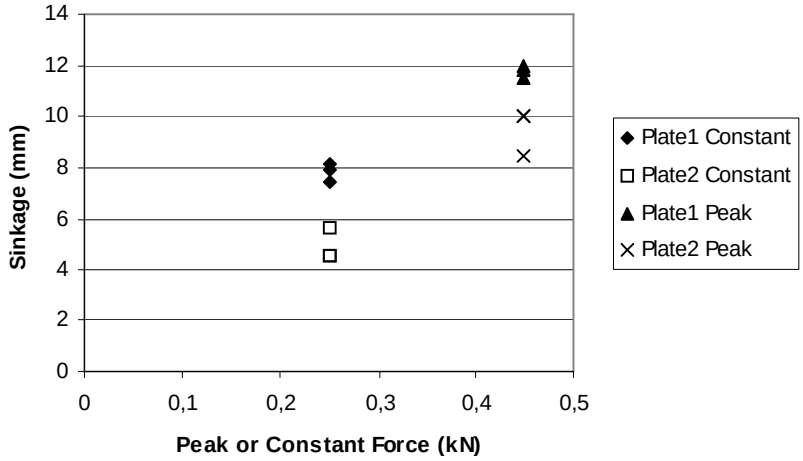

Figure 132: The influence of peak pressure vs. constant pressure while the average pressure is the same both times

7.5 Consideration of Vertical Soil Failure

The vertical soil failure indicated by the vector diagrams of soil movement found after the passage of tyres and tracks indicated in this work (e.g. Figure 8) and Ansorge (2005, a) was first reported by Seig (1985) who refered to it as “punching type of soil failure”. Trein (1995) reported the same characteristic. This characteristic contradicts the soil movement expected from the pressure bulbs of the theory of Söhne (1953). In the following plate sinkage and passive earth pressure theory are taken into consideration aiming to explain the punching failure.

Terzaghi (1943) and Meyerhof (1951, 1963, 1974) have studied the failure pattern below superficial foundations. These experiments used a loaded plate and thus static conditions. Earl (1997) extended plate sinkage theory and has studied the problem of a plate which is forced into the soil at constant speed. This is comparable to the sinkage of tyres. If a tyre has a constant forward velocity and causes a constant rut depth, the soil, while passing underneath the tyre from the front of the tyre to the rear, is compressed vertically at a speed depending on tyre radius, rut depth, forward velocity, and inclination angle of the tyre.

Earl (1997) suggests three modes of compaction below a plate during a plate sinkage test at constant speed. In the first mode the soil compacts with constant lateral stress, followed by the second mode during which lateral stress increases while the soil compacts. In the last mode lateral displacement and compaction take place. Based on the previous observations and experimental results from literature showing the formation of a cone under the plate (Terzaghi, 1943; Meyerhof, 1963; Earl, 1997), Earl and Alexandrou (2001) developed mathematical expressions to predict the mode and define three distinct phases in the displacement process during plate sinkage tests. These phases are shown in Figure 133. Initially (Phase I) soil compacts due to the penetration of the plate. This is followed by a transition period (Phase II) during which a cone starts to form and lateral stress increases. In the final stage a cone has developed and the soil fails (Phase III).

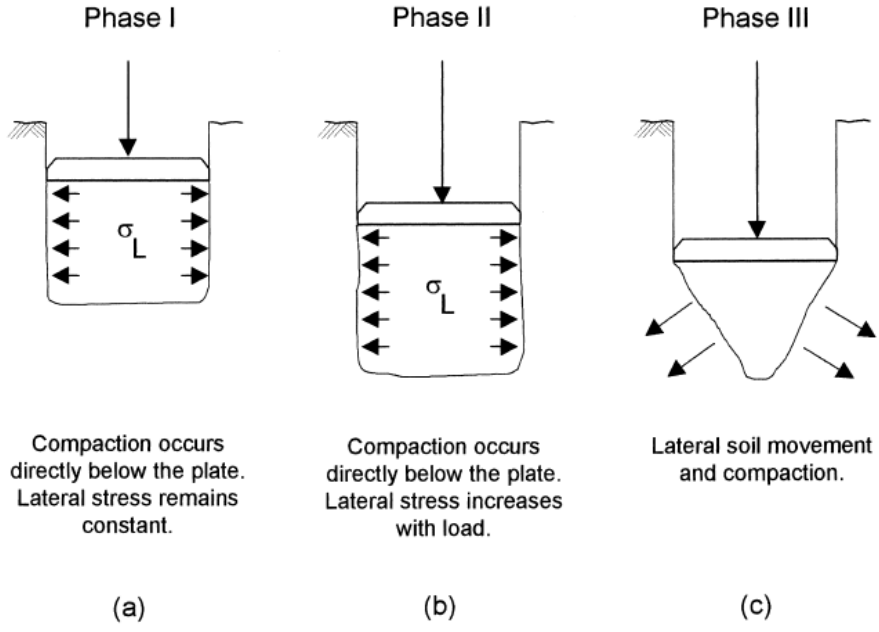

Figure 133: Three phases (a, b, and c) of soil displacement during a plate sinkage test (from Earl and Alexandrou (2001))

Benoit and Gottelund (2005) have continued the work from Earl and Alexandrou (2001) and gave the following equation for the sinkage depth Z_I at which Phase II is initiated:

$$Z_I = \frac{B}{2}\left(\frac{\gamma_c}{\gamma_i} - 1\right)$$

Eq. 12

whereby *B* is equal to the diameter of the plate and at the same time equal to the maximum extend of soil compression below the plate following the classical calculations of soil compression below foundations based on Boussinesq (1885), γ_c is the critical density necessary below the plate to initiate the formation of a cone, and γ_i is the initial density of the soil. Whether the transition form and therefore the initiation of a cone development takes place can be investigated, if the rut depth and the final density γ_f below the implement are known and Eq. 12 is rearranged to:

$$\gamma_c = (1 + \frac{2 * Z_I}{B}) * \gamma_i$$

Eq. 13

If $\gamma_c \geq \gamma_f$ Phase II will not be reached. An estimation of the situation for the experiments in the soil bin laboratory I have values for γ_i = 1.38 Mg/m^3, Z_I = 0.1 m (assuming the rut depth is the critical depth) and *B* = 0.7 m results in γ_c = 1.78 Mg/m^3. As $\gamma_c \geq \gamma_f$ is satisfied because γ_f is smaller than 1.6 Mg/m^3 no cone formation and thus no sideways movement has taken place. Consequently the vector diagrams show a clear vertical soil failure. This shows that the results from the soil bin agree with the theory developed for plate sinkage tests.

A further justification of the vertical soil failure reported by this work, Ansorge (2005, a), Trein (1995), and Seig (1985) can be derived from the passive earth pressure theory after Rankine (1847) and Terzaghi (1943).

The earth pressure at rest theory is used to calculate the horizontal pressure component σ_h in the soil which (below the tyre) pushes the soil horizontally against soil outside the

contact area. σ_h is restrained by the passive earth pressure σ_p and depending on which is larger the soil moves or moves not sideways.

For the sandy loam soil of the soil bin cohesion *c* is 5 kN/m^2 and the angle of internal friction ϕ is 39 degree (Ansorge, 2005, a). σ_h is calculated with the following equation:

$$\sigma_h = k_0 \times \sigma_v$$

Eq. 14

whereby k_0 equals:

$$k_0 = 1 - \sin\phi$$

Eq. 15

from the above equation follows $k_0 = 0.37$.

Taking a load of G = 105 kN on a contact area A = 0.94 m^2 and assuming that the soil has a density of 14kN/m^3 and assuming a depth z = 0.4 m results for σ_v from the following equation which takes the surcharge and the additional tyre load into account:

$$\sigma_v = \frac{G}{A} + \gamma \times z$$

Eq. 16

σ_v = 117.3 kN/m^2

putting σ_v in Eq. 14 results in the horizontal pressure component σ_h = 43.4 kN/m^2. This is the force pushing the soil sideways. The force which restrains this movement is the passive earth pressure equation of Rankine (1943) Theory which results for σ_p in:

$$\sigma_p = \gamma \times z \times \tan^2(45 + \frac{\phi}{2}) + 2 \times c \times \tan(45 + \frac{\phi}{2})$$

Eq. 17

with the given numbers from above σ_p = 45.6 kN/m^2

As $\sigma_p > \sigma_h$ the soil can not move sideways. For the softer soil condition used by Antille (2006) whereby sideways movement was detected for a DBD of 1.2 g/cm^3 and cohesion of 4kN/m^2, the resulting σ_p is equal to 37.9 kN/m^2 whereby σ_h was marginally smaller with 43.2 kN/m^2 and consequently the soil can move sideways. Quod erat demonstrandum.

The results in general agree with Koolen and Vaandrager (1984) who did not detect lateral soil movement at a relationship of $\sigma_3 \div \sigma_1 \approx 0.5$ which is close to the relationship assumed for minor and major principal stresses in Section 6.3.2 for a concentration factor of five and equal to the relationship at a concentration factor of four.

In an investigation of Gibson (1967) the surface did not settle outside the loaded area. Chancellor and Schmidt (1962) report a circular pattern of soil movement whereby with increasing rut depth the soil is pushed more sideways, but none or only small amounts are pushed above the original surface. Nevertheless Chancellor and Schmidt (1962) state as well, that a high percentage of volume reduction was caused by vertical displacement and suggest to measure rut depth to measure soil displacement supporting the procedure described to gain the increase in DBD in Section 6.3. In their case contact pressures were higher and thus they observed sideways soil movement. Issensee (2007) reported the same finding from horizontal penetrometer resistance measurements whereby no increase in resistance could be detected outside the loaded area. All this agrees with the findings of Kirby et al. (1997) who detected the largest vertical shear displacement underneath the tyre edge and ties back to the effect of the LPPL derived in Section 7.3.

Hence it has been possible to clearly explain the nature of the vertical soil failure with two independent soil mechanics theories, plate sinkage and passiv earth pressure theory, respectively. Therefore it can be concluded that if the pressure bulbs of Söhne (1953) reach outside the loaded area, they at least do not to influence the direction of soil movement. Results from Lamade et al. (2006) suggest that these pressure bulbs do not reach outside the contact area.

7.6 Conclusions on Ancillary Experiements

- The benefit of the tracks could be attributed to the dense layer created at the soil surface and their small contact pressure. This layer is caused by an alternating backward forward soil movement below a track. Overall backward soil movement was more pronounced below a track whereby the surface 150 mm of soil tilted significantly backwards (-4 mm). In comparison to this the passage of a tyre tilted the

soil forward (+2 mm) which was not significantly different from zero. In both cases this is limited to the top 150 mm in weak soil conditions.

- The influence of lugs on variation in soil displacement could statistically be proven to a depth of 100 mm. At 200 mm depth and below the influence of lugs could not be statistically verified.
- Load per perimeter length describes measured increase in DBD more accurately than contact pressure for full size tyres. Overall relative soil density increase can accurately be described by the reciprocal of contact area, perimeter, and an interaction term for both full size and small scale sinkage results. The validity is emphasized by an insignificant intercept making the prediction zero when it should be zero.
- The time history of pressure application has an important influence on sinkage. A pressure peak lead to 1/3 more sinkage than constant pressure.
- The punching soil failure observed by this study and others can be explained by plate sinkage theory and passive earth pressure theory.

8 CONCLUSIONS

- The benefit of tracks with respect to reduced soil displacement, penetrometer resistance, rut depth, and density increase shown by Ansorge (2005, a) is maintained for entire machine configurations after the additional passage of the rear axle in both laboratory and field studies.
- Alternative wheel configurations could reach the performance of tracks if the tyre load does not exceed 5 t. It was shown that a combine harvester equipped with TerraTracs at a total weight of 33 t maintains soil displacement similar to that of a wheeled combine harvester of one third of the weight The track at 2.67 times the load of a tyre causes similar soil displacement.
- The superiority of the tracks towards additional soil displacement caused by the rear tyres could be attributed to the dense layer created at the soil surface.
- The differences between different tracks can be attributed to the number of rollers and belt tension as they can significantly affect soil displacement. However, the effect of belt tension of the friction driven TerraTrac on soil physical properties proved to be small within the range of belt tensions available.
- The draught force necessary to loosen soil after the passage of a wheeled machine is significantly higher than after a tracked machine and can reach a factor of 3 if the additional working depth resulting from deeper reaching higher compaction after a wheel is taken into consideration.
- An in-situ method was developed to gain the slope and intercept of a virgin compression line basically from 2 different tyre passes in the field with known weight, inflation pressure and rut depth. Using these in-situ VCL parameters in the model COMPSOIL of O'Sullivan et al. (1998) it was possible to predict the input data and independent data within the LSD. The entire method was successfully validated in field conditions and small scale plate sinkage tests.
- Soil density increase after the passage of tracks could be predicted using a track specific in-situ VCL. Hence, it became obvious that tracks show a different compaction behavior than tyres.
- Triaxially derived VCLs are sensitive to the relationship of major and minor principal stresses. Only if their relationships replicates true field conditions, a suitable VCL for soil compaction prediction can be gained.

- The longitudinal soil movement below a track is tilted significantly backwards whereas the soil is tilted forward below a tyre in low slip applications. In both cases this movement is limited to the top 150 mm in weak soil conditions.
- The influence of lugs on variation in soil displacement is limited to a depth of approximately 150 mm.
- Load per perimeter length appeared to describe measured increase in DBD more accurately than contact pressure alone. Soil density increase for individual treatments could be described by the reciprocal of three trems: area, perimeter, and an interaction term. The intercept was not significant which means that there is no offset. Hence, it has been possible to define the sinkage from a tyre contact area perspective.
- Peak pressures replicating the pass of a tyre cause 1/3 more sinkage than the application of the constant average pressure.
- The vertical "punching" soil failure found in the laboratory studies supports the findings of Seig (1985) and others and can be explained by both plate sinkage theory (Benoit and Gotteland, 2005) and passive earth pressure theory.

9 FURTHER REQUIREMENTS AND PRACTICAL SUGGESTIONS

- An investigation of vertical and horizontal soil displacement characteristic under the application of higher track and tyre slippage.
- Future work would need to show whether there is a difference on total soil displacement due to lug height; ideally with a lugged and an unlugged tyre.
- Linking pressure transition throughout the soil to soil displacement.
- Improving the prediction of contact pressure particularly for under and overinflated tyres as existing predictions proofed to be unsatisfactory in this range.
- Agronomical study enlightening the monetary benefit from tracked vs. wheeled machinery and ideally comparing tracked vs. wheeled mechanization schemes.
- A different attachment system for the tracks might be useful in order to evenly balance the tracks under traction, thereby improving their performance in context with soil compaction.
- The influence of VCL parameters on the predicted shape of the soil displacement curve would be interesting as from the in-situ track VCL it appears as if the curvature is slightly different than after tyres.
- The VCL, however obtained, obviously depends on the stress configuration of minor and major principal stresses. Therefore it would be beneficial to set up a more general relationship between those properties.
- If it was possible to link drop cone data (Godwin et al., 1991) to small scale plate sinkage data deriving an in-situ VCL, a second field - possible method for deriving in-situ VCL parameters was available besides full size machinery.
- A further improvement of track design with respect to belt width and tension and roller distribution would be beneficial. Smoothening pressure peaks while simultaneously maintaining the insensitivity of the system against dirt would be beneficial.
- Confirming the findings of the LPPL with TexScan due to a better defined contact area and measuring displacement simultaneously with pressure would allow more detailed information about tracks.
- An investigation into the effect of concentration factor onto pressure transition throughout soils at different densities to confirm/validate/evaluate the findings of this study and Etienne and Steinemann.

10 BIBLIOGRAPHY

Aboaba, F.O., 1969. Effects of Time on Compaction of Soils by Rollers. Trans. ASAE 11, 302-304.

Adam, K.M., and Erbach, D.C., 1995. Relationship of tire sinkage depth to depth of soil compaction. *Trans. ASAE* 38/4:1011-1016.

Adams, B.A. and Wulfsohn, D.J., 1998. Critical-state behavior of an agricultural soil. *J. Ag. Eng. Res.* 70: 345-354.

Alexandrou, A., 1995. The development of techniques for assessing compactability of field soils. PhD Thesis Cranfield University, Silsoe College. Thesis D/95/153

Ansorge, D., 2005, a. Comparison of soil compaction below wheels and tracks. M. by. Res. Thesis, Cranfield University at Silsoe. Classified until 10/2008

Ansorge, D., 2005, b. Design of a single wheel soil interaction test rig. Master Thesis, University of Hohenheim.

Ansorge, D. and Godwin, R.J., 2007. The Effect of Tyres and a Rubber Track at High Axle Loads on Soil Compaction: Part 1: Single Axle Studies. *Biosystems Engineering*, doi:10.1016/j.biosystemseng.2007.06.005

Arvidsson, J. and Hakansson, I., 1996. Do effects of soil compaction persist after ploughing? Results from 21 long – term field experiments in Sweden. *Soil & Tillage Res*. 39: 175 – 197.

Bailey, A. C. and Johnson, C.E., 1989. A soil compaction model for cylindrical stress states. *Trans. ASAE* 32: 822-825.

Baumgartl, Th. and Koeck, B., 2004. Modeling volume change and mechanical properties with hydraulic models. *Soil Science of America Journal* 68: 57-65.

Bekker, M.G. (1960) Off the road locomotion: research and development in terramechanics. Univ. of Michigan Press, Ann Arbor, MI:220 pp.

Benoit, O. and Gotteland, Ph., 2005. Modelling of sinkage tests in tilled soils for mobility study. *Soil & Tillage Res.* 80: 215-231.

Berli, M., Eggers, C.G., Accorsi, M.L., and Or, D., 2006. Theoretical Analysis of Fluid Inclusions for In Situ Soil Stress and Deformation Measurements. *Journal of Soil Science of America* 70: 1441-1452.

Bernstein, R., 1913. Probleme zur Experimentellen Motorpflugtechnik. *Der Motorwagen* 16: 199-227.

Blatz, J.A. and Graham, J., 2003. Elastic-plastic modelling of unsaturated soil using results from a new triaxial test with controlled suction. *Geotechnique* 53/1: 113-122.

Brandhuber, R. Geischeder, R. and Demmel, M., 2006. Effects of heavy agricultural machines for sugar beet harvesting on subsoil physical properties. Proceedings of the 17th Triennale Conference of the International Soil and Tillage Research Organisation, Kiel, Germany, August, 28th – September, 3rd 2006.

Chancellor, W.J. and Schmidt, R.H. 1962. Soil Displacement below surface loads. *Trans. ASAE* 5: 240-246, 249.

Chi, L., S. Tessier, E. McKyes, and C. Lague. 1993. Modelling of mechanical behaviour of agricultural soils. *Trans. ASAE* 36 (6): 1563-1570.

Davis, D.B., Finney, J.B. and Richardson, S.J., 1973. Relative effects of tractor weight and wheel slip in causing soil compaction. *Journal of Soil Science* 24 (3): 399-409.

Defossez, P. and Richard, G., 2002. Models of soil compaction due to traffic and their evaluation. *Soil & Tillage Res.* 67: 41-64.

Defossez, P., Richard, G., Boizard, H. and O'Sullivan, M.F., 2003. Modelling change in soil compaction due to agricultural traffic as a function of soil water content. *Geoderma* 116: 89-105.

Delie, F. and Bouvard, D., 1997. Experimental characterization and modeling of the densification of powder mixtures. In: Powders and Grains, Durhan, North Carolina; 18. – 23. May 1997. Eds. Behringer, R.P. and Jenkins, J.T. pp. 117 –120.

Diserens, E. and Spiess, E., 2004. Wechselwirkung zw. Fahrwerk und Ackerboden. TASC: Eine PC-Anwendung zum Beurteilen und Optimieren der Bodenbeanspruchung. FAT – Berichte Nr. 613/2005. Schweiz.

Dresser, M.L. and Godwin, R.J., 2004. "Improved Soil Management to Reduce Runoff and Flood Flows". AgEng 2004, Leuven, Belgium, 2004.

Dresser, M.L., Blackburn, D.W.K., Stranks, S.N., Dain-Owens, A. and Godwin, R.J., 2006. Effect of tillage implements and vehicle loads on buried archaeology. In: Proceedings of the 17th Triennial International Soil and Tillage Research Organisation Conference, Kiel, Germany. August, 28th – September, 3rd 2006.

Earl, R., 1997. Assessment of field soils during compression. *J. Ag. Eng. Res.* 68: 147-157.

Earl, R. and Alexandrou, A., 2001. Displacement processes below a plate sinkage test on sandy loam : theoretical approach. *J. Terramech.* 38 (3): 163-183.

Etienne, D. and Steinmann, G., 2002. Calculation of pressure distribution in moist arable soils in eastern Switzerland: A simple model approach for the practice. *Environ. Geomechanics*: 413-421.

Froehlich, O.K., 1934. Druckverteilung im Baugrunde. Springer Verlag, Wien, 178 pp.

Fraysse, N.; Thome, H., and Petit, L., 1997. Effect of humidity on quasi – static behavior of granular media. In: Proceedings of the 3rd International Conference on Powders and

Grains, Durhan, North Carolina; 18. – 23. May 1997. Eds. Behringer, R.P. and Jenkins, J.T. pp. 147 –150.

Gallipoli, D., Gens, A. Sharma, R. and Vaunat, J., 2003. An elasto-plastic model for unsaturated soil incorporating the effects of suction and degree of saturation on mechanical behaviour. *Geotechnique* 51/1:123-135.

Gameda, S., Raghavan, G.S.V., McKyes, E. and Theriault, R., 1987. Single and Dual Probes for Soil Density Measurement. *Trans. ASAE* 30/4: 932-934.

Gibson, R.E., 1967. Some results concerning displacements and stress in a non-homogeneous elastic half space. *Geotechnique* 17: 58-67.

Ghezzehei, T.A. and Or, D., 2001. Rheological properties of wet soils and clays under steady and oscillatory stresses. *Soil Sc. Am., J.* 65: 624-637.

Godwin, R.J., 1975. An extended octagonal ring transducer for use in tillage studies. *J. Ag. Eng. Res.* 20: 347-352.

Godwin, R.J., Warner, N.L., and Smith, D.L.O., 1991. The development of a dynamic drop – cone device for the assessment of soil strength and the effects of machinery traffic. *J. Ag. Eng. Res.* 48: 123-131.

Godwin, R.J and Dresser, M.L., 2003. "Review of soil management techniques for water retention and minimising diffuse water pollution in the River Parrett Catchment." Environment Agency R&D Technical Report P2-261/10/TR. ISBN 1844321460, 2003.

Godwin, R.J. and O'Dogherty, M.J., 2003. Integrated soil tillage force prediction models. *Proceedings of the 9th European Conference of the International Society for Terrain Vehicle Systems*, Harper Adams University College, UK.

Godwin, R.J. and Spoor, G. 1977. Soil failure with narrow tines. *J. Ag. Eng. Res.* 22: 213-228.

Gregory, A.S.; Whalley, W.R.; Watts, C.W.; Bird, N.R.A.; Hallett, P.D. and Whitmore, A.P., 2006. Calculation of precompression index and precompression stress from soil compression test data. *Soil & Tillage Res.* 89: 45-47.

Gupta, S.C. and Larson, W.E., 1982. Chapter 10 – Predicting soil mechanical behavior during tillage. In: Predicting tillage effects on soil physical properties and processes. American Society of Agronomy, Special Publication 44, 151 – 178.

Gupta, S.C. and Raper, R.L., 1994. Prediction of Soil Compaction under Vehicles, pp 71-90 in Development in Agricultural Engineering 11. Soil Compaction in Crop Production. Soane, B.D. and van Ouwerkerk, C. Eds. Elsevier, Amsterdam, Netherlands.

Gurtug, Y. and Sridharan, A., 2002. Prediction of compaction characteristics of fine grained soils. Technical Note. *Geotechnique* 52/10: 761-763

Haff, P.K., 1997. Why the prediction of grain behavior is difficult in geological granular systems. In: Proceedings of the 3rd International Conference on Powders and Grains, Durhan, North Carolina; 18. – 23. May 1997. Eds. Behringer, R.P. and Jenkins, J.T. pp. 61 – 64.

Hakansson, I., 2005. Machinery induced compaction of arable soils. Incidence - Consequences – Countermeasures. Reports from the Division of Soil Management No. 109. Department of Soil Science. Swedish University of Agricultural Science.

Hettiaratchi, D.R.P. and O'Callaghan, J.R., 1980. Mechanical behavior of agricultural soils. *J. Ag. Eng. Res.* 25: 239-259.

Hettiaratchi, D.R.P., 1987. A critical state soil mechanics for agricultural soils. *Soil Management* 3/3: 94-105.

Hinrichsen, H. and Wolf, D.E., (Eds.) 2004. The physics of granular media. Wiley – VCH Verlag, Weinheim, Germany.

Issensee, KK. 2007. Personal Communication at Soil Compaction Expert Meeting at IfZ in Göttingen, Germany, 19.4.2007.

Jakobsen, B.F. and Dexter, A.R., 1989. Prediction of soil compaction under pneumatic tyres. *J. Terramech.* 26/2: 107-119.

Jennings, J.E.B. and Burtland, J.B., 1962. Limitations to the Use of Effective Stresses in Partly saturated soils. *Geotechnique* 12: 125-144.

Keller, T., Defossez, P., Weisskopf, R, Arvidsson, J., Richard, G., 2007. SoilFlex: A model for prediction of soil stresses and soil compaction due to agricultural field traffic including a synthesis of analytical approaches *Soil and Tillage Research 93/ 2: 391-411*

King, D.W., 1969. Soils of Bedford and Luton District. Soil Series of England and Wales, Harpenden, UK.

Kirby, J.M., 1989. Measurements of yield surfaces and critical state of some unsaturated agricultural soils. *J. Soil Sc.* 40: 167-182.

Kirby, J.M., 1998. Estimating critical state soil mechanics parameters from shear box tests. *Europ. J. Soil Sc.* 49: 503-512.

Kirby, J.M., Blunden, B.G., and Trein, C., 1997. Simulating soil deformation using a critical state model: II. Soil compaction beneath tyres and tracks. *Europ. J. Soil Sc*. 48: 59-70.

Kirby, J.M., O'Sullivan, M.F.O., and Wood, J.T., 1998. Estimating critical state soil mechanics parameters from constant cell volume triaxial tests. *Europ. J. Soil Sc.* 49: 85-93.

Keller, T.; Defossez, P.; Weisskopf, P.; Arvidsson, J. and Richard, G., 2007. SOIL FLEX: A model for prediction of soil stresses and soil compaction due to agricultural field traffic including a synthesis of analytical approaches. *Soil & Tillage Res.* 93: 391-411

Kurtay, T. and Reece, A.R., 1970. Plasticity theory and critical state soil mechanics. *J. Terramech.* 7: 23-56.

Lamande, M., Schjonning, P. and Togersen, F.A., 2006. Tests of Basic Aspects of Stress Transmission in Soil. In: Proceedings of the 17th Triennial International Soil and Tillage Research Organisation Conference, Kiel, Germany. August, 28th – September, 3rd 2006.

Leeson, J.J. and Campbell, D.J., 1983. The variation of soil critical state parameters with water content and its relevance to the compaction of two agricultural soils. J. Soil Sc. 24: 33-44.

Li, X.Y., Tullberg, J.N. and Freebairn, D.M., 2006. Wheel traffic and tillage effects on runoff and crop yield. Soil and Tillage Research: IN PRESS.

McKyes, E. and Fan, T., 1985. Multiplate penetration tests to determine soil stiffness moduli. J. Terramech., 22/3: 157-162.

Meyerhof, G.G., 1951. The ultimate bearing capacity of foundations. *Geotechnique* 2.

Meyerhof, G.G., 1963. Some recent research on the bearing capacity of foundations. *Can. Geotech. J.* 1 (1).

Meyerhof, G.G., 1974. Ultimate bearing capacity of foundation on sand layer overlying clay. *Can. Geotech. J.* 11.

Muro, T. and Tran, D.T., 2006. Effects of vertical exciting force of a tracked vehicle on the dynamic compaction of a high lifted decomposed granite. *J. Terramech.* 43: 365-394.

Nelder, J.A., 1985. Discussion of Dr. Chatfield's paper. *Journal of the Royal Statistical Society*. Series A, 148 (3): 238.

Newmark, N.M., 1940. Stress Distribution in Soils. Proceedings of Conference on Soil Mechanics and its Applications; Purdue – University, September 1940. PP 295 – 303.

Ning, Z.; Boerefijn, R.; Ghadiri, M. and Thorton, C., 1997. Effect of particle size and bond strength on impact breakage of weak agglomerates. In: Proceedings of the 3rd International

Conference on Powders and Grains, Durhan, North Carolina; 18. – 23. May 1997. Eds. Behringer, R.P. and Jenkins, J.T. pp. 127 – 130.

Oda, M.; Iwashita, K., and Kakiuchi, T., 1997. Importance of particle rotation in the mechanics of granular materials. In: Proceedings of the 3rd International Conference on Powders and Grains, Durhan, North Carolina; 18. – 23. May 1997. Eds. Behringer, R.P. and Jenkins, J.T. pp. 207 –210.

O'Sullivan, M.F., Henshall, J.K., Dickson, J.W., 1998. A simplified method for estimating soil compaction. *Soil & Tillage Res.* 49: 325-335

Piepho, H.P., Buechse, A., and Richter, C., 2004. A mixed modeling approach for randomized experiments with repeated measures. *Journal of Agronomy and Crop Science* 190: 230 – 247.

Radjai, F.; Wolf, D.E., Roux, S., Jean, M., and Moreau, J.J., 1997. Force networks in dense granular media. In: Proceedings of the 3rd International Conference on Powders and Grains, Durhan, North Carolina; 18. – 23. May 1997. Eds. Behringer, R.P. and Jenkins, J.T. pp. 211 –214.

Raghavan, G.S.V., McKyes, E., and Chasse, M., 1977. Effect of Wheel Slip on Compaction. *J. Agric. Eng. Res.* 22: 79-83.

Rankine, W., 1857. On the stability of loose earth. *Philosophical Transactions of the Royal Society of London*, Vol. 147.

Rubinstein, D., Upadhyaya, S.K. and Sime, M., 1994. Determination of *IN-SITU* engineering properties of soil using response surface methodology. *J. Terramech.* 31/2: 67-92.

Rusanov, V.A., 1997. Methods for determining the effects of soil compaction produced by traffic and indices of efficiency for reducing these effects. *Soil & Tillage Res*. 40, 239-250.

Schafield, A. and Worth, P., 1968. Critical State Soil Mechanics. Mc-Graw Hill, London, UK.

Seig, D., 1985. Soil Compactability. PhD – Thesis, Cranfield Institute of Technology, Silsoe College.

Sime, M. and Upadhyaya, S.K., 2004. Experimental verification of an inverse solution technique for determining physical properties of soil. *Trans. ASAE* 48/1: 13-21.

Soehne, W., 1953. Druckverteilung im Boden und Bodenverformung unter Schlepperrei fen. (Pressure distribution in the soil and soil displacement under tractor tires). *Grundlagen Landtechnik* 5: 49-63.

Spoor, G. and R.J. Godwin. 1984. Influence of autumn tilth on soil physical conditions and timing of crop establishment in spring. *J. Ag. Eng. Res.* 29: 265-273.

Spoor, G. and Godwin, R.J., 1978. An experimental investigation into the deep loosening by rigid tines. *J. Ag. Eng. Res.* 23: 243 – 258.

Spoor, G. and R.J. Godwin. 1979. Soil deformation and shear strength characteristics of some clay soils at different moisture contents. *J. Soil Sc.* 30: 483-498.

Soane, B.D., Godwin, R.J., and Spoor, G., 1986. Influence of deep loosening techniques and subsequent wheel traffic on soil structure. *Soil & Tillage Research* 8: 231-237.

Terzaghi, K., 1943. Theoretical soil mechanics. Wiley, New York, NY.

Toll, D.G. and Ong, B.H., 2003. Critical-State parameters for an unsaturated residual sandy clay. *Geotechnique* 53/1: 93-103.

Towner, G.D., 1983. Effective stresses in unsaturated soils and their applicability in the theory of critical state soil mechanics. *J. Soil Sc.* 34: 429-435.

Trein C R (1995). The mechanics of soil compaction under wheels. PhD-Thesis in Agricultural Engineering. Cranfield University, Silsoe College, UK.

Tullberg J.N., Li, Y., McHugh, A.D., and Pangnakorn, U., 2006. Random Field Traffic is not Sustainable. In: Proceedings of the 17th Triennial International Soil and Tillage Research Organisation Conference, Kiel, Germany. August, 28th – September, 3rd 2006.

Tyrrell, T., 2005. Personal Communication on Depreciation of Combine Harvesters in the UK, 19.2.2005.

Van den Akker, J.J., 2004. SOCOMO: a soil compaction model to calculate soil stress and subsoil carrying capacity. *Soil & Tillage Research* 79: 113-127.

Van den Ploeg, R.R., Ehlers, W., Horn, R., 2006. Schwerlast auf dem Acker. *Spektrum der Wissenschaft*, August 2006. PP 80 – 88.

Verhorst, J.W., 2006. Personal Communication on CLAAS Lexion Combine Harvester Specifications, 10.5.2006

Watts, C.W., Clark, L.J., Chamen, W.T.C. and Whitmore, A.P., 2005. Adverse effects of simulated harvesting of short-rotation willow and poplar coppice on vertical pressure and rut depths. *Soil & Tillage Res.* 84: 192-199.

Way, T.R., Bailey, A.C., Raper, R.L. and Burt, E.C., 1993. Tire lug height effect on soil stresses and bulk density. *ASAE – Paper No* 93-1033.

Wheeler, S.J. and Sivakumar, V., 1995. An elasto-plastic critical state framework for unsaturated soil. *Geotechnique* 45/1: 35-53.

Wong J Y (2001). Theory of ground vehicles. Third Edition. John Wiley & Sons, INC.New York, USA.

Wong, J.Y., 2007. Development of High-Mobility Tracked Vehicles for over Snow Operations. Proccedings of the Joint North America, Asia-Pacific ISTVS Conference and Annual Meeting of Japanese Society for Terramechanics, Fairbanks, Alaska, USA, June 23-26, 2007.

11 APPENDIX

11 Appendix

List of Figures - Appendix

List of Tables - Appendix

Appendix 1 Further Details on Soil Compaction Models

Appendix 1 contains additional detailed information concerning Sections 6.2 throughout to 6.8. Consequently, some of the figures given in the thesis sections will be repeated in the Appendix allowing the reader to easily follow the argumentation

11.1.1 Comparison of Soil Compaction Models

The variety of approaches used to model and indicate soil compaction rose the question how it would be possible to compare them directly, ideally comparing the same parameters. Most soil compaction models give different final outputs ranging from final real DBD (O'Sullivan, 1998) over the prediction of an area of excess of soil stability (van den Akker, 2004/SOCOMO) to just a danger of soil compaction (Etienne and Steinmann, 2002/TASC). Their common basis is the calculated stress propagation in the soil leading to the final prediction of soil compaction. Thus comparing their performance in stress prediction to measured soil stresses in the soil bin can determine the accuracy of the stress prediction of the models. Therefore this section contains a comparison of soil compaction models with respect to pressure prediction and a sensitivity analysis of COMPSOIL and SOCOMO.

11.1.1.1 Comparison of Pressure Prediction

The vertical stress propagation predicted by SOCOMO, COMPSOIL, and TASC will be compared in this section.

During the project conducted by Ansorge (2005) in the soil bin soil stresses were also determined. The vehicle support mechanics were both the rubber track and the 800 mm section width tyre laden to different values and inflation pressures. The pressure in the soil below the treatments was measured using ceramic pressure transducers embedded on aluminum tubes as described in Ansorge (2005). The pressure was measured at depths of 250 mm, 400 mm, and 650 mm. As the ceramic pressure transducers were embedded into the soil parallel to the surface the pressure measured is the vertical normal stress component. All three models (TASC, SOCOMO and COMPSOIL) give vertical normal stress values at the measured depths. The model by O'Sullivan however, can not predict the stresses deeper than 475 mm. In consequence of this limit the O'Sullivan model was excluded from the

comparison at the deepest reading. The second difficulty with the O'Sullivan model was that it could not account for tracks. Tracks were mimicked for this investigation with a conceptual load limitation to 10 t given by the spreadsheet. To get an average pressure the measured data was averaged over the time period it took to pass over the pressure transducer. Table 1 shows the measured and predicted vertical soil stress values for different implements and soil compaction models.

Table 1: Measured and predicted vertical soil stress values for different implements and models

Treatment and load	Depth (mm)	Measured vertical stress (bar)	Predicted TASC soft/*half firm*(bar)	Predicted O'Sullivan (bar)	Predicted SOCOMO (bar)	Closest Model / Deviation pos/neg (not considering half firm of TASC)
Track 12 t	250	0.80	1.10/*0.97*	0.95	0.85	SOCOMO (+6 %)
Track 12 t	400	0.49	0.80/*0.67*	0.94	0.79	SOCOMO (+92 %)
Track 12 t	650	0.38	0.49/*0.43*	- - - - - -	0.67	TASC (+26 %)
Track 5 t	250	0.26	0.46/*0.40*	0.66	0.37	SOCOMO (+42 %)
Track 5 t	400	0.10	0.33/*0.28*	0.58	0.36	TASC (+330 %)
800/10/2	250	1.18	1.86/*1.73*	1.70	1.34	SOCOMO (+14 %)
800/10/2	400	0.88	1.23/*1.11*	1.47	1.24	SOCOMO (+41 %) / TASC (+40 %)
800/10/2	650	0.50	0.64/*0.62*	- - - - - -	1.02	TASC (+28 %)
800/10/1	250	0.96	1.77/*1.49*	1.54	0.922	SOCOMO (-4 %)
800/10/1	400	0.53	1.20/*1.07*	1.35	0.90	SOCOMO (+70 %)
800/10/1	650	0.32	0.63/*0.62*	- - - - - -	0.81	TASC (+97 %)
800/10.5/2.5	250	1.6	1.98/*1.77*	1.85	1.42	O'Sullivan (- 11%)

The resulting pattern of proximity between measured and calculated values is very interesting. The model COMPSOIL overpredicted the stresses compared to the measured stresses and it never showed the closest agreement between measured and predicted values. For the surface it seems as if SOCOMO shows the closest connection to the measured parameters. Apart from one case the predicted soil stresses were always too high. At depth the TASC model gave good estimations and predicted soil pressures closer to the measured ones than SOCOMO. It is not clear why or how, yet interestingly stress decrease with depth seems too small for SOCOMO compared to reality. For the pressure prediction in Table 1 a soft surface was assumed for the TASC model. The author had checked the appropriateness of this with a screw driver test (developed in that model to measure surface soil strength similar to a

penetrometer) in the soil bin and it appeared correct, yet maybe close to the border to half firm. If the soil strength is set to half firm the TASC model performs even better (these are the stress values in italics of the TASC column). Taking into account the fact that Etienne and Steinmann (2002) included a simple surface screw driver test to account for soil variability the results change exceptionally well with surface soil conditions. Comparing the results of TASC to those of SOCOMO, which misses such an easy determinable variable like soil measuring soil strength with a screw driver, highlights the possibility for an improvement of predicting soil behaviour utilizing an easily obtained soil physical parameter.

All models showed sufficient agreement with the measured data. Overall SOCOMO corresponded most closely with the measured values as shown in Table 1. The close agreement between the models and comparing them with the measured data cannot explain the differences of a factor of 3 – 4 between measured and predicted soil displacement by Ansorge (2005). Therefore parameters translating the pressure distribution into soil behaviour have to be responsible for the disagreement.

The semi-empirically estimated contact pressure from O'Sullivan et al. (1998), which is equal to σ_1 in their model, is in agreement with the contact pressure determined from measured contact area and tyre load from Ansorge (2005) and this study as shown in Figure 1. The slope of the regression line is close (-2.5%) to 1 and the coefficient of determination (R^2) is also high. In comparison to this the contact pressure estimation utilizing the super ellipse of Keller (2005) shown in Figure 2 has a smaller R^2 and the slope differs more from 1 and the intercept is larger.

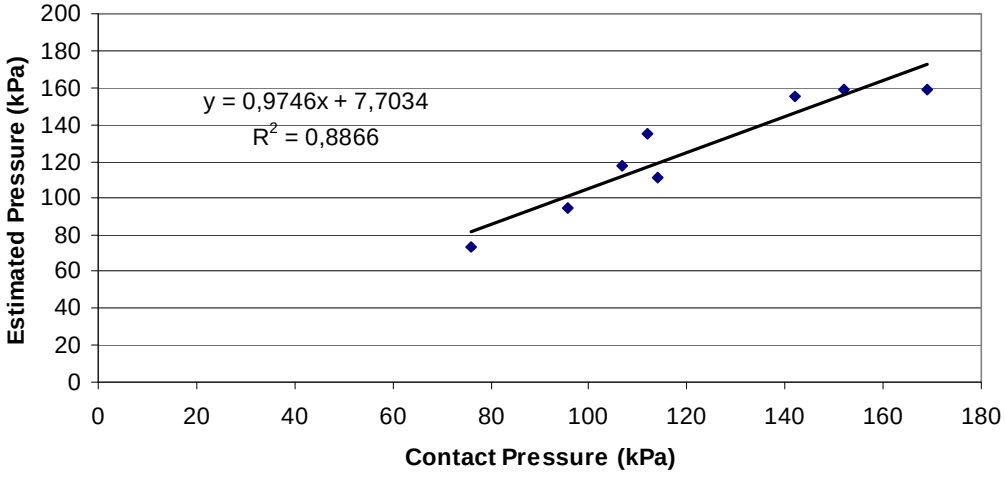

Figure 1: Estimated (from O'Sullivan et al. (1998)) vs. contact pressure for tyre loads including regression line

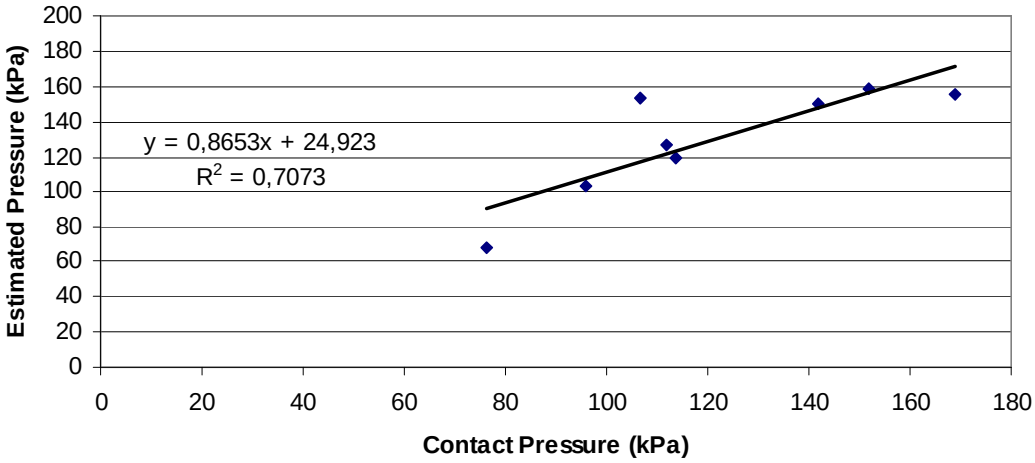

Figure 2: Estimated pressure from Keller (2005) vs. contact pressure for tyre loads including regression line

Utilizing the possibility to predict stress distribution in the soil with different approaches in the contact stress distribution permits comparison of the new approach by Keller (2005) utilized in SOILFLEX to the traditional approach such as the one used by O'Sullivan (1998). The measured and predicted data is shown in Table 2.

Interestingly there is no benefit observed from the adjusted contact pressure distribution in relation to the performance of soil stress prediction at depth. As shown in Table 1 utilizing the original O'Sullivan (1998) spreadsheet this always had the largest difference between predicted and measured soil stresses. Utilizing the Keller (2005) approach resulted in an even larger offset between predicted and measured soil stress values. It is very interesting to note that the setting using the O'Sullivan approach for contact stress distribution did not result in the same stress values as in the traditional O'Sullivan spreadsheet. The predicted pressure values for O'Sullivan through SOIL FLEX are higher than the ones predicted COMPSOIL; although SOIL FLEX simulates to the user the same approach as the original COMPSOIL spreadsheet.

Table 2: Pressure measured and predicted with Soil Flex using O'Sullivan (1998) surface approach or Keller (2005) approach

Treatment	Depth (mm)	O'Sullivan (1998) in Soil Flex (kPa)	Keller (2005) approach in Soil Flex (kPa)	Measured Stress (kPa)
800/10.5/2.5	250	219	276	160
800/10/2	250	199	253	118
800/10/2	400	167	194	88
800/10/2/	650	110	118	50
800/10/1	250	148	198	96
800/10/1	400	131	166	53
800/10/1	650	94	109	32
Plane Strain				
800/10.5/2.5	250	219	276	160
800/10/2	250	199	253	118
800/10/2	400	167	194	88
800/10/2/	650	110	118	50
800/10/1	250	148	198	96
800/10/1	400	131	166	53
800/10/1	650	94	109	32
Varying	Concentration	Factors (c) for	800/10.5/2.5 treatment	(c=5 standard)
c = 3	250	209	257	160
c = 4	250	191	228	160
c = 6	250	225	289	160

11.1.1.2 Sensitivity Analysis of Soil Compaction Models

The small differences in predicted stress propagation from the previous section cannot be the reason for the significant differences between predicted and measured soil deformation found by Ansorge (2005). This raises the question as to whether the default initial soil parameters used by the models are appropriate for the given soil type and conditions. Consequently a sensitivity analysis of SOCOMO and COMPSOIL will be conducted.

11.1.1.2.1 SOCOMO

One of the most important parameters determining soil compaction is the value of preconsolidation stress in the soil for the SOCOMO model (van den Akker, 2004). Preconsolidation stress is the amount of stress a soil can carry without further permanent compaction, i.e. the soil responds elastically up to this stress. For a detailed explanation of preconsolidation stress see Ansorge (2005) or Gregory et al. (2006).
Preconsolidation stress or structural strength was set to 200 kPa for the modeling undertaken by Ansorge (2005). This value shows sufficient agreement compared with the experimentally determined values of preconsolidation stress for sandy loam in the soil bin by Alexandrou (1995) who for DBD values between 1.35 – 1.38 g/cm^3 and a gravimetric moisture content of approximately 12 % determined an average preconsolidation stress of 236 kPa with a standard deviation of 69 kPa. Both angle of internal friction and cohesion were set to the specific values for the soil in soil bin laboratory. Therefore all parameters of the SOCOMO model represented real soil laboratory values.

An increase in preconsolidation stress in the SOCOMO model for the 680 mm section width tyre and the 800 mm section width tyre at half inflation pressure, which were compared by Ansorge (2005), did not influence the area where initial soil strength was exceeded. In a subsequent step, first preconsolidation stress was increased to 250, 300, 400 and 600 kPa, respectively, and second initial DBD increased from 1.37 to 1.47 g/cm^3. Neither changed the result. The result for a preconsolidation stress of 200 kPa is shown in Figure 3. A reduction in preconsolidation stress to 100 kPa changed the results for the output as shown in Figure 4. SOCOMO indicates the area where soil compaction happens with letters in a section perpendicular to the travel direction. The area stayed the same, yet the letters changed from P in Figure 3 to C and S closer to the surface in Figure 4. These letters did not appear before and are not explained in the model description. Therefore a personal discussion with van den Akker gave the following explanation. The letter P indicates only the excess of preconsolidation stress, the letter S indicates the excess of shear strength and C indicates the excess of both shear strength and preconsolidation stress. Therefore the results of SOCOMO seem resistant to higher preconsolidation stresses, although the soil bin soil was relatively weak and an increase in DBD accompanied by an increase in preconsolidation stress is expected to reduce soil displacement and as shown by Antille (2006).

The results from above agree to a certain extend with the expected results. A larger soil displacement and therefore increase in soil density is expected with a weaker soil. In consequence of the weaker soil conditions the increase in soil failure is appropriate, which was indicated by the different letters. However, the expected reduction in soil compaction with an increase in preconsolidation stress could not be shown using the model.

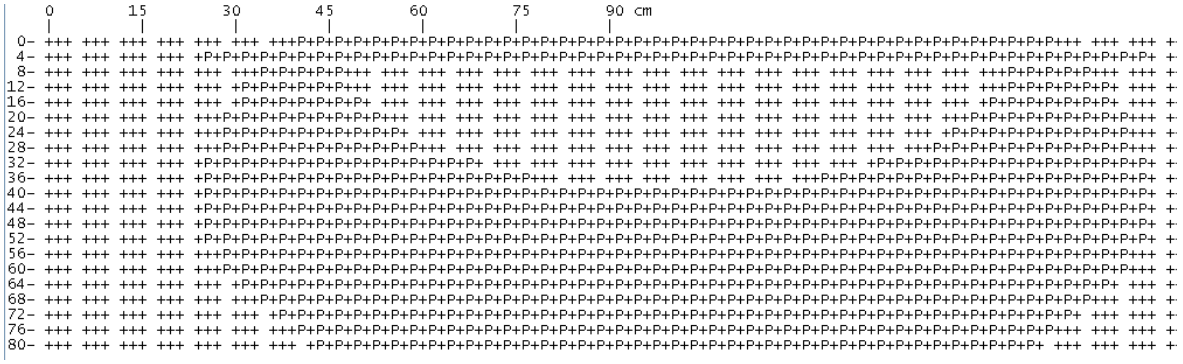

Figure 3: Estimated combined failure area for 680/10.5/2.2 at a preconsolidation stress of 200 kPa (P = excess of preconsolidation stress)

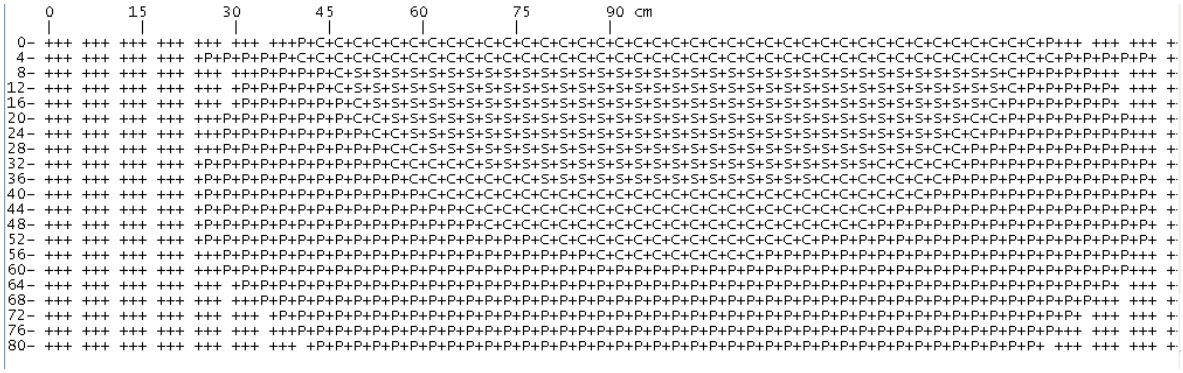

Figure 4: Estimated combined failure area for 680/10.5/2.2 at a preconsolidation stress of 100 kPa (P = excess of preconsolidation stress, S = excess of shear strength, C = excess of both)

11.1.1.2.2 COMPSOIL

As the original spreadsheet embedded in COMPSOIL was locked, soil critical state parameters could not be changed directly in the O'Sullivan model, therefore only soil density and soil water content were changed. Soil water content and dry bulk density with corresponding outputs of the model are shown in Table 3. The discussion and explanation of the changed parameter and results follow after the table.

Firstly, the contact area of a track can be mimicked by a 2 m wide and 1.2 m diameter tyre, yet it is not possible to assess the implications on soil mechanical properties in the model as in reality the contact area is turned by 90 degrees. The influence of contact shape was calculated

by Seig (1985) who showed a benefit for a long narrow contact patch compared to a short wide one. The same benefit was shown in this study as detailed in Section 7.2. However, for simplicity the turning approach was chosen.

Table 3: Initial DBD and moisture content values in O'Sullivan model and resulting parameters

γ [g/cm^3]	Water content [%]	Average increase in γ for tracks [%]	Average increase in γ for wheels [%]	Rut depth track [mm]	Rut depth wheels [mm]	Minimal Depth of similar compaction [mm]
1.37	10	2.9	3.9	15	20	325
1.27	10	10.3	11.4	52	58	325
1.20	10	17.2	18.4	86	93	375
1.15	10	22.3	23.3	112	117	275
1.2	15	19.5	20.7	98	104	425
1.36	15	4.5	5.6	23	28	325
1.36	20	12.8	13.5	64	68	125

When mimicking tracks, soil compaction is slightly reduced compared to that of tyres, yet on average only by 1 % compared to 5 % during the experiment.

The next three paragraphs discuss the predicted results for varying initial dry bulk density shown previously in Table 3.

Comparison of prediction behaviour of COMPSOIL for a range of soil densities and moisture contents

Initial dry bulk density of 1.27 g/cm^3

At an initial soil density of 1.27 g/cm^3 the difference in average increase in DBD between the "track" and the tyres is still merely 1.1 % although the total increase in soil density has increased to 10.3 % for the track and 11.4 % for the tyre. Again, as already discussed by Ansorge (2005), the increase caused by the tyre at half inflation pressure is bigger than the one caused by the 900 mm section tyre. The resulting displacement is not consistently decreasing with depth. Decrease is higher close to the surface and less at depth. Total displacement at the surface increased from about 15 – 20 mm to about 52 – 55 mm. Similar to the model run with the true soil conditions, the last 4 layers have the same displacement independent of the treatment. This can not be supported with the findings by Ansorge (2005).

Initial dry bulk density of 1.2 g/cm^3

At an initial density of 1.2 g/cm^3 the difference in average DBD between the "track" and the tyres increased to 1.2 %, total density increase was 17.2 % and 18.4 % for the track and the tyres, respectively. The surface rut depth increased to about 86 – 93 mm. Hereby the deepest 5 layers show the same increase in DBD.

Initial dry bulk density to 1.15 g/cm^3

Changing initial dry bulk density to 1.15 g/cm^3 reduced the difference between the track and the tyre to 1 % and the total increase in DBD increased to 22.3 % for the tyres. Rut depth varies from 112 mm for the track to 117 mm for the 800 mm section width tyre. Interestingly, in this case only the last two layers have the same increase in density over all treatments and in the third layer the 900 mm section width tyre has the smallest.

As varying initial dry bulk density did not lead to sufficient agreement with the measured data initial water content was varied in a second approach. Changing soil water content is the only possibility in the original O'Sullivan spreadsheet to influence the write protected critical state soil mechanics parameters, i.e. slope of the virgin compression line and recompression lines. The next three paragraphs discuss the results of varying soil water content while taking both, real initial dry bulk density and some of the modified results from above.

Soil water content 15 % and initial dry bulk density 1.36 g/cm^3

Keeping initial dry bulk density at 1.36 g/cm^3 and increasing soil water content to about 15 % increased soil density on average to about 5 %. Still the difference between the track and the tyres is about 1 %. Again, the bottom four layers show the same increase in soil density over all treatments. Surface rut depth is between 23 to 28 mm.

Soil water content 20 % and initial dry bulk density 1.36 g/cm^3

For very wet conditions with a soil water content of about 20 % and an initial dry bulk density of 1.36 g/cm^3 the difference in increase in DBD decreased to about 0.7 %. The different tyres increase density by 12.8 % nearly identical over all treatments. Only the top two layers differ when looking at the soil displacement over depth for single treatments. At all other depths soil displacement is the same for all treatments.

Soil water content 15 % and initial dry bulk density 1.2 g/cm^3

Setting soil water content to 15 % and reducing soil density to 1.2 g/cm^3 gave an average difference between the track and the tyres of 1.2 %. The resulting increase in soil density is nearly uniform with depth for the track, whereas for all others the increase decreases with depth. Interestingly the track is now the worst at the 3rd layer from the bottom. Close to the surface all are similar and surface displacement is about 100 mm .

The average difference between the track and the wheel was about 1 % for the increase in DBD. Surface rut depth was between 4 to 7 mm deeper for the wheels than for the track. No trend can be recognized for the different treatments at different initial DBD and/or soil water content. The same is true for varying DBD with respect to the depth from which all treatments cause the same soil displacement. However, these depths become shallower with an increase in soil water content.

From a soil mechanics point of view the model supports the hypothesis that soil displacement, e.g. increase in soil density at the surface is determined by contact pressure whereas at depth it is determined by the overall load. This cannot be confirmed when looking at the results of Ansorge (2005). Here the tracks caused less displacement and therefore less increase in soil density over the entire depth range.

With a reduction in initial soil strength, i.e. an increase in soil water content or a decrease in initial DBD soil compaction increases. This is in agreement with all findings in literature. For an initial DBD of 1.27 g/cm^3 the increase in DBD comes into the range measured by Ansorge (2005). The same is true with an increase in moisture content to 20 %. This puts emphasis on the fact that the slope and intercept of the virgin compression line should be changed as the original soil for which the model was designed for must have been stronger than the one used in the soil bin.

Comparison of prediction behaviour of COMPSOIL for a range of VCL slopes and intercepts

The model SOIL FLEX provides the ability to change critical soil mechanics parameters embedded in COMPSOIL directly while keeping both initial DBD and soil moisture content as given in the experiment. From theory an increasing slope of the virgin compression line means that increases in DBD result from smaller pressure changes. With a decreasing slope

more pressure is necessary. A decreased intercept means less pressure for the same DBD, too. With an increased intercept the opposite is true. In Table 4 the functionality of critical soil mechanics parameters and their implications on the predicted results is summarized. This aims on investigating whether a change in critical state soil mechanics parameters will get the predictions of the model closer to the range of the real results.

Table 4 shows the given parameters and their corresponding maximum predicted DBD, whereby the increase of the DBD is given at the surface and at depth, too. Predicted rut depth is shown, too. In a first step the slope of the virgin compression line was reduced which in consequence reduced soil compaction as expected. With a reduction in the intercept soil compaction increased significantly. With a slope of about 0.15 the results came into the range measured in the soil bin by Ansorge (2005). The recompression lines were not changed because their influence can be ignored as they influence the response to multiple loadings and have no impact on single passes which are investigated at this stage.

Table 4: Variation in predicted soil compaction with changes in critical state soil mechanics parameters

Slope	Y Axis	Recompression lines	Final max.DBD [g/cm^3]	Increase top [%]	Increase Bottom [%]	Rut depth [mm]
0.123	2.422	0.0087/0.0327	1.41	3	0	12
0.1	2.422	0.0087/0.0327	1.39	1		3
0.123	2.0	0.0087/0.0327	1.80	43	25	250
0.15	2.422	0.0087/0.0327	1.51	12	3	45
0.123	3.0	0.0087/0.0327	1.38	0	0	0
0.15	2.422	0.008/0.0327	1.51	13	3	50
0.15	2.422	0.0095/0.0327	1.50	12	3	45
0.15	2.422	0.0087/0.025	1.51	12	2	45
0.15	2.422	0.0087/0.04	1.51	12	4	50

Changing critical state soil parameters to fit the data seems a promising way to make the data fit existing soil mechanics models.

11.1.1.2.3 Conclusion and Outlook

The comparison of measured pressure to calculated pressure showed some deviation, yet the magnitude is too small to explain the large differences seen especially in COMPSOIL.

Adapting critical state soil parameters to fit the data seems a promising way to make the data fit existing soil mechanics models. An approach to gain information about the virgin compression line is to investigate the slope of the soil displacement curves from this work and the work by Ansorge (2005). The virgin compression line basically describes the reciprocal of soil density in dependence of exerted stress. The corresponding contact pressure can be assigned to the slope of each soil displacement curve by calculating the stress below a tyre from the known area and known load, assuming uniform stress distribution over the contact area. This contact pressure is in some relation to the exerted stress for the VCL model. As in detail explained by Ansorge and Godwin (2007a) from the slope of a soil displacement line the corresponding increase in soil density can be gained. Knowing the initial soil stress exerted by the roller during soil bin preparation and knowing the resulting initial soil density gives the first point on the virgin compression line. Knowing the increase in density for different contact pressures the virgin compression line can be created and the recompression line could be gained from multi passes.

If in a future step it was further possible to determine the virgin compression line just from tyre sinkage at two different inflation pressures, a very important characteristic of soil compaction could easily be determined in the field.

11.1.2. Derivation of VCL Parameters from Soil Bin and Validation/Evaluation

In a first step this “in-situ virgin compression line” will be created utilizing the different treatments from the soil bin. The approach will be validated in-field conditions, too. After gaining the slope and intercept of the virgin compression line, these parameters will be traditionally verified in a pressure cell.

11.1.2.1 Theoretical Considerations

The Cam-Clay model COMPSOIL (O’Sullivan et al., 1998) provides an estimation of soil displacement for a sandy loam soil from tyre, bulk density and moisture content data whereby COMPSOIL assumes VCL parameters.

An initial comparison of soil displacement measured by Ansorge 2005 on a sandy loam to the data predicted by COMPSOIL using the virgin compression line (VCL) parameters suggested

by O'Sullivan et al. (1998) is given in Figure 5. This shows a very large deviation for both uniform and stratified soil. This suggests that either the soil specific parameters used to describe the sandy loam soil of the model do not adequately describe the sandy loam soil used in the soil bin or there are substantial errors in the model. The latter is unlikely as O'Sullivan et al. (1998) showed close agreement for other soil types. Consequently the VCL parameters for the sandy loam of the Cottenham Series (which was used by Ansorge (2005) and this study) have to be different from the sandy loam soil described by O'Sullivan et al. (1998) and used by the original COMPSOIL model and hence need to be determined.

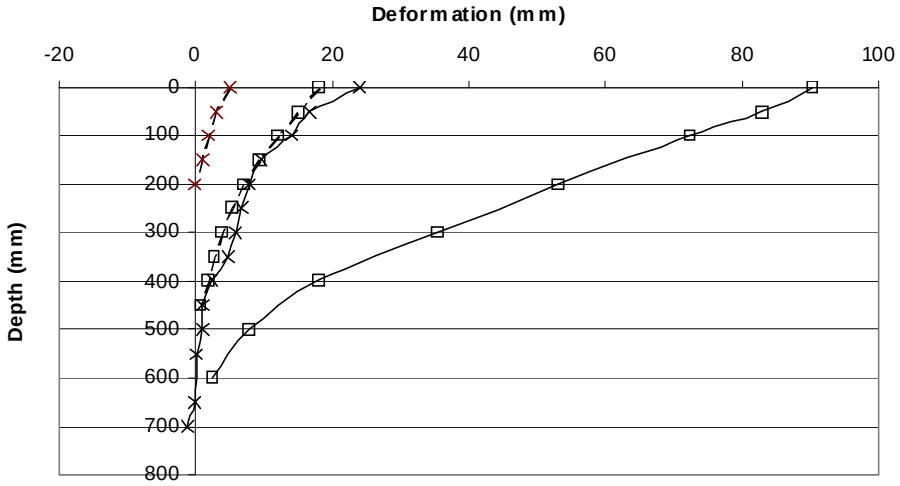

Figure 5: Measured (solid line) and predicted (broken line) soil displacement for 900mm section width tyre at 10.5t load and 1.9bar inflation pressure on uniform (□) and stratified (×) soil conditions (measured data from Ansorge (2005))

The VCL as defined by Schofield and Wroth (1968) is a unique linear function relating the relative density of a soil at given moisture content to the natural logarithm of the spherical pressure it is subjected to. According to their definition spherical pressure is the arithmetical average of major, intermediate, and minor principle stress, σ_1, σ_2, and σ_3, respectively. As mathematically this is the definition of the mean normal pressure p, this paper will use the term mean normal pressure after O'Sullivan et al. (1998) when developing the COMPSOIL model.

The VCL is usually obtained from plotting the relative density (ratio of the maximum soil density (2.66 g/cm^3) to the resulting dry bulk density) against mean normal pressure measured with triaxial cell tests. For the assessment of the in-situ VCL in the soil bin the relative

density is obtained by adding the average density increase measured by Ansorge 2005 and this study to the initial soil density. Mean normal pressure is obtained from the contact pressure following a transformation after O'Sullivan et al. (1998).

This approach does not take into account the elastic recovery of the soil, and consequently will potentially yield a virgin compression line indicating the soil to be slightly too strong. Figure 6 demonstrates this problem. Mean normal pressure P_1 is related to a measured relative density D_1 representing the density after the elastic recovery has taken place. However, to determine the VCL correctly, P_1 should be linked with D_2 where elastic recovery had not taken place.

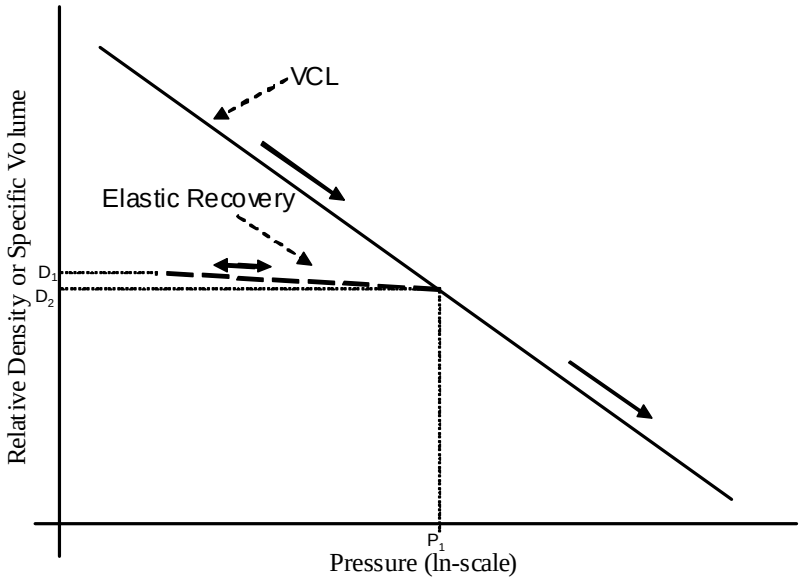

Figure 6: VCL Theory

The following calculation shows that this error can be neglected. For a relative density of 1.72 (which corresponds to a final DBD of 1.55 g/cm^3), a slope of the recompression / elastic recovery line of 0.0087 (ln(p)) $^{-1}$ (O'Sullivan et al., 1998) and an applied pressure of 100 kPa (equal to 4.61 ln (p)) the change in density from D_2 to D_1 is 4.61 times 0.0087 equal to 0.040. This yields a 0.87 % error for the relative density measurement indicating a marginally stronger soil. This error is accepted as it will affect all treatments similarly.

11.1.2.2 Practical Derivation of VCL Parameters

As shown in Section 6.2.1 the semi-empirically estimated contact pressure from O'Sullivan et al. (1998), which is equal to σ_1 in their model, is in good agreement with the contact pressure determined from measured contact area and tyre load from Ansorge (2005) and this study. The confining pressures σ_2 and σ_3 can be derived from the following equation gained by O'Sullivan et al. (1998) from empirical regression lines:

$$\ln \frac{\sigma_1}{\sigma_n} = c_1 \times z - c_2 \times A + c_3 \times \xi$$

Eq. 1

where z is the depth (m), A is the contact area (m^2) and ξ is the concentration factor. c_1, c_2, and c_3 are constants whose values are given in Table 5 and depend on the calculated stress ratio.

To calculate σ_2 and σ_3 Eq. 1 would have to be solved for all tyres at each depth within the soil according to O'Sullivan et al. (1998). To simplify the approach a depth z of 0.4 m representing the average depth in the soil profile and a contact area A of 0.8 m^2 were assumed and ξ was varied from three to five representing possible soil conditions (dense to soft) as proposed by Fröhlich (1934). The resulting dependencies of σ_2 and σ_3 on σ_1 are listed in Table 7 including the sum of σ_2 and σ_3 as this eases the calculation of mean normal pressure.

In a first approximation $\xi = 5$ was chosen to calculate p from the contact pressures given in Table 7 of the treatments by Ansorge (2005) and this study. Knowing the initial density of 1.38 g/cm^3 and the average increase, final density can be calculated. Relative density (RD) is gained by dividing final dry bulk density (Final DBD) into 2.66. The average increase (AvI), the final DBD and RD are also given in Table 7.

Figure 7 shows relative density vs. pressure. A logarithmic regression line was fitted to the data points representing a VCL for the sandy loam soil at a moisture content of approximately 9 % at which the experiments were conducted. The VCL for the sandy loam soil given by O'Sullivan et al. (1998) is also included for reference.

Table 5: Values of constants c_1, c_2, and c_3 to estimate stress ratio depending on depth, contact area and ξ (O'Sullivan et al., 1998)

Constant	σ_1 / σ_2	σ_1 / σ_3
c_1	5.30	4.66
c_2	2.08	2.06
c_3	0.21	0.32

Table 6: σ_2 and σ_3 depending on ξ

ξ	σ_2	σ_3	Sum of σ_2 and σ_3
3	σ_1 / 2.96	σ_1 / 3.24	0.65 σ_1
4	σ_1 / 3.65	σ_1 / 4.46	0.50 σ_1
5	σ_1 / 4.51	σ_1 / 6.147	0.38 σ_1

Table 7: Treatments and corresponding increase in DBD, final DBD, relative DBD and σ_2 and σ_3, contact pressure and mean normal pressure for $\xi = 5$

Treatment (Section width[mm]/Load [t]/Inflation Pressure [bar])	AvI	Final DBD	RD	$\sigma_2 + \sigma_3$	Contact Pressure (σ_1)	P
900/5/0.5	5.66	1.458	1.817	29	76	35
500-70/4.5/2.3	14.27	1.577	1.681	54	142	65
500-85/4.5/1.4	11.06	1.533	1.729	42	110	51
600/4.5/1.4	11.00	1.532	1.730	43	114	52
700/4.5/1.0	10.59	1.526	1.736	36	96	44
900/10.5/1.9	17.30	1.619	1.637	43	112	52
800/10.5/2.5	17.36	1.620	1.636	64	169	78
800/10.5/1.25	11.59	1.540	1.721	41	107	49
680/10.5/2.2	17.73	1.625	1.631	58	152	70
Roller		1.380	1.928	22	58	26

The intercept and slope of the VCL were used in COMPSOIL. In order to see how the prediction performs with these modified parameters, the measured data is compared to the predicted data in Figure 8 for six individual tyres and close general agreement was achieved. Soil displacement is successfully predicted using COMPSOIL and the parameters of the VCL from the soil bin with a heuristically chosen concentration factor of ξ =5.

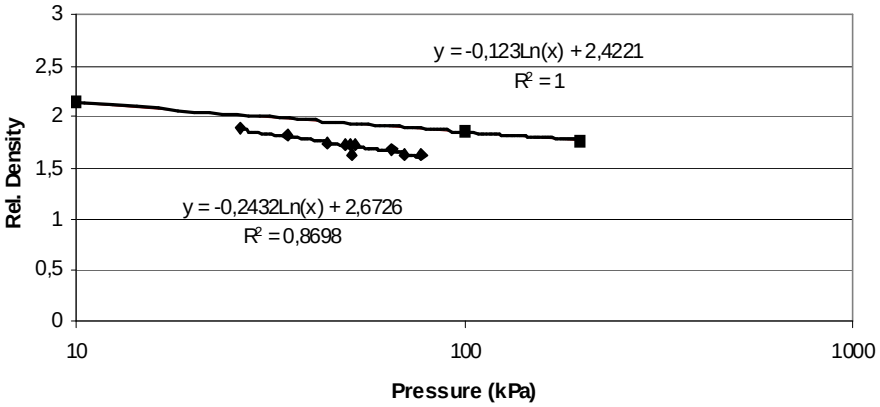

Figure 7: Virgin compression line for sandy loam soils ■ from O'Sullivan et al. (1998) and ♦ from the soil bin studies based on the average density increases from Ansorge and Godwin (2007)

To validate the heuristically chosen ξ = 5 the 900/10.5/1.9 experiment was evaluated for a smaller ξ of 4, representing a denser soil. P for ξ = 4 was calculated using the dependencies of σ_2 and σ_3 on σ_1 from Table 6. The slope (-0.2432) of the resulting VCL is identical to the slope for ξ =5. The intercept of 2.6929 is larger than the one which was derived from ξ =5 (2.6726). The overall effect of changing ξ is evaluated in Figure 9 whereby the prediction of the 900/10.5/1.9 for ξ = 4 is compared to both the measured data and the predictions for ξ =5. The smaller ξ results in a larger deviation of the rut depth at the surface and only a close agreement between measured and predicted data below 400 mm compared to the measured soil displacement. The smaller rut depth for ξ = 4 is followed by a larger decrease in soil displacement within the top 250 mm resulting in a smaller soil displacement over the entire depth of the soil profile. Transferring the observations from Figure 9 for the 900/10.5/1.9 back to the other treatments, shown in Figure 8, results in a general reduction in predicted soil displacement which consequently reduces the overall close agreement shown Figure 10. Therefore the selection of ξ =5 is justified as this shows overall a closer agreement.

Fitting linear regression functions through the top 500 mm of the measured and predicted data of Figure 8 estimating the average increase in soil density as described by Ansorge and Godwin (2007a) and plotting the measured against predicted average density increase results in close agreement as shown in Figure 10 to within +/- 2 % errors. The data is spread uniformly around the line of slope 1 and does not exhibit a general offset confirming the

choice of a concentration factor equal to 5. Fitting a linear regression line shows a marginal overprediction of 0.8 % and the $R^2 = 0.85$ confirms the general fit.

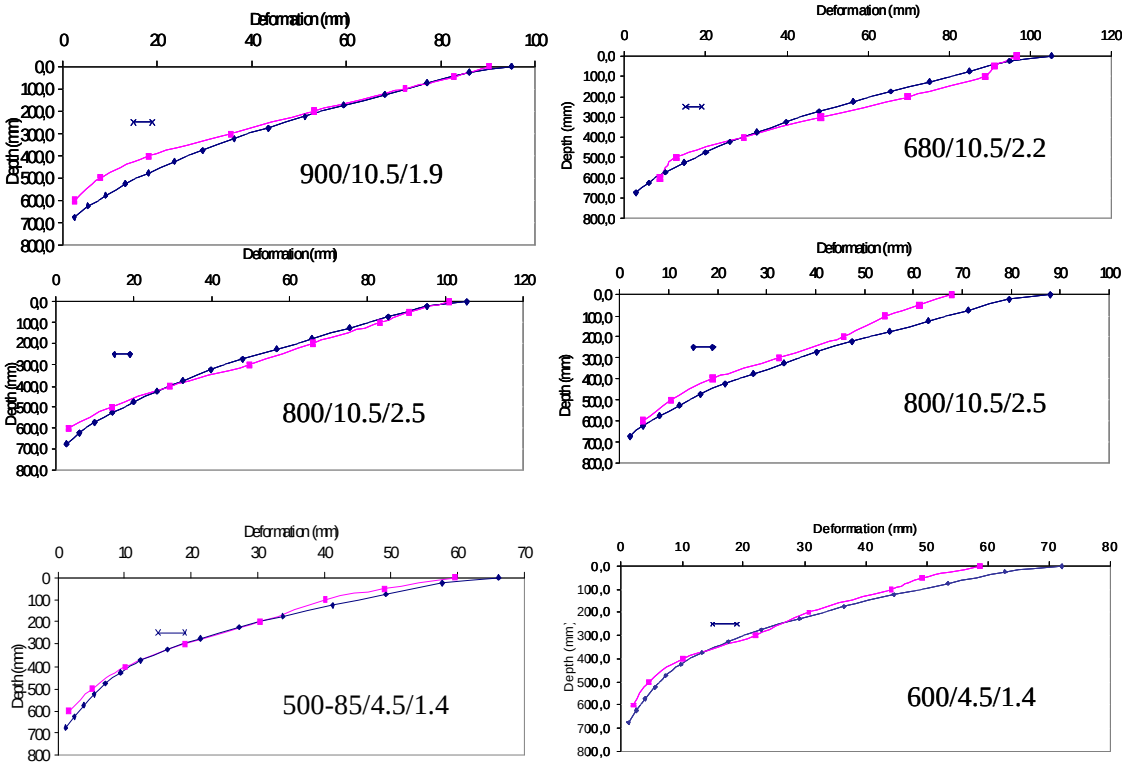

Figure 8: Measured (■) and predicted (♦) soil displacement for tyres with a concentration factor of 5. The least significant difference (LSD) at 95 % is also shown

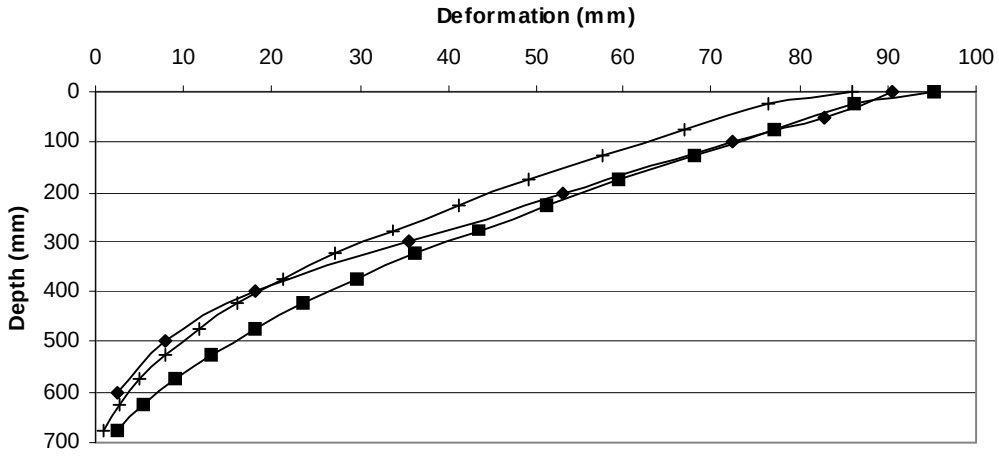

Figure 9: Measured soil displacement (♦), predicted soil displacement with concentration factors of 4 (+) and 5 (■), respectively, vs. depth for a 900/10.5/1.9 tyre

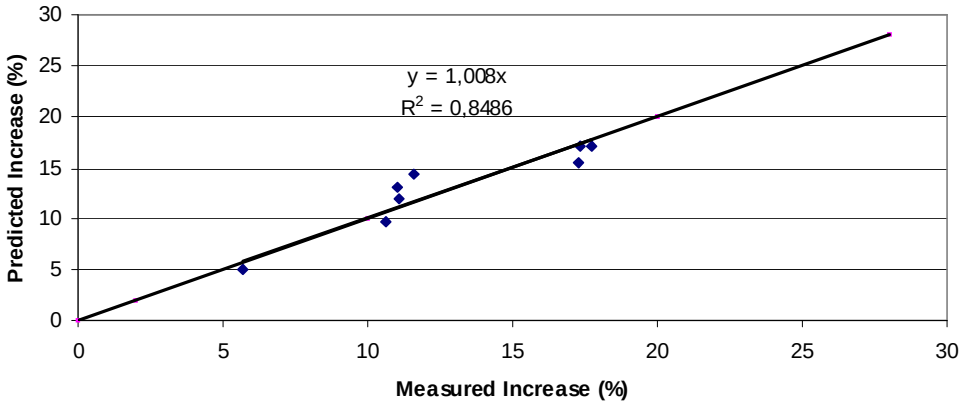

Figure 10: Measured vs. predicted average percentage increase in soil density

11.1.3 Prediction of Independent Data

It was an important step to be able to show that COMPSOIL is self consistent with a soil specific VCL which is able to reproduce the input data used to derive the specific VCL. For a justification of the approach the modified model will be compared with four other data sets from the same soil but not utilized for the development of the in-situ model. To do this:

1. Data generated by Antille (2006) using the single wheel tester designed by Ansorge (2005) with the same tyres at identical loads and inflation pressures with more dense (1.6 g/cm^3) and less dense (1.2 g/cm^3) soil conditions. This aimed at justifying the appropriateness of this VCL more generally for different initial dry bulk densities.
2. Data generated by a pass of the 900/10.5/1.9 tyre on stratified soil conditions mimicking real field conditions and investigating the ability of the model to deal with different bearing capacities within the same profile. This data is originally from Ansorge and Godwin (2007).
3. Data generated by two multi passes on the uniform medium soil condition. The tyre used was the 900 mm section width tyre, once having the 900/10.5/1.9 configuration and passing three times over the soil and then having the 900/5/0.5 configuration. This was targeting the performance of the model with respect to loading-unloading cycles and included the opportunity to adjust the recompression and reloading parameters.
4. Data which was generated by the passage of whole combine harvesters and used to explore the possibility to predict the soil displacement after a pass of whole combine harvesters over medium soil conditions.

11.1.3.1 Dense/Hard and Loose/Weak Soil

Following the ability to reproduce the input results as shown above, the prediction is extended onto different bearing capacities of the same soil type. Therefore the results from Antille (2006) were compared to the theoretical predictions. Antille (2006) used the same high axle load tyre configurations as Ansorge (2005) with the same soil type and water content, only at a lower bearing capacity with a DBD of 1.2 g/cm^3 DBD and at a higher bearing capacity with a DBD of 1.6 g/cm^3.

The measured and predicted results are plotted in Figure 11 and show in general a close agreement. On dense soil the 680/10.5/2.2 and the 800/10.5/2.5 are in good agreement with the predictions. On the soft soil overall a closer agreement is achieved.

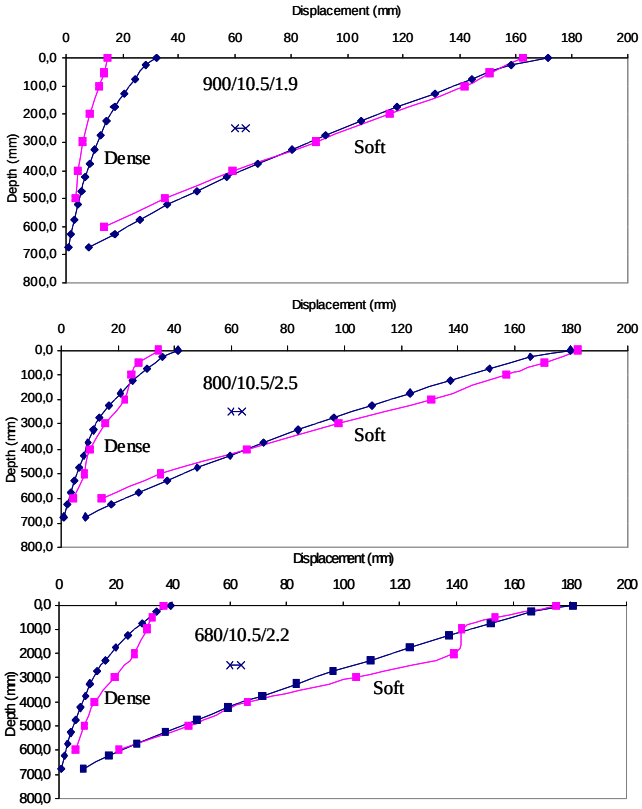

Figure 11: Measured (■) and predicted (♦) soil displacement for tyres on soft and dense soil conditions. LSD at 95 % is also shown

The accuracy was evaluated from the calculated average density changes for the predicted and the measured soil displacement shown in Figure 11 and plotted against each other in Figure 12.

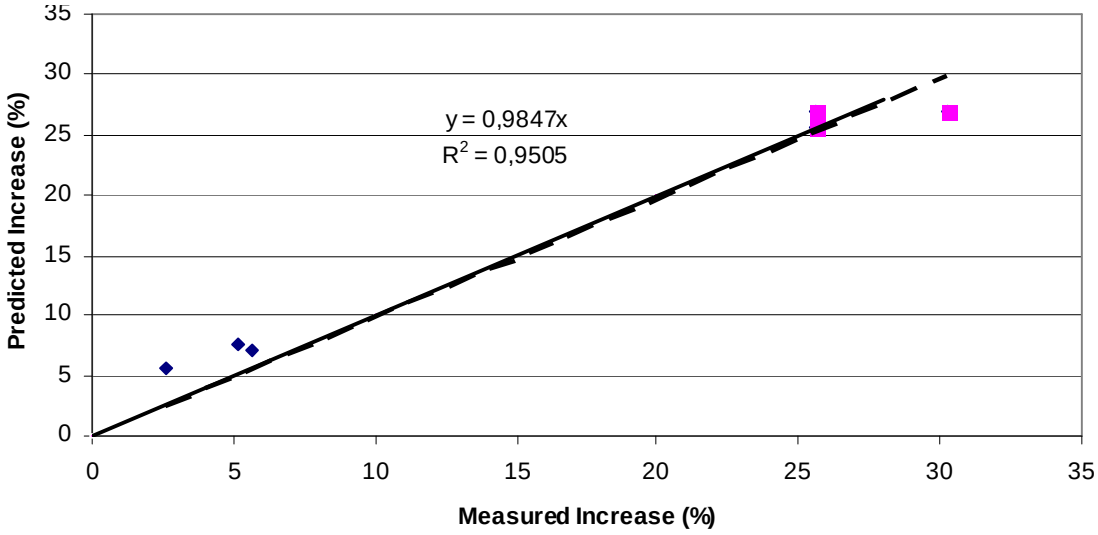

Figure 12: Predicted vs. measured increase in soil displacement for the data from Antille (2006) on high (♦) and low (■) bearing capacity. Also shown is the 1:1 relationship (solid line)

From Figure 12 a close agreement can be seen between the measured and the predicted increase in soil density for the data from Antille (2006). The accuracy is within an absolute error of +/- 3 %. The linear regression line shows that the increase is underpredicted by 1.5 % compared to the 1:1 line, however, linearity of the data is confirmed with an R^2 of 0.95.

Data from the medium bearing capacity was used to derive the VCL parameters and it is capable of predicting soil density increase for different initial DBD's. Thus this justifies the concept of a VCL for a soil at given moisture content in general and in particular for this soil type. Moreover the initial DBD from which VCL parameters are derived allows a prediction of soil density increase in denser and in weaker soil conditions. Thus the VCL appears to be independent of the initial density it was created for. The close agreement was achieved with a concentration factor of 5 and shows the robustness of the approach against this parameter which technically influences pressure distribution within the soil and is depending on the initial density. The close agreement on higher and lower bearing capacities justifies an extension of the investigation of the capability of the model to predict soil compaction in the more complex cases given below.

11.1.3.2 Stratified Soil Conditions

After having shown the capability to predict soil compaction on different bearing capacities, the next step was to compare the performance of the in-situ model for different bearing capacities within one soil profile. Hence, the stratified soil conditions used by Ansorge (2005) were simulated with the in-situ model using densities of 1.45, 1.62, and 1.55 g/cc for the zones: above 200 mm, between 200-325 mm and 300-750 mm, respectively. As can be seen from

Figure 13 the predicted and measured soil displacement agree well in shape indicating that the compaction behaviour of the soil is correctly predicted. However, a general over prediction is visible over the whole depth starting with 14 mm at the surface and decreasing to 2 mm at depth, overall typically 4 mm. This could be attributed to the tendency to overestimate soil displacement on dense soil, a tendency which was already marginally visible by the comparison of prediction to measurement on dense soil in the previous paragraph (3.1). The large difference at the surface can as well be attributed to the influence of lugs and a sampling error.

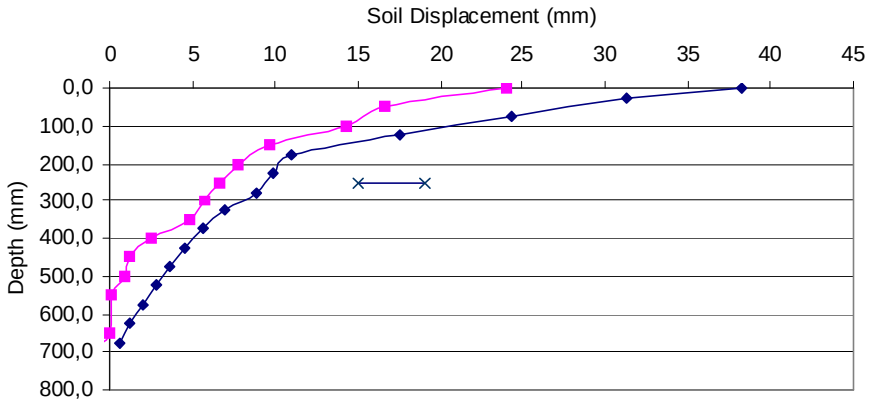

Figure 13: Predicted (♦) and measured (■) soil displacement on stratified soil conditions after the pass of a 900/10.5/1.9. The least significant difference (LSD) at 95 % is also shown

11.1.3.3 Multi Pass Experiment

Figure 14 shows the results of predicting soil displacement after 3 passes of 900/10.5/1.9 and 900/5/0.5 tyres over a uniform weak soil with an initial DBD of 1.38 g/cm^3. These were compared to the measured values from Ansorge (2005). This comparison aims particularly at

the evaluation of the behaviour of the model with respect to the slope of the recompression line (RCL) which determines soil behaviour at the beginning of reloading (the second cycle in a loading-unloading sequence). The smaller the slope of the RCL the faster soil compacts in the consecutive loading cycles and has undergone less strengthening than one with a larger RCL slope.

As the close agreement between measured and predicted data shows, the model predicts the soil behaviour correctly for subsequent passes without the necessity to adjust the RCL. The slope of the RCL = 0.0327 as defined by O'Sullivan (1998) can be maintained for this sandy loam, too. In general a close agreement at the surface is achieved and only displacement behaviour at depth differs slightly when the displacement approaches zero anyway and the deviation is still within the error of measurement.

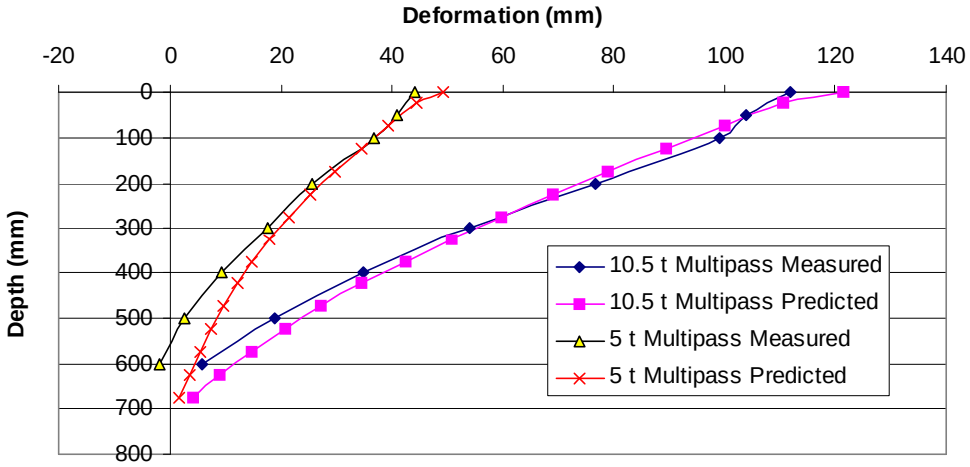

Figure 14: Predicted and measured soil displacement after multipasses of a 900 mm tyre

11.1.3.4 Passes with complete vehicles

Figure 15 shows the predicted soil displacement below vehicles after the pass of the front and the rear axle. In general a close agreement was obtained between measured and predicted soil displacement. A close agreement was found for both the 900/10.5/1.9 followed by the 500-70/4.5/2.3 (900-500) and the 590/4/1.2 followed by the 290/1.5/2 (590-290). For the 900/10.5/1.9 followed by the 700/10.5/1.0 (900-700) combination rut depth prediction was significantly smaller than the measured value, but the slope was similar. The 680/10.5/2.2 followed by the 500-85/4.5/1.4 (680-585) had closer agreement with respect to the predicted rut depth, but overall the slope differed more.

To summarize the ability to predict soil displacement after multiple passes from either a three front axle pass or whole machines the slope of the measured and predicted soil displacement lines were calculated and plotted against each other in Figure 16. The agreement between measured and predicted soil displacement is high. The average increase in DBD was predicted to within +/- 1.5 % for all treatments except the 680-585 with +3%. The slope shows that the increase is underpredicted by 5 % compared to the 1:1 line with an R^2 of 0.85.

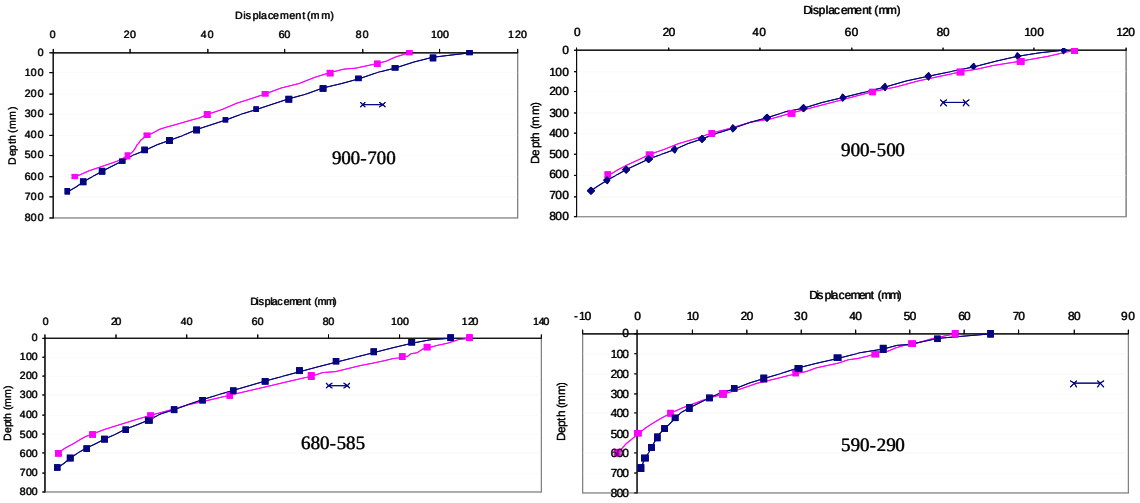

Figure 15: Predicted (♦) and measured (■) soil displacement on stratified soil conditions after the pass of a combine harvester with different tyre and load combinations. The least significant difference (LSD) at 95 % is also shown

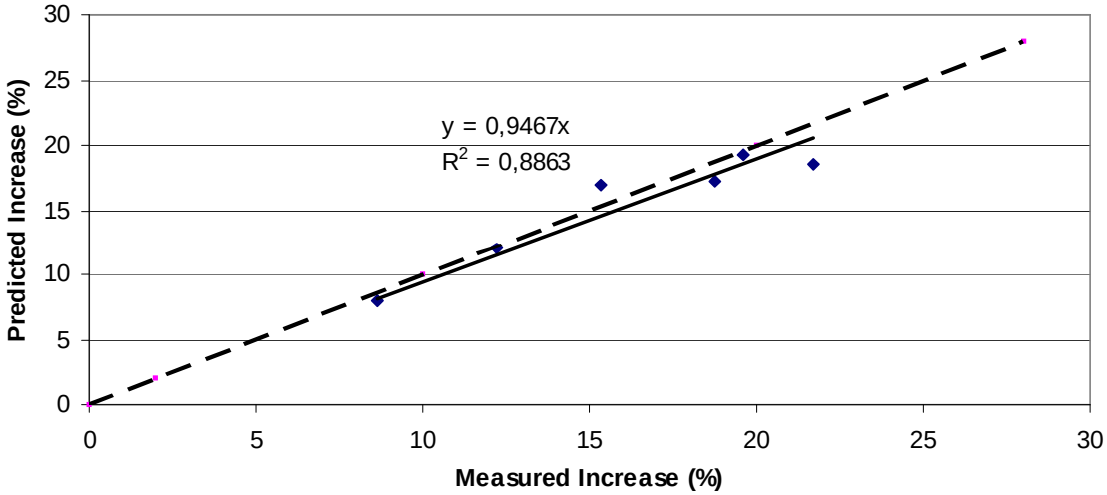

Figure 16: Predicted vs. measured increase in soil displacement for multi passes from whole machines or front axles. Also shown is the 1:1 relationship (broken line)

11.1.4 In-field determination of VCL

This section contains the data from field experiments and the approach to gain the slope and intercept from tyre passes as explained in Section 6.3 will be validated on a clay soil and a sandy loam soil. On both soils concentration factors of 4 and 5 will be compared. On the sandy loam three VCLs are gained from shallow tilled and subsoiled soils and by pooling the data from both treatments.

11.1.4.1 Clay Soil

The approach of defining a VCL from contact pressure and rut depth was also verified with the field experiments. On the clay loam from rut depths of 57.5 mm and 82 mm for low and high inflation pressure, respectively, an average increase in DBD of 9.6 and 13.7 % was calculated assuming 600 mm of uniformly increased DBD. Initial DBD was 1.27 g/cm^3 and resulted in 1.911 and 1.843 relative density when adding the increase in DBD for the low and high inflation pressure, respectively. Contact pressure was estimated according to O'Sullivan et al. (1998), and resulted in a mean normal pressure of 52.9 kPa and 55.9 kPa for the low and high inflation pressure, respectively at a concentration factor of 5 following the calculations given in detail in Section 6.3.2. At a concentration factor of 4 the corresponding pressures were 57.5 kPa and 60.8 kPa. In Figure 17 the relative density is plotted vs. mean normal pressure for both concentration factors and a logarithmic regression line is fitted to each set of data resulting in the corresponding VCLs for the clay soil.

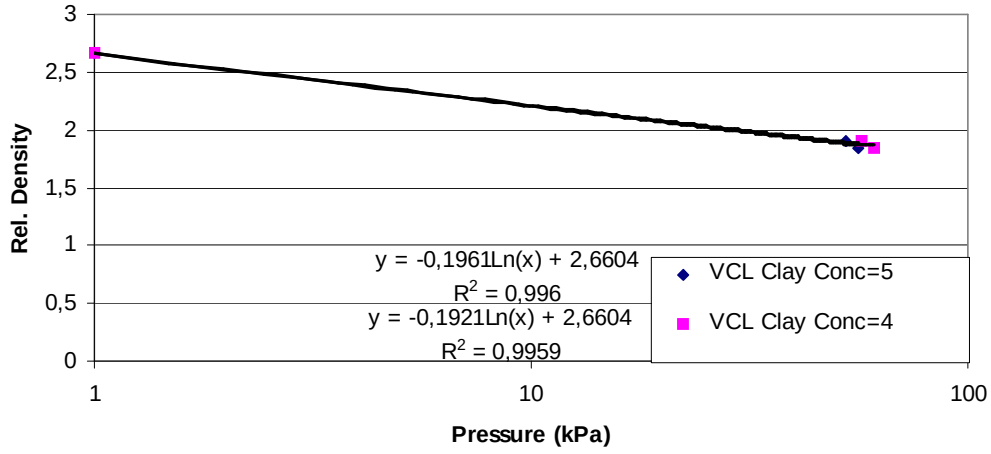

Figure 17: VCL for clay soil gained in field experiment

In the following the prediction performance of the VCLs for the two concentration factors will be evaluated. If the slope of -0.1961 and the intercept of 2.6604 corresponding to a concentration factor of 5 are fed into COMPSOIL, soil displacement for these field conditions is predicted for the high and normal inflation pressure machine configuration and compares to the measured data as shown in Figure 18 by the dash-point-dash line. Doing the same with slope and intercept gained from a concentration factor of 4, the prediction compares to the measured data as shown by the blue line in Figure 18. When comparing the concentration factor to the data for both inflation pressures, a concentration factor of 4 is closer to the measured data and therefore on the clay soil a concentration factor of 4 seems more appropriate. However, the difference between the predicted and measured soil displacement at both inflation pressures is small. In general soil displacement at the higher inflation pressure shows a greater variation and was more difficult to predict due to the high inflation pressure as the estimated contact pressure is too low.

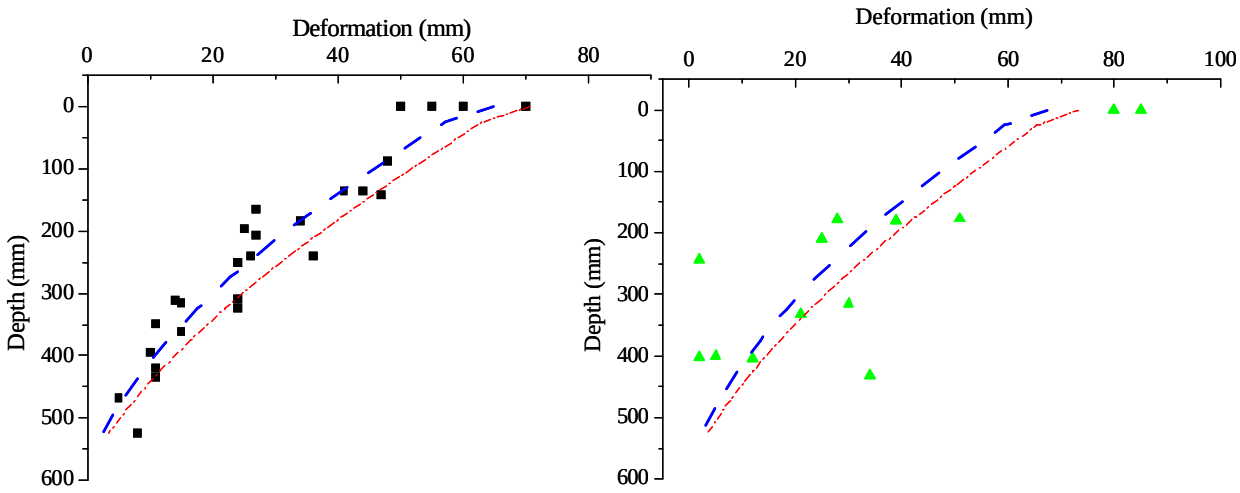

Figure 18: Predicted vs. measured soil displacement on clay soil in field for a concentration factor of 4 (- - -) and 5 (- • -) at normal (250 kPa) [squares] and high inflation pressure (350 kPa) [triangles]

11.1.4.2 Sandy Loam Soil

As explained earlier in this section the data from both the sandy loam shallow tilled, subsoiled and pooled experiments will be used to gain the slope and intercept of VCLs. The identical procedure as described in the previous section was used to gain the slope and intercept of the VCLs and hence no details are given. The DBD profile was 1.33 g/cm^3 for the sandy loam subsoiled to 350 mm depth and 1.6 g/cm^3 below to 750 mm. For the shallow tilled profile, the

impact at the surface was ignored due to settlement as explained later. For the maximum working depth of 350 mm a uniform DBD of 1.49 g/cm^3 was assumed. Below 350 mm it was similar to before with 1.6 g/cm^3 to 750 mm.

Starting with the sandy loam which received the shallow disc tine cultivation an offset of 15 mm was taken out similar to the clay as both soils received the same cultivation. As obvious from Figure 19 predicted soil displacement is larger for a concentration factor of 5 compared to a concentration factor of 4. The influence of the actual pressure calculation when soil displacement is calculated in the model is marginal, however, the influence of the concentration factor on the slope and intercept of the VCL causes this difference. Overall a concentration factor of 4 fits better, however, using the VCL created in the soil bin on the same soil type with a concentration factor of 5 fits the data best. This is due to the fact that the VCL from the soil bin contains more data points. The field experiment was conducted at a moisture content of approximately 20 % whereby the soil bin experiment was conducted at about 9 %. The good agreement in predicted soil displacement using the soil bin VCL is due to a similar distance from optimum moisture content for compaction which is at about 15 % moisture content for a sandy loam soil. Taking the three different VCLs into consideration which were used to predict soil displacement and created from tyre passes only on shallow tilled soil, only subsoiled soil and the pooled one, shows the best agreement for the VCL prediction gained from the shallow tilled plot only. Using the one gained from the subsoiled plot estimates soil displacement higher and the pooled one (called “both”) predicts intermediate soil displacement. The three different VCLs are shown in Figure 20.

Predicted vs. measured data for the sandy loam soil subsoiled is shown in Figure 21. A concentration factor of 4 fits the data for the normal inflation pressure better than a concentration factor of 5. However, at high inflation pressure a concentration factor of 5 seems more appropriate because it overcomes the under estimated soil displacement for this passage. Thus on this soil condition no clear recommendation can be given concerning the concentration factor. Similar to the shallow tilled part the VCL gained from the soil bin gives the best estimation of soil displacement. Interesting to note is the relation between the estimation gained from the pooled data (“both”) and the one only utilizing the data gained on the subsoiled plot (“subsoil”). At a concentration factor of 5, the prediction for “both” is bigger than for “subsoil” at normal and high inflation pressure. Nevertheless at a

concentration factor of 4, “subsoil” is bigger than “both” as expected from previous results on the shallow tilled soil.

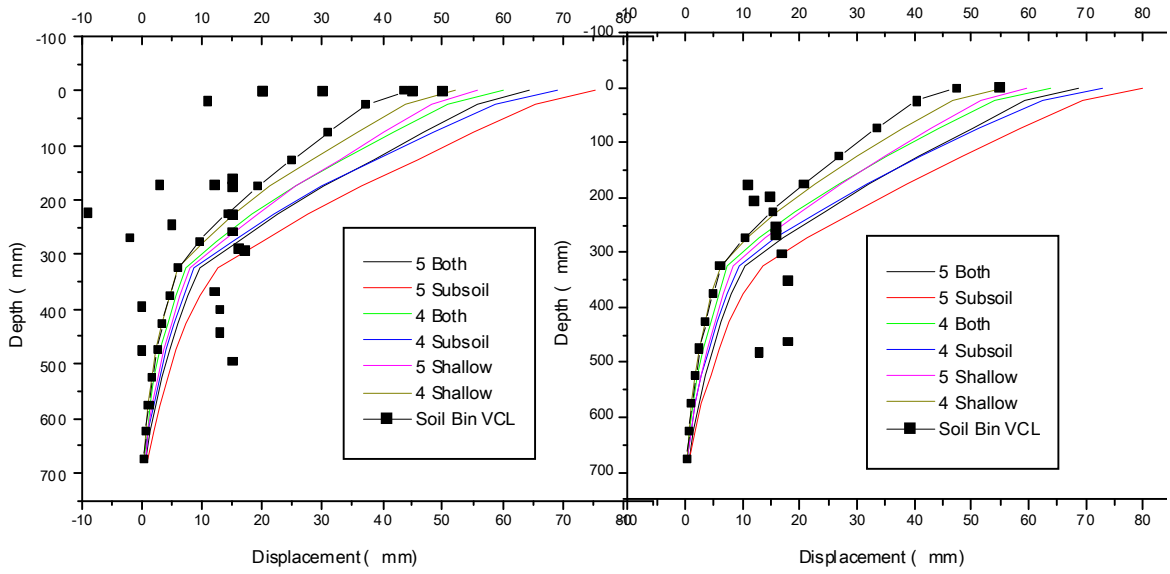

Figure 19: Measured (points) and predicted (lines) soil displacement for the normal (2.5 bar) (left hand side) and high inflation pressure (3.5 bar) (right hand side) treatment on shallow tilled sandy loam soil

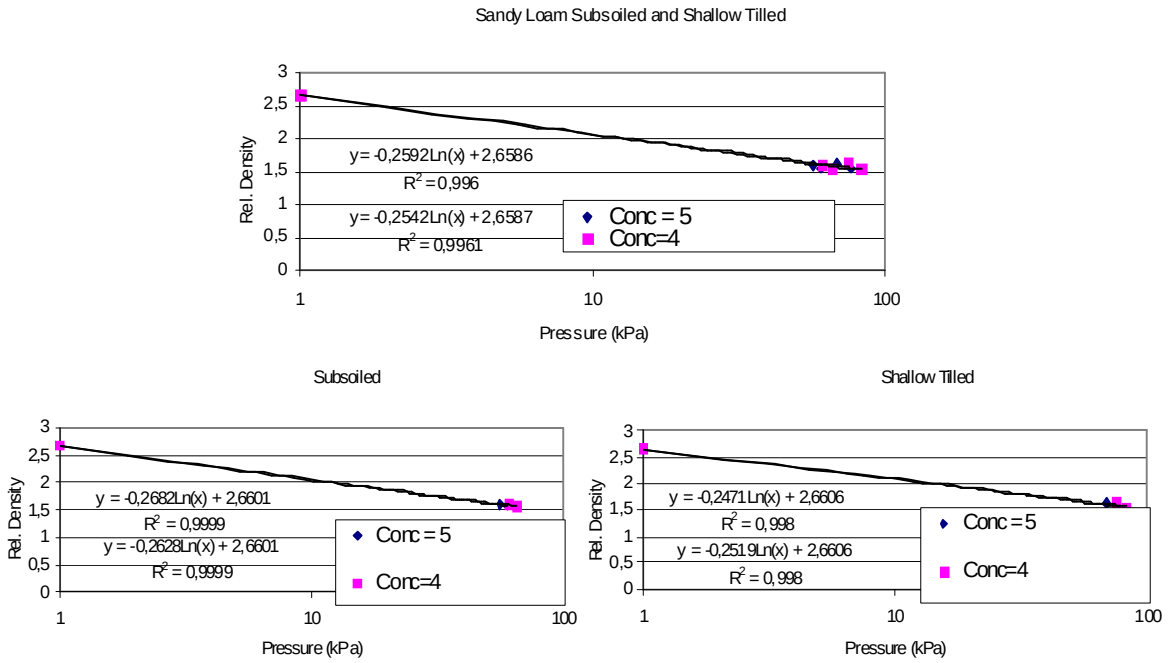

Figure 20: Virgin compression lines from different grouping of field experiments on sandy loam soil

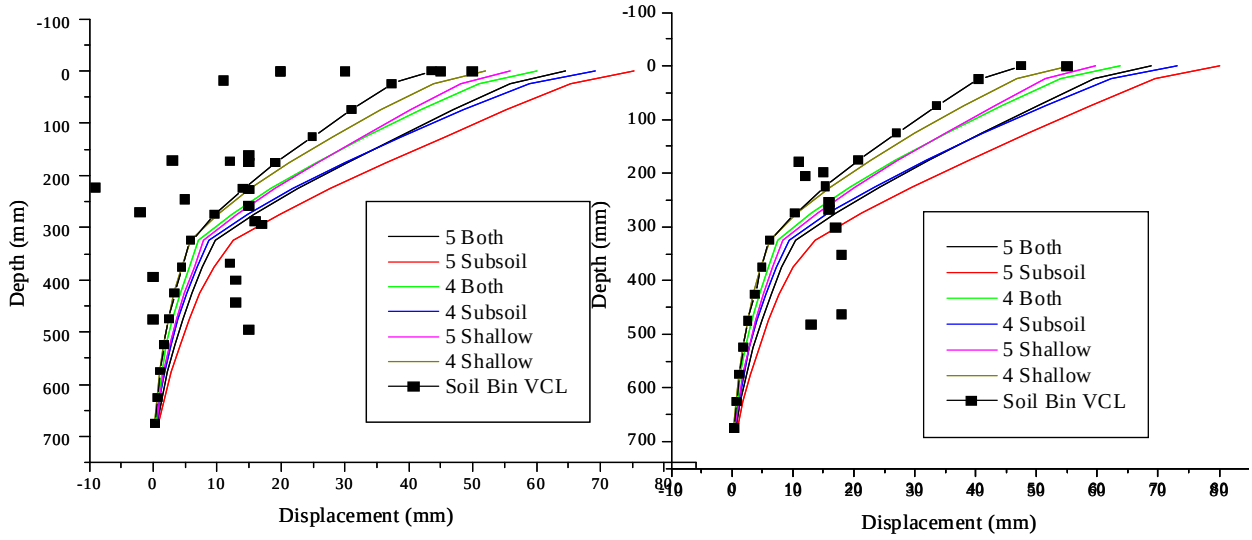

Figure 21: Measured (points) and predicted (lines) soil displacement for the normal (2.5 bar) (left hand side) and high inflation pressure (3.5 bar) (right hand side) treatment on subsoiled sandy loam

Overall it seems as if a concentration factor of 5 seems appropriate to describe the pressure propagation for a sandy loam soil and a concentration factor of 4 to describe a clay soil. This can be explained from their different particle size distribution which overall gives the sandy loam a coarser network compared to the clay which is due to the smaller particle sizes much finer. Due to the finer network the pressure decreases less with depth and is transmitted to deeper layers more easily than with the coarser network of a sandy soil.

In future work consideration should be given to the behaviour of tyre contact patches at different inflation pressures when they vary from the recommended inflation pressure either positively or negatively as in either case prediction results are not satisfactory.

11.1.5 Triaxial Justification of VCL

In this section the soil bin approach to gain a VCL will be evaluated by gaining an adequate VCL with a triaxial test equipment. Initially confining pressure will be applied followed by an investigation of the water compressibility and finally axial and radial pressure will be applied trying to mimic real soil bin conditions. At the end all the different prediction results of the varying VCLs will be compared. In Appendix 1.6 the soil bin approach to gain a VCL will be taken by utilizing small scale plate sinkage tests rather than tyres.

11.1.5.1 Confining Pressure Applied

In the first sequence only confining pressure was applied as this is the commonly referred way in literature to gain a virgin compression line according to Leeson and Campbell (1983). In the second subchapter a higher axial stress will be applied.

11.1.5.1.1 Influence of Time of Loading

In the first set of tests only confining pressure was applied to the soil samples. The samples were loaded to 100 kPa, unloaded and then reloaded up to 250 kPa. The short loading time from the soil bin can not be repeated because cell pressure can not be changed instantaneously. The influence of loading time on virgin compression parameters was investigated by allowing the system different amounts of time to reach each set pressure. Figure 22 shows the results from the experiments with different time spans used for loading. The different starting points at the beginning are due to slightly different initial densities. However, the curves merge at approximately 100 kPa indicating that differences in initial density do not affect the final results which agrees with the theory. The shortest loading time allowed 30 min to reach the set pressure, the medium loading time allowed 120 min to reach each set pressure and the slow curve was allowed 360 min to reach the maximum pressure. As obvious from the diagram there are no differences amongst the treatments and no clear tendency with loading time is visible either. Natural variation has a larger influence than the allowed time scale. This is shown with the slow VCL, which is expected to be the weakest due to the amount of time allowed to compact, but on the contrary, it is in fact the strongest.

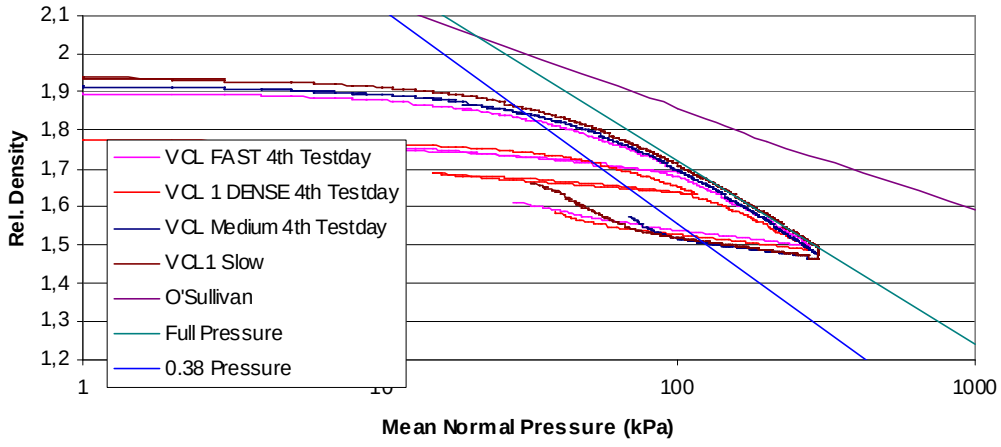

Figure 22: The influence of loading time on the shape of virgin compression lines and virgin compression lines from tyre data (pressure) and from literature (O'Sullivan et al, 1998)

The straight lines in Figure 22 represent the virgin compression lines which are gained from tyre data as described in section 3 and from O'Sullivan et al. (1998). It is interesting to observe that the virgin compression lines determined in the triaxial cell agree very well with the full pressure curve which assumes the mean normal pressure to be equal to σ_1, but is theoretically not sound and indicates a soil being too strong when its parameters are fed into the prediction model COMPSOIL.

11.1.5.1.2 Influence of Moisture and Initial Soil Density

The influences of moisture content and initial soil density in Figure 23 were conducted at the fast loading range. The curves of all samples appear independent of moisture content in the range of 8.2 – 12.5 % and initial density as they merge between 100 – 200 kPa depending on their initial densities. These curves are close to the full pressure tyre data of the soil bin. Only the densest sample with 10.8 % moisture content does not to merge with the other curves at the same point, but this might be due to the denser initial state of the sample at the beginning or an anomalous soil behaviour.

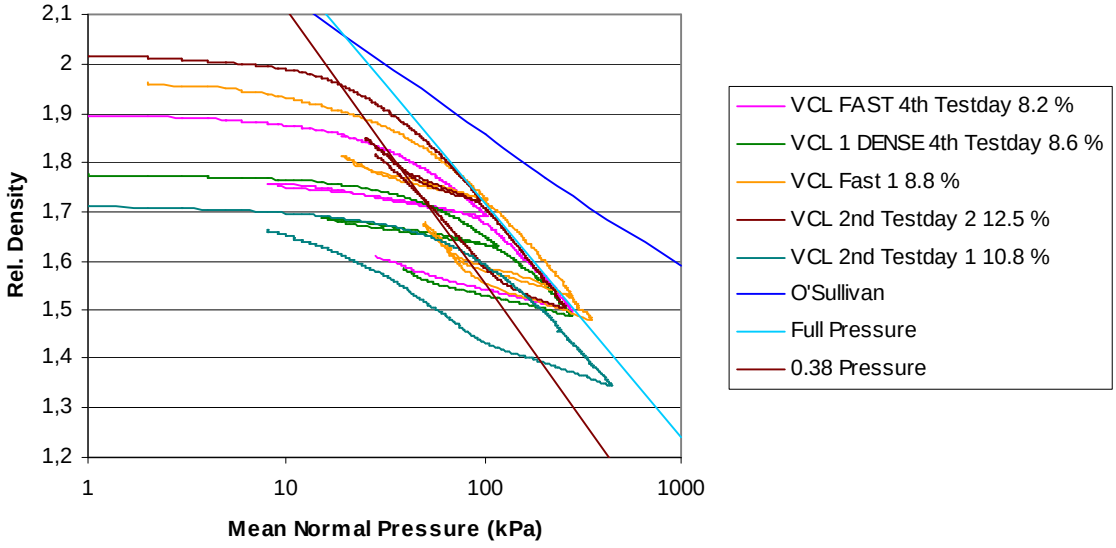

Figure 23: Influence of different initial densities and moisture contents on final VCL

Overall the repeatability of results only applying confining pressure is very good as can be seen from the results in both Figure 22 and Figure 23. The necessity to actually adjust a VCL for different sandy loam soils can be seen when comparing the VCLs of different authors in

Figure 24. The VCL created in this experiment is intermediate between the ones from O'Sullivan et al. (1998) and Leeson and Campbell (1983).

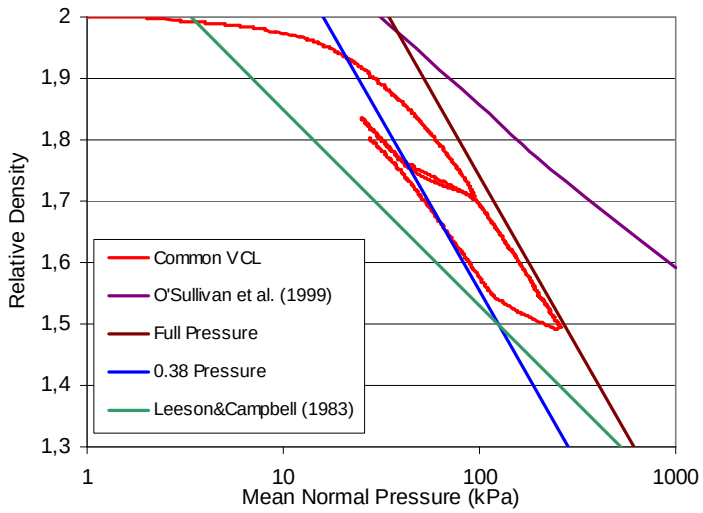

Figure 24: VCLs from O'Sullivan et al. (1998), Leeson and Campbell (1983), and the one gained by mere confining pressure

11.1.5.1.3 Water Compressibility

All the previous curves do not take water compressibility and the elasticity of the triaxial system into account. Therefore the elastic response of the system including the water was evaluated by pressurizing the cell without a sample three times up to 350 kPa and relieving the pressure again. As the graph in Figure 25 shows there is a close agreement between pressurizing and relieving the pressure. Only leaving the total pressure applied to the system as in the last run shifts the curve slightly but on depressurizing it reaches the origin again. Compressibility has an influence on the results because approximately 25 cm^3 are necessary to reach a cell pressure of 250 kPa. With a sample volume of 538 cm^3, 25 cm^3 represent 4.6 % of the entire sample volume. Taking the compressibility into account which has been disregarded in the previous figures, however, shifts the virgin compression line further away from the origin on the horizontal axis thereby making the soil to appear even stronger.

To evaluate the influence of the water compressibility Figure 26 shows one arm of the pressurizing curves from Figure 25 including a quadratic regression function. The regression

function was used to calculate the necessary volume to pressurize the system exemplarily for the VCL shown in Figure 27.

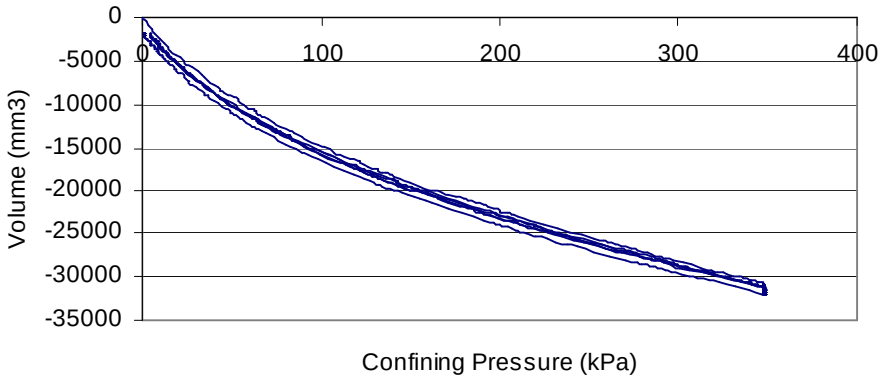

Figure 25: Volume necessary to pressurize cell (neg. volume means increase in water in triaxial cell)

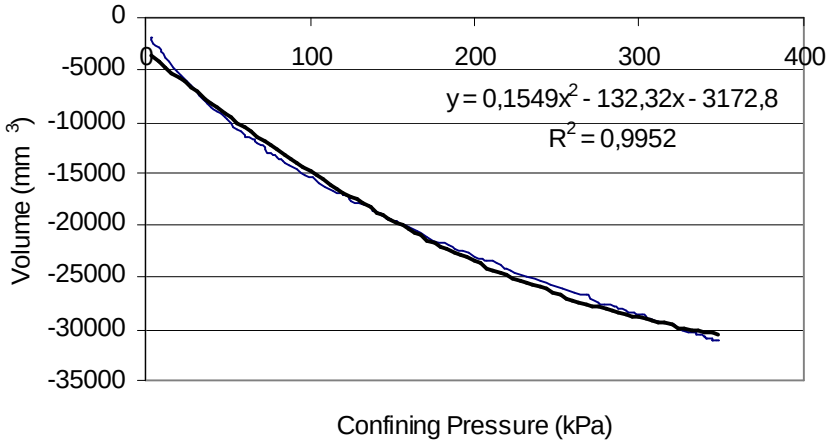

Figure 26: Regression line of one arm used to estimate a regression function for the volume response at a given pressure. (neg. volume means increase in water in triaxial cell)

The influence of the water compressibility is significant as apparent from Figure 27, however as it is identical for all curves it would only shift them in total and not have an influence on their relations amongst each other. Resulting from this the water compressibility was not taken into account in the previous discussion.

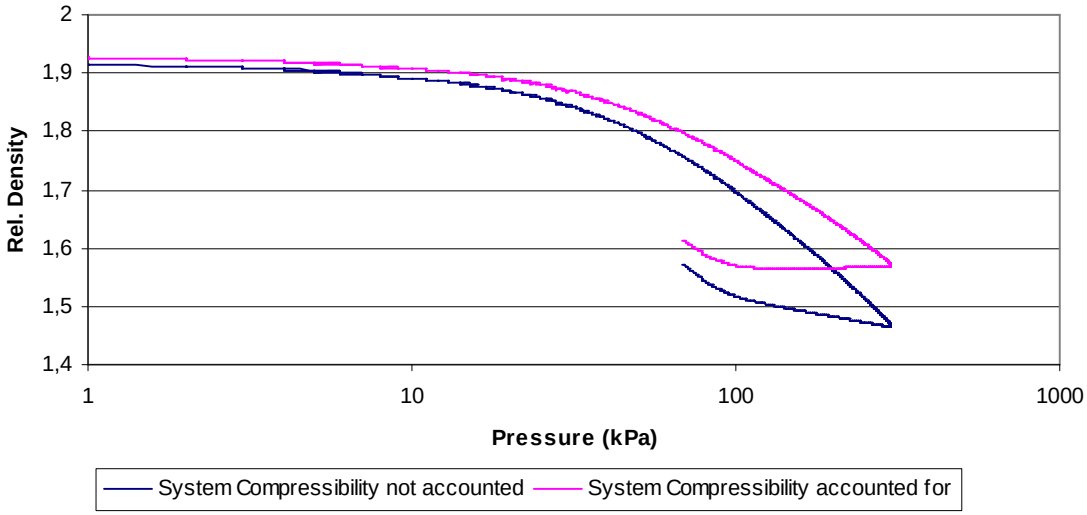

Figure 27: VCL with and without compensation for water compressibility

11.1.5.2 Axial and Radial Pressure

As there was poor agreement for the VCL from the soil bin gained by the tyre passes and the VCLs created with radial pressure in the triaxial test apparatus the idea rose to apply radial and axial pressure simultaneously replicating stress conditions implied by Eq. 1 which has been discussed earlier. Radial pressure has been set to 25 kPa and axial load was applied replicating a tyre pass in the soil bin. According to Eq. 1 the resulting σ_1 should be approximately 130 kPa because of the relation of σ_1 to the sum of σ_2 and σ_3 being approximately 0.38 as shown in Table 6. The resulting virgin compression line is shown in Figure 28. The density change was calculated from the change in cell volume as before and additionally from the height change of the sample assuming that the entire height is taken up by the sample and the sample does not squeeze sideways. For the 1.8 s in which axial load was applied no change in cell volume was measured and therefore measuring the height change was the only suitable measurement parameter. However, when looking at the sample afterwards it failed sideways during the test which resulted in a VCL weaker than in reality (this will be shown later).

Figure 29 shows the loading cycle for the virgin compression line plotted in Figure 28 with σ_1 against σ_2 and σ_3, i.e. axial load vs. radial load. It can be seen that σ_1 does not get close to 130 kPa and is only in the second half of the test about 4 times larger than both σ_2 and σ_3. Due to the slow response time of the cell volume/pressure controller the radial pressure could

not be maintained at the set value of 25 kPa after the beginning of the application of axial load and the resulting compaction of the sample allowed the cell pressure to drop as the sample volume decreases (because the soil compacted further).

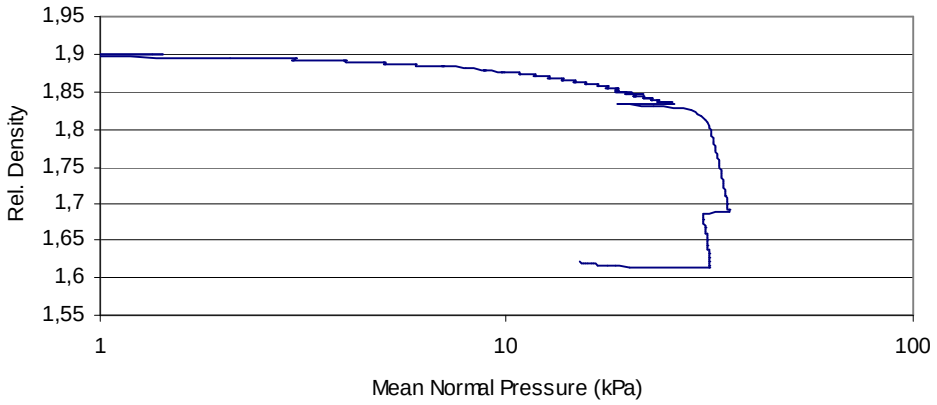

Figure 28: VCL _2_231106 radial pressure up to 30 kPa followed by an axial load application simulating the passage time of a tyre in the soil bin

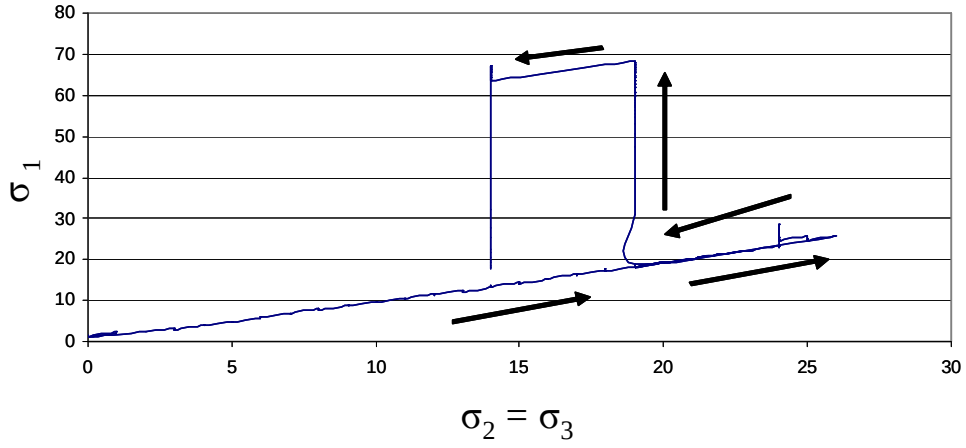

Figure 29: σ_1 in relation to σ_2 and σ_3 during the trial of VCL_2_231106

From these experiences resulting in a VCL which was too weak (as shown later) compared to soil bin VCL, followed the idea to apply axial load by moving the piston a known distance in a given amount of time while recording the resulting axial force. As the axial load is applied slowly, radial pressure can be maintained and the cell volume change is equal to the compacted soil volume as beforehand when only applying confining pressure. The resulting diagram is shown in Figure 30.

Using the parameters of the VCL created only from cell volume change results in a better prediction of the soil displacement by COMPSOIL. However, as shown in Figure 31 the

relation of σ_1 to σ_2 and σ_3 is never larger than three which means that the stress state expected from Eq. 1 in the soil bin was not reached in the triaxial cell. The stress difference at this state can not become larger because the sample started to fail in shear which was realized when the sample was taken out of the triaxial cell and the rubber membrane was taken off. The shear planes can clearly be seen in Figure 32.

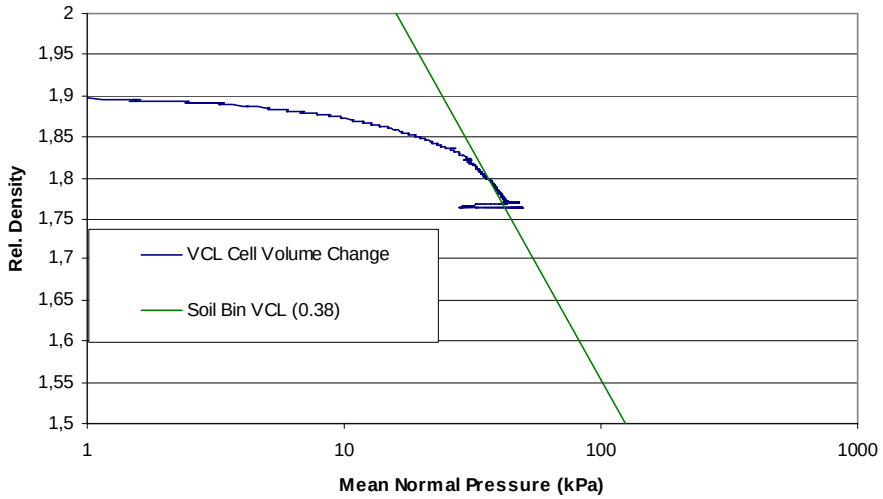

Figure 30: VCL for VCL_1_241106 with cell volume change

The sample was just about to start shearing when reloading it again as shown in Figure 33 where axial load is plotted against axial displacement. After loading the sample to 20 mm displacement all the load had been taken off and it was reloaded to 25 mm displacement. In this reloading phase the shear planes must have started to develop as the slope of the axial load vs. axial displacement curve exhibits a difference in shape in Figure 33 - if extrapolated it would not merge with the same curve anymore as initially.

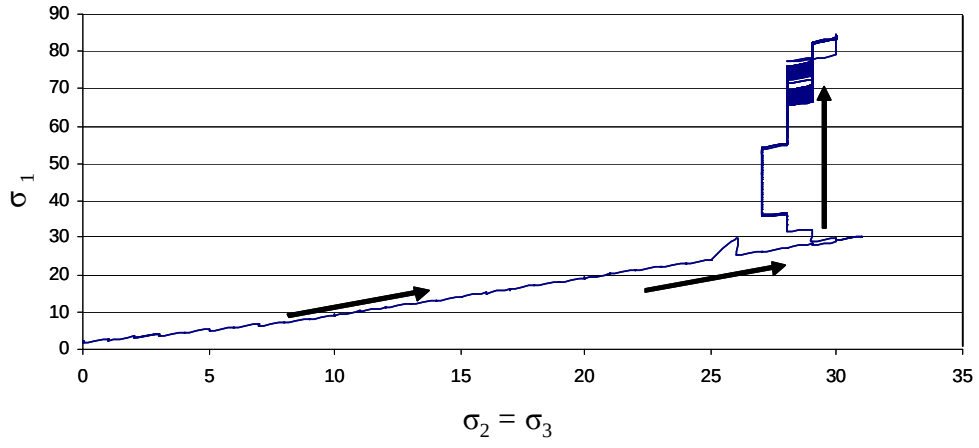

Figure 31: σ_1 in relation to σ_2 and σ_3 during the virgin compression test loading

Figure 32: VCL_1_241106 sample at the point of incipient shear failure

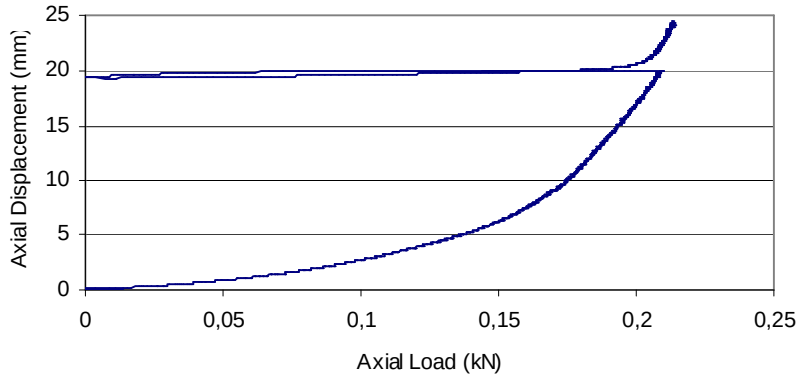

Figure 33: Axial displacement vs. axial load on sample VCL_1_241106

Summarizing this section the influence of differences in σ_1 to σ_2 and σ_3 can be seen in Figure 34 where the virgin compression lines differ significantly if σ_1 is bigger than σ_2 and σ_3. The VCL with radial and axial load is much closer to the VCL created from the tyre pass data than if only radial pressure is taken into account.

The result of the VCL with the radial-axial loading shown in Figure 34 was repeated with five more samples shown in Figure 35. VCL 1 came very close to the previous VCL. VCL 3 was weaker than the other one initially and the VCL 6 was slightly weaker. VCL 4 was even weaker. The VCL 2 from the second day was stronger than all the others.

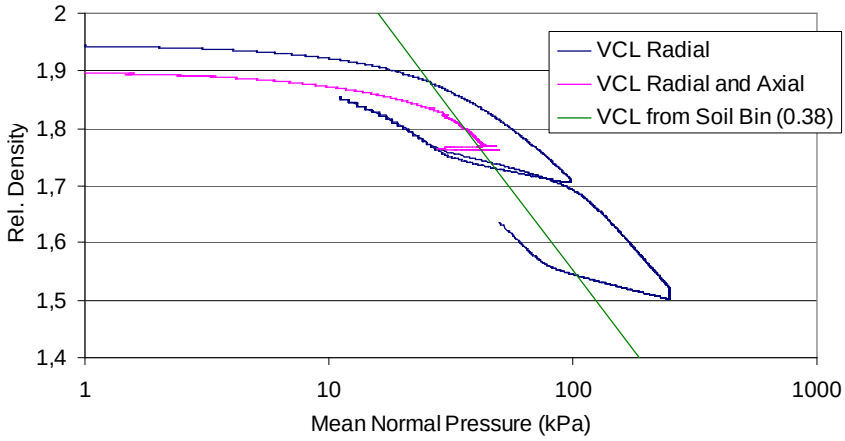

Figure 34: Virgin compression lines for radial and radial-axial loading with sandy loam soil at 9 % moisture content

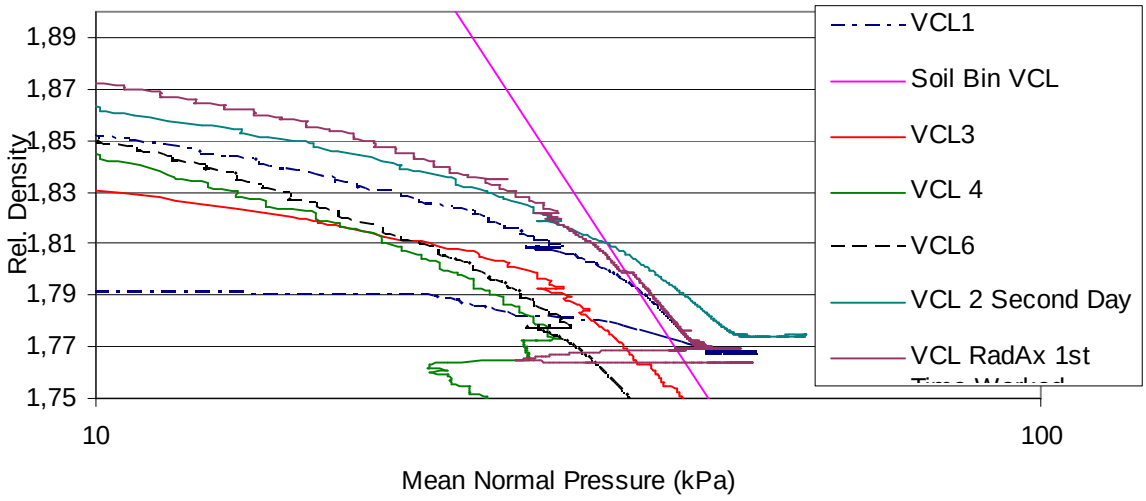

Figure 35: Replication of radial-axial loading to get a feeling for the variation

The data in Figure 35 shows that it is difficult to reproduce similar results with this method. To judge which one of these curves would represent the appropriate VCL for the soil bin soil without the Soil Bin VCL as reference would be impossible. Therefore in a next step all five curves were averaged to gain an overall average VCL. Additionally the three VCLs, closest to the soil bin VCL, were averaged, VCL1, 3, and VCL2 second day, respectively. Both average VCLs were obtained by accounting for water compressibility, too. The initial curves had not been adjusted as the confining pressure is the same for all since the adjustment does not influence total variance. The average VCLs are shown in Figure 36 including the soil bin VCL as reference. The average of all five VCLs exhibits a good agreement with the soil bin VCL. Only taking the three closest VCLs into consideration, results in a VCL which would indicate the soil to be too strong.

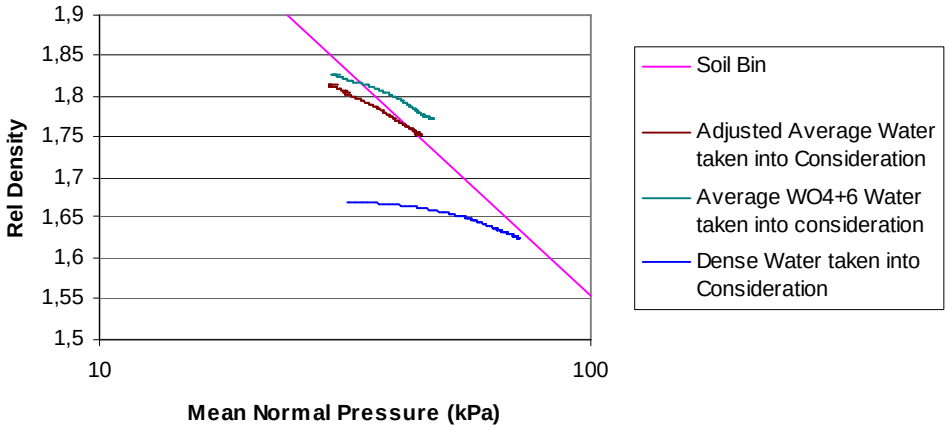

Figure 36: Averaged VCLs with water compressibility taken into consideration

One approach to reduce variation was to utilize a much denser initial soil condition. Having done this for three samples shown in Figure 37 indicates as well some variation and more importantly the samples fail before they reach the VCL indicating the soil to be too weak. Thus to get to the soil bin VCL at this higher initial density, a larger confining pressure would be necessary. A VCL created by averaging the VCL data from the dense samples has also been included in Figure 36. Interesting to note is that the average VCL does not reach the soil bin VCL and moreover, shows a different slope.

Because of the different slope for the average VCL from the dense soil samples it is strongly argued that a VCL is not a unique line which only depends on the mean normal stress. In contrast it is a line describing soil strength in relation to ratio of the axial and radial stress state. As Figure 38 shows with a denser sample at the same confining pressure a much higher axial loading can be achieved. With the density representing the density commonly used in the soil bin a relationship of 1/3 could be achieved between Sigma 1 and Sigma2/3. In contrast to this, for the dense sample this ratio increased to 1/5. Thus depending on this configuration different VCLs can be gained.

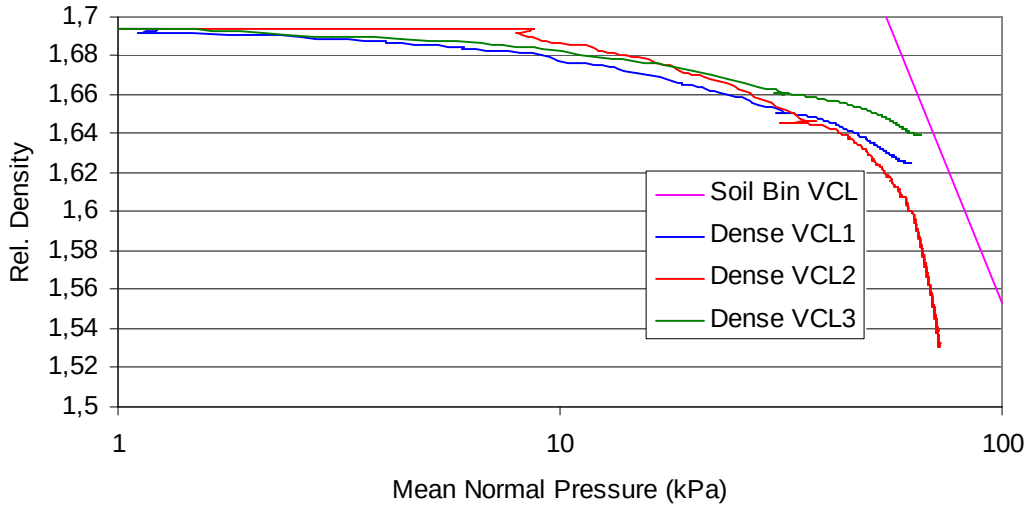

Figure 37: VCLs from radial-axial loading at a denser state and their comparison to the soil bin VCL

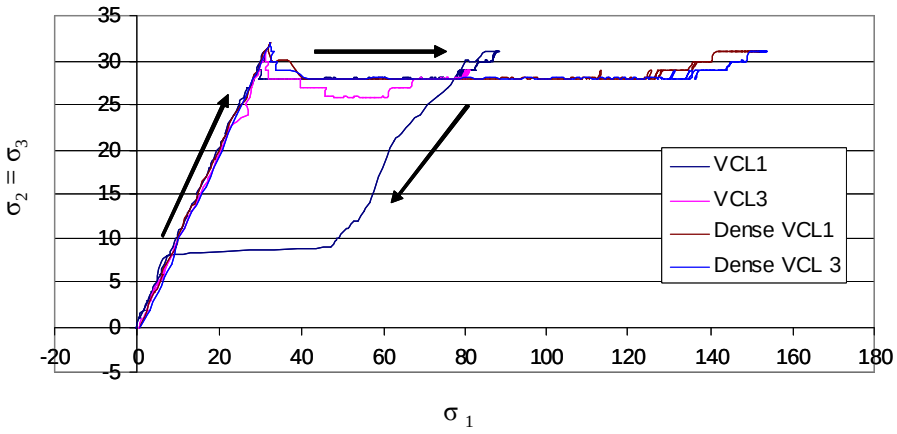

Figure 38: σ_1 in relation to σ_2 and σ_3 depending on intial soil density at same confining pressure of approximately 30 kPa

11.1.5.3 Implications of Triaxial VCLs on predicted Soil Displacement

If regression lines are put through the different virgin compression lines and their slope and intercept is fed into COMPSOIL the predicted outcome is compared in Figure 39 for the different approaches. The “Mean Norm = Contact Pressure” gained by assuming contact pressure being equal to mean normal stress agrees well with a typical VCL from the triaxial tests whereby only radial pressure has been applied (VCL only Spherical Pressure). However, this underestimates soil displacement by a factor of 2. If constant confining stress is applied and an axial load impact similar to that in the soil bin is applied, as can be seen from “VCL A+R Cell+Height Quickly”, and if the height change is additionally to the cell volume change

taken into account soil displacement is totally overestimated. With only cell volume (VCL A+R Cell Quickly) change the approach is closer to the prediction with the tyres, however, underestimates the resulting sinkage.

If the axial load is applied slowly by a constant strain rate and only cell volume change is taken into consideration "VCL A+R Cell Slow" shows the correct shape and underestimates total displacement less than "VCL A+R Cell Quickly " did. If in the slow case height change is taken into consideration, too, "VCL A+R Cell+Height Slow" shows a closer agreement at the surface, but the entire shape of the curve changed making it less appropriate.

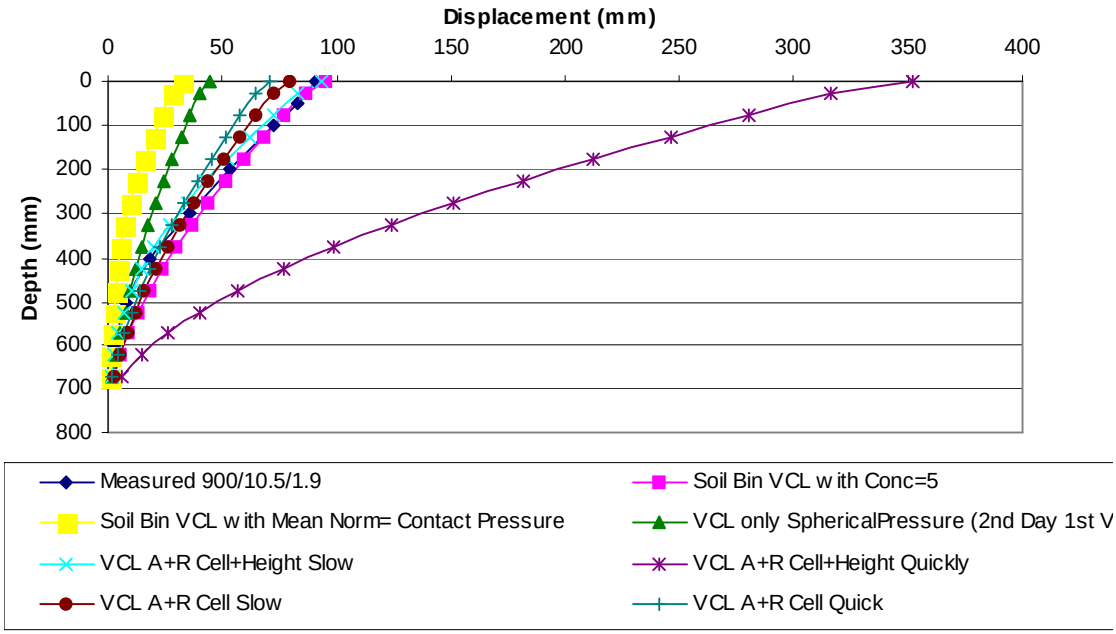

Figure 39: Different ways of gaining VCL to describe 900/10.5/1.9 treatment

The following figure will compare the average VCLs gained in the previous section to both, the unique "VCL A+R Cell Slow" from the previous diagram and the initial soil data. Using the VCL parameters gained from "VCL Average Dense" soil displacement is overestimated at depth, although in the top 150 mm it agrees most closely to the measured soil movement. The prediction of soil displacement for "VCL Average 5" agrees with the "VCL A+R Cell Slow" which shows that this VCL created initially "randomly" without replications is in fact not random. As discussed before soil displacement for these two lines is overestimated at depth and underestimated at the surface. Pre-selecting the 3 from the 5 VCLs to gain an average actually lead to an even larger error between measured and predicted soil displacement.

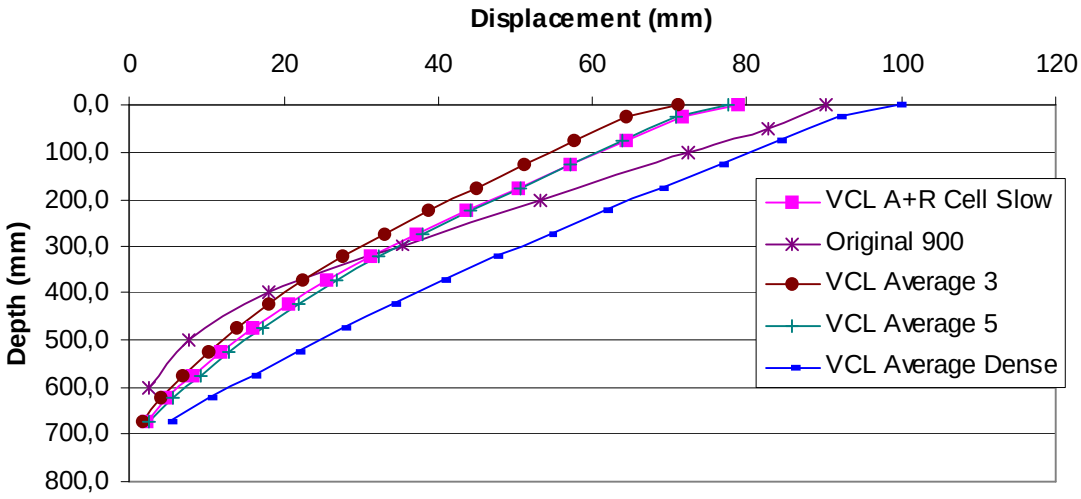

Figure 40: Predicted soil displacement using averaged VCLs at 1.4 g/cm^3

These results lead to a comparison of the predicted and measured soil displacement on dense and soft soil condition for the averaged VCLs. The "VCL A+R Cell Slow" was not included anymore as it agrees well with the "VCL Average 5". Overall all averaged VCLs agree well with measured soil displacement for the 900/10.5/1.9 on both weak and dense soil conditions. The average of the VCLs gained on dense soil shows the closest agreement on the dense soil and has the biggest overprediction on the weak soil. This overprediction is probably due to the weaker soil structure at a higher axial load while maintaining confining pressure. The average of 5 and 3 are virtually identical on dense soil conditions and only show some deviation on the weak soil conditions. On weak soil conditions as shown previously in Figure 40 the preselected averaged 3 curves show a larger underestimation of soil displacement than the average of 5. The average of 5 agrees over the entire depth well with the measured soil displacement. It only shows a very slight underestimation of soil displacement in the top 300 mm and a slight overestimation in the bottom 300 mm.

Very interesting is the general fact that virgin compression lines which should uniquely describe soil density change with pressure depending on mean normal pressure differ significantly if σ_1 is larger than σ_2 and σ_3, i.e. if additional axial load is applied. The virgin compression line depends on the stress state of σ_1, σ_2, and σ_3 and only if these represent real field conditions the VCL does correspond to the VCL gained from the pass of the tyres. Moreover as Figure 41 showed, if the soil conditions which are used to measure soil displacement are replicated in the triaxial cell, the predictions from resulting VCL will most

closely agree with the real data. Overall the approach by O'Sullivan et al. (1998) to set the confining pressure in relation to the axial load appears justified.

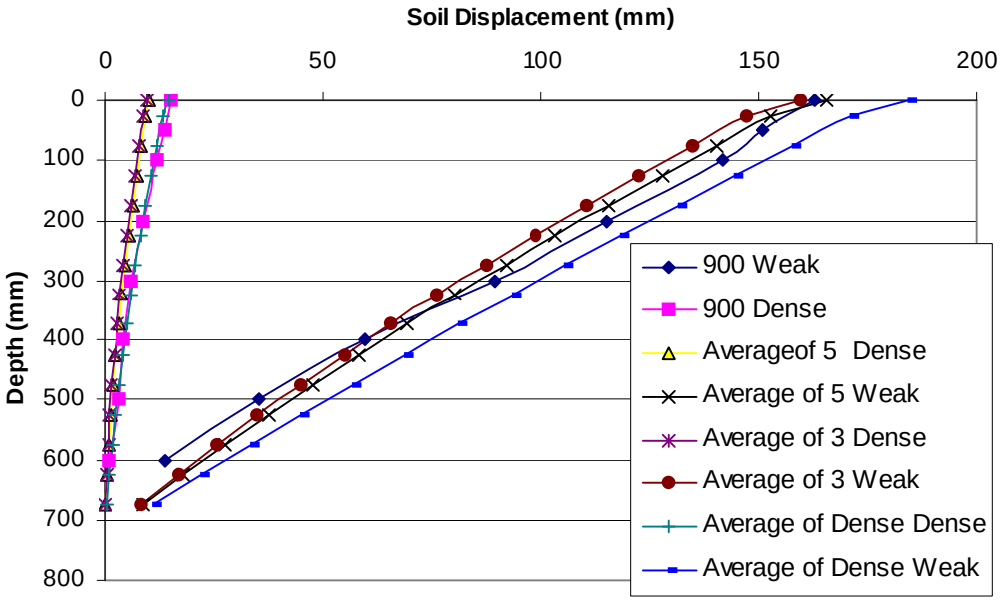

Figure 41: Predicted and measured (Antille, 2006) soil displacement on denser and weakr soil conditions for the 900/10.5/1.9

11.1.6 VCL from Plate Sinkage Data from Triaxial Cell

As it proved to be difficult to gain a virgin compression line describing the soil in such a way as the tyre experiences it, a different approach to gain a virgin compression line was to use the contact patches, pressures and sinkage data of Section 6.3. Similar to the soil bin a uniform soil density increase over the entire depth was assumed as no sideways movement of the soil could be detected. Again the punching type of soil failure appeared in all measurements and is shown in Figure 42. No heave is visible at the surface indicating hardly sideways movement of the soil. The plate sinkage experiment was conducted as specified in Section 2.8.

The virgin compression line of the soil was calculated in the same way as for the tyre data. The plate sinkage divided by soil depth resulted in the average increase of soil density assuming uniformity with depth. With the average increase and the known initial density the final density was calculated and then 2.66 divided by it to gain the relative density. As with the soil bin, contact pressure was transformed into mean normal pressure as shown in Section 6.3.3 and the resulting virgin compression line is shown in Figure 43. The function for the different plates (left hand side of Figure 43) indicates a slightly weaker soil as the one for the same plate with different loads on the right hand side.

Figure 42: Plate in cooking pot after compression. No sideways heave visible

Feeding the slope and the intercept of these virgin compression lines into the O'Sullivan model gave a close agreement to the measured data as shown in Figure 44. Figure 44 shows as well the predictions if the contact pressures were taken for mean normal pressures. Similar to the real tyre data then soil displacement is significantly underestimated.

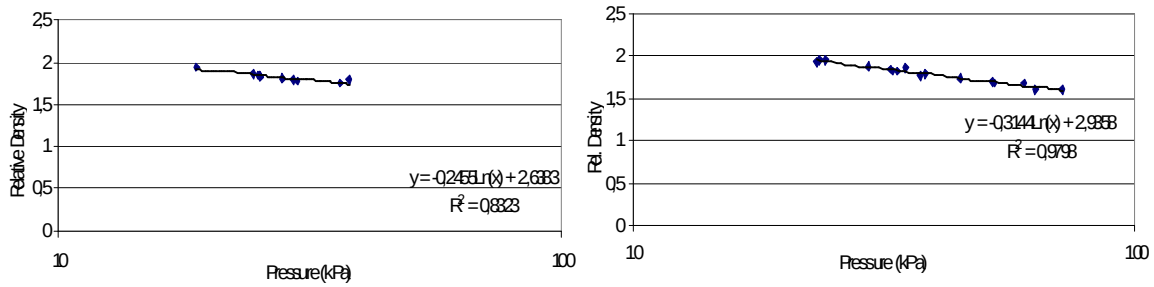

Figure 43: Virgin compression line for plate sinkage tests with different plate sizes (left) and different pressures on same plate (right)

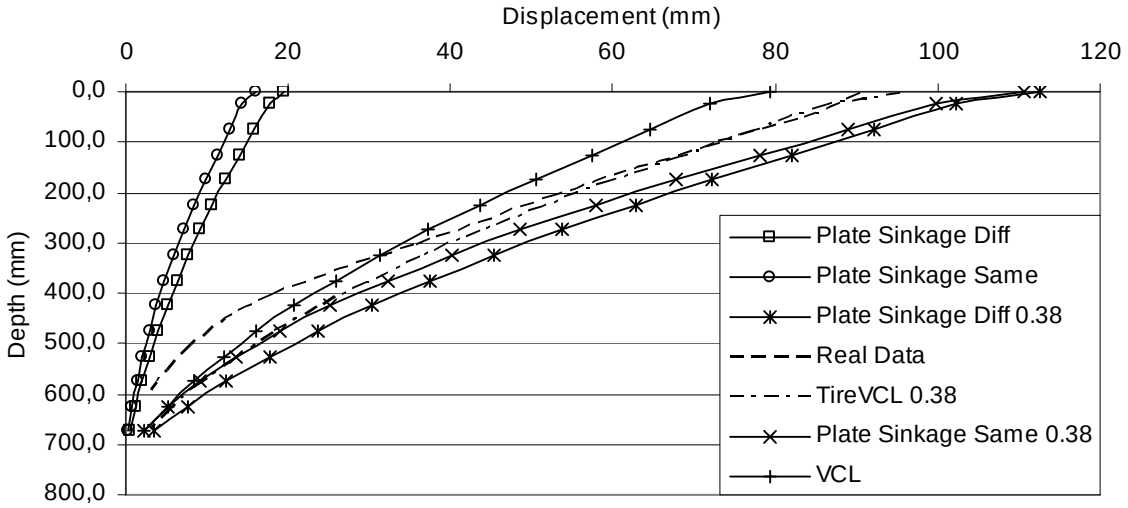

Figure 44: Measured and differently predicted soil displacement for the 900/10.5/1.9 on uniform soil conditions

The VCL parameters created with the plate sinkage tests predict the 900/10.5/1.9 tyre closer to its real data than the best estimation using the triaxial data for the VCL parameters whereby axial and radial load is applied at the same time as described in Appendix 1.5.2. Still the best estimation is gained with tyre data itself. This result justifies moreover the approach taken with the estimation of the VCL parameters only from contact pressure and rut depth when knowing the DBD profile with depth of the soil.

11.1.7 Sinkage Prediction from Real and Small Scale Plate Sinkage Data

Plate sinkage data of the soil bin was available and utilized to predict plate sinkage parameters k and n, which were in turn used with the approach from Bekker (1960) to predict rut depth.

11.1.7.1 Theory of Bekker – Sinkage Equations for Tyres

The general plate sinkage equation according to Bekker (1960) is as follows:

$$p = k * z^n$$

Eq. 2

whereby *p* is the pressure in kPa, *z* is the sinkage depth in m and *n* (dimensionless) and *k* in kPa are empirical factors describing soil behaviour. *k* and *n* are empirically gained when plotting pressure of a plate [kPa] on the y – axis against sinkage [m] on the x-axis in double logarithmic scale. *K* is the intercept at 1 m sinkage and *n* is the slope of the linear function on log-log scale. The plate geometry influences *k* and for higher accuracy *k* can be derived from:

$$k = (k_c / b + k_\phi)$$

Eq. 3

K_c and k_ϕ are empirical factors describing soil behaviour in relation to the shortest length of the contact area or the diameter of the plate *b* in m. K_c and k_ϕ are gained by plotting *k* for different plate sizes on the Y-axis and the corresponding *1/b* on the x-Axis. Both axis are on linear scale. When a linear regression line is fitted, k_ϕ is the intercept at *1/b*=0 and k_c is the slope of the line which could be negative. Eq. 3 is substituted into Eq. 2 and solved for *z*:

$$z = \left[\frac{p}{k_c / b + k_\phi} \right]^{\frac{1}{n}}$$

Eq. 4

However, the tyre differs in its sinkage behaviour from a flat plate due to its curvature. Consequently Bekker (1960) gives the approximate sinkage depth *z* depending on tyre load *W* [kN] and diameter *d* [m]of the tyre as follows:

$$z = \left[\frac{3W}{(3-n) * (k_c + b * k_\phi) * \sqrt{d}} \right]^{\frac{2}{2n+1}}$$

Eq. 5

Eq. 5 shows that an increase in diameter reduces sinkage much quicker than a comparative increase in width of these elements. According to Bekker (1960) “when ground pressure is kept constant, it is advisable to limit the width and to increase the length proportionally”.

Multiplying Eq. 3 by b gave the “alternative term” for Eq. 5. Therefore Eq. 5 can be expressed either ignoring the shape factor of k_c and k_ϕ or having *k* calculated from Eq. 3 earlier on:

$$z = \left[\frac{3W}{(3-n) * k * b * \sqrt{d}} \right]^{\frac{2}{2n+1}}$$

Eq. 6

11.1.7.2 Theory of Bekker – Sinkage Equations for Tracks

For the sinkage of a track, the terms look different as it is not one contact area, rather several contact areas split up between the different rollers and influenced by the belt tension. Whether in general it is more favourable to equip tracks with many small rollers or less bigger ones no coherent answer can be given. According to Bekker (1960) small rollers provide a uniform load spread, but bigger ones are necessary for load suspension of high speed vehicles. In consequence, the smaller number of large rollers may destroy the uniform load distribution. The problem of finding an optimum solution for wheel size and number of wheels is not only a problem of soil scientists, but also that of design, particularly if weight is taken into consideration.

According to Bekker (1960) the sinkage z_x at any point below a track supported by small diameter wheels can be determined in the following way:

$$z_x = \frac{W}{2*l*k*s} - 0.41*s*\sqrt{\frac{l_0}{l}-1} + \frac{1{,}23*x^2}{s}*\sqrt{\frac{l_0}{l}-1}$$

Eq. 7

Whereby the sinkage depends on the load *W*, the length of the track in contact with the soil *l* [m], the parameter *k* (*n* is assumed to be one in this case), half the distance between the rollers *s* [m], the track slag l/l_0, and the position *x* [m] for which the sinkage should be calculated along the track line. For the sinkage below the last roller *x* equals *s* and the equation reduces to:

$$z_x = \frac{W}{2*l*k*s} + 0.82*s*\sqrt{\frac{l_0}{l}-1}$$

Eq. 8

Both equations assume an n-factor = 1 which is a very soft soil. The implications of this and possible changes will be discussed later. The following drawing will explain the dimensions further:

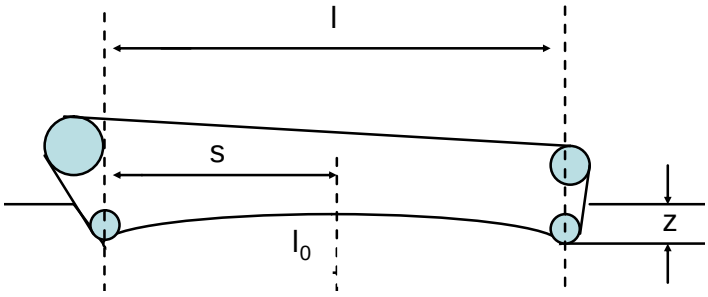

Figure 45: Track dimensions

11.1.7.3 Bekker-Theory applied

The necessary diagrams to gain n and k were drawn from plate sinkage data of a 142 mm diameter plate from the soil bin for a DBD of 1.2 g/cm^3, 1.4 g/cm^3, 1.6 g/cm^3, respectively. Measurements were replicated three times. For a first approximation, no correction for plate geometry was introduced and no statistical analysis was carried out. The spread of the data for each soil condition looked reasonable. The corresponding n and k values for the given soil conditions are summarized in Table 8.

Table 8: n and k depending on initial DBD

Soil Density	n	k
Soft 1.2 g/cm^3	0.89	700
Medium 1.4 g/cm^3	0.62	2150
Dense 1.6 g/cm^3	0.42	2400

11.1.7.3.1 Sinkage of Tyres

The values from Table 8 were used in Eq. 6 to calculate the sinkage of the rear tyres only on medium soil condition; however the front tyres were calculated on all three soil conditions. The sinkage data for the soft and dense soil condition is from Antille (2006) and the medium condition from Ansorge (2005). The tracks have not been included at this stage. As breadth of the tyre once the width of the tyre was used and in a second step (as suggested by Bekker, 1960) half the length of the foot print as this was always shorter than the width of the tyre. The estimated rut depth is plotted against the measured rut depth in Figure 46.

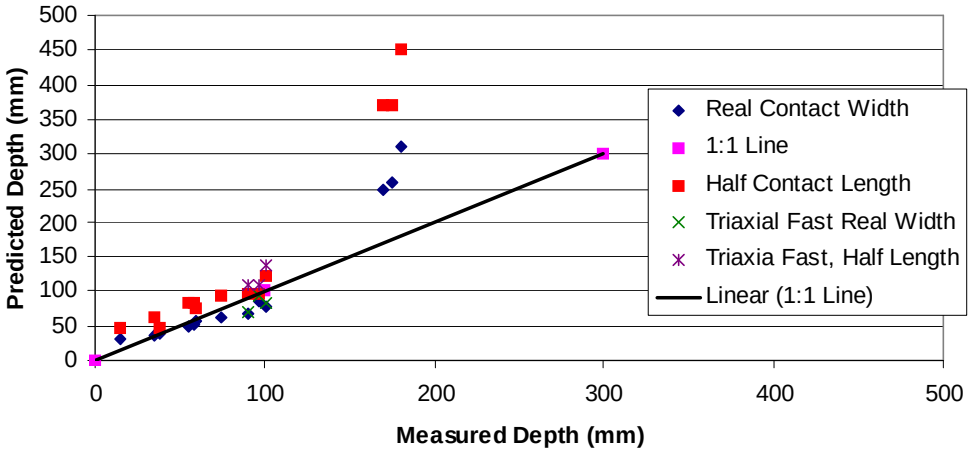

Figure 46: Predicted vs. Measured depth of the tyres from plate sinkage data

The predicted and measured rut depths for the dense and medium soil condition show tolerable deviation, whereby using the tyre width for the shortest contact length results in a slightly underpredicted sinkage compared to using half the contact length which results in a slightly overpredicted rut depth. However, on soft soil conditions, the deviation is about 100 %. This might be due to the fact that the Bekker model assumes an infinite soil depth below, whereas in the soil bin, the maximum depth is 750 mm. On medium soil conditions, the results could be replicated using the plate sinkage data gained from tests in the triaxial test as described in Section 2.8. This shows that plate sinkage tests can be used for both the

estimation of VCL parameters and Bekker-parameters. Section 6.7 showed a mathematical justification of this from Sime and Upadhyaya (2004).

The advantage of the Bekker approach is, that its parameters can be measured much easier than traditional critical state soil mechanics parameters, however, still needs plate sinkage tests performed to gain the parameters. Therefore the assessment is not as straight forward as the one proposed in Section 6.3 whereby the measurements can be taken from rut depths created by tyres. Figure 47 shows that the predicted rut depths from COMPSOIL are intermediate between the Bekker approach utilizing the contact width and the one using half the contact length.

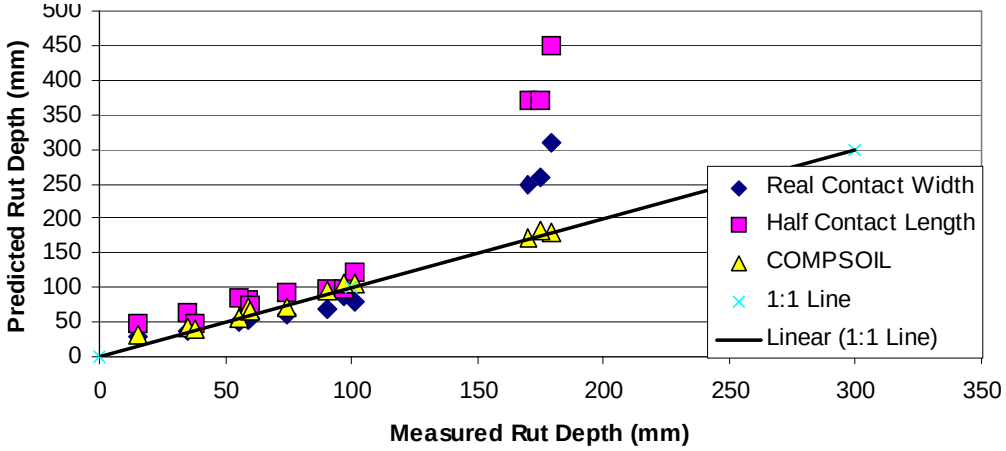

Figure 47: Predicted vs. Measured depth of the tyres from plate sinkage data and from COMPSOIL

An adjustment for plate sizes was not conducted due to the insufficient result on the soft soil conditions. For a more detailed approach and in order to reduce the errors further a sinkage study would need to be undertaken using different plate sizes to estimate k_c and k_{phi} properly. According to McKyes and Fan (1985) at least 3-4 plate sizes have to be used to reduce the coefficient of variation to 27 % and 16 %, respectively.

11.1.7.3.2 Sinkage of Tracks

The track sinkage equation could possibly be utilized to explain the different behaviour of different tracks. However, it has not been used for a proper evaluation of the sinkage, as it assumes n to be equal to 1 which is only the case on very soft soils. Nevertheless Table 9 includes predictions of track sinkage gained from the plate sinkage approach of Eq. 4 whereby only k*b has been considered, the track equation Eq. 8 (which for a slag of 0 reduces

to the plate sinkage equation of Eq. 4 with an n-factor of 1). Additionally the following Bernstein equation is included, too:

$$z = \frac{6 * W}{5 * r * b * k * \sqrt{D}}$$

Eq. 9

whereby r is the number of rollers in the track unit and D is equal to the diameter of the largest roller of the track unit.

Table 9: Measured and predicted track sinkages using different approaches

Unit / Belt Slag	Plate (Eq. 4) (mm)	Track (Eq. 8) (mm)	Bernstein (Eq. 9) (mm)	Measured Sinkage (mm)
Stocks/0.05	0.2	80	51	55
Stocks/0.02	No Slag	64	No Slag	
PTS/0.05	0.2	102	58	85
PTS/0.02	No Slag	79	No Slag	
Westtrack/0.05	0.1	70	36	55
Westtrack/0.02	No Slag	57	No Slag	
TerraTrac/0.05	0.15	77	29	55
TerraTrac/0.02	No Slag	62	No Slag	

According to Table 9 the general plate sinkage equation would predict sinkages too small. The track equation assuming a slag of 0.02 estimates sinkage too high in a range of 2 – 9 mm depending on the unit except for PTS whereby sinkage would be underestimated. This is sensible as it is the unit with the least belt tension. Consequently a track slag of 0.05 results in a sinkage prediction even larger and less appropriate except possibly for the PTS. The Bernstein equation significantly underestimates sinkage except for the Stocks. Thus in general the track equation (Eq. 8) predicts sinkage most accurately. Unfortunately true track slag has not been measured during the experiments and therefore no further calibration/adjustment can be made.

Appendix 2 Footprint Characteristics

The footprint of a tyre depended on the width, diameter and its inflation pressure. The wider the tyre was the larger had the resulting footprint been. The same was true for tyres with larger diameter and less inflation pressure. The data for the rear tyres used in this investigation is shown in Table 10.

Table 10: Footprint characteristics and average contact pressure for different treatments

Treatment	Area (m^2)	Max. Width (m)	Max. Length (m)	Length/Width Ratio	Av. Contact Pressure (kN/m^2)
500-70/4.5/2.3	0.03161	0.525	0.66	1.26	142
500-85/4.5/1.4	0.04086	0.55	0.81	1.47	110
600/4.5/1.4	0.03933	0.60	0.75	1.25	114
700/4.5/1.0	0.04711	0.67	0.75	1.12	96
900/5/0.5	0.05887	0.83	0.98	1.18	76

Appendix 3 Gravimetrically measured dry bulk density

The DBD values for the different types of investigations are shown in Figure 48. Overall the tendency of the data corresponded to the estimated increase in DBD from the soil displacement measurement for each treatment group. The initial DBD was significantly lower than any other group. The results of the rear tyre group and the speed system group caused a similar DBD. The results from different track types and the result of the undercarriage systems fell within the same range, too. All other combinations were significantly different (LSD shown in Figure 48). The tendency of the DBD agreed for gravimetric DBD compared to the estimated increase in DBD utilizing the slope of the soil displacement graphs. The resolution of the soil displacement measurement was greater than that of the DBD.

The evaluation of the under carriage systems can be split up in the average wheel and average track type system shown in Figure 49. Hereby the average gravimetric DBD values did not correspond to the groups of soil displacement seen in Section 3.2

With a volume of 145613 mm^3 for an ideal cylinder having an internal length of 51.5 mm and an internal radius of 30 mm totally filled with soil, the measurement would be correct. Yet

with a slight deviation from the circular shape leading to a reduction of 1 mm in diameter, which would hardly be noticed, the volume decreases by 3.3%. By cutting off the soil from the top and bottom of the cylindrical ring, no soil particles can reach higher than the cylinder. If particles were sticking out initially a cavity remains after cutting the surplus soil. These cavities are only relevant for the sand fraction ranging from 0.1 mm to 2 mm. Consequently it can be assumed, that both ends of the cylinder are filled to 0.25 mm less in average. This again reduces the volume by an additional 1% than is assumed. Handling mistakes, e.g. hammering the ring too far into the soil, thus compacting the sample additionally, are not taken into consideration which would also increase the measurement errors significantly. The individual DBD data is shown in Table 12. The grouped DBD data is shown in

.

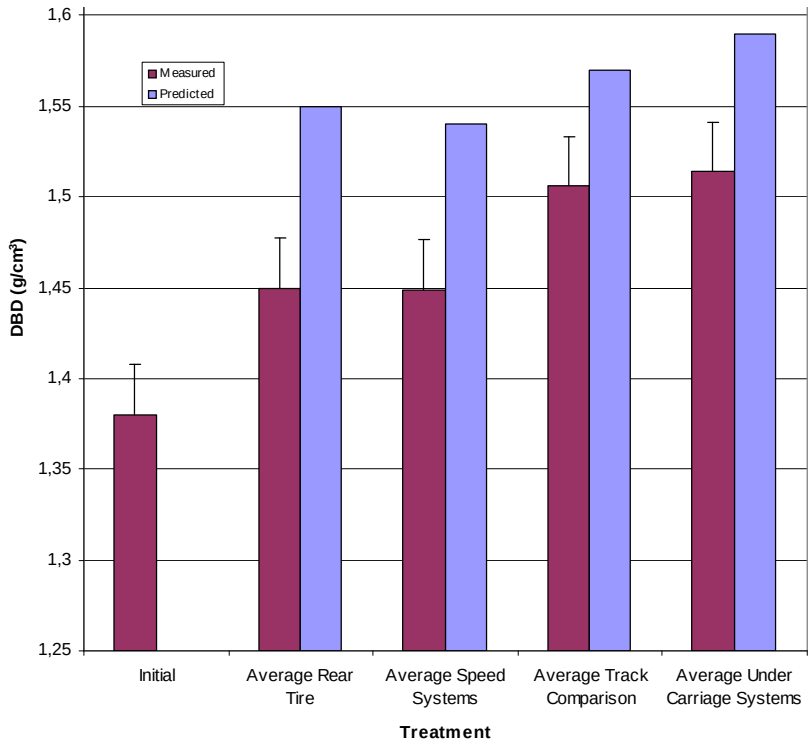

Figure 48: DBD values for different treatment groups averaged together

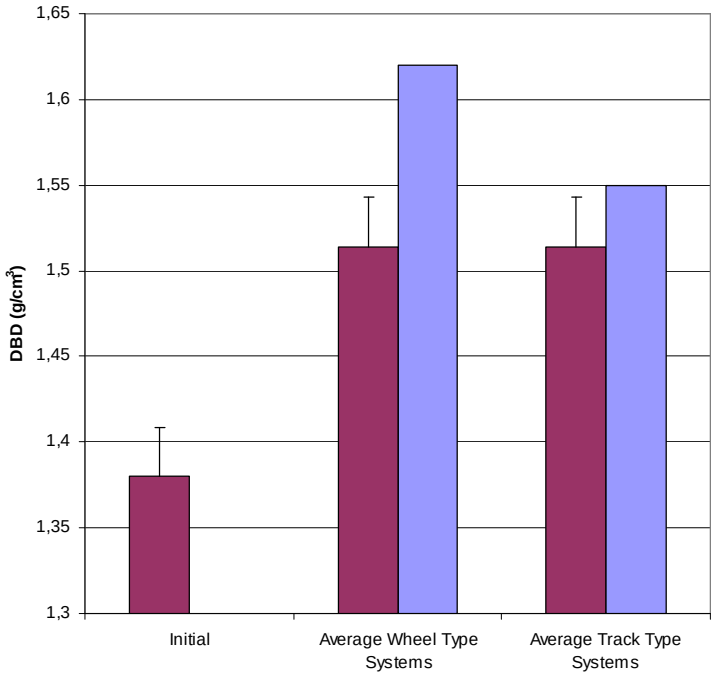

Figure 49: DBD for undercarriage systems split up in wheel and track type soil compaction characteristics

Table 11: DBD values for treatment groups

Treatment	DBD (g/cm^3)	SE	DF
Control	1.380	0.016	15
Rear Tyre	1.450	0.016	8
Speed Investigation	1.449	0.018	13
Undercarriage Systems	1.514	0.016	17
Track Type	1.514	0.016	10
Wheel Type	1.514	0.015	7

Table 12: DBD values for all treatments

Treatment	DBD (g/cm^3)	Standard Error	Degrees of Freedom
Rear Tyres			
500-70	1.4645	0.03911	66
500-85	1.4512	0.03911	66
600	1.5201	0.03911	66
700	1.4245	0.03911	66
680/5.5/1.5	1.3897	0.03911	66
Speed Systems			
900 Slow	1.4301	0.03911	66
900 Normal	1.4145	0.03911	66
900 Fast	1.4212	0.03911	66
900 Multipass	1.5301	0.03911	66
Whole Machine Systems			
T3/12 followed by 500-70	1.5023	0.03911	66
T3/12 followed by 700	1.5023	0.03911	66
900/10.5/1.9 followed by 500-70	1.5457	0.03911	66
900/10.5/1.9 followed by 700	1.5090	0.03911	66
680/10.5/2.2 followed by 500-85	1.5212	0.03911	66
680/7/1.6 followed by 500-70/3.5/1.3 followed by 500-85/3.75/1.1	1.5334	0.03911	66
680/7.5/1.5 followed by 680/7.5/1.5	1.4808	0.03911	66
680/5.5/0.9 followed by 700/4.5/1.0	1.5502	0.03911	66
Dominator 23.1-26/4/1.2 followed by 11.5/80-15.3/1.5/2	1.4829	0.03911	66
Tracks			
Westtrack	1.5025	0.04106	77
Stocks	1.5346	0.04221	83
Steve	1.5163	0.03911	66
TerraTrac@ 200 bar	1.4905	0.03911	66
TerraTrac@ 160 bar	1.5060	0.03911	66
TerraTrac@ 50 bar	1.4875	0.03911	66